JYVÄSKYLÄ STUDIES IN COMPUTING 28

Seppo Hämäläinen

WCDMA Radio Network Performance

Esitetään Jyväskylän yliopiston informaatioteknologian tiedekunnan suostumuksella
julkisesti tarkastettavaksi yliopiston Agora rakennuksessa (Ag Aud. 2)
helmikuun 8. päivänä 2003 kello 12.

Academic dissertation to be publicly discussed, by permission of
the Faculty of Information Technology of the University of Jyväskylä,
in the Building Agora, (Ag Aud.2), on February 8, 2003 at 12 o'clock noon.

UNIVERSITY OF JYVÄSKYLÄ

JYVÄSKYLÄ 2003

WCDMA Radio Network Performance

JYVÄSKYLÄ STUDIES IN COMPUTING 28

Seppo Hämäläinen

WCDMA Radio Network Performance

UNIVERSITY OF JYVÄSKYLÄ

JYVÄSKYLÄ 2003

Editors
Tommi Kärkkäinen
Department of Mathematical Information Technology, University of Jyväskylä
Pekka Olsbo, Marja-Leena Tynkkynen
Publishing Unit, University Library of Jyväskylä

ISBN 951-39-1931-5 (PDF)

ISBN 951-39-1402-X (nid.)
ISSN 1456-5390

Jyväskylä University Printing House, Jyväskylä 2003

ABSTRACT

Hämäläinen, Seppo
WCDMA Radio Network Performance
Jyväskylä: University of Jyväskylä, 235 p.
(Jyväskylä Studies in Computing,
ISSN 1456-5390; 28)
ISBN 951-39-1931-5
Finnish summary
Diss.

In this thesis the WCDMA radio network performance and the radio network performance simulations are discussed. As research results, simulation tools are developed that can be used when investigating the WCDMA radio network performance, the effects of the various parameters on the performance and the effects of the various algorithms on the performance. Another research result is performance analysis for a set of WCDMA system parameters and algorithms based on simulations. In addition, two new methods to improve WCDMA and cdma2000 system performance have been developed.

By using the developed radio network simulator, parameters and algorithms of the WCDMA system can be studied for standardization purposes. The developed tools can be used for the development of radio resource management algorithms, radio network planning tool development and as a tool for radio network optimisation. Here two kinds of simulators are considered – static and dynamic tools. Static simulators are simple computer software, which can be used to generate sufficient results in a short time. Dynamic simulators are more complex tools, which model time span, user mobility, traffic, multiple access and realistic radio resource management.

In this work, the WCDMA radio network capacity has been investigated by using the developed tools. The WCDMA base station receiver can be implemented by using a so-called multi-user detection. In this work the capacity gain due to the multi-user detection has been studied. Base station transmission can be based on orthogonal codes or the mobile station receiver can employ interference cancellation. Here the gains from the orthogonal codes and the interference cancellation were investigated. In addition, gains from soft handover were studied.

Due to the linearity of the mobile stations power amplifier and selectivity of the mobile station receiver filter, the base stations or the mobile stations operating in the adjacent frequency can cause interference in the desired channel. Here the requirements for the linearity and selectivity have been studied based on static simulations. By using simulations capacity losses due to interference from having the source in the adjacent frequency has been studied.

In this thesis the effect due to power control and its parameters, random access, handover algorithms and their parameters, and compressed mode have

been studied by using a dynamic radio network simulator. The performance of High Speed Downlink Packet Access (HSDPA) has also been studied with the dynamic tool.

In order to improve the performance of CDMA systems two novel methods – diversity random access and Site Selection Diversity Transmit (SSDT) - has been developed. Both methods are in use in both the WCDMA and cdma2000 systems.

Several WCDMA system parameters have been modified or agreed in the 3GPP project based on the research shown here. Such parameters are e.g. the linearity requirement of the mobile station power amplifier, the selectivity requirement of the mobile stations receiver filter and the minimum power requirement of the mobile station.

Keywords: WCDMA, Radio Network Simulation, Radio Network Performance, Capacity, Radio Resource Management, Multi-User Detection, Adjacent Channel Interference, Random Access, Power Control, Handover, Compressed Mode, High Speed Downlink Packet Access, Site Selection Diversity Transmit

Author's Address Seppo Hämäläinen
Beijing Riviera, Villa 123
No.1 Xiang Jiang Bei Road
Chaoyang District
100103 Beijing
P.R.China

Supervisor Prof. Tapani Ristaniemi
Department of Mathematical Information Technology
University of Jyväskylä

Reviewers Prof. Jukka Lempiäinen
Institute of Communications Engineering
Tampere University of Technology

Prof. Risto Wichman
Signal Processing Laboratory
Department of Electrical and Communications Engineering
Helsinki University of Technology

Opponent Prof. Riku Jäntti
Department of Computer Science
Vaasa University

This thesis is dedicated to my wife Terja, to my children Lina-Maria and Leevi and to my parents Aune and Toivo

Beijing, January 7, 2003

Seppo Hämäläinen

PREFACE

I would like to thank the whole Mobile Networks laboratory of the Nokia Research Centre for generating a good atmosphere for my research. I would especially like to thank Dr. Seppo Granlund and Mr. Jukka Soikkeli.

I would like to thank my co-authors of the conference and journal articles and patents – Antti Toskala, Harri Holma, Tero Henttonen, Hannu Häkkinen, Jere Keurulainen, Tero Ojanperä, Jussi Numminen, Seppo Granlund, Oscar Salonaho, Antti Lappeteläinen, Peter Slanina, Magnus Hartman, Kari Sipilä, Harri Lilja, Ari Hämäläinen, Sari Korpela, Jukka Vikstedt and Mika Rinne.

My supervisor, Prof. Tapani Ristaniemi, also needs to be acknowledged. Thank you for pushing me forward with my thesis.

Special thanks go to Mr. Jussi Numminen who generated many problems to be solved and simulated during the standardization phase. Big thanks go also to Mr. Mika Kolehmainen who helped me a great deal during the years this research was made.

Beijing, January 7, 2003

Seppo Hämäläinen

TABLE OF CONTENTS

ABBREVIATIONS

1x	cdma2000, single carrier
1xEV	1x EVolution
1xEV-DO	1xEV – Data Only
1xEV-DV	1xEV – Data and Voice
16QAM	16-point Quadrature Amplitude Modulation
2G	2nd Generation Mobile Systems
3G	3rd Generation Mobile Systems
3GPP	3rd Generation Partnership Project
3GPP2	3rd Generation Partnership Project 2
64QAM	64-point Quadrature Amplitude Modulation
8PSK	8-array Phase Shift Keying
ACI	Adjacent Channel Interference
ACIR	Adjacent Channel Interference Ratio
ACK	ACKnowledgement
ACLR	Adjacent Channel Leakage Ratio
ACP	Adjacent Channel leakage Power
ACS	Adjacent Channel Selectivity
ACTS	Advanced Communication TechnologieS
AI	Acquisition Indicator
AICH	Acquisition Indicator CHannel
AMC	Adaptive Modulation and Coding
AMPS	Advanced Mobile Phone Service
AMR	Adaptive MultiRate
ARIB	Association for Radio Industry and Business
ARQ	Automatic Repeat reQuest
ATDMA	Advanced TDMA Mobile Access
AVI	Actual Value Interface
AWGN	Additive White Gaussian Noise
BCH	Broadcast CHannel
BER	Bit Error Rate
BLER	BLock Error Rate
BPSK	Binary Phase Shift Keying
BS	Base Station
BSIC	Base Station Identity Code
CCCH	Common Control CHannel
CCPCH	Common Control Physical CHannel
CCSS	ConCurrent System Studio
CDF	Cumulative Density Function
CDMA	Code Division Multiple Access
cdma2000	code division multiple access for the year 2000
ChEG	China IMT-2000 radio transmission technology and coordination Evaluation Group

C/I	Carrier to Interference Ratio
CODIT	COde DIvision Test bed
COST	European Co-Operation in the field of Scientific and Technical research
CM	Compressed Mode
CPCCH	Common Power Control CHannel
CPICH	Common PIlot CHannel
CWTS	China Wireless Telecommunications Standards
D-AMPS	Digital-AMPS
DCA	Dynamic Channel Allocation
DCH	Dedicated CHannel
DCS1800	Digital Cellular System 1800 (operating in 1800 MHz band)
DECT	Digital Enhanced Cordless Telecommunications
DL	DownLink
DPCCH	Dedicated Physical Control Channel
DPCH	Dedicated Physical CHannel
DPDCH	Dedicated Physical Data CHannel
DRC	Data Rate Control
DS-CDMA	Direct Sequence – CDMA
DSCH	Downlink Shared CHannel
DTX	Discontinuous Transmission
E_b/I_0	Energy per bit to interference ratio
E_b/I_0_target	E_b/I_0 target for closed loop power control
E_b/N_0	Energy per bit to noise ratio
$E_b/(N_0 + I_0)$	Energy per bit to noise and interference ratio
E_c/I_0	Energy per chip to noise ratio
EACAM	Early Acknowledgement Channel Assignment Message
EDGE	Enhanced Data rates for Global Evolution
ETSI	European Telecommunications Standards Institute
EVM	Error Vector Magnitude
FBI	FeedBack Information
F-CACH	Forward - Common Assignment CHannel
FCS	Fast Cell Selection
FDD	Frequency Division Duplex
FER	Frame Error Ratio
FHARQ	Fast Hybrid ARQ
FIFO	First In - First Out
FMA	FRAMES Multiple Access
FMA1	FRAMES Multiple Access mode 1, TDMA based option
FMA2	FRAMES Multiple Access mode 2, CDMA based option
FPLMTS	Future Public Land Mobile Telephone System
FRAMES	Future Radio widebAnd Multiple accEss Services
FTP	File Transfer Protocol
GDP	Gross Domestic Product
G_p	Processing gain
GPRS	General Packet Radio Service

GSM	Global System for Mobile communications
GSM1800	Global System for Mobile communications, 1800 MHz band
GSM1900	Global System for Mobile communications, 1900 MHz band in the USA
HARQ	Hybrid ARQ
HCS	Hierarchical Cell Structure
HDR	High Data Rate, same as 1xEV-DO
HPSK	Hybrid Phase Shift Keying
HSDPA	High Speed Downlink Packet Access
HS-DSCH	High Speed – Downlink Shared CHannel
IC	Interference Cancellation
ID	IDentification
IFHO	Inter-Frequency HandOver
IMT-2000	International Mobile Telecommunication – 2000
IP	Internet Protocol
IPv6	Internet Protocol version 6
IS-41	Interim Standard 41
IS-95	Interim Standard 95
IS-136	Interim Standard 136, Same as D-AMPS
ISCP	Interference Signal Code Power
ITU	International Telecommunication Union
ITU-R	ITU-Radio Communication sector
ITU-T	ITU-Telecommunication Standardization sector
I_0	Interference power spectral density
I_{ub}	Interface between Node-B and RNC
L3	Layer 3
LOS	Line-of-Sight
MAC	Medium Access Control
MAI	Multiple Access Interference
MCL	Minimum Coupling Loss
MCS	Modulation and Coding Set
MF	Matched Filter
MII	Ministry of Information Industry in China
MIMO	Multiple Input – Multiple Output
MPT	Ministry of Post and Telecom in China
MS	Mobile Station
MUD	Multi-User Detection
N_0	Noise power spectral density
NLOS	Non-Line-of-Sight
Node-B	Base station in 3GPP vocabulary
NR	Noise Rise
ODMA	Opportunity Driven Multiple Access
OFDM	Orthogonal Frequency Division Multiplexing
OFDMA	Orthogonal Frequency Division Multiple Access
OL	Outer Loop
OVSF	Orthogonal Variable Spreading Factor

PA	Power Amplifier
PC	Power Control
PCCAM	Power Control Channel Assignment Message
PCS1900	Personal Communication System 1900 (operating in 1900MHz band)
P_d	Detection error probability
PDC	Personal Digital Cellular
PDF	Probability Density Function
PDU	Protocol Data Unit
P_{fa}	False alarm probability
PIC	Parallel Interference Cancellation
PRACH	Physical Random Access CHannel
QPSK	Quadrature Phase Shift Keying
RACE	Research of Advanced Communications technologies in Europe
RACH	Random Access CHannel
RAN	Radio Access Network
RF	Radio Frequency
RLC	Radio Link Control
RNC	Radio Network Controller
RRC	Radio Resource Control
RRM	Radio Resource Management
RSCP	Received Signal Code Power
RSSI	Received Signal Strength Indication
RT	Real Time
RX	Receive
RxP	Received power
SF	Spreading Factor
SF/2	Spreading Factor halving
SINR	Signal to Interference + Noise Ratio
SIR	Signal to Interference Ratio
SMG2	Special Mobile Group 2
SNR	Signal-to-Noise Ratio
SPW	Signal Processing Worksystem
SSDT	Site Selection Diversity Transmit
STD	STandard Deviation
T1	Committee that develops technical standards and reports
T1P1	Subcommittee of T1 in areas of wireless/mobile services and systems
T300	RRC timer related to connection request and setup
TDD	Time Division Duplex
TDMA	Time Division Multiple Access
TD-SCDMA	Time Division Synchronous CDMA
TFC	Transport Format Combination
TFCI	Transport Format Combination Indicator
TGCFN	Transmission Gap Connection Frame Number

TGD	Transmission Gap start Distance
TGL1	Transmission Gap Length 1
TGL2	Transmission Gap Length 2
TGPL1	Transmission Gap Pattern Length 1
TGPL2	Transmission Gap Pattern Length 2
TGPRC	Transmission Gap Pattern Repetition Count
TGSN	Transmission Gap Starting slot Number
TIA	Telecommunications Industry Association
TPC	Transmit Power Control
TSG	Technical Specification Group
TTA	Telecommunications Technology Association
TTA1	TTA's WCDMA track
TTA2	TTA's cdma2000 track
TX	Transmit
TxP	Transmit power
TTC	Telecommunications Technology Committee
TTI	Transmission Time Interval
UDD	Undefined Delay Data
UE	User Equipment in 3GPP vocabulary, same as MS
UMTS	Universal Mobile Telecommunication System
US-TDMA	Same as IS-136
UTRA	Universal Terrestrial Radio Access (3GPP) or UMTS Terrestrial Radio Access (ETSI)
UTRAN	UMTS Terrestrial Radio Access Network
UWC-136	Universal Wireless Communications 136
UWCC	Universal Wireless Cellular Consortium
WB-CDMA	Same as WCDMA
WB-TDMA	Wideband TDMA
WCDMA	Wideband Code Division Multiple Access
W-CDMA	Same as WCDMA
W-CDMA N/A	WCDMA North America
WG4	Working Group 4. 3GPP working group doing specifications for radio performance and RF parameters
WIMS	Wireless Integrated services digital network Multimedia Services
WP-CDMA	Wideband Packet CDMA
WTDMA	Same as WB-TDMA
WWW	World Wide Web

1 INTRODUCTION

1.1 Background

Today, communications enter our daily lives in many different ways. Speech transmission has moved to digital and is becoming more and more wireless. At the moment the second generation digital mobile telephone systems - GSM (Global System for Mobile communications) in Europe, China, the USA and some other parts of the globe, PDC (Personal Digital Cellular) in Japan, IS-95 (Interim Standard 95) and TDMA (Time Division Multiple Access) in the USA – allow for a large capacity of digital speech and for low-rate data transmission. Extensions to the second generation systems, such as GPRS (General Packet Radio Service) and cdma2000 1x (code division multiple access for the year 2000, 1 carrier) will offer services that approach that which is required from the third generation networks. To fully meet these requirements new system, UMTS (Universal Mobile Telephone System), have been developed.

From the air interface point of view the key requirements of UMTS are: the system should be able to serve high data rates of 2 Mbps for mobile speed less than 10 km/h, 384 kbps for mobile speed less than 120 km/h and 144 kbps for mobile speed less than 500 km/h. Speech quality has to correspond to the fixed link quality when using low data rates. The system should be able to serve packet and circuit switched services for the different bitrates and the different radio environments. Dual band and dual mode operation of UMTS and GSM including roaming between UMTS „islands“ should be possible. Roaming between UMTS and GSM networks is required. The system should be able to operate in any suitable band that becomes available, e.g. GSM, DCS1800 (Digital Cellular System 1800) or PCS1900 (Personal Communication System 1900). [UMTS30.01]

1.1.1 Background in Europe

In Europe 3G (3rd Generation mobile systems) research already started in 1988 in the RACE I (Research of Advanced Communications technologies in Europe) programme followed by the RACE II program during 1992–1995. In the RACE

II CDMA (Code Division Multiple Access) based CODIT (COde DIvision Test bed) and TDMA based ATDMA (Advanced TDMA Mobile Access) air interfaces were developed. In 1995, the ACTS (Advanced Communication TechnologieS) programme was started. Within the ACTS the FRAMES (Future Radio widebAnd Multiple accEss Services) project was established having the objective to define a proposal for a UMTS radio access system. The FRAMES project had participants from major industrial parties and universities. [Hol00]

At the beginning of the FRAMES project participants gave proposals for the FRAMES multiple access scheme. Based on the initial proposal evaluations two options TDMA-based FMA1 with and without spreading and CDMA based FMA2 were formed. FMA stands for Frames Multiple Access. Proposals were submitted to ETSI (European Telecommunications Standards Institute, [ETSI]) as candidates for the UMTS air interface and the ITU (International Telecommunication Union, [ITU]) IMT-2000 (International Mobile Telecommunication 2000) submission [Hol00]. In June 1997 the received air interface proposals were grouped into five groups in ETSI [UMTS30.06]:

- α group: WB-CDMA (WCDMA, Wideband CDMA)
- β group: OFDM (Orthogonal Frequency Division Multiplexing)
- γ group: WB-TDMA (WTDMA, Wideband TDMA)
- δ group: WTDMA/CDMA
- ε group: ODMA (Opportunity Driven Multiple Access)

The evaluation of the proposals was based on the requirements in the ITU-R (ITU – Radio communication sector) IMT-2000 framework.

The α concept group was formed from WCDMA proposals from FRAMES, Fujitsu, NEC and Panasonic, and contributions were made from several companies from Europe, the USA and Japan. The physical layer of the WCDMA uplink was based on the FRAMES proposal, while the downlink was based on other proposals. The basic features of the WCDMA proposal were wide 5 MHz bandwidth, physical layer flexibility for integration of all data rates on a single carrier and re-use 1. The possible enhancements included transmit diversity, adaptive antennas and support for the advanced receiver structures. [Hol00]

The α group achieved the greatest support within ETSI. WCDMA was seen as taking advantage of the flexibility in the physical layer for accommodating the different service types simultaneously. As a drawback for WCDMA, it recognized the usage of an unlicensed band. Since WCDMA requires a continuous transmission and reception for the closed loop power control it is not easily usable in the unpaired TDD (Time Division Duplex) band. [Hol00]

The β group was based on the OFDM proposal mainly from Telia, Sony and Lucent. The features of the OFDM proposal were operation with slow frequency hopping with TDMA and OFDM multiplexing, a 100 kHz wide bandslot as the basic resource unit, higher rates were built by allocating several

bandslots, creating a wideband signal and diversity was provided by dividing the information among several bandslots over the carrier. The possible enhancement mechanisms were transmit diversity, multi-user detection for interference cancellation and adaptive antenna solutions. [Hol00]

The proposal in the γ group was based on the non-spread option of the FRAMES FMA1 proposal, WTDMA. The basic features of WTDMA were: 1.6 MHz carrier bandwidth, equalization with training sequences in TDMA bursts, interference averaging with frequency hopping, link adaptation, two basic burst type, $1/16^{th}$ and $1/64^{th}$ burst lengths for high and low data rates respectively and low re-use. The possible enhancements included inter-cell interference suppression, support for adaptive antennas, TDD operation and a less complex equalizer for large delay spread environments. The main limitation of WTDMA seen was the range of bitrates – especially low bitrates. This is due to the fact that the slot duration – even if only $1/64^{th}$ of the frame time – did not offer low bitrates. Thus a narrow band TDMA would be needed together with the wideband option to offer low bitrates. [Hol00]

The proposal in the δ group was based on the spreading option in the FRAMES FMA1. WTDMA/CDMA features were: 1.6 MHz carrier bandwidth, TDMA burst structure with midamble for channel estimation, CDMA concept applied on the top of the TDMA structure for additional flexibility, reduction of intra-cell interference by multi-user detection for users within a timeslot on the same carrier and low reuse down to three. The possible enhancements included frequency hopping, inter-cell interference cancellation, support of adaptive antennas, operation in TDD mode and DCA (Dynamic Channel Allocation). Receiver complexity was seen as a drawback to this proposal. [Hol00]

The ε group was based on ODMA proposed by Vodafone. ODMA is not a multiple access method as such, but rather a relaying protocol. It was later integrated into the WCDMA and WTDMA/CDMA concept groups. In ODMA users out of coverage use another terminal as a relay to transmit to the base station. [Hol00]

In principle all the proposed technologies were able to fulfil the UMTS requirements. WCDMA and WTDMA/CDMA were the main candidates. WCDMA received support from a selection made in Japan; in Japan ARIB (Association of Radio Industries Businesses, [ARIB]) selected WCDMA as a 3G technology which increased the global potential of WCDMA. In 1998 ETSI selected WCDMA as the standard on the paired band and WTDMA/CDMA on the unpaired band. [Hol00]

1.1.2 Background in Japan

In Japan three main proposals were based on WCDMA, WTDMA and OFDMA (Orthogonal Frequency Division Multiple Access). WCDMA technology in Japan was similar as in ETSI, since the members of ARIB contributed WCDMA in both organizations. The outcome of the ARIB selection process in 1997 was WCDMA with FDD (Frequency Division Duplex) and TDD modes. [Hol00]

1.1.3 Background in Korea

In Korea TTA (Telecommunications Technology Association, [TTA]) adopted a 2-track approach. The TTA1 (TTA's cdma2000 track) proposal was similar to the cdma2000 while the TTA2[1] (TTA's WCDMA track) similar to the WCDMA. Several TTA1 details were submitted to ETSI and ARIB, which lead to a high degree of commonality in ARIB, ETSI and TTA solutions. [Hol00]

1.1.4 Background in the USA

In the USA there are several 2G (2nd Generation mobile systems) systems that have a natural path of evolution to the 3G. The most important of them are GSM1900 (GSM, 1900 MHz band in the USA), US-TDMA (IS-136[2], D-AMPS[3]) and IS-95. GSM1900 related standards work was made in T1 (A US Committee that develops standards and reports, [T1]) in its subcommittee T1P1 (a sub-committee of T1 in areas of wireless/mobile services and systems). T1P1 submitted W-CDMA N/A (Wideband CDMA, N/A = North America) proposal to the ITU-R IMT-2000 process. This proposal has many commonalities with ETSI and ARIB WCDMA technologies since the contributing companies were also active in ETSI and ARIB. IS-136 3G evolution was made in TIA (Telecommunications Industry Association, [TIA]) work package TR45.3. Result was a combination of narrow band and wide band TDMA - UWC-136 (Universal Wireless Communications 136). Narrowband TDMA was identical to the EDGE (Enhanced Data rates for Global Evolution) concept in ETSI and in T1P1. Wideband TDMA is based on the FRAMES WTDMA concept. TR45.5 proposed cdma2000 air interface to ITU. cdma2000 is evolution of IS-95 and it is based partly on IS-95, such as synchronized network and common pilot channels. cdma2000 is very similar to the Global cdma 1 ITU proposal from TTA, Korea. In TR46.1 WIMS (Wireless Integrated services digital network Multimedia Services) W-CDMA was made. WIMS W-CDMA is based on a constant spreading factor with high numbers of multicodes. WP-CDMA (Wideband Packet CDMA) resulted from convergence between W-CDMA N/A and WIMS W-CDMA. The merged proposal was submitted to the ITU-R IMT-2000. [Hol00]

1.1.5 Background in China

China can be seen as a special case for wireless mobile communications. The population of P.R. China was 1300 million at the end of 2001. At the same time, the number of fixed line subscribers was 179 million and the number of mobile subscribers 145 million. In the second quarter of 2002 the number of mobile subscribers reached 180 million, see FIGURE 1.1-1. Despite of the fact that the number of mobile subscribers in China is the highest in the world, the penetration rate was only 11.2 % at the end of 2001. It is estimated that the number of Chinese mobile subscribers will increase to 260–290 million that

---

1 TTA1 and TTA2 systems were later renamed as global cdma 1 and 2, respectively

2 Interim Standard - 136

3 Digital AMPS, AMPS = Advanced Mobile Phone Service

corresponds to a 20–22 % penetration rate (assuming 1300 million population). The Chinese economy is developing rapidly – the growth of the Chinese GDP (Gross Domestic Product) in 2001 was very high, 7.3 %. The developing economy also boosts expansion in the telecom sector. In 2001 growth in the telecom sector was over 20 % and for mobile communication almost 70 %. Quarterly, about 15 million new mobile subscribers emerge in China. [Wu02, Tel02]

In addition to the high population, population density is also very high in China if compared to other countries. The average Chinese city population density is 11 160/km^2. In cities where the population is over 2 million population density is 17 935/km^2 and in cities such as Shanghai, Chengdu, Chongqing, Shenyang, Qingdao and Wuhan the density is 20 000/km^2. In Hong Kong the average density is 27 000/km^2 and in dense areas even up to 50 000/km^2. This high density of people sets special requirements for the cellular capacity. [Wu02]

The history of Chinese 3G standardization activity starts from 1997 when the ChEG (China IMT-2000 radio transmission technology and coordination) group was founded by the China MPT (Ministry of Post and Telecom) and registered in ITU. At the beginning purpose of the ChEG group was to evaluate WCDMA and cdma2000 standards. In 1998 ChEG together with the national 863-project called candidate proposals for the Chinese 3G system. One of the proposals, TD-SCDMA (Time Division Synchronous CDMA), was then submitted to ITU where it became part of the ITU recommendation. The ChEG had also harmonization activities of WCDMA and cdma2000. Currently CWTS (China Wireless Telecommunications Standards, [CWTS]) actively participates in international standardization activities. CWTS was founded in 1999 by MII (Ministry of Information Industry) and it is an organizational partner of 3GPP (3rd Generation Partnership Project) and 3GPP2 (3rd Generation Partnership Project - 2) where it has submitted numbers of contributions and proposals. [Cao02]

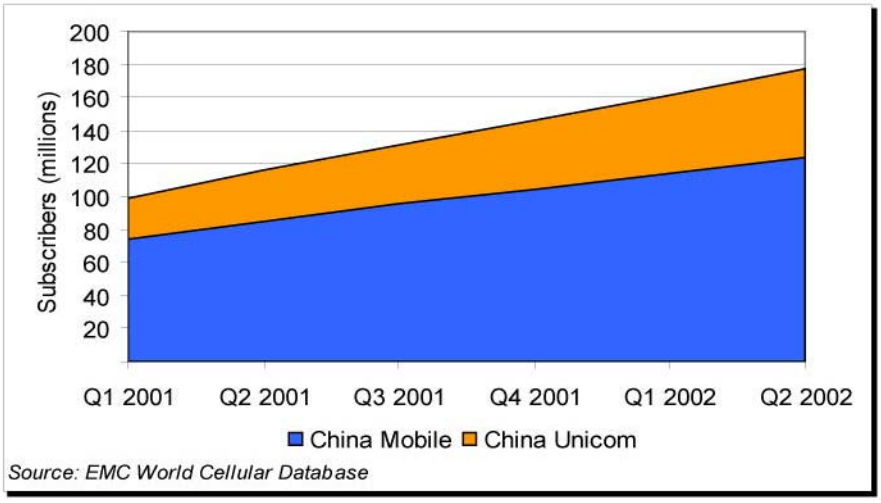

FIGURE 1.1-1. China subscriber growth - China Unicom and China Mobile.

1.1.6 3GPP Initiative

Since similar technologies were standardized parallel in several regions around the world, it was a waste of resources. In addition, to be able to achieve identical specifications common WCDMA specification work was desired. Therefore initiatives were made to create a single forum for WCDMA standardization, 3GPP ([3GPP]). Standardization organizations involved in the creation of 3GPP were ARIB, ETSI, TTA, TIA, TTC (Telecommunications Technology Committee, [TTC]) and T1P1. In 3GPP a joint effort for the standardization of UTRA (Universal Terrestrial Radio Access) was agreed. Later CWTS joined 3GPP and contributed its TD-SCDMA system. In addition, to the above members 3GPP has market representation partners (GSM Association, UMTS forum, Global Mobile Suppliers Association, IPv6[4] forum, UWCC[5]). 3GPP constitutes four TSGs (Technical Specifications Group): RAN (Radio Access Network) TSG, Core Network TSG, Service and System Aspects TSG and Terminals TSG. The most relevant TSG for WCDMA is RAN TSG that is further split into working groups WG1- Radio layer 1, WG2 – Radio layer 2/3, WG3 – Architecture and interfaces, WG4 – Radio performance and RF (Radio Frequency) parameters and ITU Ad-hoc – ITU activity coordination. [Hol00, Sto98, 3GPP]

During the first half of 1999 the input from the various participants were merged. The target was to get a finalized first release, Release 99, of UTRA ready by the end of 1999. The member organizations have undertaken individual actions to produce standards publications identical to 3GPP. During 2000 further work on GSM evolution was also moved under 3GPP. [Hol00]

1.1.7 3GPP2 Initiative

Work done in the USA in TR45.5 and in Korea in TTA was merged and 3GPP2 was created. 3GPP2 work runs parallel to 3GPP work. 3GPP2 work focuses on the development of cdma2000 and multi-carrier mode of cdma2000. 3GPP2 has participants from ARIB, TTC and CWTS. [3GPP2]

1.1.8 Harmonization of 3GPP and 3GPP2

During the spring 1999 several operators and manufactures held a series of meetings in which the target was to seek a harmonization between WCDMA and cdma2000. The results was a harmonized 3G CDMA standard with 3 modes: Multicarrier (based on cdma2000), direct sequence (based on UTRA FDD) and TDD (based on UTRA TDD) modes. Selection was a modular approach in which both core networks, IS-41 (Interim Standard 41) and GSM, could be used with all air interface alternatives. Technical impacts of harmonization were a change of WCDMA chip rate from 4.096 to 3.84 Mchps

---

4 Internet Protocol version 6

5 Universal Wireless Cellular Consortium

and addition of a common pilot. In cdma2000 a direct sequence mode was abandoned and replaced by WCDMA. [Hol00]

1.1.9 IMT-2000 process in ITU

In ITU 3rd generation systems used to be called FPLMTS (Future Public Land Mobile Telephone System), but are now called IMT-2000. In ITU, ITU-R TG8/1 handles radio-dependent aspects, while radio-independent things are handled by ITU-T (ITU – Telecommunications Standardization sector) SG11. ITU-R TG8/1 received several proposals as IMT-2000 candidate during IMT-2000 candidate process. In the second phase evaluation results were received from proponents as well as from the other evaluators. During the first half of 1999 recommendation IMT.RKEY was created containing the IMT-2000 multimode concept. It was finalized at the end of 1999 when a detailed specification of IMT.RSCP was created. The detailed implementation of IMT-2000 continues in regional standardization bodies. [Hol00]

ITU-R process has an important role as an external motivation and timing source for IMT-2000 activities in regional standardization bodies. It also sets requirements that have been reflecting to regional standard as UMTS since they need to fulfil IMT-2000 requirements. [Hol00]

ITU-R IMT-2000 is grouped to TDMA and CDMA groups. TDMA group consists of UWC-136 and DECT (Digital Enhanced Cordless Telecommunications). UWC-136 is the single carrier mode and DECT multi-carrier mode of TDMA group. CDMA group consists of UTRA FDD, cdma2000, UTRA TDD and TD-SCDMA. UTRA FDD is the single carrier direct sequence mode and cdma2000 multicarrier mode. UTRA TDD and TD-SCDMA form TDD mode of CDMA group. [Hol00]

1.1.10 Beyond Release –99

In 3GPP work after release –99 contains the specifications of the new features and making corrections to release -99. The required corrections are identified as implementation proceeds. The next releases after release –99 are named as release 4, 5 and so on. Originally it was assumed that new versions appear annually. [Hol00]

In release 4 only minor adjustments to the RAN were done. In release 5 bigger changes such as HSDPA (High Speed Downlink Packet Access) are involved. During the coming years specifications that allow the use of IS-41 core network with UTRA FDD will be specified. Correspondingly, on the cdma2000 side specifications that allow the use of the GSM core network with cdma2000 radio will be specified. On the TDD side further alignment between UTRA TDD and TD-SCDMA will be made. IP (Internet Protocol) -based technology will be used more in future releases. First in release 4 transport will have an IP-based option and later the IP will shape the internal architecture of UTRAN (UMTS Terrestrial Radio Access Network). [Hol00]

1.2 Motivation of This Thesis

This thesis presents research made for the WCDMA air interface and the radio resource management algorithms performance. In addition the basic principles and modelling of WCDMA radio network simulators is discussed.

The motivation of this research is to develop tools and execute simulations for standardization purposes, radio resource management algorithm development purposes, network planning purposes and WCDMA radio network optimisation purposes. As the WCDMA system is highly complicated, an analytical approach is almost impossible to investigate WCDMA system behaviour.

Several parameters defined by 3GPP were first tested with static and/or dynamic simulators presented here. Such parameters are for example the minimum power requirement for the mobile station, the adjacent channel interference requirements and the compressed mode parameters.

When radio resource management algorithms were developed for the real system, they were tested with the dynamic WCDMA simulator. By doing simulations, it was ensured that the developed algorithms function as expected.

When network-planning tools were developed they were tested with the dynamic system level simulator, see [Lai01]. In [Lai01] the used simulator was the dynamic WCDMA simulator described in this thesis.

In 2002 Nokia Networks launched a new service that is based on the developed dynamic WCDMA simulator, see [Nok02]. By using the developed tool, WCDMA radio networks can be optimised before the network launch. This saves on investment and makes it possible to have better performance in the network in the very beginning of the network opening.

Yet another and very important application is the training of WCDMA engineers. Since the developed simulator models WCDMA behaviour well it can be used for educational purposes – engineers may change the parameters of a WCDMA network and can see from the simulation what is its effect on the system's performance and thus learn how the WCDMA system behaves.

Modelling of the static (W)CDMA simulator already started in 1993 by the author. The first simulation results were available shortly after that. First, the capacity of the WCDMA uplink taking benefit from multi-user detection was investigated. Next, the downlink capacity using soft handover and interference cancelling was investigated. In 1996 simulations for the WCDMA power control were made. In 1996–1999 simulation analysis for the adjacent channel interference requirements were made. This also included modelling and implementation of the adjacent channel interference to the static simulator. Late 1996 the modelling and implementation of the dynamic WCDMA simulator were started. The concept of actual value interface was created in 1996. First simulation results from the dynamic WCDMA simulator were made available in 1997. The performance of the random access, the acquisition indication channel, the handover and the compressed mode were investigated in 2001.

The author of this thesis also participated in the development of the WCDMA system at Nokia's internal projects and in the European ACTS FRAMES project and later in ETSI SMG2 (special Mobile Group 2) and in 3GPP TSG RAN WG4. Diversity random access and site selection diversity transmit concepts were developed in 1994.

1.3 List of Contributions

Research for this thesis has been conducted in the Mobile Networks laboratory at the Nokia Research Centre, Helsinki, Finland during the years 1994–2001. Part of the research results have been documented in several conference and journal papers, book chapters and patents. In addition to that, some research that has not been documented previously is shown here. This thesis gathers text from those sources into a form of monograph.

Previously presented research has been reported in the following journal and conference papers, book chapters and patents. The role of the author in contributions is described in Chapter 1.4.

1. Keurulainen, J., Häkkinen, H. and Hämäläinen, S., "Handover Method, and a Cellular System", US Pat. No. 6,198,928 B1, 6.3.2001. PCT filed 31.8.1995.
2. Häkkinen, H., Granlund, S. and Hämäläinen, S., "A Connection Establishment method, a subscriber terminal unit and a radio system", Australian patent no. 719096. Application no AU199716041 B2, 1997.02.04, Priority data: number 960541, date 06.02.1996, filed with Finland.
3. Holma, H, Hämäläinen, S. and Toskala, A., "Interference Analysis of CDMA Uplink with Hard and Soft Handovers", in the proceedings of CIC97 conference, pp. 37–41, 1997, Seoul, Korea.
4. Hämäläinen, S., Holma, H., Toskala, A. and Laukkanen, M., "Analysis of CDMA Downlink Capacity Enhancements", in proceedings of PIMRC97 conference, pp. 241–245, 1–4 September, 1997, Helsinki, Finland
5. Hämäläinen, S., Slanina, P., Hartman, M., Lappeteläinen, A., Holma, H. and Salonaho, O., "A Novel Interface Between Link and System Level Simulations", in proceedings of ACTS97 conference, pp. 599–604, 7–10 October, 1997, Aalborg, Denmark
6. Holma, H., Toskala, A., Hämäläinen, S. and Ojanperä, T., "Performance Analysis" Chapter 7, pp. 195–247 in book "Wideband CDMA for Third Generation Mobile Communications" edited by T. Ojanperä and R. Prasad. Artech House, 1998
7. Toskala, A., Holma, H. and Hämäläinen. S., "Link and System Level Performance of Multiuser Detection CDMA Uplink", Wireless Personal Communications 8, pp. 301–320, 1998
8. Hämäläinen, S., Holma, H, Sipilä, K., "Advanced WCDMA Radio Network Simulator", in proceedings of PIMRC99 conference, pp. 951–955, 19–22 September, 1999, Osaka, Japan
9. Rinne, M., Hämäläinen, S and Lilja, H., "Effects of Adjacent Channel Interference on WCDMA Capacity", in proceedings of ICT99 conference, pp. 127–132, 1999 Cheju, Korea
10. Hämäläinen, S., Lilja, H and Hämäläinen, A., "WCDMA Adjacent Channel Interference Requirements", in proceedings of VTC99fall conference, pp. 2591–2595, 19–22 May, 1999, Amsterdam, Netherlands

11. "Multi-operator Interference", Chapter 8.5, pp. 180–186 in book "WCDMA for UMTS" edited by H. Holma and A. Toskala. John Wiley & Sons, Ltd. 2000.
12. Henttonen, T. and Hämäläinen, S., "Network Effects of WCDMA Random Access and Acquisition Procedures", in proceedings of CIC2001 conference, 30 October – 2 November, 2001, Seoul, Korea
13. Korpela, S., Hämäläinen, S., "Comparison of Narrow Band and Wide Band SIR Based Handover Criteria in WCDMA", in proceedings of CIC2001 conference, 30 October – 2 November, 2001, Seoul, Korea
14. Hämäläinen, S. and Henttonen, T., "Comparison of Filtering and Reporting Schemes for WCDMA Handover", in Proceedings of ICT2002 conference, pp. 178–182, 23–26 June, 2002, Beijing, China
15. Hämäläinen, S., "High Speed Packet Access in WCDMA", in proceedings of CIC2001 conference, 30 October – 2 November, 2001, Seoul, Korea, Invited paper to technical session
16. Hämäläinen, S., Henttonen, T., Numminen, J. and Vikstedt, J., "Network Effects of WCDMA Compressed Mode", submitted to VTC2003 spring conference, Cheju, Korea

This thesis is organized as follows. First the system simulation principles and the developed static and dynamic simulators are described in Chapter 2. This includes the description of UMTS30.03 propagation, traffic and mobility models. In addition, the simulated environments have been presented. The interface between the link and the system level has been introduced. Division between the static and dynamic simulation methods have been discussed. It is shown that there are certain needs and restrictions with the dynamic system level simulations as well as with the static system level simulations. The description of the implemented simulators includes a description of the signal reception in the base stations and the mobile stations, the modelling of the most crucial radio resource management algorithms such as power control and handovers and fundamental WCDMA receiver models. The modelling of the RAKE receiver, RAKE allocation, maximal ratio combining, orthogonal codes and multi-user detection has been given.

In Chapter 3, the WCDMA radio network capacity is discussed. The simulation results are shown for the MUD (Multi-User Detection) uplink and for the downlink using orthogonal codes. Performance gain due to the MUD and soft handover has been discussed. In addition, capacity issues related to the WCDMA adjacent channel interference performance have been evaluated by the means of a system simulation.

In Chapter 4, the WCDMA radio resource management algorithms performance is discussed. The network capacity effects of power control, random access, acquisition, handover and compressed mode are shown. It has been shown that the un-ideal performances of the above-mentioned algorithms have their effects on the system performance. The reasons for the performance effects are discussed. In addition, the developed diversity random access and site selection transmit diversity methods are presented.

In Chapter 5, a High Speed Downlink Packet Access has been evaluated by means of simulation. It has been shown that the HSDPA provides high capacity and is robust against system impairments.

Finally, the conclusions are drawn in Chapter 6. In addition, future work is discussed in Chapter 6.

1.4 The Role of the Author

The author of the thesis has been working as a team member of a research team and as a project manager of a research team. The author of this thesis has been doing modelling of simulators, the implementation of simulators, planning simulation cases, running simulations and analysing simulation results. In the following, the role of the author is depicted chapter by chapter.

In Chapter 2 the author of this thesis created the concept of AVI (Actual Value Interface). He was also the leader of the research team that created the presented dynamic simulator. The static simulator was created by the author. The author mainly created the modelling principles of both simulators.

In Chapter 3, the author of this thesis made most of the simulator modelling and implementation. The author was responsible for planning and analysing system level simulations. The author also executed most of the simulations.

In Chapter 4, the author of this thesis made most of the simulator modelling and participated in simulator implementation in a smaller role. The author had the main responsibility of planning and analysing simulations.

In Chapter 5, the author of this thesis made the first model for HSDPA and gave guidance for the simulations. The author of this thesis also participated in the simulation results analysis in a smaller role.

In Chapter 4.2 the diversity random access method is presented. The author of this thesis was the first who presented the diversity random access principle.

In Chapter 4.6 SSDT (Site Selection Diversity Transmit) concept is presented. The author of this thesis contributed to the development of the SSDT concept by proposing the addition of signalling to the method first developed by the co-authors.

1.5 Related Work

The interface between the link and the system level simulations has been discussed in [Mal95, Wig96, Olo97, Eng99]. In [Mal95] an interface has been given which does not include a multipath propagation model in the system level simulator. In [Wig96] an actual value interface is shown for a GSM system using frequency hopping. [Wig96] suggests separate look-up tables for different mobile station speeds and interference scenarios. In [Olo97] an actual value interface has been shown, using raw BER (Bit Error Ratio) deviation in addition to mean in mapping from raw BER to FER (Frame Error Ratio). In [Eng99] an actual value interface with a two-step lookup procedure for WCDMA has been given and analysed.

In [Ari91, Ari92, Lab96, Ben98, Akh99, Eng99, Chh99, Wac99a, Kwo99, Dzi99, Gio00, Neu00, Pin00, Lai00a, Car00, Lai01, Hop01, Tri01, Tig01, Zha01a, Zha01b] system level radio network simulators and network planning tools are presented for WCDMA, IS-95/cdma2000 and for CDMA in general. In [Zha01a, Zha01b] WCDMA capacity analysis and static simulation tools are presented for both uplink and downlink. In [Ari91, Ari92, Gio00] static simulators and in [Eng99] a dynamic simulator used with power control studies are presented. In [Chh99] a dynamic simulator has been used when comparing handover algorithms. In [Lab96] a dynamic IS-95 radio network simulator is presented and the simulation results compared with the field results. In [Akh99, Pin00, Tri01] dynamic simulators using the model given in [UMTS30.03] are described. In [Hop01] a dynamic simulator for network planning is presented. In [Ben98] simulation tools to analyse WCDMA has been presented. For system level studies a static simulator has been presented. In [Wac99a, Lai00a, Car00, Tig01] static simulators for network planning purposes are discussed. In [Kwo99] a static simulator is used to evaluate the capacity effect due to adjacent channel interference. A static simulator that combines the analytical capacity evaluation with simulation has been presented in [Dzi99]. The size of the simulation area to be used with static simulations has been evaluated in [Neu00]. The accuracy of the simulation results of static and dynamic tools is discussed in [Lai01].

In [Gil91, Mil92, Sha92, Jal93a, Jal93b, Jan93, Vit93a, Vit93b, Sha94, Bur94, Jan94, Jal94, Jan95a, Jan95b, Man95, Lau95, Due95, Sol96, Hua96, Vem96, Yan97, Sam97b, Jal97, Wu97, Tam97a, Tam97b, Sch98, Moh99, Ism00, Cas00, Lee00, Lee01a, Lee01b, Wib01, Kim01b] CDMA performance has been analysed. In [Gil91, Mil92] analysis for the CDMA uplink and downlink capacity is given. Performance with different bandwidths is investigated in [Jal94]. In [Sol96] CDMA capacity is investigated by taking the power control error and soft handover into account. Capacity effect of power control is discussed in [Tam97a, Tam97b]. In [Jan93, Jan94, Jan95b, Sol96, Wib01, Kim01b] performance in presence of imperfect power control and sectorisation is treated. In [Jan95a] performance in the downlink is analysed by using measured channels. Performance in the fading channel has been investigated for the uplink and downlink in [Jal97] and [Moh99], respectively. According to [Yan97] the downlink capacity increases 3-fold when orthogonality becomes ideal. In [Jal93a] the importance of downlink power control for the downlink capacity has been studied. It has been shown that fast power control is needed, if a high number of multipath components is not available. Based on [Jal93b] it can be seen that the uplink is not very sensitive to the number of antennas and large bandwidth offers gains from statistical multiplexing. According to [Jal93a, Jal93b, Ism00] capacity is remarkably reduced when the propagation exponent is decreased. The same can also be seen in [Lau95] where the effect of the propagation exponent and the number of surrounding cell tiers and the number of users are investigated. In [Lee00, Lee01a, Lee01b] simulation for the capacity effects due to the different propagation environment, pathloss exponent, downlink orthogonality, noise floor, sectorisation, handover threshold and power control step has been analysed for both uplink and downlink. In [Sch98]

the maximum uplink capacity per km^2 is calculated. Performance of a power controlled and coded CDMA uplink is discussed in [Vit93a]. In [Vit93b] the Erlang capacity of the CDMA uplink is analysed. Analysis is based on the Erlang-B formula that has been replaced by the condition that the noise rise exceeds 10 dB with 1 % probability. In [Man95, Sam97b] the Erlang capacity for the variable rate data is studied. In [Hua96] CDMA uplink capacity is investigated when voice and data share the same bandwidth. In [Sha92, Sha94] network planning approach for hierarchical cell structure networks is given in which the same frequency is used in both hierarchy layers. In [Wu97] the same kind of approach is selected. The analysis given for two CDMA tiers shows large capacity losses in the system. In [Cas00] an architecture is presented in which frequency re-use is used for the macro cell layer and unused frequencies in a certain area are allocated for the micro cells. In [Due95] an overview on multi-user detection schemes are given. In [Vem96] capacity of an IS-95 network with and without multi-user detection has been analysed. According to [Vem96] multi-user detection does not provide any capacity gain.

In [Wal94, Hoz99, Lai99a, Wac99b, Pie99, Jon00, Hil00a, Owe00, Lai00b, Sip00, Pin00, Deh00, Hol01, Wac01, Hei02, Sch02, Hil02, Joh02, Smi02] radio network performance of WCDMA has been analysed. In [Hoz99] the downlink performance has been evaluated. In [Pie99] the limiting transmission direction is studied. In [Lai00b] the effect of site configuration, in [Wac99b] the effect of sectorisation and in [Lai99a] the effect of a subscriber profile to the capacity has been analysed. In [Jon00, Owe00] WCDMA capacity and coverage has been analysed with a simple static simulator. In [Pin00] a dynamic system simulator has been used to evaluate capacity and soft blocking in the system. WCDMA downlink capacity estimation has been investigated in [Sip00, Hil00a]. WCDMA downlink coverage estimation is studied in [Hil02]. In [Hol01] WCDMA capacity has been analysed with simulations and measurements with a WCDMA experimental system. In [Wac01, Hei02, Sch02, Joh02, Smi02] capacity effects of adjacent channel interference has been analysed. Interference between narrow band second-generation systems and WCDMA is discussed in [Smi02, Hei02]. Hierarchical cell structure for WCDMA in which cell layers use different frequencies is discussed in [Joh02]. In [Wac01] two WCDMA operators operate the same type of networks on adjacent frequencies. Network planning of WCDMA has been discussed in [Wal94, Deh00].

IS-95/cdma2000 capacity and comparison with WCDMA has been discussed in [Pad94, Jal98a, Jal98b, Jal00, Sar00, Mac00, Gho00, Sar01, Jun01, Luu01, Est02, Ren02, Bi02]. The performance of the IS-95 uplink has been discussed in [Pad94] and the capacity of cdma2000 in [Sar00, Sar01]. Coverage and capacity of cdma2000 has been discussed in [Jun01]. The downlink performance of multi-carrier cdma2000 and WCDMA systems has been compared in [Jal98a, Jal98b, Mac00]. From the simulation analysis it was observed that two systems have almost equivalent performance. The performance of cdma2000 1xEV-DO (1x Evolution- Data Only) has been analysed in [Jal00, Est02, Bi02]. The performance of 1xEV-DV (1x Evolution –

Data and Voice) is given [Gho00, Luu01]. In [Ren02] the performance of HDR (High Data Rate, same as 1xEV-DO) and 1xEV-DV has been compared.

In [Bai94] CODIT system and in [Nik98] FRAMES system has been presented. In [Bai94 and Nik98] also the power control, random access and other radio resource management of those systems has been presented.

CDMA power control has been studied in [Lee91, Cha91, Sol92, Dia92, Gej92a, Gej92b, Zan92, Wan93, Ari93, Sim93, Ari94, Zan94, Vit94a, Yun94, Lin94, Zor94, Yun95, Sam95, Sam97a, Mor97, Son98, Dar98, Wu99, Sip99a, Sip99b, Bak00, Chu00, Qiu00, Lin00b, Hig00, Tra01, Wen01, Hol01, Sam01, Jes01, Kim01b, Gun01, Att02]. Optimum and theoretical power control algorithms have been investigated in [Zan92, Zan94, Lin94, Wu99, Wen01]. WCDMA uplink and downlink power control has been described in [Bak00]. In [Chu00] cdma2000 power control algorithms and performance simulations for them has been given. In [Lee91] nth-power-of-distance power control for CDMA downlink power control is presented and further analysed in [Gej92a, Gej92b, Wan93, Zor94]. Improvement to the IS-95 downlink slow closed loop power control has been given in [Son98]. In [Dar98] a downlink power control algorithm for soft handover situation is presented in which allocated power levels in different base station involved in soft handover is allocated. In [Lin00b] IS-95 uplink power control under soft handover has been analysed. Effects to the CDMA uplink closed loop power control due to a fading channel has been investigated in [Cha91, Dia92, Ari93, Ari94]. In [Cha91] also effects due to the power control rate and delay has been investigated. In [Sim93] the uplink power control together with coding and interleaving has been investigated. In [Hig00] the uplink power control with coherent RAKE combining has been investigated through experiments. Performance of WCDMA SIR (Signal-to-Interference Ratio)-based closed loop power control for the uplink has been discussed in [Kim01b, Gun01]. In [Hol01] the performance of WCDMA uplink power control has been measured using the trial system and compared to the simulations. The effect of mobile stations speed, multipath diversity and antenna diversity has been analysed. Uplink power control effects such as an increase in the average power due to a fading channel and fast power closed loop power control has been discussed in [Sip99a, Sip99b]. In [Sip99a] theoretical analysis, simulations and measurements are shown. In [Sip99b] the soft handover impact to a power increase is studied. CDMA uplink open loop power control has been studied in [Sol92]. Open loop power control is useful to combat against sudden changes in pathloss. In [Yun94, Yun95, Sam95, Mor97, Qiu00, Tra01] power control algorithm for variable quality of service has been presented. The purpose of the algorithm is to minimize transmission power while the quality of service is maintained separately for each service class. Intra-cell and inter-cell interference in power controlled CDMA has been investigated in [Vit94a]. A well-known outer loop power control algorithm is presented in [Sam97a]. In [Att02] outer loop power control for 1xEV-DO is discussed. SIR estimation methods have been discussed in [Sam01, Jes01, Kim01b]. SIR estimation is needed with closed loop power control, which compares the target SIR value to SIR estimate.

Random access has been discussed in [Esm97, Kha98, Lim99, Fra99, Sch99, Sch01, Lin00a, Cho01, Vuk01, Shi01, Coo02]. Slotted-Aloha based random access methods for WCDMA have been discussed in [Esm97, Lim99, Fra99, Sch99]. WCDMA random access performance has been further analysed in [Lin00a, Cho01, Vuk01, Coo02]. It has been shown that WCDMA random access that is slotted-Aloha type scheme with fast acquisition indication performs better than the pure slotted-Aloha scheme. The advantage comes mainly from the fact that the long message part and the short preamble parts are separated. The performance and implementation of acquisition is investigated in [Sch99, Sch01]. The performance of common channel packet access has been discussed in [Kha98]. Common channel packet access in the uplink is based on the random access method of WCDMA. In [Shi01] 1xEV with IS-95 type access channel that is based on pure slotted-ALOHA method and WCDMA random access with separate preamble and message part has been compared. According to [Shi01] WCDMA random access is better than IS-95 type access in terms of throughput and channel occupancy. The advantage of IS-95 type access method is that it is backwards compatible to the existing IS-95 systems.

Handover have been discussed in [Mur91, Chi91, Gud91b, Gri91, Hol92, Aus93, Vij93a, Vij93b, Aus94, Zha94, Kum94, Sam94, And94, Vit94b, Sei94, Cho95, Reg95, Hol95, Zha96, Gor96, Won97, Lin97, Yan97, Lee98, Zha98, Jug99, Wor99, Lai99b, Yan00a, Yan00b, Nag00, Lin00b, Ucr01, Ber00]. In [Mur91] a method with two different filtering lengths and hysteresis values was proposed so that handover would work well in both micro- and macro-cell environments. In [Chi91] the conventional backward handover is proposed to be used in the macro-cell environment where timing of the handover is less critical and faster forward handover in micro-cells where rapid signal loss due to corner effects may cause sudden deterioration in the signal level and increase in the interference level. In [Gri91] mobile assisted handover algorithm in micro-cellular environment has been investigated. To solve the trade-off between long filtering that causes the delays in handover execution and short filtering that may lead to ping-ponging, adaptive filtering has been proposed in [Hol92, Hol95]. A method in which the averaging length of handover measurements is determined from signal amplitude deviation was proposed. In [Aus93, Aus94] a method in which the sampling window is adjusted based on a velocity estimation has been proposed. In [Gud91b] a simple analytical model for handover analysis is presented in which probability for handover, false handover and call drop due to the handover can be evaluated. In [Vij93a] a model for handover analyses has been given. The model assumes field strength measurements and is based on the Poisson model for the level crossing. The developed model is used to analyse handover algorithm sensitivity in [Vij93b]. The model given in [Vij93a] is further developed for evaluating handover algorithms based on both absolute and relative measurements [Zha94, Zha96], handover algorithms using both BER and relative signal strength measurements [Kum94] and handover algorithm in which a handover filtering window and hysteresis are set based on shadowing parameters [Sam94]. Soft handover coverage and capacity advantages have been discussed in [Vit94b,

Cho95, Reg95]. It has been shown that soft handover improves the coverage 2 to 2.5 times and capacity more than 2 times. Network performance effects of the handover delays due to synchronization, execution, measurement error and control rate have been studied in [And94]. In [Gor96] soft handover benefits has been evaluated. It was noted that increased soft handover area also increases the capacity that has to be served through a base station. In [Nag00] the blocking effect caused by the increased load due to soft handover has been analysed. In [Sei94] optimal size for the soft handover area is proposed. The optimum is reached when the same error probability is achieved for both transmission directions. Soft handover, its benefits and drawbacks and handover parameter optimisation has been discussed in [Won97]. According to [Lin97, Lin00b] multiple links under soft handover are negatively correlated, since power control commands from the strongest link dictate the power control. In [Lee98] it has been shown that soft handover causes slight capacity loss in the downlink due to the increased number of transmissions. However, in [Ucr01] capacity loss is claimed to be substantial 13–25 %. The gain from softer handover is roughly 2.9 in the uplink and the downlink if compared to non-sectorized case [Lee98]. In [Jug99] it has been shown that soft handover and mobility reduce sectorisation gain. Adaptive adding and dropping thresholds are discussed in [Wor99, Yan00a, Yan00b]. Adaptive thresholds decrease call blocking and outage and help to balance traffic between cells. Analysis and simulations for CDMA handover algorithm are shown in [Zha98]. In [Lai99b] different CDMA handover algorithms has been compared by using measurement data. In [Yan97, Ber00] the impact of various design parameters to the CDMA performance has been evaluated including the handover drop and add thresholds.

WCDMA handover has been discussed in [Mih99, Luo00, Akh00, Bin00, Hil00b, Sta01, Kim01a, Gra01, Yin02a, Fla02]. In [Mih99] handover effects on the downlink SIR is compared when hard and soft handovers are used and the handover margin is varied. The effects of handover delays caused by timers are investigated in [Luo00, Kim01a]. When delay is increased mean and variance between handover occurrences increase. Too long a timer also worsens the BER and increases interference. In addition, in [Kim01a] the effects due to handover margins and thresholds are studied. According to [Akh00] SIR-based handover reduces uplink transmission power and interference as the mobile station connects to the base station that provides the best SIR. In [Bin00] coverage effect due to soft handover are investigated. It was noticed that additional interference in the downlink decreases capacity. In addition, loading has its impact to macro diversity gain in the downlink. Event and periodic handovers are compared in [Hil00b]. According to [Hil00b] periodic reporting performs better than event-triggered reporting. In [Sta01] 3dB gain from soft handover is demonstrated. In [Gra01] a new power control algorithm used together with soft handover in presented. The given algorithm is based on soft symbols, when reliability from the power control commands from several base stations is combined. In [Yin02a] the received signal code power based and narrow band SIR based measurements are compared for inter-frequency handover. It is

shown that narrow band SIR based inter-frequency handover triggers more handovers and performs worse. In [Fla02] the cost function approach to optimise window add of WCDMA handover algorithm is proposed and studied.

The compressed mode has been discussed in [Gus97, Yin02b]. In [Gus97] compressed mode principles and simulation results for different compressed mode options has been presented. In [Yin02b] event-triggered and periodic entrance to the compressed mode and their capacity effects has been investigated.

A high speed downlink packet access has been discussed in [Fre01, Das01, Lov01, Par01, Mou01, Lov02, Kol02, Hor02, Fre02]. HSDPA has been introduced in [Par01]. In [Fre01, Das01, Lov02, Fre02] HARQ (Hybrid Automatic Repeat reQuest) methods are analysed and compared for HSDPA. Performance of the HSDPA network is discussed in [Lov01, Mou01, Kol02]. In [Hor02] interference cancellation together with HSDPA has been discussed.

Site Selection Diversity Transmit has been presented and analysed in [Fur00, Akh01, Tak01, Mor01, Wan01]. In [Fur00] SSDT concept and analysis of its advantages are given. Downlink performance with generalized RAKE reception is investigated in [Wan01]. It has been noticed that SSDT gives optimal performance as it minimizes interference. In [Akh01] SSDT is compared together with the power drift algorithm. It is proposed to use the hybrid algorithm in which the power drift algorithm is used for high loading and SSDT for low loading. In [Tak01] enhancement to the basic SSDT algorithm has been proposed in which several base stations can be active instead of only a single one. In [Mor01] a method is presented in which base stations are not shut down, but their transmission power is reduced.

In [Rao99, Ben00, Qua01, Gho01] cdmaOne and its evolution 1x, 1xEV and 1xEV-DO and 1xEV-DV have been presented. In [Ete01] cdma2000 enhanced random access and reservation schemes such as diversity random access discussed in Chapter 4.2.2 are presented.

2 MODELLING OF WCDMA SYSTEM SIMULATORS

A single simulator approach would be the preferred solution for air interface simulations. However, such simulator would require modelling of a single radio link with modulation waveforms, coding/decoding, spreading/ despreading and other transmitter/receiver algorithms, modelling for a radio network with a multitude of base stations and a high number of mobile stations generating traffic and interference and transmitting signals, and modelling for the protocols. Computational power required by such a simulator would be massive. Thus, the simulator has to be divided into smaller parts each specialized to their specific tasks. A practical division of a simulation is link level simulation, radio network level simulation and protocol level simulation. For link and protocol level simulations commercial platforms exist, such as CCSS (CoCentric System Studio) [CCSS] and SPW (Signal Processing Worksystem) [SPW] for the link level and OPNET Modeler [OPNET] for the protocol simulations. OPNET Modeler also offers a platform for system simulations. However, this platform is limited and is not suitable for full-range system simulations with a time-driven approach and detailed modelling of WCDMA radio and radio resource management algorithms.

System simulation involves several characters that are modelled and implemented to the simulator: traffic models, mobility models, propagation models, antennas, multipath environment, map data, multiple access dependent modelling and modelling of RRM (Radio Resource Management) algorithms. A simulator may employ all the above models or a sub-set of them.

A radio network simulator can be static or dynamic. A static simulator refers to a simple simulator with no mobility or traffic models, while a dynamic simulator is a simulator with detailed level modelling for a network's dynamic behaviour.

Static simulator is a simplified simulator employing a simple map that is usually hexagonal or Manhattan layout, propagation model, simple model for multiple access and a very limited set of radio resource management algorithms. In a static simulator only snap-shots are taken from the network. Static simulators can be used when rough and fast estimates are needed.

Dynamic system simulator is a complex simulator, employing map data (Manhattan, Hexagonal or real maps), propagation model, multipath model, antennas, detailed modelling for the multiple access, traffic model, mobility model and a comprehensive set of radio resource management algorithms with realistic modelling. In a dynamic simulation users move in the simulated area, establishing calls, transmitting a signal to the receiver and performing handovers and other radio resource management tasks. The output of the simulation is a high number of numeric data, e.g. a number of bad quality and dropped calls, noise rise in the base station, transmission power of the base station and the mobile station and other outputs that can be useful when developing radio resource management algorithms and network planning methods.

The usage of radio network level simulators is diverse. Simulators can be used to compare different technologies as was done in 1997 when ETSI evaluated technical solutions and selected the air interface solution for UMTS (see [UMTS30.06]), specify parameters in radio specifications such as power amplifier requirements (see Chapter 3.3), do research for radio resource management algorithms (see Chapter 4), support radio network planning (see [Lai01]) and optimise the operators' network (see [Nok02]).

2.1 Static and Dynamic Radio Network Simulations

Both, static and dynamic simulations are needed. Both methods have their pros and cons, and one cannot replace another. The advantage of static simulators is a very short simulation time if compared to dynamic tools. The advantage of dynamic tools is very accurate modelling of the WCDMA air interface. The problem for dynamic simulation is the long calculation time due to high complexity.

Even though static tools do not model the radio interface and its procedures in detail they are accurate enough to provide information needed for example for network planning purposes. Since static tools are very lightweight, simulations with high numbers of base stations and mobile stations can be made in a reasonable time. In [Lai01] the accuracy of static simulation tools has been analysed and compared to that of dynamic tools. It was shown that even though some differences in results exist, accuracy of static simulator is sufficient.

Dynamic simulation tools, however, are needed when the effects due to dynamic behaviour in the network is studied. Static tools lack the possibility to investigate interference changes due to the dynamic nature of the network that is due to for example user mobility and user traffic. Dynamic tools that model in detail RRM algorithms are able to pinpoint the problems caused by the dynamics of the network. For example, as discussed in Chapter 4.4, a simulator with a detailed modelling for handover algorithms with imperfections can be used to show the possible problems caused by user movement.

The WCDMA radio network planning uses a more simple interference and dynamical modelling than the dynamic WCDMA simulator presented here but the network planning tools can be calibrated with the simulator. It is clear that any simulation tools need to be verified by real measurements from the WCDMA test network.

2.2 Interface Between Link and System Level Simulation

For an accurate receiver performance evaluation a chip level or a symbol level simulation model is needed, i.e. at least 3.84 Mcps or 15 ksps (the lowest symbol rate supported by the WCDMA physical channel) time resolution. On the other hand, in the system level the traffic models and the mobility models require simulations of at least 10-20 minutes with a large number of mobiles and base stations. Simulation with high resolution and long duration would lead to very long simulation time. Therefore, a separate link and system level simulators are needed. The link level simulators usually operate at symbol or chip level, while the dynamic system level simulators operate with the resolution determined by the feature that most often changes the interference. In WCDMA the fast closed loop power control operating of a 1.5 kHz frequency is the algorithm which has the highest frequency, and therefore, 1.5 kHz frequency is used in the dynamic system simulator. In the static simulator a lower frequency can be used.

The link level simulator is needed to build such a model that is able to predict the receiver FER or BER performance, taking into account the channel estimation, interleaving and decoding. The system level simulator is needed to model a system with a large number of mobile terminals and base stations, and algorithms operating in such a system.

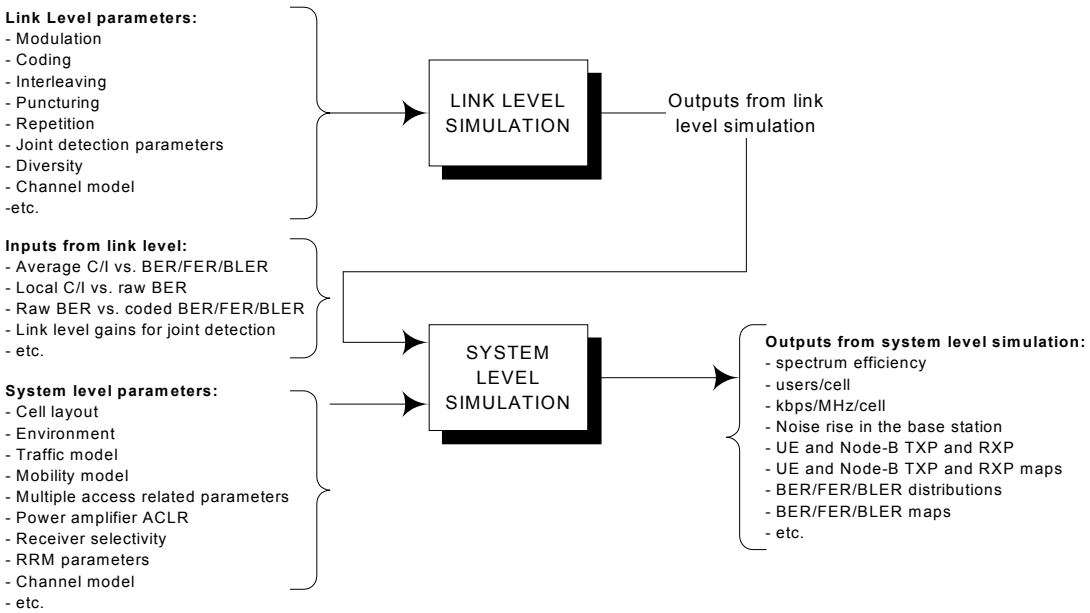

FIGURE 2.2-1. Relation of link and system level simulation.

Due to the fact that the simulation is divided into two parts, a method to interconnect the two simulators has to be defined. A system level simulation requires parameters such as C/I (Carrier-to-Interference Ratio) thresholds as input parameters. On the other hand, those parameters are outputs from the link level simulation, see FIGURE 2.2-1. However, it is not obvious in what kind of format the link level simulation outputs should be from the point of view of the system level simulator.

The conventional interface between the link and system level tools is a so-called *average value interface*. The average value interface describes the receiver BER/FER performance by average C/I, E_b/I_0 (Energy per bit to interference ratio), E_b/N_0 (Energy per bit to noise ratio), $E_b/(I_0 + N_0)$ (Energy per bit to interference and noise ratio), E_c/I_0 (Energy per chip to noise ratio) requirements. The average value interface is not accurate if there are fast changes in interference due to, e.g. high bitrate packet users. This kind of approach is suitable for static snapshot simulations, but cannot be used when simulating systems with fast power control and other algorithms having frequent impacts to interference. The new method, referred to here as *actual value interface*, is a more accurate way to do the interface between the link and the system level simulations from the point of view of 3rd generation systems. This study was originally given in [Häm97c].

2.2.1 Average Value Interface

The average value interface is widely used especially with the static snapshot simulations. The characteristics of the average value interface are link level simulations where BER is measured as a function of average C/I[6] over a long period (tens or hundreds of seconds). By doing so, the effects from multipath fading, interleaving and interference variations are taken into account according to their average characteristics. Usually the measured BER is the average value over the whole link level simulation run.

In the system level a snapshot C/I value that is produced without multipath or fast fading corresponds to the link level C/I. Link and system level C/I values can match each other if the resolution of the system level simulation is so low that the effects from interleaving and fast fading can be assumed as averaged out and if the fading, interleaving and interference characteristics are on average the same as those assumed in the link level simulations. If fast fading is included in the system level simulation, it has to be averaged over a long period before a snapshot can be taken.

The drawback of the average value interface is that the resolution of the system simulation must be in magnitude of 100 ms or more. The resolution depends on the mobile station speed, the interleaving length and the channel model. The resolution has to be sparse enough so that it can be assumed that variations are averaged out. On the other hand, packet data and fast RRM

---

[6] Note: C/I is the average value of C over the whole simulation divided by the average value of I over the simulation.

algorithms operate with the resolution of 10 ms (the shortest interleaving length) or 0.667 ms (fast closed loop power control period). This means that radio resource management algorithms whose frequency is higher than 10 Hz (100 ms) can be simulated only in the link level.

Traffic models are usually only considered in the system level. Since packet data may be very bursty (duration of data bursts incoming to the radio network may be less than 5 ms), the multiplexing gain from packet data cannot be observed if the resolution of the simulator is sparser than the resolution of the packet radio algorithm. Therefore, a very considerable phenomenon that has impacts on the system performance is ignored.

RRM and processes such as ARQ (Automatic Repeat reQuest) and fast power control run with the resolution in order of 100 Hz or higher. These processes can be taken into account only in the link level simulations if the average value interface is used. Unfortunately, these algorithms have their impacts on the interference situation of the network. Since the link level simulations are carried out only for a single link with certain interference characteristics, the effects due to the changing interference conditions in the network cannot be seen. This is another significant phenomenon that is ignored with the average value interface.

The modelling of inter- and intra-cell interference in the link level simulations is restricted to a low number of interferers due to complexity reasons. Usually inter-cell interference is assumed Gaussian. If the spreading factor is high enough and random codes are assumed, this assumption is valid based on the Central limit theorem. Intra-cell interference can also be assumed Gaussian or real interferers can be simulated. If the number of users causing interference is low (due to e.g. low spreading factors) the link level simulation cannot model the interference situation in the network properly. In this case simulation where the interference situation is considered in the system level and the link level performance comes through the actual value interface is suggested.

2.2.2 Actual Value Interface

The actual value interface is a novel way to connect link and system level simulations. In the actual value approach the link level simulation data e.g. bit errors are measured for every slot of a radio frame. The system level simulation also runs with the slot resolution. Due to slot resolution possible deinterleaving and decoding has to be taken into account in the system level simulation. Their performance, however, comes through link level inputs.

If the system level simulation is carried out with the actual value interface, fast fading has to be taken into account in addition to slow fading and pathloss. The same kind of correlated fading process is used both in the link and the system level simulations, modelled as e.g. the Rayleigh distributed process, with a certain Doppler frequency. The fading process is explained in Chapter 2.3.4.

The strength of the actual value interface, compared to the average value interface, is that all the RRM can be simulated accurately on the system level. RRM algorithms can be included to the system level simulation since the simulation resolution is as accurate as the resolution of those algorithms. The actual value interface enables possible gain or loss of power control, ARQ and link adaptation algorithms. If ARQ was simulated in the link level, the varying interference conditions in the network cannot be taken into account. Link adaptation can be simulated thoroughly only on the system level since adaptation decisions depend strongly on the changing interference conditions. If the link adaptation algorithm is fast the average value interface cannot be used.

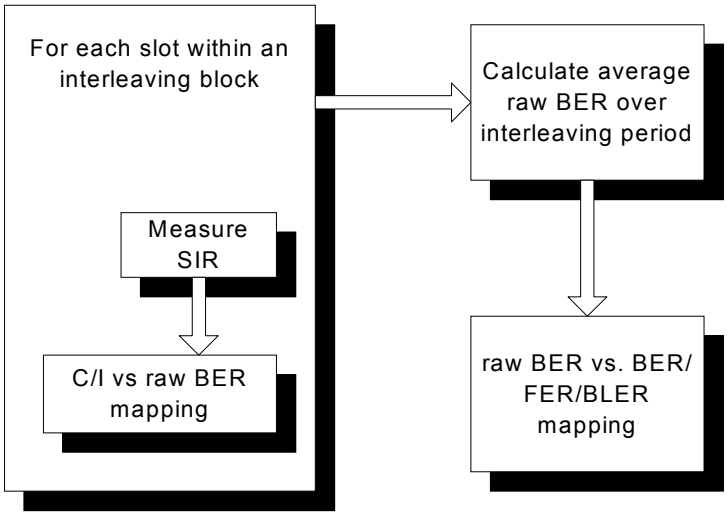

FIGURE 2.2-2. Block diagram of interface for RT (Real Time) bearers.

An example of actual value interface is shown in FIGURE 2.2-2. In the presented method, link level simulation results are collected on a slot-by-slot basis, i.e. C/I and BER values are collected for each slot and coded BER/FER values for each interleaving period. E.g. if the target service has interleaving over 15 slots, then C/I and the corresponding raw BER values (BER before decoding and deinterleaving) for 15 slots are observed directly from the fading channel and BER/FER of the coding block is measured over the interleaving period. In the system level the C/I ratio is measured for each slot within the interleaving block and is mapped to raw BER by using a raw BER vs. C/I look-up table from the link level simulation. Deinterleaving is modelled so that the average raw BER within the interleaving block is calculated. Further, decoding is modelled by mapping the deinterleaved raw BER to the coded BER/FER by using the measured mean raw BER vs. coded BER/FER look-up table.

All link level algorithms including coding, interleaving, fast power control and receiver algorithms are modelled in the link level simulation and their performance can be seen in BER/FER performance.

It should be noticed that with the actual value interface the system simulator includes fast fading and fast power control. This is needed in order to

model the interference caused by the rapidly changing output powers. The power control non-idealities are modelled in the link level. Simple ARQ schemes can be modelled in the system level and neglected in the link level. However, the combining of packets requiring soft information from demodulator must be done in the link level.

A drawback of the actual value interface is the complexity of the calculation – the actual value interface requires that the WCDMA system level simulation is running in power control slot resolution, i.e. 1500 Hz. Since all the calculation has to be done with high frequency for all the users and the base stations in the simulated system, simulations become longish.

2.3 Cellular, Traffic, Propagation and Mobility Models

2.3.1 Cellular Structures

A third generation system must be able to support a wide range of services in different radio operating environments. Different types of cells are needed for different requirements: large cells guarantee continuous coverage while small cells are necessary to achieve good spectrum efficiency and high capacity. Low mobility and high capacity terminals use small range cells, while high range cells serve high mobility and low capacity terminals. In addition, different cell types should be able to operate upon one another. The HCS (Hierarchical Cell Structure) describes a system where at least two different cell types, e.g. macro-cell and micro-cell, operate upon one another. Micro-cells are small cells covering areas of a few hundred-meter radius. Low powered base stations are typically placed at lamp post level and they serve a block of a street. Macro-cells or umbrella cells cover a radius of one kilometre or more. Macro-cells cover rural areas, provide continuous coverage also in areas, which are covered by micro-cells, and serve rapidly moving users. Pico-cells cover indoor areas with cell radius of a few dozens meters. A low power base station usually covers an office, the floor of a high building or a residence. Whenever possible, traffic should be directed to the smallest available cell, so that the system's spectral efficiency is improved. [And92]

Developed simulators offer models for macro-, micro- and pico-cell environments. Also a combination of different cell types can be used. For different types of environments different pathloss, shadowing and multipath models and parameters apply. In addition mobility models are different depending on the environment.

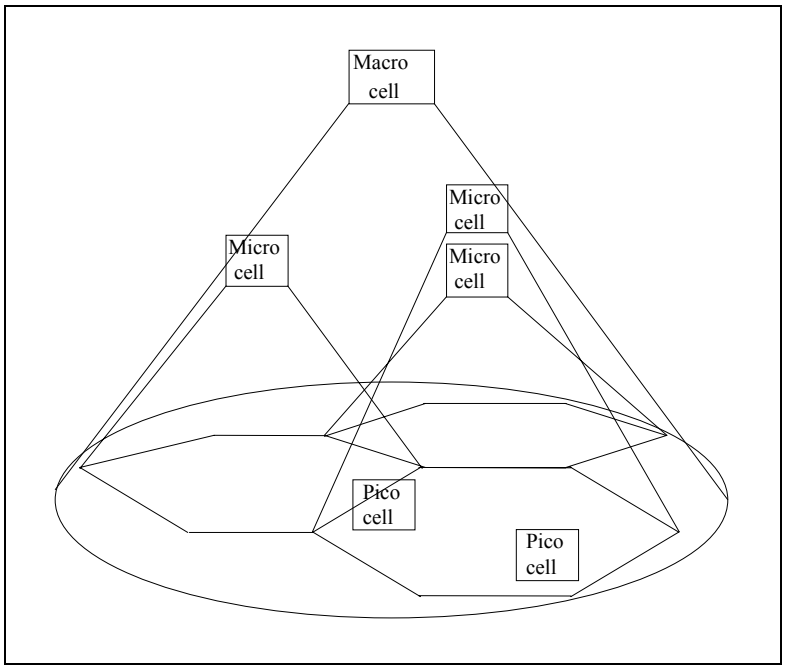

FIGURE 2.3-1. Hierarchical cell scenario.

2.3.2 Path Loss Modelling

The pathloss model used with the simulators is separately defined for indoors, Manhattan micro-cellular (outdoor-to-indoor) and macro-cellular (vehicular) environments according to [UMTS30.03]. Also, measured propagation data can be used if real maps are available, see FIGURE 2.3-3.

The indoor pathloss model in [UMTS30.03] is derived from COST[7]231 indoor model [COST231]. In indoor cells pathloss versus distance is

$$L = 37 + 30\ \mathrm{Log10}(R) + 18.3\ n((n+2)/(n+1)-0.46), \tag{2.3-1}$$

where:

R is the transmitter-receiver separation given in metres;

n is the number of floors in the path.

In Equation (2.3-1) *L* shall in no circumstances be less than free space loss.

Micro-cell model in [UMTS30.03] is called as indoor-to-outdoor model. This model considers LOS (Line-Of-Sight) and NLOS (Non-Line-Of-Sight) situations and is used in the urban Manhattan environment. The proposed model is a recursive model according to [Ber95]. The shortest path along streets between the base station and the mobile station has to be found within the Manhattan environment. The pathloss is then calculated as

---

[7] COST = European Co-Operation in the field of Scientific and Technical research

$$L = 20 \cdot \log_{10} \frac{4\pi d_n}{\lambda}, \tag{2.3-2}$$

where

d_n is the "illusory" distance,

λ is the wavelength,

n is the number of straight street segments between the BS (Base Station) and the MS (Mobile Station)

The illusory distance is the sum of these street segments and can be obtained recursively as

$$k_n = k_{n-1} + d_{n-1} \cdot c, \tag{2.3-3}$$

$$d_n = k_n \cdot s_{n-1} + d_{n-1} \tag{2.3-4}$$

In Equation (2.3-3) c is a function of the angle of the street crossing and gets the value 0.5 in case of a 90-degree street crossing. In Equation (2.3-4) s_{n-1} is the length of the last segment in metres. A segment is a straight path. The initial values for k_0 and d_0 are 1 and 0, respectively. The illusory distance is obtained as the final d_n when the last segment has been added. The model is extended to cover the micro-cell dual slope behaviour, by modifying the expression to

$$L = 20 \cdot \log_{10}\left(\frac{4\pi d_n}{\lambda} \cdot D\left(\sum_{j=1}^{n} s_{j-1}\right)\right) \tag{2.3-5}$$

where

$$D(x) = \begin{cases} x / x_{br}, x > x_{br} \\ 1, x \le x_{br} \end{cases}.$$

Before break point x_{br} the slope is 2, after the break point it increases to 4. Break point x_{br} is set to 300 m. x is the distance from the transmitter to the receiver.

To take into account the effects of propagation going above rooftops it is also needed to calculate the pathloss according to the shortest geographical distance. This is done by using the commonly known COST231 Walfish-Ikegami Model [COST231] and with antennas below rooftops

$$L = 24 + 45 \log(d + 20). \tag{2.3-6}$$

Here d is the shortest physical geographical distance from the transmitter to the receiver in meters.

The final pathloss value is the minimum between the pathloss value from the propagation through the streets and the pathloss based on the shortest geographical distance:

Pathloss = min(street pathloss, above roof-tops pathloss). (2.3-7)

In macro-cells path loss versus distance is [UMTS30.03]

$$L = 40(1-4\cdot 10^{-3}\Delta hb)Log10(R) - 18Log10(\Delta hb) + 21Log10(f) + 80 \text{ dB}, \quad (2.3\text{-}8)$$

where:

R is the base station - mobile station separation in kilometres;

f is the carrier frequency of 2000 MHz;

Δhb is the base station antenna height, in metres, measured from the average rooftop level.

The base station antenna height is fixed at 15 meters above the average rooftop (Δhb = 15 m). Considering a carrier frequency of 2000 MHz and a base station antenna height of 15 meters, Equation (2.3-8) condenses as

$$L = 128.1 + 37.6\ Log_{10}(R). \quad (2.3\text{-}9)$$

In Equation (2.3-9) *L* shall in no circumstances be less than free space loss. This model is valid for NLOS case only and describes the worst-case propagation. The path loss model is valid for a range of Δhb from 0 to 50 metres.

2.3.3 Shadowing Modelling

The transmitted signal attenuates because of pathloss, shadowing and multipath fading. The amount of the attenuation depends greatly on the environment. Obstacles, such as hills and buildings, create shadowing to radio connections. The most severe shadowing effects are in human made environment where high buildings cause steep boundaries to the signals received. Due to the fact that the shadowing process is rather slow as compared to multipath fading, it is often referred to as *slow fading*. Locally, the mean value of shadowing can be generated from a lognormal deviation. Therefore, shadowing is often called as *lognormal fading*.

The shadowing modelling is adopted from [UMTS30.03]. Shadowing is given in the logarithmic scale around the mean path loss. Shadowing is as a Gaussian distributed random variable with zero mean and STD (STandard Deviation) as an environment dependent parameter. Due to the slow fading process versus distance Δx, adjacent fading values are correlated. Its normalized autocorrelation function R(Δx) can be described with sufficient accuracy by an exponential function [Gud91a]

$$R(\Delta x) = e^{-\frac{|\Delta x|}{d_{cor}}\ln 2} \quad (2.3\text{-}10)$$

with the decorrelation length dcor, which is dependent on the environment.

The mean value for the long-term fading is 0 dB Standard deviation is a parameter. Often used value for standard deviation is 6 dB in micro-cells and 8 or 10 dB in macro-cells. In the macro-cellular environment the decorrelation length of 20 meters is selected. In the micro-cellular environment the selected decorrelation length is five metres.

For a more realistic simulation shadowing can be modelled so that the fading process is correlated between the base stations.

2.3.4 Fast Fading Modelling

Signals travelling different paths between the transmitter and the receiver arrive at the receiver at different times. The received signal strength may differ as well as its phase depending on length of the path, number of reflections and diffractions and number of penetrated walls and their parameters. At times phases are adding destructively. When that occurs, the resultant received signal gets weak. Then the signal is said to be in fade or in a fading dip. Depending on the operated environment the delay spread and the number of multipath components may differ. The *coherence bandwidth* is the maximum frequency difference for which received signals are still correlated. The coherence bandwidth is approximately inversely proportional to the delay spread and it is measured as a bandwidth where correlation is at least 3 dB (i.e. 0.5). The channel is *frequency selective* if more than one multipath component exists, otherwise channel is *flat*. If signal goes through frequency selective channel signal waveform is not retained.

The delay spread is often described with a so-called tapped-delay-line model in which for each path or tap the average relative strength and delay to the strongest path are shown; see example in FIGURE 2.3-2 and TABLE 2.3-1. Each tap of tapped-delay-line model has a certain The *Doppler spectrum* caused by the movement of the user. The *Doppler spread* is the range of values over which the Doppler spectrum is essentially non-zero. The *Coherence time* of the channel is approximately inversely proportional to the Doppler spread. In TABLE 2.3-1 "CLASSIC" Doppler spectrum corresponds to the *time selective* Rayleigh fading channel. The fading is said to be slow if the coherence time is clearly longer than the duration of symbol. If the coherence time is less than the symbol duration, the channel is said to be fast fading. Otherwise the channel fading is relatively fast [Lat98].

The WCDMA RAKE receiver (see more about RAKE receiver in Chapter 2.4.2) enables the separation of multipath components if the time difference between multipath components is at least *1 / chip rate* (0.26 μs in case of 3.84 Mcps). When different paths are summed coherently together, so-called micro-diversity is gained that attenuates fading and improves received signal quality. If signals are summed together non-coherently, as happens inherently in the case of narrow band systems, product signal remains Rayleigh distributed. In an outdoor environment the amplitude of the received signal is typically a Rayleigh distributed value. In indoor environment amplitude can be often

modelled as a Rician distributed variable due to line-of-sight component between the transmitter and the receiver.

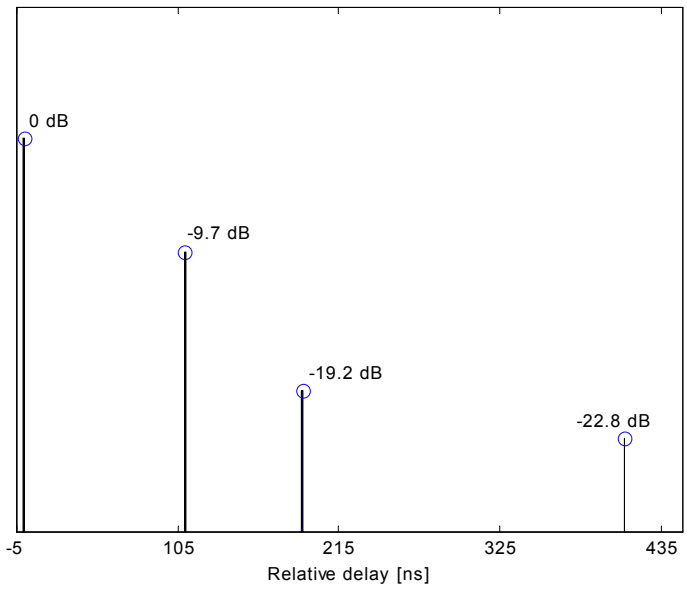

FIGURE 2.3-2. An example of tapped-delay-line model for ETSI indoor-to-outdoor A model [UMTS30.03].

In order to properly support the studies of RRM, the multipath propagation environment is modelled on the simulator. The number of multipaths, their path gains and fading processes can be obtained from channel models such as ATDMA [Str93], CODIT [Jim94] or ITU [Xia97]. The Rayleigh distributed fading process is generated by using the Jakes model [Jak74]. Parameters for the used channel models are given in Appendix A.

TABLE 2.3-1. ETSI Outdoor-to-Indoor and Pedestrian Test Environment Tapped-Delay-Line parameters [UMTS30.03].

Tap	Channel A		Channel B		Doppler Spectrum
	Rel. Delay (nsec)	Avg. Power (dB)	Rel. Delay (nsec)	Avg. Power (dB)	
1	0	0	0	0	CLASSIC
2	110	-9.7	200	-0.9	CLASSIC
3	190	-19.2	800	-4.9	CLASSIC
4	410	-22.8	1200	-8.0	CLASSIC
5	-	-	2300	-7.8	CLASSIC
6	-	-	3700	-23.9	CLASSIC

2.3.5 Real Propagation Maps

In [UMTS30.03] cellular models are regular hexagonal models for a macro-cellular environment and the Manhattan model with equal size house blocks

and streets with a micro-cellular environment. In the simulator real maps can be used in addition to UMTS30.03 models. Then the propagation data is generated by other tools, e.g. by Ray tracing, or by measurements, and imported to the simulator. An example of a real map from Helsinki City is shown in FIGURE 2.3-3. The propagation data is obtained from a network planning tool by using ray tracing, and it is verified by measurements.

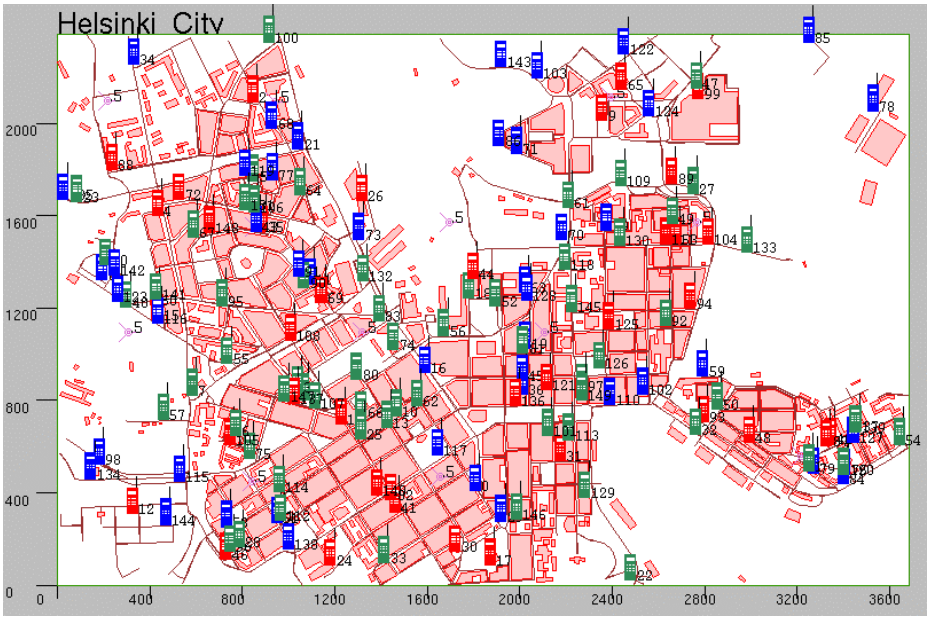

FIGURE 2.3-3. An example of a real map used with simulations. The simulated scenario is a multi service scenario. The colour of the mobile station indicates the used service (speech, circuit switched or packet data).

2.3.6 Antenna

For every sector of each base station sector specific antenna patterns are defined. Both horizontal and vertical patterns are considered. The antenna pattern is given as a matrix where antenna gain is given as a function of angle from the main bearing, see FIGURE 2.3-4. The resolution of the matrix can be for example 1 radius. When pathloss between a base station and a mobile station is calculated, horizontal and vertical angles are first defined. The measured angle is mapped for antenna gain by using separately defined look-up tables. Finally, the pathloss that is calculated assuming the isotropic antenna is multiplied by the defined antenna gain. In FIGURE 2.3-4 an example of antenna pattern is given.

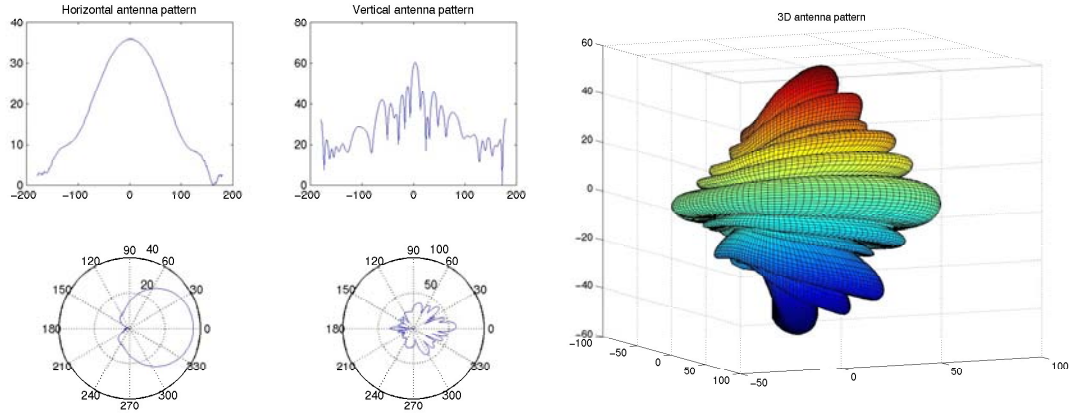

FIGURE 2.3-4. An example of antenna pattern.

2.3.7 Traffic Modelling

In dynamic simulations the users make calls and transmit the data according to the traffic models. The call generation process for real time services, such as speech and video, is made according to a Poisson process [UMTS30.03]. For speech, voice activity and discontinuous transmission have to be considered. The speech traffic model is an on-off model, with activity and silent periods being generated by an exponential distribution. The mean value for active and silent periods are equal to 3 seconds and independent on the uplink and downlink. For circuit switched data services, the traffic model is a constant bitrate model, with 100 % of activity.

FIGURE 2.3-5 depicts a typical WWW (World Wide Web) -browsing session [UMTS30.03]. A session consists of a sequence of packet calls that can be considered as web page downloading. The bursty nature of the fixed network is modelled by assuming that one packet call constitutes several packets arriving to the network. A packet service session contains one or several packet calls depending on the application. After the page is entirely downloaded to the terminal, the user spends a certain amount of time studying the information. This time interval is called reading time. If FTP (File Transfer Protocol) type service is simulated, it is assumed that there is only one packet call per session.

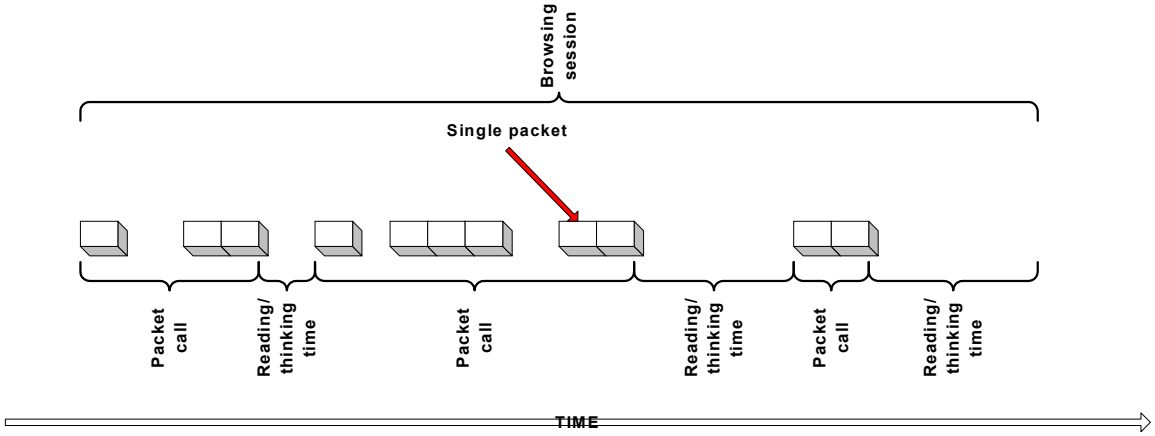

FIGURE 2.3-5. World Wide Web traffic characteristic [UMTS30.03].

The session arrival process is a Poisson process. The number of packet calls within a session as well as the length of the reading time is generated randomly from geometric distribution. The number of individual packets within a packet call and interval between two consecutive packets is also set randomly according to the geometric distribution. The size of the packet is generated according to the Pareto distribution with cut-off. Cut-off is needed to limit the highest sizes so that the simulation can converge. Parameters for distributions are given as simulation parameters. In TABLE 2.3-2 parameters for different types of packet sessions are given. [UMTS30.03]

The simulator supports mixed traffic scenarios where speech users together with packet data users are simulated. For example, the speech load can be set to a certain number of Erlangs and the remaining capacity can be allocated for the best effort packet data. Then packet data throughput and delay can be studied.

TABLE 2.3-2. Characteristics of packet data connections, UDD (Undefined Delay Data) service [UMTS30.03].

Packet based information types	Average number of packet calls within a session	Average reading time between packet calls [s]	Average amount of packets within a packet call []	Average interarrival time between packets [s][8]
WWW surfing, UDD 8 kbit/s	5	412	25	0.5
WWW surfing, UDD 32 kbit/s	5	412	25	0.125
WWW surfing, UDD 64 kbit/s	5	412	25	0.0625
WWW surfing, UDD 144 kbit/s	5	412	25	0.0277
WWW surfing, UDD 384 kbit/s	5	412	25	0.0104
WWW surfing, UDD 2048 kbit/s	5	412	25	0.00195

2.3.8 Mobility Modelling

In a dynamic simulator users move in the simulation area according to the mobility model. In [UMTS30.03] separate mobility models are developed for indoor pico-, outdoor micro- and outdoor macro-cellular environments.

When new users are generated in the macro-cell simulation they are uniformly distributed over the simulation area. The direction to which a new user is moving is randomly selected when the mobile station entity is created. The direction of movement is updated according to the decorrelation length and direction can be changed at each position update according to a given probability. [UMTS30.03]

---

[8] The different interarrival times correspond to average bit rates of 8, 32, 64, 144, 384 and 2048 kbit/s.

The micro-cell model is made for an environment in which mobile stations move in a street net. Such environments are micro-cellular Manhattan environment and the environment with a real map. In such a structure, mobiles move along streets and may turn at street crossings with a given probability. The turning probability is illustrated in FIGURE 2.3-6. Mobiles are uniformly distributed in the streets and their direction is randomly chosen at the initialisation. [UMTS30.03]

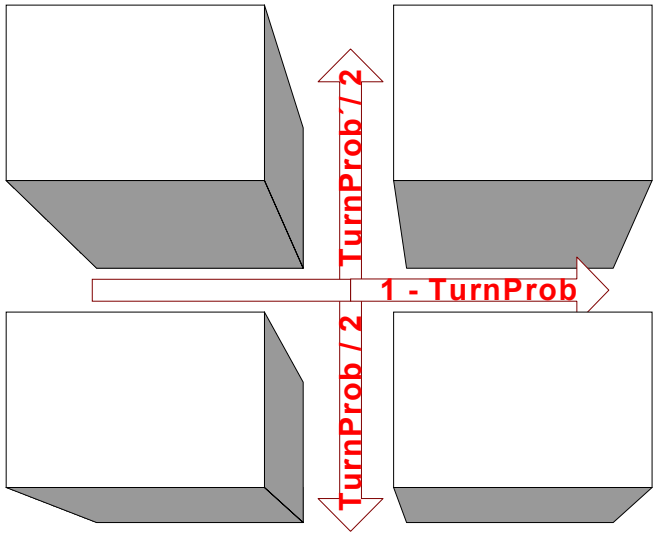

FIGURE 2.3-6. Turning probability when the mobile station enters to a street crossing [UMTS30.03].

The indoor mobility model models user mobility in an office building. Mobile stations are either stationary or moving with a constant speed from an office room to a corridor or vice versa. Time duration that a mobile station spends in the stationary state is drawn from the geometric distribution. Different mean values are assumed depending on whether the mobile station is in an office room or in the corridor. If a mobile station is in an office room, it has a higher probability to be stationary. The transition from the moving state to the stationary state takes place when the mobile station reaches its destination. [UMTS30.03]

When a mobile station is in an office room and it is switched to the moving state it starts to move into the corridor. First the destination co-ordinates in the corridor are selected with uniform distribution. Each place in the corridor has equal probability to become the destination point. Then the mobile station starts to move from its current location to the destination location so that first the vertical (y) co-ordinate is matched with the new co-ordinate and next the horizontal co-ordinate is matched to the destination co-ordinate. The speed is constant during the movement. When the mobile station reaches the destination point it is transferred into the stationary state. It is assumed that the door dividing each office room and corridor is as wide as the office room itself. [UMTS30.03]

When a mobile station is in a corridor and it is switched to the moving state it moves to any of the office rooms with equal probability. First the destination office room is selected by using discrete uniform distribution. Then the destination co-ordinates are selected with uniform distribution. Each place in an office room has equal probability to become the destination point. The mobile station moves from its current location so that first the horizontal (x) co-ordinate is matched to the new co-ordinate and next the vertical (y) co-ordinate is matched to the destination co-ordinate. The speed is constant during the movement. When the mobile station reaches the destination point it is transferred into the stationary state.

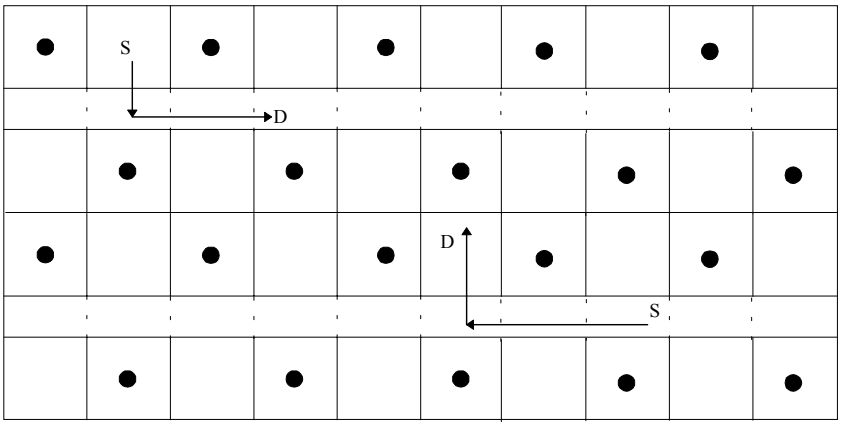

FIGURE 2.3-7. Indoor layout and movement from corridor to room and vice versa [UMTS30.03].

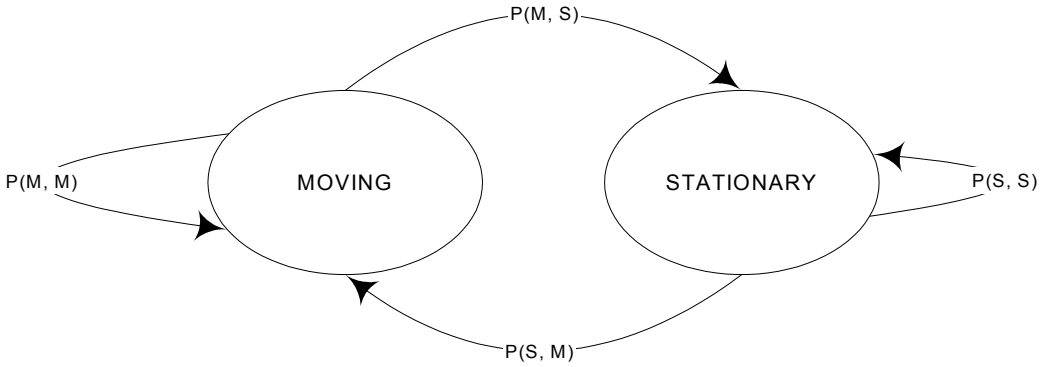

FIGURE 2.3-8. State automate presentation of the mobile station movement [UMTS30.03].

When the transition probabilities from the stationary state to the move state are derived the ratio of mobile stations at office rooms (r), mean office room stationary time (mr) and iteration time step (Δt) has to be defined. With these parameters the transition probabilities per iteration time step (1 - Δt / mr, 1 - Δt / mc) and mean corridor stationary time (mc) can be derived so that the flow to the office rooms equals the flow from the office rooms [UMTS30.03]:

$$r \cdot \frac{\Delta t}{mr} = (1 - r) \cdot \frac{\Delta t}{mc} \qquad (2.3\text{-}11)$$

with the default parameters, enlisted in the table below, the following values are obtained

- P(S,S) in office room = 1 - 0.005 / 30 = 0.999833
- P(S,M) in office room = 0.005 / 30 = 0.0001667
- P(S,S) in corridor = 1 - 0.0009444 = 0.9990556
- P(S,M) in corridor = 0.005 · 85 / (30 · 15) = 0.0009444

The average stationary time in the corridor becomes Δt / P(S,M) = 5.294 seconds.

TABLE 2.3-3. Example parameter values for mobility model [UMTS30.03].

Macro	Micro	Pico
▪ Speed = 120 km/h ▪ Probability to change direction at position update = 0.2 ▪ Maximal angle for direction update = 45° ▪ Decorrelation length = 20 meters	▪ Mean speed = 3 km/h ▪ Minimum speed = 0 km/h ▪ Standard deviation for speed (normal distribution) = 0.3 km/h ▪ Probability to change speed at position update = 0.2 ▪ Probability to turn at cross street = 0.5	▪ ratio of mobiles at office rooms = 85 % ▪ Mean office room stationary time = 30 s ▪ simulation time step = 0.005 s ▪ mobile speed = 3 km/h

2.3.9 Mixed Indoor-Outdoor Environment

In [Nok00b] a mixed indoor pico – outdoor micro environment is presented. Base stations may locate both indoors and outdoors. Mobile stations may move outdoors in street canyon according to the micro-cell mobility model [UMTS30.03] and in indoors according to the indoor mobility model [UMTS30.03]. If an outdoor mobile station enters a so-called entrance point (door) it may go indoors with a certain probability. At the same time its mobility model is changed to the indoor model. Correspondingly a mobile station moving inside may enter outdoors.

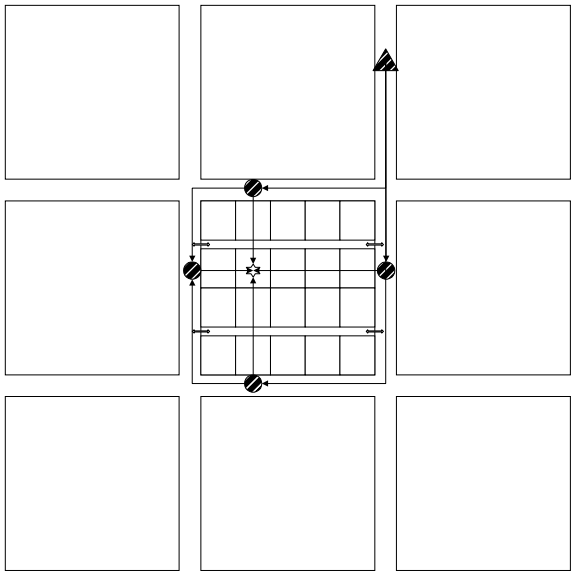

FIGURE 2.3-9. Mixed indoor and outdoor model. Triangle in the street canyon is the transmitter (receiver) outdoors and star the receiver (transmitter) in indoors [Nok00b].

The used outdoor propagation model is as presented in [UMTS30.03] and an indoor model is the Motley-Keenan model [Mot88]. Propagation from outdoors to indoors is modelled as follows. First, propagation between the transmitter and wall is calculated (four dots in FIGURE 2.3-9). Then the indoor path loss is calculated between each dot and the receiver. Finally, pathloss with the lowest value is selected for further calculations. It is assumed that propagation from indoors to outdoors is reciprocal.

2.4 Dynamic Simulator

Sophisticated RRM algorithms - such as handovers, load control, admission control, power control and packet scheduling - are important for the WCDMA radio network operation. The dynamic WCDMA radio network simulator supports the development of all RRM algorithms. It should also be noticed that RRM algorithms depend heavily on each other, e.g. power control directly affects load control, handovers and packet scheduling. Therefore, joint development of RRM algorithms is needed. This WCDMA simulator supports the analysis of the interactions of the algorithms. The presented simulator also supports the tuning and optimisation of the parameters of RRM algorithms. Such tuning is important in providing the maximum capacity from the radio network. Most important RRM algorithms have been modelled and implemented very precisely because it has been seen that they have essential effects on WCDMA networks' behaviour and performance. For example, the simulator has realistic and accurate models for power control (open, closed loop, outer loop) and handovers with measurement errors, processing and signalling delays and errors. Interactions between different RRM algorithms

force us to have as detailed and realistic models as can be possible. Naturally, available computational power sets limits for modelling accuracy.

Here modelling and implementation of a dynamic WCDMA radio network simulator is given. The study shown in this chapter was first given in [Häm99b].

2.4.1 Modelling of Radio Network Entities

The functional split between radio network elements is similar to that as in real life. In the simulator MSs, BSs and RNCs (Radio Network Controllers) are modelled. Modelling for radio network controllers is needed since most RRM algorithms locate at the radio network controller. One of the key ideas in the simulator is to implement the features and algorithms to those objects (here network elements) that they exist in real life. Thus, access from a certain network element to some algorithm or data must be done like in real life. For example, if a mobile station needs to provide propagation data for the radio network controller, data must be sent via the base station serving the mobile station. Further more, this makes it easy to model signalling in the network, including signalling delays and errors. FIGURE 2.4-1 depicts the functional split and locations for radio resource management and radio algorithms in the simulator.

The implemented simulator is designed to support multi-service (different users have different service) and multi-bearer (a user may have several services) simulations. The relation amongst connection, links and logical channels is as follows. The physical link is used to tie a transmitter (MS or BS) and a receiver (BS or MS) together. The bearer ties the physical channels and a logical channel together. There may be one or more traffic bearers active at the same time. The connection ties bearers together and the connection is also used to manage physical channels.

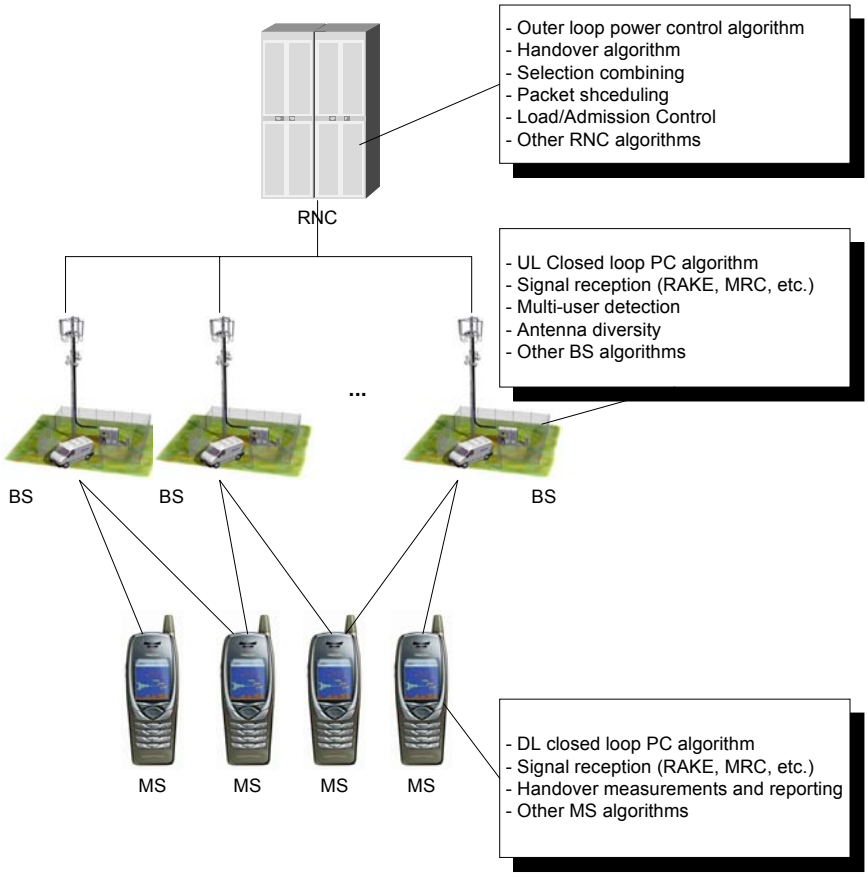

FIGURE 2.4-1. Functional split and location of radio and radio resource management algorithms.

2.4.2 Modelling of RAKE Receiver

Since the multipath propagation model is included in the simulation model, a model for the RAKE receiver is needed. The RAKE receiver is an efficient system designed to operate in multipath environment. The principle of the RAKE receiver is depicted in FIGURE 2.4-2. The RAKE receiver constitutes of several fingers that are allocated to receive different resolvable multipath components. The MF (Matched Filter) is used to determine the current multipath profile. It can also provide initial code phase (code acquisition) for the code generators [Pic92]. The matched filter can be designed to locally generate code with delays of half chip apart from each other. By doing so it is ensured that the right code phase is found. E.g. if the code length is 256 chips, then 512 code phases are generated. From 512 correlation results, the strongest ones are selected to be used with RAKE fingers. The matched filter can find code phase for every finger of the RAKE receiver.

The received wideband signal is correlated with the spreading code. The resulted narrowband signal is then phase adjusted in a phase rotator so that the output from several fingers can be coherently combined in the combiner. The combiner is typically a maximal ratio combiner in which the signals to be

combined are weighted with their channel coefficients. The phase information is found by the channel estimator that uses pilot symbols for estimating the channel state.

The state of the channel changes continuously. Code tracking is needed to ensure the highest possible correlation result. Code tracking is made separately for each finger and it can be much simpler than the initial code acquisition. It can be based for example on the sliding correlator or an early-late delay locked loop [Pic92, Oja98]. The sliding correlator uses a single correlator that correlates the received signal by sliding the code phase. Sliding is made with half chip accuracy. The code phase is slid whenever correlation results goes below a threshold [Pic92]. In an early-late delay locked loop method two correlators are used half chip apart from the on time correlator (one early and one late). Thus three correlation results are obtained – one with current code phase, one half chip early and one half chip late. The strongest of the three correlation results is then selected and the code phase corrected accordingly [Oja98]. Here we assume two samples per chip for code acquisition and tracking, but also higher over sampling rates are possible.

In the simulator the number of RAKE fingers is limited and given as a parameter. In certain environments the number of RAKE fingers may be smaller than the number of resolvable multipath components. This is the case especially if the mobile station is connected to several base stations in soft handover. The mobile station RAKE finger allocation is made so that multipaths with the highest average tap gains are selected for signal receiving. This is possible in the simulator since tap gains can be calculated in an ideal way from pathloss and the channel profile that is a simulation parameter. This is an optimistic assumption since in real life exact values cannot be calculated. On the other hand, since the RAKE finger allocation is based only on the average tap gains this model may be pessimistic – if a path that is on average strong fades due to fast fading RAKE finger is not reallocated to a stronger tap. The code acquisition and tracking are assumed ideal (or their performance comes through the link level inputs).

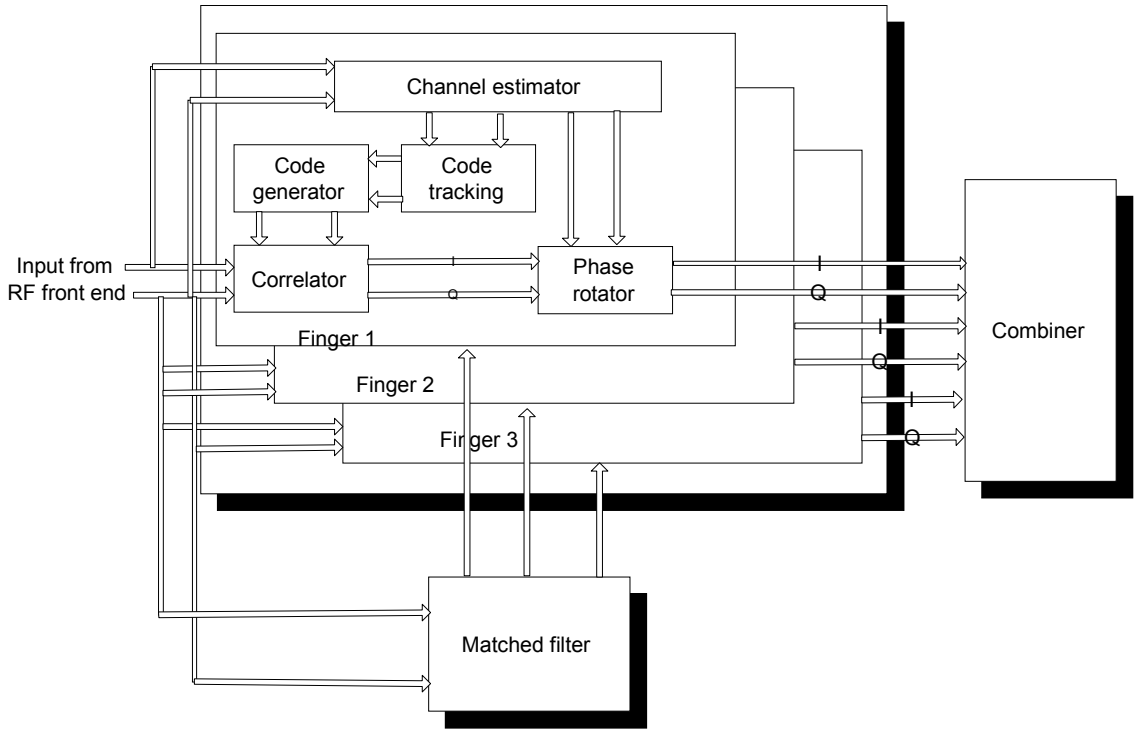

FIGURE 2.4-2. Block diagram of the RAKE receiver.

The signal to interference ratio is determined separately for each finger. The maximal ratio combining is modelled by summing the SIR-values from all the received fingers together. This model holds if the interference is noise like [Pro95]. Interference can be assumed as noise like in the case of WCDMA with low and medium data rates. For high data rates some inaccuracy may exist. The model for the RAKE receiver is discussed more in the following chapter (Chapter 2.4.3), which describes how interference and signal-to-interference ratio are calculated.

2.4.3 Modelling for Interference

The calculation of interference is an essential process of the system simulator. The better the interference modelling is, the more accurate the results can be obtained. On the other hand, the interference calculation is very computer time consuming: the received interference has to be calculated every time when the interference situation changes due to the fast power control.

The total wideband interference power $I_{bs(k)}$ received by a base station k is calculated as follows

$$I_{bs(k)} = \sum_{\substack{n=1 \\ n \neq m}}^{N} \left[L_{n,k} \cdot \frac{\sum_{i=1}^{L} g_{i,n,k}}{\sum_{i=1}^{L} \hat{g}_{i,n,k}} \cdot p_{ms(n)} \right] \tag{2.4-1}$$

where N is the total number of active mobile stations in the system and m is index for the observed user. Ln,k is pathloss (attenuation due to distance and slow fading) between the base station k, and the mobile station n. $\hat{g}_i$ is the average tap gain for path i, $\Sigma g/\Sigma\hat{g}$ is the multipath fading normalized to having long term average equal to one and L is the number of multipath components. $p_{ms(n)}$ is the transmission power of the mobile station n.

After the interference calculations, the uplink SINR (signal-to-interference and noise ratio) $SINR_{ul}$ can be calculated for the user m connected to the base station k as

$$SINR_{ul(m,k)} = \sum_{i=1}^{R} \frac{G_p p_{ms(m)} a_i^2}{I_{bs(k)} + N}, \tag{2.4-2}$$

where G_P is the processing gain, a_i is amplitude attenuation of received path i and R is the number of allocated RAKE fingers. In the simulator it is assumed that the number of RAKE fingers in the base station is always sufficient to receive all multipath components. In Equation (2.4-2) it is assumed that the received signals are combined coherently with maximal ratio combining.

In the downlink the effect due to orthogonal codes has to be taken into account, because of the multipath propagation perfect orthogonality cannot be assumed. For optimal maximal ratio combining, the downlink $SINR_{dl}$ for a user m can be calculated as

$$SINR_{dl(m)} = \sum_{k=1}^{M} \left(\sum_{i=1}^{R_k} \frac{G_p \cdot p_{bs(m,k)} a_{k,i}^2}{I_{ms(m)} - P_{bs(k)} a_{k,i}^2} \right), \tag{2.4-3}$$

where $I_{ms(m)}$ is the total interference power received by the mobile station m, M is the number of base stations in the active set, $p_{bs(m,k)}$ is the transmitting power for the observed user from the base station k, $P_{bs(k)}$ is the total power transmitted from the base station k, $a_{k,i}$ is amplitude attenuation of the channel tap i and R_k is the number of allocated RAKE fingers from base station k.

2.4.4 Modelling for Radio Resource Management Algorithms

The simulator has sophisticated modelling for radio resource management algorithms, such as random access, acquisition indication, power control, handover and compressed mode. The modelling of those algorithms is given below. In addition, other radio resource management algorithms have been modelled and implemented, such as admission control, load control and packet scheduling but not discussed here. The simulator supports a realistic division of the radio resource management algorithms between the base station and the radio network controller and the required signalling over I_{ub} (Interface between BS and RNC) interface.

2.4.4.1 *Random Access and Acquisition Indication*

The model for the random access includes the transmission of preambles, transmission of message part and open loop power control with the desired error distribution. The AICH (Acquisition Indication CHannel) is modelled with two conditional probabilities: The probability that preamble is not received by the base station given that the mobile station has sent one and the probability that an acknowledgement is erroneously detected when the base station has not sent it.

In the call setup phase, the mobile station first selects the base station to which it has the lowest pathloss. After the base station is selected, random access uses the open loop power control to estimate the initial power needed to connect to that base station. In the simulator, the mobile station estimates pathloss from the measured CPICH (Common PIlot CHannel) RSCP (Received Signal Code Power) and the pilot transmission power information. Then the initial power is calculated as described in Chapter 2.4.4.2. Random access and acquisition indication are discussed in Chapters 4.2 and 4.3, respectively.

According to specification [TR25.922] the random access preamble length is 1 ms. Simulator runs in a slot level and thus the used preamble length is set to two slots (with WCDMA 2 slots equals ca. 1.3 ms). The C/I of a preamble is measured and compared to a threshold value that is a simulation parameter. If C/I is greater than the threshold the base station receives the preamble and sends an acknowledgement by using AICH to the mobile station. Otherwise the preamble is lost and the mobile station will continue random access normally.

Even if the base station receives a preamble it is possible that the mobile station does not receive the AICH message. There is also a probability that the mobile station makes a decoding error while waiting for ACK (ACKnowledgement) for sent preamble and decides that it has received one. These error sources are modelled as two probabilities: The detection error probability (the probability that a preamble is not detected) is referred to as $1 - P_d$ and the false detection probability (the probability that an ACK is falsely detected) is called P_{fa}. There is also a limit on the number of preambles that the random access sends before a failure in connection; if the number of sent preambles reaches the maximum allowed value, the mobile station suspends random access, waits for a while and then resumes random access. However, if the length of random access exceeds the maximum allowed length random access is terminated. If the preamble is not acknowledged after a specified number of slots the mobile station increases its transmission power and sends another preamble. Otherwise the terminal receives the AICH ACK after a delay of a few slots and then starts sending the message part.

The modelling with the simulator only allows positive acknowledgements: The mobile station either succeeds in random access or the call is dropped when its random access fails.

When the capacity effects of random access have been investigated, the average number of users in the random access state and the dedicated state is kept constant. This is done by defining a user separately either a random access

state user or a dedicated state user. In the simulator, when a random access of a random access state user ends the mobile station restarts the random access procedure after 1–2 frames. This can be seen as a very simple model for sending packets through RACH (Random Access CHannel). Simulation results give an idea of what to expect from a more detailed treatment of packet traffic through common packet channels.

The mobile station uses a timer (T300 in [TR25.922]), which starts when the random access begins, to detect false detection.

2.4.4.2 *Power Control*

The power control is one of the most important RRM algorithms in a real system as well as in the simulator. The power control consists of the fast closed loop, the outer loop and the open loop power control. The outer loop power control controls the SIR set point for the fast closed loop power control both in the uplink and the downlink, and the open loop power control is used to set the initial transmission powers for the mobile terminals. The simulator has detailed modelling and implementation for all power control loops.

The open loop power control is based on the mobile station pathloss estimates. The pathloss is estimated from the measured pilot signal power (CPICH RSCP) and pilot transmission power information

$$TxP_{RACH} = SIR_{Threshold} - L + NoiseRise_{Threshold} \text{ [dB]}, \quad (2.4\text{-}4)$$

where $SIR_{Threshold}$ is predefined threshold for the quality and $NoiseRise_{Threshold}$ is the base station threshold for received interference power. Both $SIR_{Threshold}$ and $NoiseRise_{Threshold}$ are simulation parameters. The pathloss between the mobile station and the base station is calculated as

$$L = \text{CPICH RSCP} - \text{CPICH TxP}, \quad (2.4\text{-}5)$$

where CPICH RSCP is the received pilot power and CPICH TxP the transmission power of the pilot, both given in dBm.

After the mobile station has established a dedicated channel connection with the base station it may start to use the fast closed loop power control. In the closed loop power control, the mobile station estimates received SIR of the received downlink signal (or in the uplink the base station estimates SIR of the received uplink signal). The closed loop power control compares SIR estimate with the SIR target provided by the outer loop power control. If the estimate is worse than the target the mobile station (or the base station) will send a power increase command to the base station (mobile station). If the SIR estimate is better than the target a power decrease command is sent. In the simulator SIR is first calculated ideally and then a bias and a lognormal noise term are added to the ideal value to model SIR-estimation. Both the bias and the noise term are function of ideal SIR. The stronger the ideal SIR is the smaller the bias and standard deviation of noise term are, see FIGURE 2.4-3. For bias and standard

deviation of noise term look-up tables are used. Look-up tables are generated by using link level simulators.

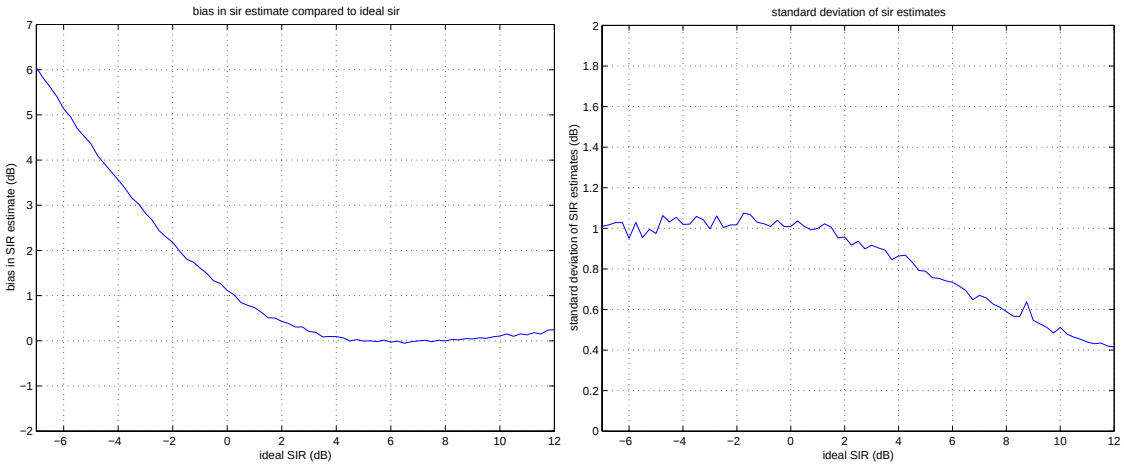

FIGURE 2.4-3. Left hand figure: Bias in SIR estimate as function of real SIR. Right hand figure: standard deviation of error in estimated SIR as a function of real SIR.

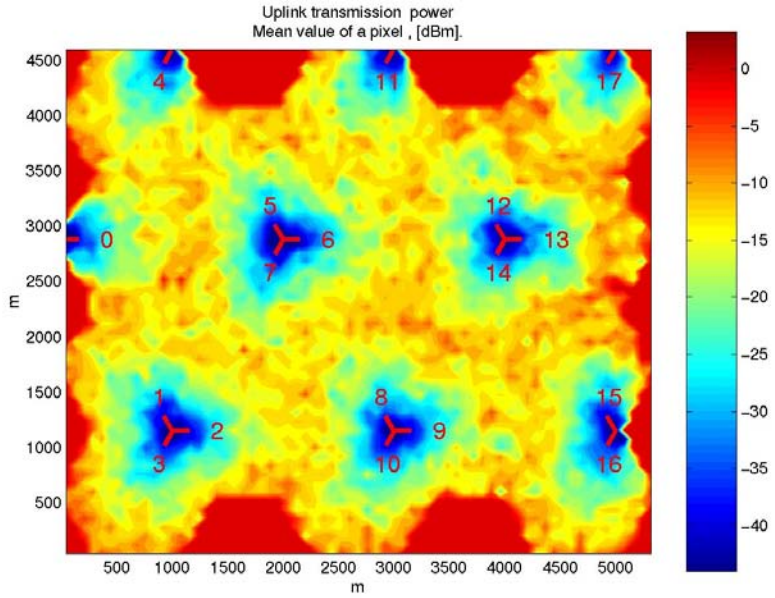

FIGURE 2.4-4. An example of mobile station transmission power as a function of position.

When the power control commands are sent in the feedback channel realistic delays are assumed. In the feedback channel errors may occur. Errors are random and their probability depends on the quality of the feedback signal. Probability for error is generated by using link level simulators. In FIGURE 2.4-4 an example of uplink power is given as a function of mobile station position.

The outer loop control in the simulator is a so-called jump algorithm [Sam97a]. After the frame has been received by the mobile station in the downlink (or the radio network controller in the uplink) frame quality is defined by using the actual value interface. If the frame was erroneous the SIR

target is increased by an up-step. If the frame was correct the SIR target is decreased by a down-step.

Open, outer and closed loop power control algorithms are discussed in more details in Chapter 4.1.

2.4.4.3 *Handover*

The simulator has realistic modelling for handover. Intra-frequency soft and softer handovers and inter-frequency hard handover are modelled. Handover decisions are based on the mobile station measurements. However, actual handover decisions are made by the radio network controller. Handover measurements involve errors that are modelled with lognormal distribution. Standard deviation of error is a simulation parameter. Mobile station measurements are signalled to the radio network controller that processes them and sends handover commands to the involved base stations and the mobile station. Delays in handover signalling and processing are taken into account.

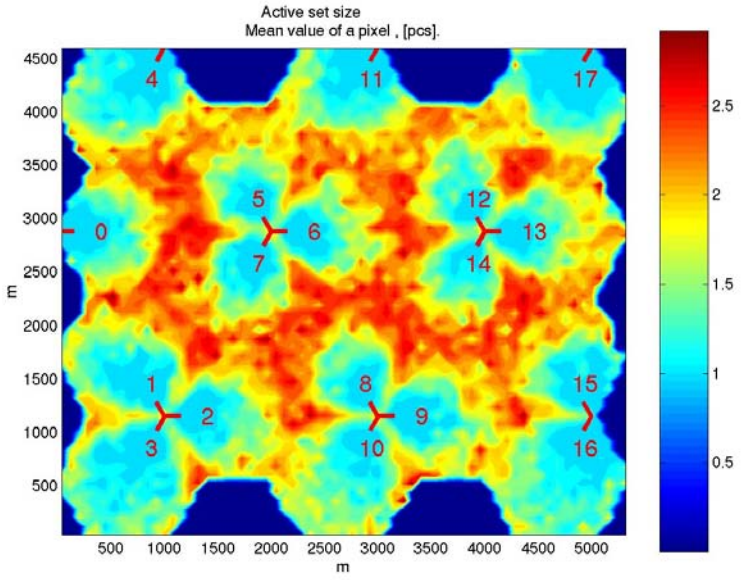

FIGURE 2.4-5. Average size of active set as a function of mobile station position.

In case of soft and softer handover the mobile station combines received signal from multiple sources by using maximal ratio combining as given in Equation (2.4-3). Since the number of RAKE fingers in the mobile station is limited (number of RAKE fingers is a simulation parameter) it may happen so that all paths cannot be captured. In this case, paths that could not be captured contribute only to the interference. In the uplink softer handover is modelled as a maximal ratio combining since combining can be made in the base station. The uplink soft handover is based on the selection combining since combining has to be made in the radio network controller. In a real system selection combining can be based e.g. on frame reliability information such as Viterbi metrics. The radio network controller selects the frame from the best source

(base station) and discards the frames from other sources. Since Viterbi metrics are not available in the simulator the mean SIR of the frame is used instead.

In simulations the maximum size of the active set can be limited. In FIGURE 2.4-5 the size of the active set is given as a function of the mobile stations position. In this example the maximum active set size is limited to three.

Handover is discussed in more details in Chapter 4.4.

2.4.4.4 *Compressed Mode*

In the uplink the compressed mode uses SF/2 (spreading factor halving) method. In the downlink SF/2 can be used, but also puncturing is possible. Both compressed mode methods are discussed in more details in Chapter 4.5.

In case of the puncturing method, part of the coding bits are punctured. This dilutes the coding gain and thus causes some loss in the link performance. In the simulator, this is modelled by multiplying the received SIR by a parameter that can have values equal or below one. This parameter describes the loss in coding performance.

After the mobile station leaves the gap (time when the signal is not transmitted) the transmission power for that user has to be set to the same value as it was before entering to the gap. However, there is an error involved to this power setting. The error is modelled as a log-normally distributed error having standard deviation as a parameter.

In the simulator the mobile station may enter to the compressed mode if a certain event occurs or according to some probability. Event-triggered compressed mode can be due to e.g. downlink transmission power exceeding a threshold value. Another modelling is to force mobile stations to the compressed mode according to the Poisson process. Parameters for the Poisson process are selected so that on average a certain pre-defined fraction of all active users are in the compressed mode.

2.5 Static Simulator

The static WCDMA system simulator has been presented first in [Häm96]. The model was also contributed to 3GPP where it was used with adjacent channel interference simulations [TR25.942]. The block diagram of the simulator is given in FIGURE 2.7-1. Simulation consists of four main building blocks – the generation of simulation environment, calculation of pathlosses, handover model and power control model. After one simulation round as many SIR samples are generated as the number of mobile stations in the simulation. In order to get sufficient statistical confidence simulation is executed several times.

The mobile stations are randomly and uniformly distributed in the simulated area. If more than one operator is simulated, for each mobile the serving operator is selected randomly with probability defined as a parameter. After the mobile stations are put to the system, the distance between each mobile station and each base station is calculated. A so-called wrap-around

method is applied when calculating distance. This means that the distance between a mobile station and a base station is calculated by using the shortest distance so that the base station is moved to the centre of the system.

Next gain matrix (pathloss matrix) is generated by using the pathloss model and by adding shadowing and in the case of a multi-operator simulation attenuation due to transmitter and receiver filters. Since wrap-around is used every base station and mobile station experiences enough interference without the edge effects of the model.

For the handover, first the candidate base stations are selected. Those base stations are candidates for handover that pathloss is inside the addition window that is calculated from the strongest base station. The size of the addition window is a simulation parameter. Active base stations are randomly selected from the candidates. The size of the active set is a simulation parameter.

In the simulator the mobile stations do not move. However, they can be simulated to have a mobile fast-fading channel. Each simulation run begins with an initial phase, where the power control operates to settle the appropriate powers for all connections to achieve the required signal-to-noise ratio for the target quality. After the power levels have been settled, the actual simulation observations are gathered. The power control modelling is similar as in [Ari92].

2.5.1 Downlink Interference Calculations and Channel Model

As was discussed in Chapter 2.2.1, channel models are not usually used with static simulators. This is also the case with the simulator presented in [TR25.942]. In the downlink another model was developed in which multipath fading was included to the interference calculation. This model was originally presented in [Häm97a].

Each base station transmits user specific dedicated signals and a common pilot signal. The power of all the transmitted signals are summed together at the base station transmitter. The signal propagates from a base station to a mobile station via several Rayleigh fading paths. The different multipath components have different average power levels as described in Chapter 2.3.4. Here, it is supposed that the received signals are combined coherently with maximal ratio combining. Maximal ratio combining is modelled by taking the sum of the SIR values of paths [Pro95]. The attained wideband SIR before despreading reads as

$$SIR = \frac{\sum_{i=1}^{N} g_i \cdot L_{p,l} \cdot P_{tx}}{\sum_{i=1}^{N} \hat{g}_i} \cdot I_{total}^{-1} \quad . \tag{2.5-1}$$

Here, N is the number of perceived paths in the channel model with the selected bandwidth. It is assumed that all paths can be received from one base station. $L_{p,l}$ is pathloss between the mobile stations and the base station l, P_{tx} is

the transmission power for the selected user and I_{total} is total interference experienced by that user. g_i is instantaneous path gain and $\hat{g}_i$ average gain for path i.

Instantaneous signal-to-interference ratio after de-spreading is calculated by dividing the received signal by the interference, and multiplying by the processing gain. Interference that arrives from the same base station as the desired signal is multiplied by an *orthogonality factor* α. The orthogonality factor of one corresponds to perfectly orthogonal intra-cell interference while with the value of zero the intra-cell interference has the same effect as inter-cell interference when downlink spreading codes are assumed as non-orthogonal pseudo-random codes. Energy per bit density to noise + interference density or narrowband SINR after despreading is

$$\frac{E_b}{N_0 + I_0} = \frac{\sum_{i=1}^{N} g_i \cdot L_{p,l} \cdot P_{tx}}{\sum_{i=1}^{N} \hat{g}_i} \cdot \frac{G_p}{(1-\alpha) \cdot I_{\text{intra}} + I_{\text{inter}} + N_0}, \tag{2.5-2}$$

where N_0 is thermal noise, G_p is processing gain, I_{intra} is intra-cell interference and I_{inter} inter-cell interference. Since the system is interference limited, thermal noise N_0 is assumed small and neglected. I_{intra} and I_{inter} are equal to

$$I = \sum_{l=1}^{M} \left[L_{p,l} \cdot \frac{\sum_{i=1}^{N} g_i}{\sum_{i=1}^{N} \hat{g}_i} \left(\sum_{k=1}^{R} P_{tx,k,l} + P_{pilot,l} \right) \right] \tag{2.5-3}$$

In the equation R is the number of interfering users in its own cell or other cells. Each path of the desired user experiences the same interference on average. M is the number of base station causing inter- or intra-cell interference and $P_{pilot,l}$ is pilot power of base station l. The pilot (CPICH) transmission power is 6 dB higher than the maximum power of single code channel. One 144 kbps user exploits 24 code channels and has the maximum power of 1 W, thus the pilot power level will be 0.17 W. In practical systems CPICH level needs to be higher since CPICH is used for handover measurement and channel estimation and should be thus received everywhere in the cell area.

The orthogonality factor α is calculated from the Equation (2.5-4). $(E_b/N_0)_n$ is the performance figure for one user case assuming intra-cell interference negligible. $(E_b/I_0)_n$ is the corresponding figure for the case in which intra-cell interference is high and noise is negligible. The produced α is

$$\alpha = 1 - \left(\frac{E_b}{I_0} \right)_n \cdot \left(\frac{E_b}{N_0} \right)_n^{-1}. \tag{2.5-4}$$

In FIGURE 3.2-1 link level simulation results are shown where E_b/I_0 is given as a function of E_b/N_0 in macro-cell environment. In FIGURE 0-1, when E_b/N_0 approaches infinity $(E_b/I_0)_n$ gets value 3.0 dB. This corresponds to the case when noise is negligible. Correspondingly, when E_b/I_0 approaches infinity (I_0 is negligible) $(E_b/N_0)_n$ gets value 4.0 dB.

Macro diversity can be modelled in two ways with the static system level simulation. The first approach is to simulate macro diversity in the link level so that separate E_b/N_0 levels are obtained for users in the soft handover state. In this model, the mobile station is able to receive all the paths directed to it. Another way is to transmit a signal from several base stations to the mobile station so that the mobile station can receive only some of the paths directed to it. Paths that are not captured by the RAKE processing are contributing to the interference. Now the same E_b/N_0 threshold is used for all the mobile stations. The latter method has been used in simulations due to straightforward modelling, although it is not quite as accurate as the preceding method.

An active set is selected randomly from the candidate set base stations. The candidate set base stations are those base stations that fit into the handover margin. This non-ideal handover selects in maximum three base stations to the active set.

2.6 Simulation Outputs

Simulation results from system levels simulations are a high number of numeric data such as capacity, outage, algorithm performance, system parameters, dropping, blocking, bad quality, interference distributions and so forth. The outage means a fraction of users that cannot satisfy the quality requirement such as SIR requirement or FER requirement. The capacity is usually given as users/carrier or kbps/MHz/cell. Capacity can be measured in such operation point where certain outage is suffered. For example with the static simulations capacity is often defined when 5 % of SIR-samples are in outage.

The definition for capacity with the dynamic simulator was initially adopted from [UMTS30.03]. This is referred to as ETSI criterion. ETSI capacity criterion is separately defined for all bearer types. For circuit-switched bearers, the number of bad frames is counted. A frame is bad quality if its C/I or FER is below requirement. A modification to the ETSI criterion was made in which erroneous frames are randomly generated according to the probability given by the simulated FER. If the number of bad quality frames is larger than e.g. 5 % of all frames during a call, the call is considered to be a bad quality call. It is required that no more than e.g. 2 % of all calls are bad quality calls. For packet bearers it is required that the average bitrate of the call is at least e.g. 10 % of the peak bitrate. Average bitrate is calculated by dividing the number of transmitted bits by the active time (time when transmitting). If the average bitrate is less than 10 % of the peak rate, the call is considered a bad quality call. It is required that no more than e.g. 2 % of all calls are bad quality calls.

In general, when capacity is spoken in this thesis, it is referred to cellular capacity, i.e. the number of users that the system can serve per MHz or carrier.

An important measurement for system performance in the uplink is noise rise and change in noise rise due to different parameters or algorithms. The loading can be calculated from noise rise as

$$Load = \eta = \frac{NR - 1}{NR}, \tag{2.6-1}$$

where NR is the noise rise in the linear scale. The load change is calculated by direct comparison to the reference value.

2.7 Discussion

A system level simulator can be static or dynamic. Static simulators are lightweight simulators that are better suited for fast capacity estimates while dynamic simulators model radio network dynamic behaviour well. Static simulators usually employ an average value interface as a snapshot corresponds to long time average simulated in the link level. In order to model the dynamic nature of the WCDMA network well, the dynamic simulator has to employ actual value interface. By using actual value interface the effect of power control, ARQ and RRM can be simulated in details.

Basic building blocks of a system simulation are cellular structures, traffic, mobility, propagation, antenna, shadowing and multipath models. Most of the models are adopted from [UMTS30.03].

Modelling of dynamic simulator includes, in addition to the basic building blocks, modelling of radio network entities with functionality that corresponds to real life, the RAKE receiver and RRM algorithms. The RAKE receiver model relates mainly to SIR calculation of a single finger, combining of outputs of fingers and finger allocation. Modelling of RRM algorithms follows the specifications (3GPP or implementation specifications in products). The simulator has models for delays and errors in RRM related measurements, signalling and decisions. Modelling of measurement and signalling impairments are urgent as they have their impacts on the network performance.

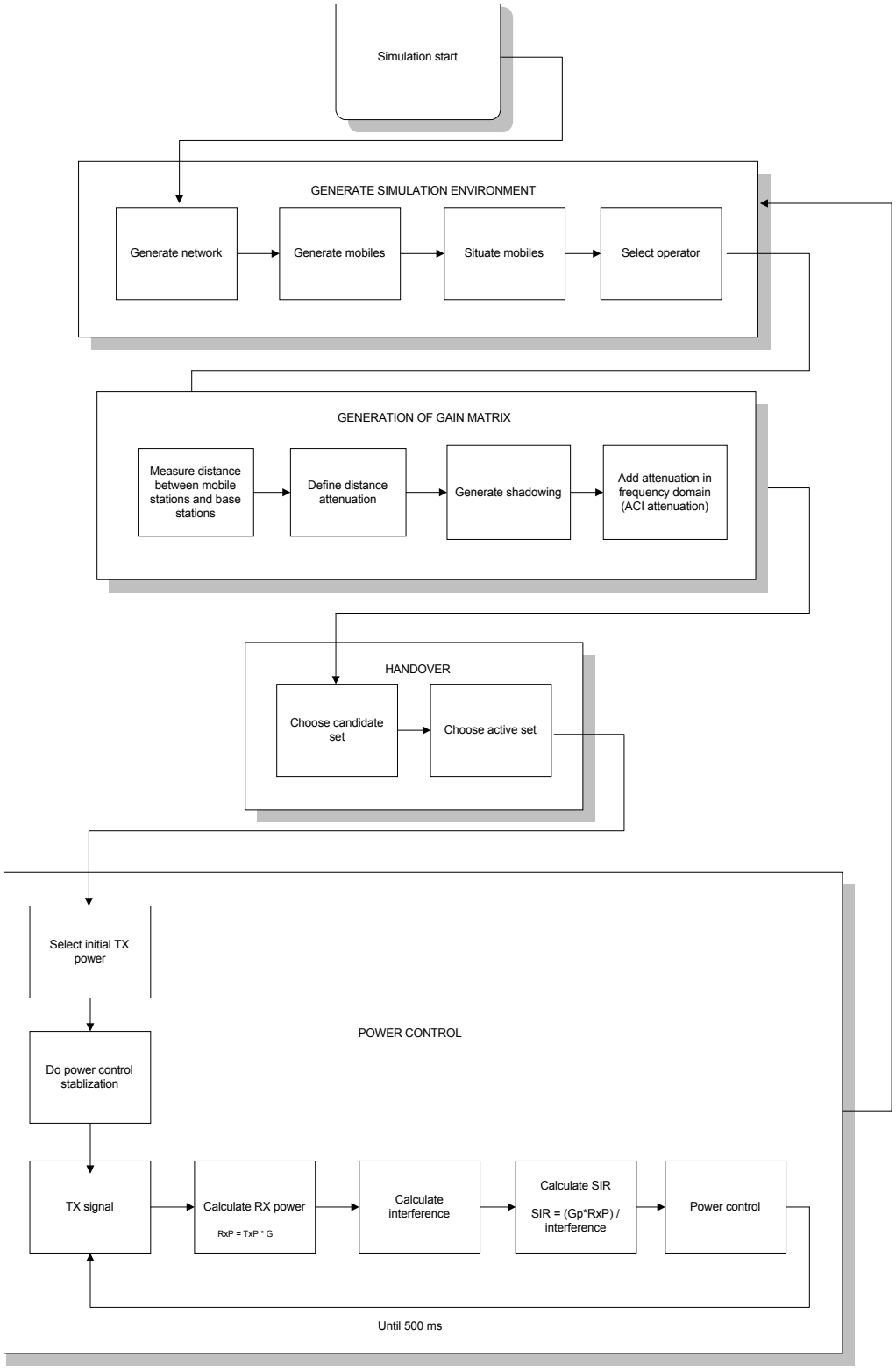

FIGURE 2.7-1. Block diagram of the static simulation tool.

3 WCDMA RADIO NETWORK CAPACITY

3.1 Uplink Capacity with Multi-User Detection

In this chapter system performance of a WCDMA radio network utilizing multi-user detection (MUD) is investigated. WCDMA specifications make it possible to use advanced receiver structures with multi-user detection. OVSF (Othogonal Variable Spreading Factor) codes are used for spreading and to separate different channels of a user in both uplink and downlink. Different length orthogonal codes can be assigned depending on the data rate. Another option would be the assignment of multiple orthogonal codes, but this would require multiple RAKE combiners in the receiver, each combiner belonging to a different code channel. This would increase the complexity of receiver. The way to generate OVSF codes and their performance analysis was first described in [Ada97].

A part of the OVSF code tree is shown in FIGURE 3.1-1. By using OVSF codes spreading factor on the DPDCH (Dedicated Physical Data CHannel) can be varied on frame-by-frame basis. The TFCI (Transport Format Combination Indicator) transmitted on the DPCCH (Dedicated Physical Control CHannel) describes data rate information and is needed to allow data detection on the DPDCH. A complex valued scrambling code is used on top of spreading. Scrambling code separates the transmission from the different sources, i.e. mobile or base stations but does not allow additional spreading. Long or short scrambling codes can be used; long codes are used with base stations using conventional RAKE receivers and short codes with base stations utilizing advanced multi-user detection receivers. Short codes are needed in order to make the multi-user detection receiver implementation easier. Short codes are based on periodically extended S(2) code family and are in length of 256. The method to generate short codes in [TS25.213] is such that it provides almost 1.7 million codes, thus code planning is not needed.

CDMA systems are inherently interference limited [Gil91]. By using Equation (3.1-6) it can be seen that the higher the SIR-target for the service is, the less users can be served by the system. Due to the non-orthogonal nature of WCDMA scrambling codes, MAI (Multiple Access Interference) is generated in the receiver when matched filter or correlator receiver is used. In case of

efficient power control all users are received on approximately equal levels. Then, assuming there is a high enough spreading factor, interference can be considered as Gaussian based on the central limit theorem. Even when multiple access interference is Gaussian, it consists of other users signal and is thus structured. This structure can be taken into account in the receiver and interference thus cancelled [Hol00]. Multi-user detection receivers have been widely investigated in literature, see for example [Due95]. Multi-user detection receivers can be classified in several ways depending on their characteristics. In [Häm96] and [Tos98] a sub-optimal non-linear PIC (Parallel Interference Cancellation) receiver is assumed. This receiver has been presented in [Var90, Var91 and Faw95]. An example of a PIC receiver is shown in FIGURE 3.1-2.

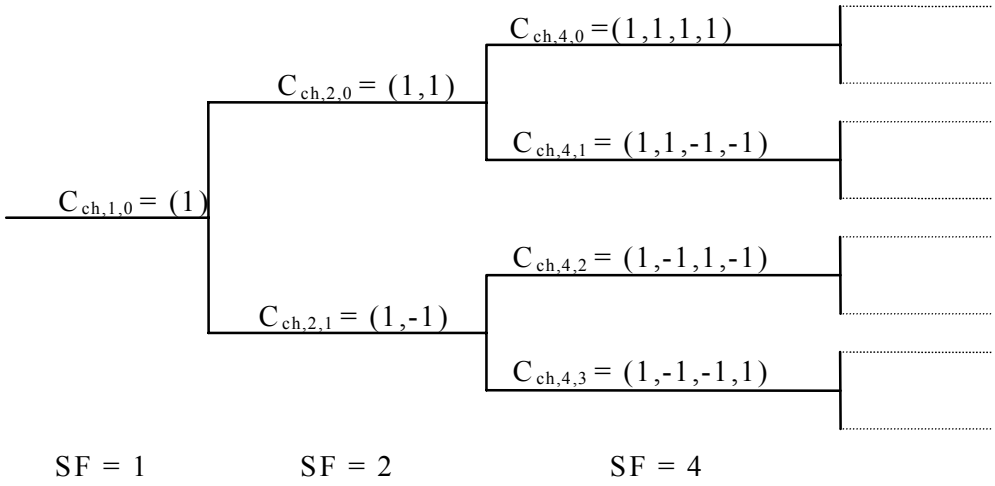

FIGURE 3.1-1. OVSF code tree [TS25.213].

In this chapter the uplink capacity is studied in urban micro- and macro-cell environments. The modelling of the environment specific and WCDMA specific features are considered in the system simulator presented in Chapter 2.5. Here the system level simulator is calibrated with analytical capacity calculations. Algorithms for multi-user detection are not described - only possible gains are evaluated. This study was originally presented in [Häm96, Tos98, Hol98] in which the link level performance and the cellular system capacity were studied.

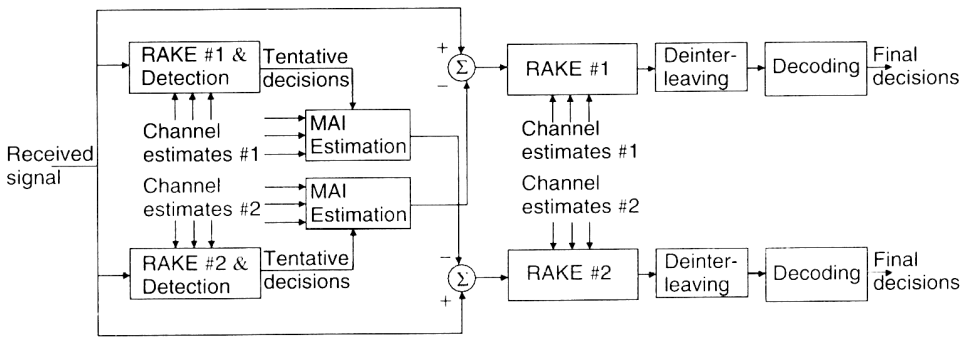

FIGURE 3.1-2. An example of parallel interference cancellation receiver. Two users received [Hol00].

3.1.1 Link Level Simulation Results

In [Häm96 and Tos98] the BER performance simulations in the link level are used to assess the efficiency of multi-user detection in the CODIT channel model. This efficiency denotes the percentage of intra-cell interference being removed by multi-user detection at the base station receiver. The efficiency of multi-user detection is estimated from the load that can be accommodated with a specific E_b/N_0 value with a conventional RAKE receiver and with a multi-user receiver. The additive white Gaussian noise, N_0, is used to represent both thermal noise and interference from neighbouring cells while intra-cell interference is represented by actual signals. The E_b/N_0 values have been chosen according to the estimated maximum cellular capacity. The target BER is 10^{-3}. In the analysis the number of users served with the RAKE receiver is denoted by K_{RAKE} and that with the multi-user detection receiver by K_{MUD}. Multi-user detection efficiency β at the given E_b/N_0 value is defined as

$$K_{RAKE} = (1 - \beta)\, K_{MUD}. \qquad (3.1\text{-}1)$$

This applies to the CODIT macro-cell channel where multipath interference is significant. In a micro-cell, the CODIT channel model is close to a single path channel and thus self-interference is negligible. Therefore the desired user can be neglected from the total number of users and calculate the multi-user detection efficiency for the micro-cellular environment as

$$K_{RAKE} - 1 = (1 - \beta)\,(K_{MUD} - 1). \qquad (3.1\text{-}2)$$

To keep the complexity of the receiver on a moderate level, only 4 RAKE fingers are assumed per antenna and per user in the base station receiver. In a macro-cellular environment 63% of the total energy can be collected on average. In the micro-cellular environment 95 % of energy can be captured with 2 RAKE fingers.

TABLE 3.1-1. Link level simulation parameters.

Parameter	Value
Chip modulation	BPSK (Binary Phase Shift Keying)
Data modulation	BPSK
Carrier frequency	2.0 GHz
Chip rate	Gold codes of length 31
Reference symbols	10%, time multiplexed
Coding	½-rate Convolutional, constraint length 9
Interleaving depth	40 ms block interleaving
User data rate	74.3 kbps
Channel model	CODIT macro cell, 50 km/h CODIT micro cell, 36 km/h
Number of RAKE fingers per antenna	4 in macro cell 2 in micro cell

Parameter	Value
Channel estimation parameters y1 and y2	0.02
Power control	2 kHz, step size 1.0 dB, 5 % errors in feedback
Antenna diversity	2 antennas, correlation 0.7, noise uncorrelated
Path combination method	Maximal ratio combining
Number of stages in MUD	2 (1 interference cancelling)
Target BER	0.001

Parameters used with link level simulations are presented in TABLE 3.1-1. As this study was made before WCDMA parameters were fixed, some assumptions are different than those in 3GPP specifications. The simulation results from link level simulations are shown in TABLE 3.1-2. In the micro-cell environment the simulated E_b/N_0 value for the multi-user detection receiver is first estimated for 15 users having BER of 10^{-3}. Next the corresponding number of users is estimated for the RAKE receiver when the same E_b/N_0 is assumed. The RAKE receiver can support 5–6 users with the selected E_b/N_0. This yields upto 64–71 % multi-user detection gain when Equation (3.1-2) is used. In the macro-cell environment the E_b/N_0 figure for the multi-user detection system with 10 users is simulated. With the RAKE receiver 3–4 users can be supported with the same E_b/N_0. By using the Equation (3.1-1) multi-user detection efficiency of 60–70 % is achieved. As the calculated multi-user detection efficiency is valid for the intra-cell interference only, it does not directly convert to gain in the cellular capacity. The interference from all the cells in the network must be included in the study to obtain the capacity for the whole network. A system level simulator is needed to estimate the network level gain from multi-user detection. Further, the efficiency used here is valid only for the selected operation point; for different E_b/N_0 requirement different efficiency would be obtained.

TABLE 3.1-2. Link level simulation results for target BER 10^{-3}.

Channel model	Number of users, no MUD, K_{RAKE}	Number of users with MUD, K_{MUD}	Efficiency of MUD β
Micro	6 – 7	15	64%-71%
Macro	3 – 4	10	60%-70%

3.1.2 Cellular Capacity

The cellular capacity of the multi-user detection system and the RAKE system is estimated by using the static system level simulator presented in Chapter 2.5. The system level simulation parameters are presented in TABLE 3.1-3. Since this study was made before WCDMA parameters were fixed some of the parameters differ from those given in 3GPP specifications. This study assumes the base stations with omni directional antennas and regular cellular layout. In

case of macro-cell simulation base stations are placed in a rectangular grid and in the micro-cell environment base stations are placed on every other street crossing. Multi-user detection efficiency obtained from the link level simulations is used when intra-cell interference is calculated. In every base station, interference generated by those mobile station connected to the observed base station is partially cancelled by using the following equation

$$I_{residual} = (1 - \beta) \cdot I_{received}. \quad (3.1\text{-}3)$$

Interference caused by other users is included as is. SIR target for the simulated service is taken from the link level simulations in a single user case.

In FIGURE 3.1-3 the outage probability is plotted as a function of load for the RAKE receiver and for the multi-user detection receiver with 65 % cancellation efficiency in the micro-cell environment. The capacity with the conventional RAKE receiver is 4.6 users/MHz/cell and for the system with multi-user detection 10.8 users/MHz/cell. The capacity gain in the micro-cell environment due to multi-user detection is thus 3.7 dB (124 % higher capacity). The network capacity obtained with the multi-user detection receiver is actually so high that it cannot be supported due to hard blocking caused by the spreading code limitation. The capacity is obtained with 5 % outage, i.e., 95% of users can achieve SIR requirement.

TABLE 3.1-3. System level parameters.

Parameter	Value
Active set size	3
Handover margin	3 dB
Voice activity	100 %
Power control step size	1 dB
Erroneous power control commands	0 %
Micro-cell mobile speed	36 km/h
Macro-cell mobile speed	50 km/h
Channel spacing	6 MHz
SIR target	Micro – 1 dB Macro – 3 dB
Slow fading deviation	6 dB

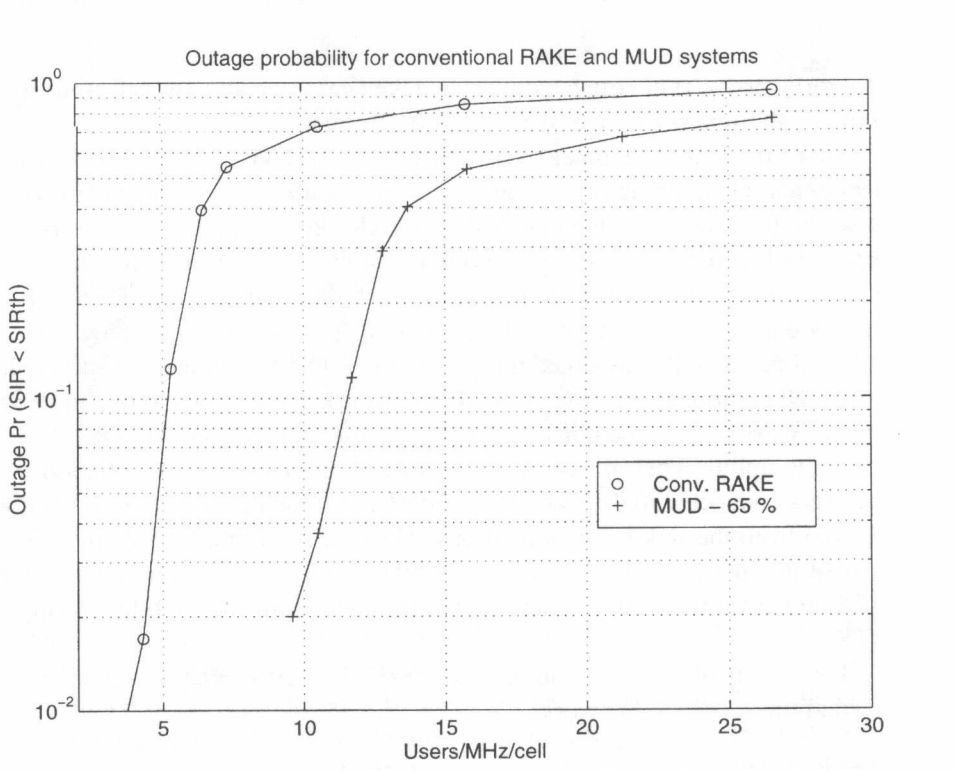

FIGURE 3.1-3. Outage probability curves for micro-cells with conventional receiver and with multi-user detection receiver with $\beta = 65$ %.

In FIGURE 3.1-4 the simulated outage figures for the macro-cell case are presented as a function of load for different multi-user detection efficiencies. From FIGURE 3.1-4 it can be seen that the capacity of the multi-user detection system with 65 % efficiency is almost doubled if compared to the conventional RAKE receiver case. This corresponds to 2.9 dB gain due to multi-user detection.

The high capacity of WCDMA with multi-user detection results from the fact that most of the interference comes from the users connected to the same cell as the observed user. Due to the soft handover, the users in a handover state can be included in the multi-user detection process, which allows an extra 20 % of interference to be included in the interference cancellation in the macro-cellular environment. In the micro-cellular environment cell separation is better. Thus fewer users are in the soft handover state. On the other hand, the amount of interference from other cells is lower which allows bigger gain from multi-user detection.

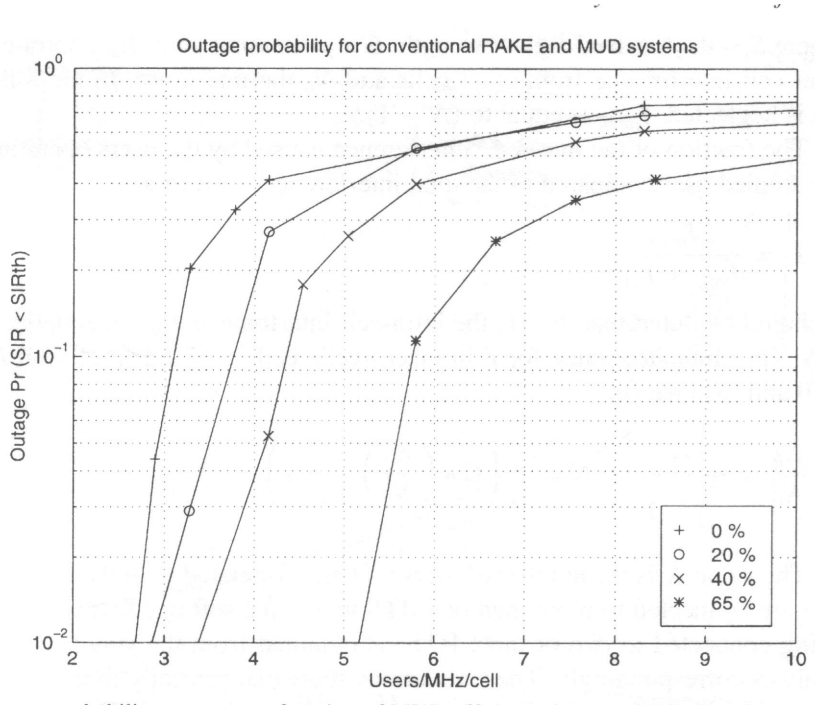

FIGURE 3.1-4. Outage probability curves as a function of multi-user detection efficiency in the macro-cell environment. The line with zero percent efficiency corresponds to the conventional RAKE receiver.

To validate the simulation results, analytical capacity calculations for the macro-cellular environment are carried out. The simulated performance compared to the analytical results are given in TABLE 3.1-4. The reason for conventional receiver results having differences between simulated and analytical results is in the power control modelling. The analytical approach assumes perfect power control whereas the simulator has the actual power algorithm running with limited dynamics and accuracy.

TABLE 3.1-4. Analytical and simulated (5 % outage) capacities in macro-cell (users/MHz/cell).

	Conventional RAKE	MUD 20 %	MUD 40 %	MUD 65 %
Simulated	2.9	3.4	4.2	5.7
Analytical	3.5	4.2	5.0	6.7

First, the capacity formula for the network without multi-user detection in base station is defined. The attained E_b/N_0 value is:

$$\frac{E_b}{N_0} = \frac{S \cdot G_p}{I_{\text{intra'}} + I_{\text{inter}} + N_0}, \tag{3.1-4}$$

where S is the received signal strength, G_p processing gain, $I_{intra'}$ intra-cell interference, I_{inter} inter-cell interference from other cells and N_0 thermal noise. In

the following thermal noise N_0 is neglected since the system is interference limited. $I_{intra'}$ is equal to $(N - 1) \cdot S$. It is assumed that each user connected to the same base station is received with equal strength S. This assumption holds since fast closed loop power control is used to solve the near-far problem.

The fraction of the intra-cell interference caused by the users operating in the same cell as the studied user compared to the total interference is given as

$$F = \frac{I_{\text{intra}}}{I_{\text{intra}} + I_{\text{inter}}}. \tag{3.1-5}$$

It should be noted that in Equation (3.1-5) the intra-cell interference I_{intra} is equal to $N \cdot S$, instead of $(N - 1) \cdot S$. It should also be noted that N also takes into account soft handover users connected to that base station. The simulated value for F in macro-cells is 0.73. For a single cell F is equal to 1. In [Vit94a] total relative inter-cell interference $f = I_{inter} / I_{intra}$ has been analysed. In macro-cells with 6 dB slow fading deviation f holds the value of 0.49 if active set size of 3 is assumed. Propagation is assumed to follow d^4 rule, where d is the distance between the mobile station and the base station. These parameter settings are approximately the same as used in this study, though not exactly the same. By converting calculated relative inter-cell interference f to F, the result F value will be 0.67. The difference between the simulated value and the calculated value according to [Vit94a] becomes from the following: the used propagation law with simulations is $d^{3.6}$ instead of d^4, some randomness in handover selection in case of simulation and in [Vit94a] only the strongest connections are considered when I_{intra} is calculated, while in the simulations interference from all users transmitting to observed base station is taken into account.

From Equations (3.1-4) and (3.1-5) we get

$$\frac{E_b}{N_0} = \frac{G_p}{\frac{N}{F} - 1} \Leftrightarrow N = F\left(G_p \left(\frac{E_b}{N_0}\right)^{-1} + 1\right). \tag{3.1-6}$$

The value N is the number of users that are associated with the base station. N also includes users that are connected to more than one base station while in a soft handover state. The number of users being connected to two or three base stations is obtained from the simulator and used to adjust the analysis correspondingly. The simulations show that typically in the simulated macro-cellular environment, 80 % of the users are connected to only one base station, while 15 % of the users are connected to two base stations and 5 % are connected to three base stations. The calculated capacity must be thus scaled with 1.25 as the effect of soft handover is seen in F and the total number of connections in the system is higher than the number of mobiles in the system.

The corresponding analysis for the multi-user detection case can be done:

$$\frac{E_b}{N_0} = \frac{SG_p}{(1-\beta)I_{intra'} + I_{inter} + N_0} . \quad (3.1\text{-}7)$$

Inter-cell interference can be calculated as

$$I_{inter} = \frac{1-F}{F} I_{intra} . \quad (3.1\text{-}8)$$

From Equation (3.1-7) we now get

$$\frac{E_b}{N_0} = \frac{S \cdot G_P}{(1-\beta)(I_{intra} - S) + \frac{1-F}{F} I_{intra}} . \quad (3.1\text{-}9)$$

Since I_{intra} is equal to $N \cdot S$, we now can write Equation (3.1-9) as

$$\frac{E_b}{N_0} = \frac{S \cdot G_p}{(1-\beta)(NS - S) + \frac{1-F}{F} N \cdot S} . \quad (3.1\text{-}10)$$

The capacity of the system is now given as

$$N = F\left(\frac{G_p (\frac{E_b}{N_0})^{-1} - (\beta - 1)}{1 - F\beta} \right) . \quad (3.1\text{-}11)$$

If β is set to 0 in Equation (3.1-11), then Equation (3.1-11) becomes the same as Equation (3.1-6). β value 0 represents the capacity of the conventional RAKE receiver based system.

The capacity as a function of multi-user detection efficiency is shown in FIGURE 3.1-5. Both analytical and simulated results are shown. The simulated results compare well to the analytical results. The offset between analytical and simulated results is due to the non-ideal power control and due to real interferers in the simulator instead of Gaussian approximation.

To calibrate the simulator, an additional verification was carried out. The macro-cell performance was compared to that presented by Gilhousen et al. in [Gil91] with the same parameters. The difference from the results in [Gil91] was less than 10 %. The difference is due to the imperfections in the power control and due to interference modelling.

It should be noted that the capacity values are valid only under the assumptions used and even then a system operating at the given capacity would be in a highly unstable state. The used 5 % outage criterion leads to approximately 20 dB noise rise, which can be considered a high load for the network. If the interference is increased by a small amount, the system outage

will increase dramatically as many users do not meet the quality criteria anymore. The power control modelling principle used leads to a relatively narrow C/I distribution resulting in high capacity. As the real C/I distribution is expected to be less ideal, degradation in the capacity is expected. Additionally, the performance of the backbone network in setting up new connections for soft handovers and managing the power balancing signalling in the network is also a critical factor to achieve a stable and high capacity WCDMA network.

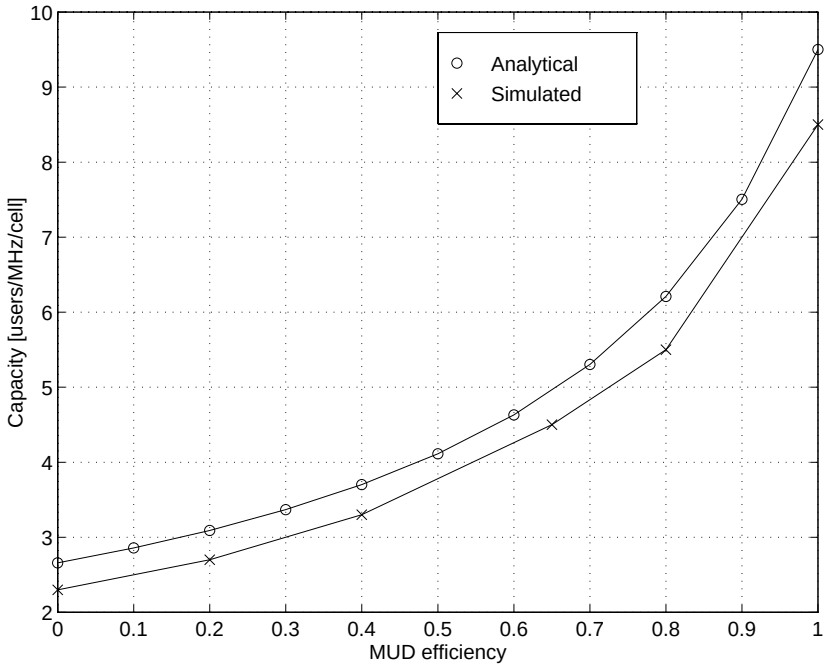

FIGURE 3.1-5. Analytical and simulated capacity as a function of multi-user detection efficiency in the macro-cellular environment.

3.2 Downlink Performance

In this chapter WCDMA downlink capacity improvements with macro diversity, with reception antenna diversity and with interference reduction techniques are analysed. This study was originally presented in [Häm97a, Hol98].

The services that are expected to be important in UMTS networks are data services like WWW-browsing. These services set high requirements for the capacity, especially in the downlink. Downlink capacity enhancement methods in a WCDMA cellular network are considered. Downlink capacity improvements that can be achieved with interference reduction techniques are analysed with the help of static cellular system simulator presented in Chapter 2.5.

With the WCDMA downlink OVSF codes are used for spreading and to separate different channels of a base station or sector. Unlike in the uplink, in the downlink the spreading factor does not vary. Variations in the data rate are

handled by rate matching (puncturing or repetition) or with a discontinuous transmission. OVSF codes are such that they preserve orthogonality between different downlink channels even data rates and spreading factor used in different channels varies. Top of spreading, scrambling is used to separate the different base stations or sectors. Scrambling does not change signal bandwidth.

In an ideal situation signals transmitted from a base station or a sector remain orthogonal in reception. However, multipath propagation distorts orthogonality as different paths arrive at different times to the receiver. Delay spread depends on the operated environment and is typically longer in the macro-cellular environment. In addition to orthogonal codes, interference can be reduced by using advanced receiver structures, i.e., IC (Interference Cancelling) receivers. In this study the possible capacity gain for IC receivers is evaluated. Algorithms for cancelling interference are not in the scope of this study. Capacity gain from orthogonal codes and interference cancellation is studied in urban macro and micro-cell environments by using environment specific orthogonality factors.

The performance measurement for the system simulations is outage percentage. A maximum of 5 % of obtained SIR values is allowed to be lower than the threshold SIR, i.e. having quality worse than required.

3.2.1 Simulation Assumptions

The main parameters for the simulated macro and micro-cell environments are shown in TABLE 3.2-1. Radio network related parameters are presented in TABLE 3.2-2. Some of the parameters differ from 3GPP specifications as this study was made before 3GPP parameters and features were fixed. The link level E_b/N_0 and E_b/I_0 values that are used are shown in TABLE 3.2-3 and FIGURE 3.2-1. The orthogonality factor is derived according to the Equation (2.5-4) from the link level results. The obtained orthogonality factor is in the order of 0.2 in the macro-cell channel and in the order of 0.7 in the micro-cell. Better orthogonality can be seen in the micro-cell environment due to lower number of multipaths.

TABLE 3.2-1. Simulation environment.

	Micro	Macro
Shadowing	Mean 0dB, STD dev 4dB	mean 0dB, STD dev 10dB
Base station amount	128	19
Base station layout	Manhattan	Hexagonal
Base station spacing	200 m	800 m
Building width	100 m	-
Street width	30 m	-
Mobile speed	5 km/h	5 km/h

TABLE 3.2-2. Simulation parameters.

Parameter	Value
Outage requirement	< 5 %
Active set size in soft handover	3
Handover margin in non-ideal handover	3 dB
Carrier spacing	6 MHz
User bitrate	144 kbit/s
Voice activity	100 %
RAKE fingers	9
PC (Power Control)dynamic range	20 dB
PC step size	1 dB
Pilot strength	0.17 W

TABLE 3.2-3. E_b/N_0 and E_b/I_0 and calculated orthogonality factor for 128 kbps service.

	Downlink E_b/N_0	Downlink E_b/I_0	Orthogonality factor
Macro	4.0 dB	3.0 dB	0.21
Micro	6.1 dB	0.9 dB	0.7

In the downlink the needed E_b/N_0 for service with 10^{-3} BER is 4.0 dB in the macro-cell environment and 6.1 dB in the micro-cell environment. In CODIT micro-cell channel delay spread is rather short, thus a downlink receiver cannot obtain diversity although the code channels remain more orthogonal. A means to improve diversity is to add an antenna branch to the mobile station receiver and thus utilize antenna diversity. The link level gain in the micro-cell environment from the antenna diversity is in the order of 3 dB. In the macro-cell environment the actual gain is very small especially if the total number of RAKE fingers is kept the same regardless of adding a second antenna branch to the mobile station.

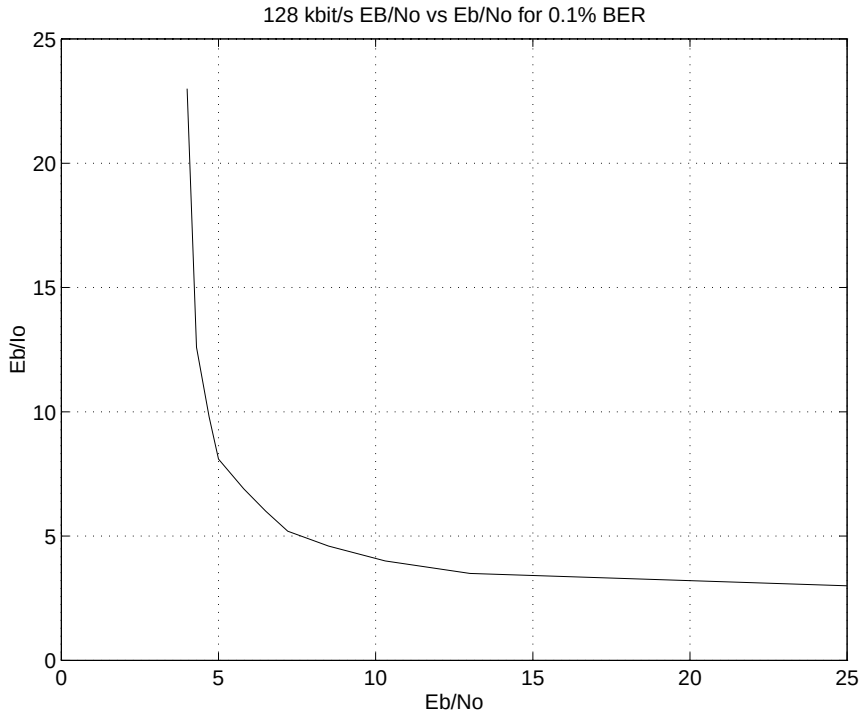

FIGURE 3.2-1. Downlink link level example performance for CODIT macro-cell channel with 128 kbit/s data service.

In TABLE 3.2-4 micro-cell and macro-cell capacity is given with 5 % outage. In FIGURE 3.2-2 outage as a function of offered load is plotted. TABLE 3.2-4 and FIGURE 3.2-2 show capacity results from basic cases that are used as reference cases when the gains from the handover and interference cancellation are investigated.

TABLE 3.2-4. Cellular capacity in kbit/s/cell/MHz. Service 144 kbit/s.

[kbit/s/cell/MHz]	Downlink
Macro	169
Micro	222

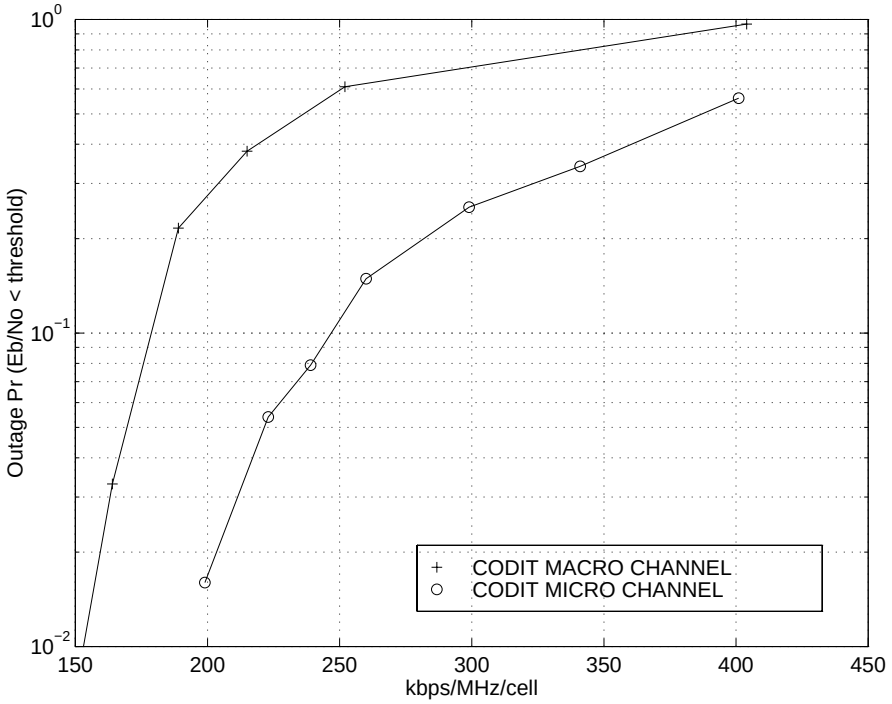

FIGURE 3.2-2. System level performance for CODIT macro-cell and micro-cell channels with 144 kbps user data.

3.2.2 Soft Handover and Macro diversity

Macro-cell capacity decreases only by 10 % if soft handover and macro diversity are not used. The simulated CODIT macro-cell channel gives sufficient multipath diversity even if the mobile station is in a hard handover state. On the other hand the limited number of RAKE fingers cannot fully exploit the attained diversity from soft handover. On the contrary, a large part of the generated energy by soft handover base stations would be lost contributing to the interference. The situation is different for the micro-cell case, since CODIT micro-cell channel provides only a little multipath diversity. Thus, macro diversity is essential for high capacity in the micro-cell environment. Similarly antenna diversity has more benefit in the micro-cell environment if compared to macro-cell environment. In TABLE 3.2-5 the capacity for hard and soft handovers is given. Soft handover and macro diversity give 0.4 dB and 2.0 dB gain in macro and micro-cell environments, respectively.

TABLE 3.2-5. Downlink capacity with hard and soft handover.

[kbit/s/cell/MHz]	Hard handover	Soft handover	Soft handover gain
Macro	155	169	0.4 dB
Micro	139	222	2.0 dB

3.2.3 Interference Cancellation in Mobile Station/Orthogonal Codes in Downlink

3.2.3.1 *Intra-cell Interference Cancellation*

Intra-cell interference can be cancelled by using such spreading codes that make user signals orthogonal or by interference cancelling techniques. In case of interference cancellation all the intra-cell interference cannot be included in the cancelling process. Here we suppose that interference cancellation can cancel 20 % of the macro-cell intra-cell interference and 70 % of the micro-cell intra-cell interference. An example of implementation for downlink interference cancellation can be found in [Wic97].

Since the serving base stations generate the major part of interference, interference cancellation or orthogonalization of signals gives high capacity gain. If orthogonalization is ideal in a micro-cellular environment, as high a gain as 7.5 dB can be achieved if compared to case where interference signal waveform is random. The results in TABLE 3.2-6 are given as lower and upper bounds for the capacity gain from interference cancellation. The value 0.0 corresponds to random codes and large number of multipaths and value 1.0 to single path case with orthogonal codes or with ideal interference cancellation. Also capacities with actual simulated orthogonality factors are presented. Capacity as a function of cancellation efficiency is shown in FIGURE 3.2-3.

TABLE 3.2-6. Downlink capacity with reduced intra-cell interference in [kbit/s/cell/MHz].

	Capacity for different orthogonality factors				
Orthogonality factor	Worst case $\alpha = 0.0$	Macro $\alpha = 0.2$, Micro $\alpha = 0.7$ (=values from link level simulations)		Ideal $\alpha = 1.0$	
	Capacity	Capacity	Gain	Capacity	Gain
Macro	141	169	0.8 dB	502	5.5 dB
Micro	78	222	4.5 dB	436	7.5 dB

3.2.3.2 *Inter-Cell Interference Cancellation*

There are several ways to implement interference cancellation in the system level. The approach studied here is to search for a certain number of strongest interferers and cancel them. Here we assume that intra-cell interference is reduced by orthogonal codes.

In FIGURE 3.2-4 and TABLE 3.2-7 simulation results for inter-cell interference cancellation is shown. Mobile station interference cancellation that cancels inter-cell interference does not offer remarkable gain since a major part (ca. 70–80 %) of the interference that a mobile station experiences is generated by the serving base stations. The capacity gain also depends on the bitrate. If lower bitrates are used, then there are more interferers and the capacity gain is lower. But if higher bitrates are used, then a higher percentage of interferers can be included

in the interference cancellation process. Capacity gain is highest in the macro-cellular environment where 0.2–0.7 dB gain can be seen, while in a micro-cell environment the gain is less than 0.2 dB. Capacity gain is higher in macro-cell environment due to worse cell isolation.

TABLE 3.2-7. Downlink capacity with reduced adjacent cell (inter-cell) interference. N is number of cancelled users.

	IC efficiency						
Efficiency	0.0	0.3		0.7		1.0	
	Capacity	Capacity	Gain	Capacity	Gain	Capacity	Gain
Macro, (N=10)	169	176	0.2 dB	188	0.5 dB	200	0.7 dB
Micro, (N=10)	222	230	0.2 dB	228	0.1 dB	228	0.1 dB

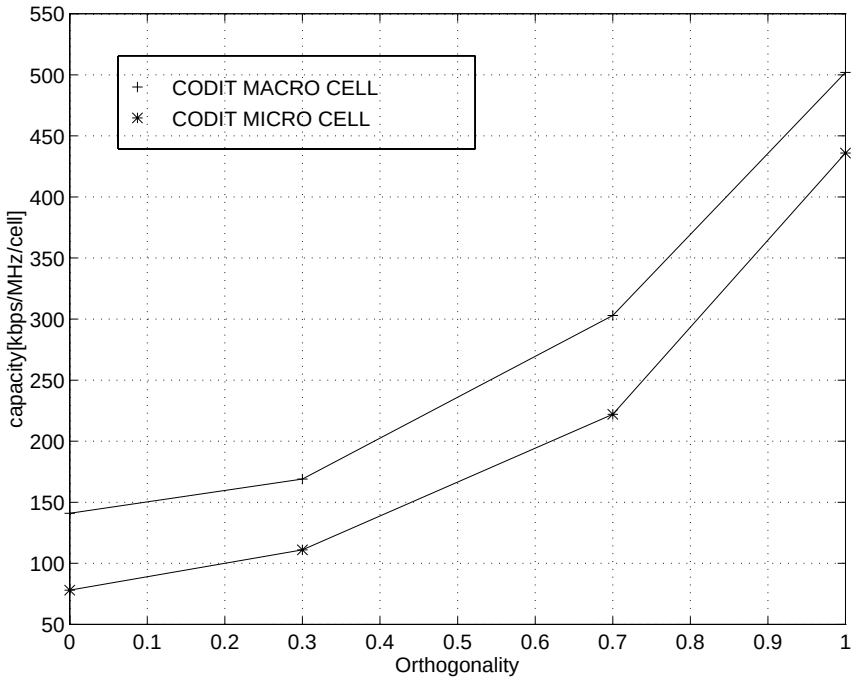

FIGURE 3.2-3. Downlink capacity as a function of orthogonality of intra-cell interference.

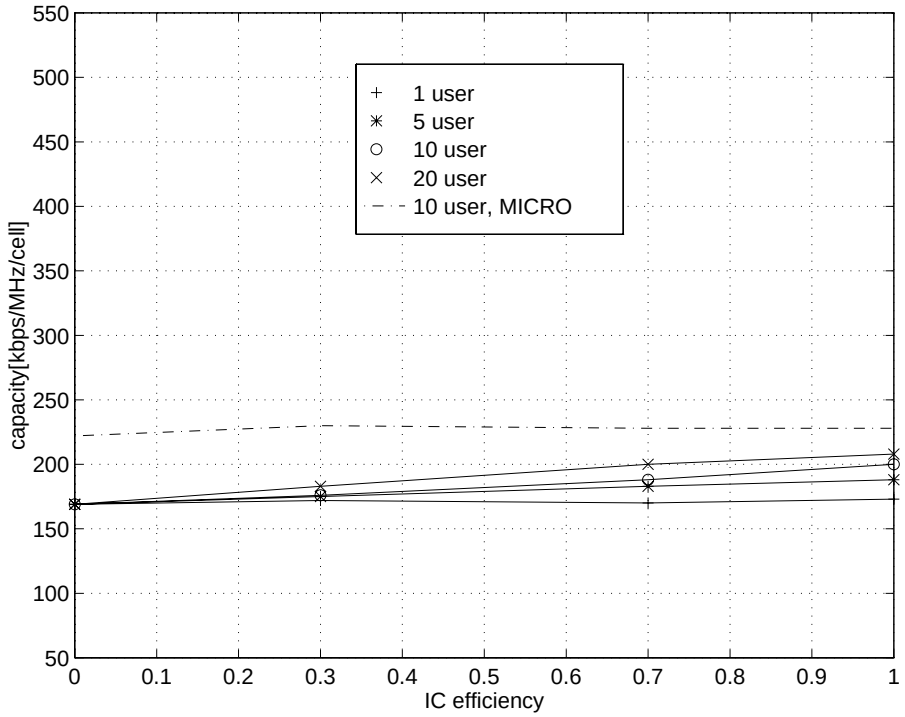

FIGURE 3.2-4. Downlink capacity as a function of orthogonality of inter-cell interference in macro-cell environment.

3.3 WCDMA Adjacent Channel Interference Requirements

In this chapter the effects of ACI (Adjacent Channel Interference) on the WCDMA capacity are studied for two adjacent frequency operators as well as for hierarchical cell structure used by one operator at adjacent frequency channels. Adjacent channel interference is one of the most critical issues for the frequency co-ordination in the IMT-2000 systems. If the adjacent frequency operators are isolated in a frequency domain by large guard bands, much of the spectrum is wasted due to the large system bandwidth. Tight spectrum mask requirements for a transmitter and high selectivity requirements for a receiver in the mobile station and in the base station, would guarantee low adjacent channel interference. However, these requirements have a great impact especially on the implementation of a small WCDMA mobile station.

Here the effect of adjacent channel interference on the system capacity is studied in a highly loaded network as well as with practical loading of the WCDMA system. Also a new model for adjacent channel interference in the uplink is introduced taking into account the behaviour of a practical WCDMA terminal power amplifier. A goal of this chapter is to find out adjacent channel interference requirements for the WCDMA system. This study has been originally given in [Häm97b, Häm98, Rin99, Häm99a and Hol00].

Adjacent channel interference consists of transmitter non-idealities and imperfect receiver filtering. In the uplink the main source of adjacent channel

interference is the mobile station nonlinear power amplifier (PA) which introduces Adjacent Channel leakage Power (ACP). Tight ACP requirements have a direct effect on the efficiency of the power amplifier and therefore also on the talk time of the WCDMA terminal. It is expected that in the downlink the limiting factor for adjacent channel interference will be the receiver selectivity of the WCDMA mobile station, since it is easier to implement tight ACP requirements in the base station than to implement highly selective receiver filters for the mobile station.

The studies concerning adjacent channel interference raised a lot of interest (especially for the uplink) during the year 1998 in ETSI UMTS standardization forum, see [Nok98a, Eri98b and Mot98]. However, the problem with these simulations was that the simulations were executed with slightly different parameters leading to different results. After the WCDMA standardization responsibility was handed to the 3GPP forum, the discussion on adjacent channel interference issues continued in TSG RAN WG4, which has the responsibility for specifying the minimum RF requirements for WCDMA [3GPP]. TSG RAN WG4 established a special ad hoc on adjacent channel interference system simulations and selected the author of this thesis as the chairman of the ad hoc. The outcome of this ad hoc was the agreed adjacent channel interference simulation scenarios and parameters [TR25.942]. In this chapter simulations are performed according to the agreed simulation parameters. In addition a few simulations with additional simulation parameters, e.g. new uplink adjacent channel interference model, are shown. The simulations are accomplished by using the WCDMA snapshot simulator presented in Chapter 2.5.

3.3.1 Adjacent Channel Interference Mechanisms

Adjacent channel interference is one source of interference summing to the other interference mechanisms present in the operating band. The operating band interference is caused by multiple-access interference or intra-cell interference, inter-cell interference and thermal noise. An extra source of interference will be adjacent channel interference caused to the operating band by all the operations in the adjacent frequency bands. Signal-to-interference ratio with adjacent channel interference is given in Equation (3.3-1) for the uplink and in Equation (3.3-2) for the downlink:

$$SIR_{UL} = \frac{G_p \cdot P_{TX} / L_p}{I_{intra} + I_{inter} + I_{aci} + N_0}, \tag{3.3-1}$$

$$SIR_{DL} = \frac{G_p \cdot P_{TX} / L_p}{(1-\alpha) I_{intra} + I_{inter} + I_{aci} + N_0}. \tag{3.3-2}$$

Here P_{TX} is the transmission power, L_p is pathloss, G_p is processing gain, I_{intra} is intra-cell interference, I_{inter} is inter-cell interference, I_{aci} is adjacent channel

interference and N_0 = kTWF is the thermal noise with thermal noise spectral density kT, bandwidth W and receiver noise figure F.

When band limited linear modulation methods are used, spectrum leakage between the adjacent channel carriers depends on the linearity of the power amplifier due to the non-constant RF-envelope. Spectrum leakage to adjacent channels can be controlled by backing off the power amplifier or using some linearization method to equalize the nonlinearities of the power amplifier. Unfortunately, both methods decrease the achievable power amplifier efficiency when compared to the modulation schemes that have a constant envelope and can be amplified with power efficient but non-linear power amplifiers [Lil96]. Linearity requirements of a WCDMA transmitter are mainly determined by the spectrum adjacent channel interference attenuation requirements. ACLR (Adjacent Channel power Leakage Ratio) is depicted as a ratio of signal power in the desired channel to signal power in the neighbouring channel, i.e., as the ratio of the transmitted power to the power measured after an ideal rectangular receiver filter in the adjacent frequency channel [Eri99a]

$$ACLR = \frac{P_{TX}}{P_{RX,a}}, \tag{3.3-3}$$

where P_{TX} is the transmitted power in the operating band and $P_{RX,a}$ is the power measured after a rectangular receiver filter in the adjacent frequency channel. ACLR requirements are usually given in dBc that is the power on the adjacent channel is compared to the in-band power. The out-of-band received power after the receiver filtering is given as

$$P_{TX} = \int_{fc1-W/2}^{fc1+W/2} S_{xx}(f)\,|H_{TX}(f)|^2\,|H_{PA}(f)|^2 df, \tag{3.3-4}$$

where S_{xx} is the signal power spectrum at the input of the transmitter filter, $|H_{TX}(f)|^2$ is the transmitter filter response and $|H_{PA}(f)|^2$ represents the non-linearity of the power amplifier in the frequency domain.

If low ACLR, i.e., larger spectrum spreading into adjacent carriers can be tolerated, more power efficient power amplifiers can be used in the mobile terminals. Here terms ACP and ACLR are used interchangeably. ACLR is depicted in FIGURE 3.3-1.

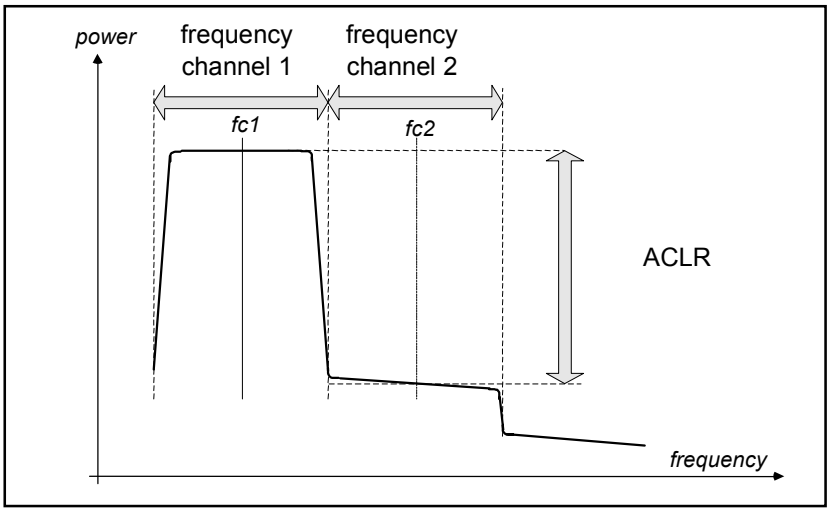

FIGURE 3.3-1. Adjacent channel interference depicted.

In case the receiver filter is non-ideal, some of the adjacent channel carrier power may leak to the receiver causing performance deterioration. In the uplink, the ACLR contributes most to the adjacent channel interference, because in practice it is more difficult to implement tight ACLR requirements with good power amplifier efficiency for the mobile station transmitter than to design high selectivity filters for the base station receiver. In the downlink, however, it is easier to implement tight ACLR requirements of the power amplifier for the base station transmitter than to implement high selectivity filters for the mobile station receiver. Simple reasoning behind this is that a base station can consume more power than a mobile station. ACS (Adjacent Channel Selectivity) is a measure of receiver's ability to receive a signal at its assigned channel frequency in the presence of a modulated signal in the adjacent channel. ACS is the ratio of the receiver filter attenuation on the assigned channel frequency to the receiver filter attenuation on the adjacent channel frequency [Eri99a]

$$ACS = \frac{P_{TX,a}}{P_{RX}} \quad (3.3\text{-}5)$$

Here $P_{TX,a}$ is the signal power in the adjacent carrier and P_{RX} the power measured in the desired channel. The in-band transmitted signal power after receiver filtering is given as

$$P_{RX,a} = \int_{fc2-W/2}^{fc2+W/2} S_{xx}(f)\ |H_{TX}(f)|^2 |H_{PA}(f)|^2 |H_{RX,a}(f)|^2 df \quad (3.3\text{-}6)$$

where $|H_{RX,a}(f)|^2$ is the receiver filter response.

Adjacent channel interference is long-term average interference caused by the operation of the mobile stations and the base stations communicating on the

adjacent frequency channel. ACIR (Adjacent Channel Interference Ratio) is the sum effect of ACLR and ACS and defined as [Eri99a]

$$ACIR = \frac{1}{\frac{1}{ACLR} + \frac{1}{ACS}}. \tag{3.3-7}$$

The total adjacent channel interference in the network can be summed over the mobile stations and integrated over time. The pathloss and fading are independent for the different connections between the mobile stations and the base stations. The adjacent channel interference is thus given as

$$ACI = I_{aci} = \int \left(\sum_{MS_i} \left(\frac{P_{TX}}{ACIR} \cdot fading / L_p \right)_i \right) dt, \tag{3.3-8}$$

where MS_i is a single mobile station operating on the adjacent frequency channel, *fading* is the multipath fast fading with Rayleigh amplitude distribution [Jak74] and L_p is the pathloss. The fading and pathloss are experienced by a base station in the uplink transmission and by a mobile station in the downlink transmission.

TABLE 3.3-1. Terms defined in [Eri99a].

ACLR	Adjacent Channel leakage Power
The ratio of the transmitted power to the power measured after a receiver filter in the adjacent RF channel. Both the transmitted power and the received power are measured within a filter response that is nominally rectangular, with a noise power bandwidth equal to the chip rate.	
ACP	Adjacent Channel Leakage power Ratio
Same as ACLR	
ACS	Adjacent Channel Selectivity
Adjacent Channel Selectivity is a measure of a receiver's ability to receive a signal at its assigned channel frequency in the presence of a modulated signal in the adjacent channel. ACS is the ratio of the receiver filter attenuation on the assigned channel frequency to the receiver filter attenuation on the adjacent channel frequency. The attenuation of the filter on the assigned and adjacent channels is measured with a filter response that is nominally rectangular, with a noise power bandwidth equal to the chip rate.	
ACI	Adjacent Channel Interference
ACI is the power measure for interference caused by transmissions in adjacent channels and given in dBm.	
ACIR	Adjacent Channel power Interference Ratio
ACIR is the sum effect of ACLR and ACS taking into account both power amplifier linearity and receivers selectivity	

ACLR and ACS requirements can be derived based on MCL (Minimum Coupling Loss)[9] calculations as shown in TABLE 3.3-2. The minimum coupling loss analysis however leads to an extremely pessimistic power amplifier linearity and filtering selectivity values. The condition described by the MCL calculation assumes that several unlike events occur simultaneously: 1) another operator's mobile station should locate in the immediate proximity of the desired operator's base station, 2) another operator's mobile station should be transmitting (continuously) with full power. This requires that the desired base station locates exactly in the cell border of another operator's base station. 3) Another operator's base station is transmitting (continuously) with full power. Thus, the simulation approach is preferred over the minimum coupling analysis.

TABLE 3.3-2. Worst-case minimum coupling loss calculations.

Parameter	Value	Remarks
Uplink		
UE[10] max power	21 dBm	
MCL	70 dB	Coupling loss to another operator BS
RxP	-49 dBm	UE TXP – MCL
Noise	-103 dBm	N_0 = kTWF, kT = -174 dBm/Hz, W = 66 dB, F = 5 dB --> N_0 = -103 dBm
ACLR	54 dBc	Assuming ACI below noise, ACLR = RxP - N_0
Downlink		
BS max power	43 dBm	Total Tx power of macro-cell BS
MCL	70 dB	
RxP	-27 dBm	BS TXP – MCL
Noise	- 99 dBm	N_0= -174dBm/Hz + 66 dB + 9dB = -99 dBm
ACS	72 dBc	Assuming ACI below noise, ACS = RxP - N_0

3.3.2 Simulated Scenarios

The adjacent channel interference term I_{aci} depends on the loading and applied power levels in the adjacent channel, which in turn depends on the designed cell range, mobility of the terminals and characteristics of the radio channels among other things. For the above-mentioned reasons, simulations have to consider the effects of adjacent channel interference on the different load conditions. In these simulations, the network is first loaded by as many mobile stations as is necessary to load the network maximally yielding an outage

---

[9] Minimum coupling loss defines the minimum pathloss expected to occur between the mobile station and the base station antenna connectors

[10] User Equipment

probability lower than but close to 5 % [11]. The outage probability defined for a single radio link is the probability that the BER exceeds the specified BER requirement. In the network, the outage probability is calculated over all active radio links. In the second phase simulations with realistic loading are carried out. Realistic loading is obtained by keeping the noise rise in the uplink on average of 6 dB in each base station. The selected 6 dB noise rise corresponds to 75 % loading in the network. Higher loading may lead to an unstable network.

For macro cell simulations three different layouts have been considered: co-sited, intermediate and worst-case layout. As the co-site case is seen as a trivial case from an interference point of view, it has been neglected in the simulations. In the other two cases base stations are placed in a hexagonal or rectangular grid separately for both operators. In the worst-case cell layout, the second operator's base stations are always in the cell border of the first operator's base stations. In the intermediate cell layout, the second operator's base stations are always in the middle of the first operator's cells. Different macro-cell layouts are depicted in FIGURE 3.3-2. In case of hierarchical cell structures 72 micro-cells locate in the middle of the simulated area as depicted in FIGURE 3.3-3. The number of macro-cells is five, but the data is collected from only those base stations that overlap with micro-cells.

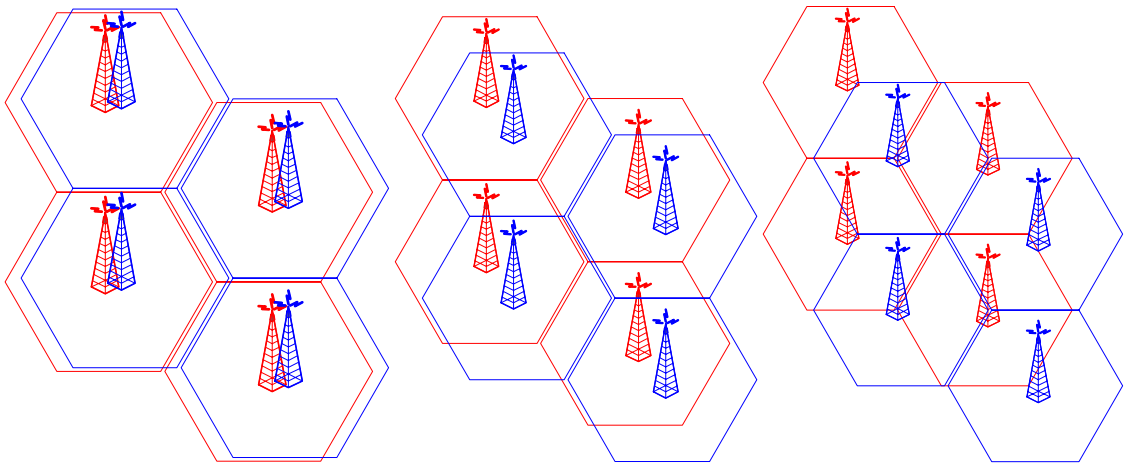

FIGURE 3.3-2. Simulated macro-cell layouts. Co-sited on the left, intermediate in the middle and worst case on the right.

[11] Capacity with 5 % outage probability corresponds close to the theoretical capacity in an interference-limited network. For capacity calculations see Chapter 3.1.2.

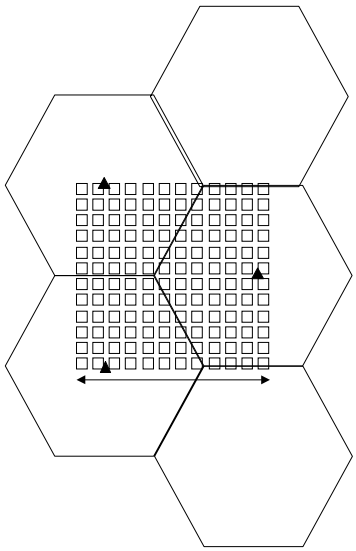

FIGURE 3.3-3. Simulated HCS cell layout.

3.3.3 Adjacent Channel Interference Simulations

3.3.3.1 *Multi-Operator Scenario with High Loading*

Simulations are performed separately for the uplink and for the downlink with different ACIR values. Base stations of both operators are placed in a rectangular grid. Simulations consider the assumed worst-case base station layout with a macro-cell propagation model and high mobile station speed. This situation leads to high mobile station power levels so that SIR-target for the guaranteed signal quality can be fulfilled. Using high powers near to the adjacent frequency band operator base station will cause large amounts of adjacent channel interference for this cell.

In the uplink, the interference distribution depends on the load as represented in FIGURE 3.3-4 and FIGURE 3.3-5. For low loading, depicted in FIGURE 3.3-4, the interference distribution is narrow as all connections in all cells experience only low levels of interference. For high loading, depicted in FIGURE 3.3-5, the distribution becomes wider. If the cell range is increased, the distributions will become narrow also in the high-load case. The mean interference value remains higher for the high-load case.

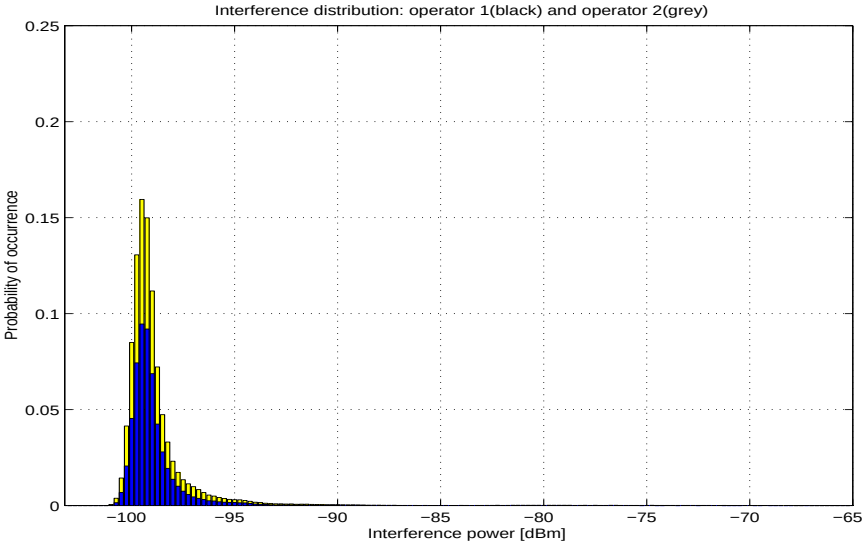

FIGURE 3.3-4. An interference distribution for a low-load case with ACIR 30 dBc for the interference-limited cells.

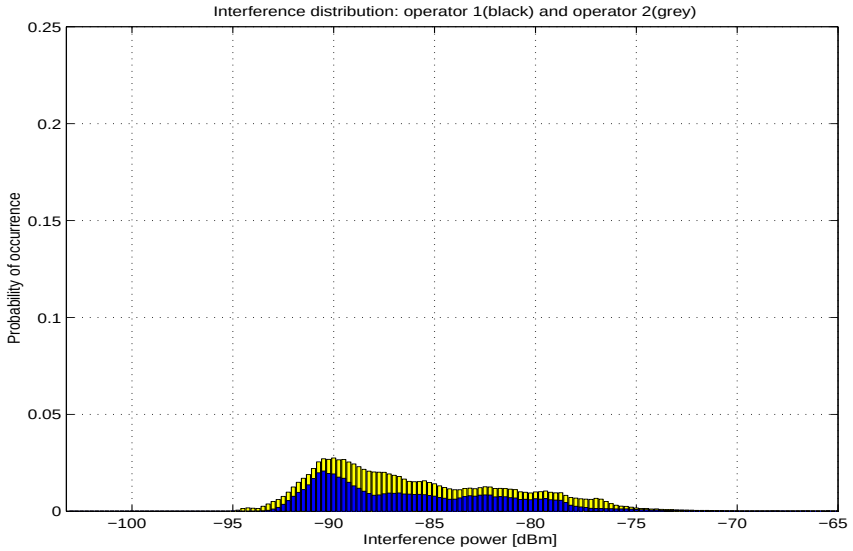

FIGURE 3.3-5. An interference distribution for a high-load case with ACIR 30 dBc for the interference-limited cells.

In FIGURE 3.3-6, the uplink average interference power as a function of load for different ACIR values is presented. The interference level behaves similarly to different ACIR values when loading is increased. The difference in the interference level for ACIR 30 dBc, ACIR 35 dBc and ACIR 40 dBc is within around 5 dB.

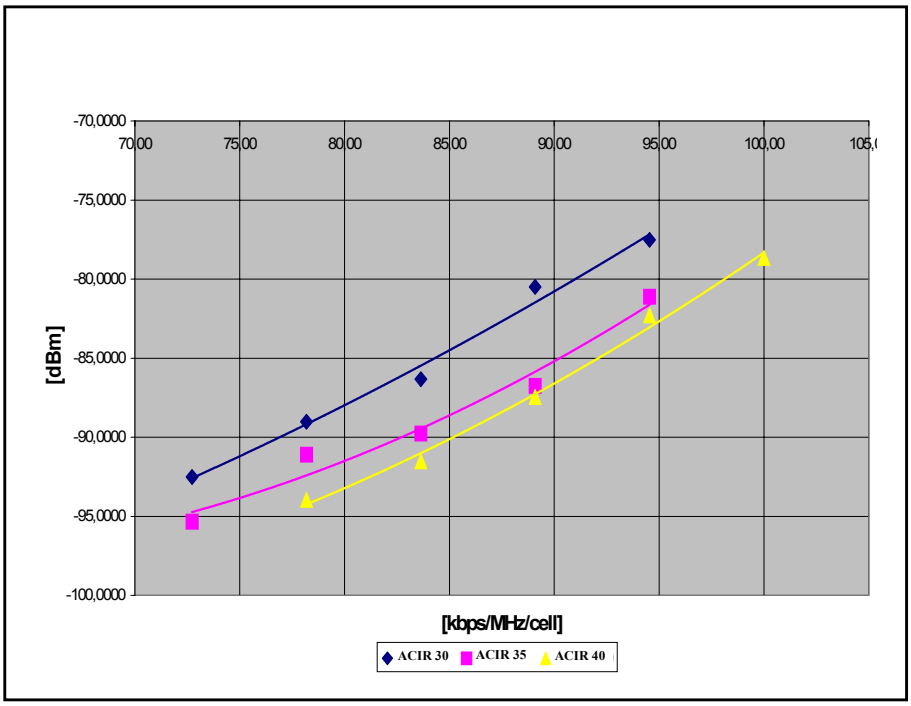

FIGURE 3.3-6. The average interference power as a function of load with different ACIR values for the interference-limited cells.

Outage probability as a function of load for different ACIR values is shown in FIGURE 3.3-7. The outage probability starts rising fast when loading becomes high. From FIGURE 3.3-7 it can be seen that with 5 % outage offered loading is in order of 90 kbps[12]. Further from FIGURE 3.3-6 it can be seen that the interference + noise power for 90 kbps loading is –87 ... -80 dBm. This corresponds to 16 ... 23 dB noise rise that makes the system operate in a highly unstable area. This is not an issue in a static simulation, but in e.g. a dynamic simulation or in a real system this would lead to a possibly unstable system, high call drop-rate and a high number of bad quality calls.

The capacity loss is summarized in TABLE 3.3-3 for two different cell ranges: a medium-size cell is interference-limited (with radius approximately 1800 m) and a large cell is range-limited (with a radius approximately 5400 m). Capacity is given in units of kbps/MHz/cell and the capacity loss is given in percentages compared to the single operator case at the outage probability of 5 %. Capacity has decreased significantly in the range-limited case even without any adjacent channel interference, because of the mobile station's power limits.

As seen from TABLE 3.3-3 adjacent channel interference has some effect on both the interference-limited case and the range-limited case. However, the difference in the capacity loss for ACIR 40 dBc and ACIR 30 dBc is minor. Taking into consideration that the downlink capacity is much more limited than the uplink capacity, it is anticipated that ACIR 30 dBc will be acceptable for the uplink. In the range-limited cells, the ACIR seems to effect more. However, it

---

12 The used SIR target for the service was 6.5 dB

can be clearly noticed that even the ACIR value of 50 dBc does not improve capacity much if compared to the ACIR value of 30 dBc.

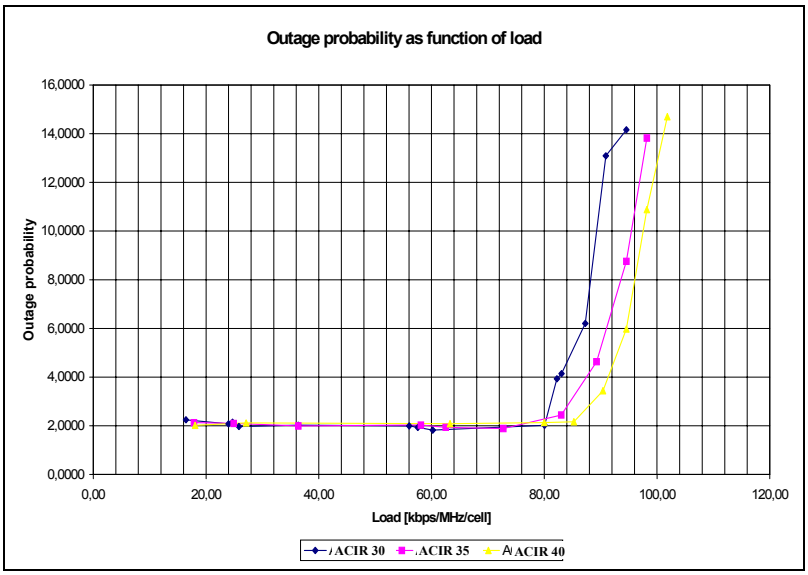

FIGURE 3.3-7. The outage probability as a function of load with different ACIR values for the interference-limited cells.

TABLE 3.3-3. The capacity loss due to the adjacent channel interference in the uplink.

	Capacity [kbps/MHz/cell]		Capacity loss due ACI [%]	
Cell radius	Interf. limited	Range limited	Interf. limited	Range limited
Single operator	99.8	71.5	-	-
ACIR 50 dBc	92.8	55.1	7	23
ACIR 45 dBc	92.8	55.1	7	23
ACIR 40 dBc	90.8	53.6	9	25
ACIR 35 dBc	88.8	52.1	11	27
ACIR 30 dBc	87.8	50.1	12	30

Downlink outage probability as a function of load is described in FIGURE 3.3-8. Outage probability behaves similarly for ACIR values of 40 dBc, 50 dBc and beyond. Outage probability, as a function of load, starts rising with a lower load when the ACIR value is 30 dBc. This implies an insignificant capacity loss with ACIR values equal to and higher than 40 dBc and some capacity loss with ACIR value of 30 dBc. ACIR values lower than 30 dBc would cause unacceptable capacity loss. Taking into account that the downlink capacity is more limited than the uplink capacity, it is important that the adjacent channel interference does not contribute too much to the interference. Therefore, it is anticipated that the ACIR value of 30 dBc to 35 dBc will be acceptable for the downlink. The selected value in 3GPP is 33 dBc.

The capacity loss is summarized in TABLE 3.3-4 for the interference limited medium-size cell case and the coverage limited large cell case. The

capacity is given in units of kbps/MHz/cell and the capacity loss is given in percentages compared to the single operator case at the outage probability 5 %.

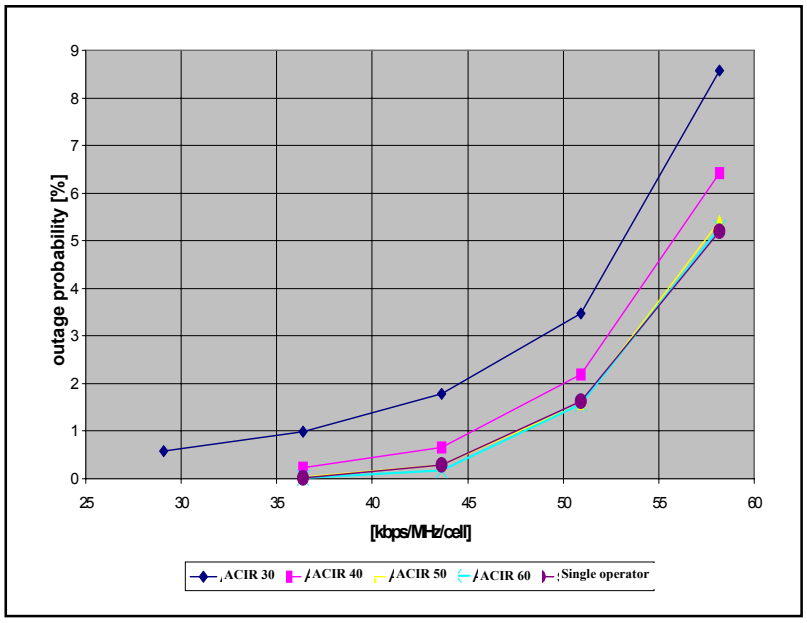

FIGURE 3.3-8. The outage probability in the downlink as a function of load with different ACIR values for the interference-limited cells.

TABLE 3.3-4. Capacity loss due to adjacent channel interference in the downlink.

	Capacity [kbps/MHz/cell]		Capacity loss due to ACI [%]	
Cell radius	Interf. Limited	Range limited	Interf. limited	Range limited
Single operator	57.8	55.1	-	-
ACIR 60 dBc	57.6	54.4	1	2
ACIR 50 dBc	57.4	54.5	1	2
ACIR 40 dBc	55.8	53.8	4	3
ACIR 30 dBc	53.2	50.9	8	8

3.3.3.2 *Multi-Operator Scenario with Realistic Loading*

When the effect of adjacent channel interference is simulated it is important to use realistic parameters. One such parameter is network loading in the uplink. Interference having the source at the adjacent channel is seen as an increase in load at the desired channel. If the used loading point is already very high, the effect of adjacent channel interference is also more significant. This can be seen from FIGURE 3.3-9, which shows a CDMA pole curve. CDMA pole curve can be generated according to [Sha94] as

$$r = \frac{1}{1-\eta}, \tag{3.3-9}$$

where r is noise rise over thermal noise and η is system loading having values from 0 to 1. If network loading is realistic (in the order of 3–6 dB noise rise), a small increase in loading causes a small increase in interference. Correspondingly, if the network loading is high (e.g. 20 dB noise rise), a small increase in loading will cause a remarkable increase in interference. In addition, it should be noticed that too high loading imply high mobile stations output powers. Therefore this effect would further emphasize the effect of adjacent channel interference on the system capacity when the load is too high. Here we can assume that the mobile station's power amplifier ACLR dictates uplink adjacent channel interference and the base station selectivity can be neglected.

TABLE 3.3-5. Important simulation parameters for ACI simulations.

Parameter	**Value**
MCL macro	70 dB
MCL micro	53 dB
Macro-to-Macro BS distance	1000 m
Micro-to-Micro BS distance	180 m
Offset between Macro cell BSs of different operators	577 m or 289 m
Offset between Macro and Micro base stations (in HCS)	See FIGURE 3.3-3
MS maximum power	21 dBm
MS power control range	65 dB
Macro-cell downlink E_b/N_0	7.9 dB
Macro-cell uplink E_b/N_0	6.1 dB
Micro-cell uplink E_b/N_0	3.3 dB

In the previous chapter capacity loss in the macro-to-macro scenario was simulated with about 16–20 dB noise rise that corresponds to 98–99 % loading from the WCDMA pole capacity. A real WCDMA system easily becomes unstable (even without adjacent channel interference) with this kind of loading as discussed previously. In this chapter most of the multi-operator macro-to-macro uplink simulations are accomplished with 6 dB noise rise criterion as proposed in [TR25.942].

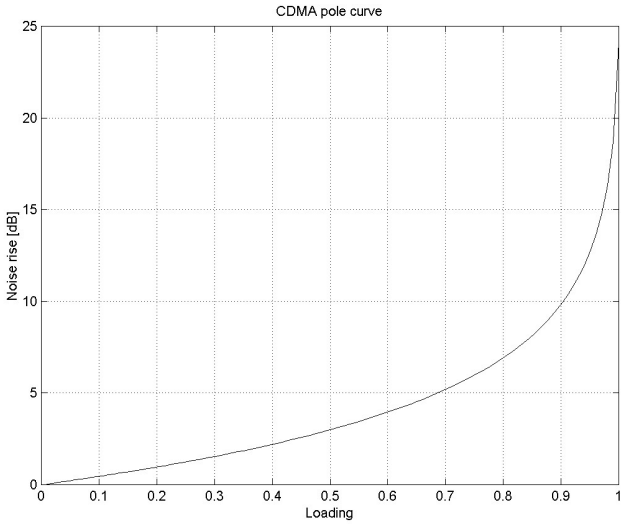

FIGURE 3.3-9. CDMA pole curve according to equation (3.3-9). Noise rise is given in decibels.

From the power amplifier point of view, maximum output powers are the most challenging to implement and have significant effects on the size of the WCDMA terminal due to thermal heating issues [Lil99a]. A practical power amplifier behaves in a way that, as the power is decreased from the maximum power level (i.e. backoff increased), also the ACP (or ACLR) improves significantly as shown in FIGURE 3.3-10. The used modulation method is HPSK (Hybrid Phase Shift Keying) that is a derivative from QPSK. HPSK is designed to reduce peak-to-average ratio of the modulation scheme [Lil99a].

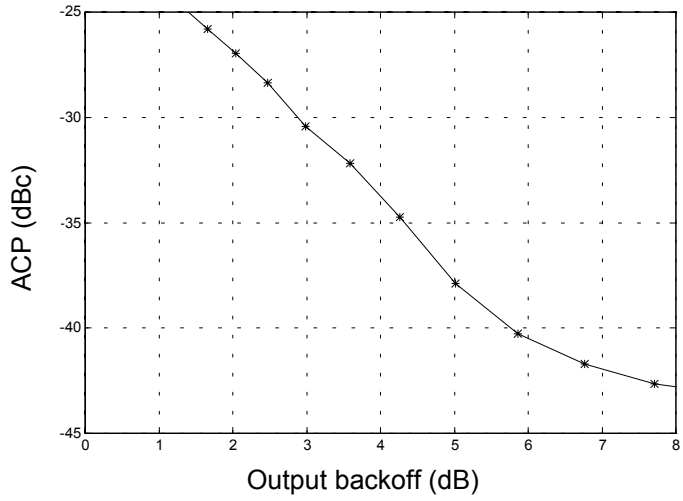

FIGURE 3.3-10. The effect of PA backoff for WCDMA HPSK modulation scheme [Lil99a].

As can be seen from FIGURE 3.3-10, ACP improves 3–4 dB as the output power is decreased 1dB. However, the improvement depends on the power amplifier characteristics and also ACP improvement "compresses" after a certain backoff. In order to make sure that the practical power amplifier really behaves as modelled in the simulator, some margin is added to the ACLR improvement. In

this chapter an additional power amplifier model, called *practical* PA *model*, is modelled in the following way: ACLR improves by 5 dB after the mobile station output power is decreased by 4 dB from the maximum transmission power. After that the ACLR remains the same.

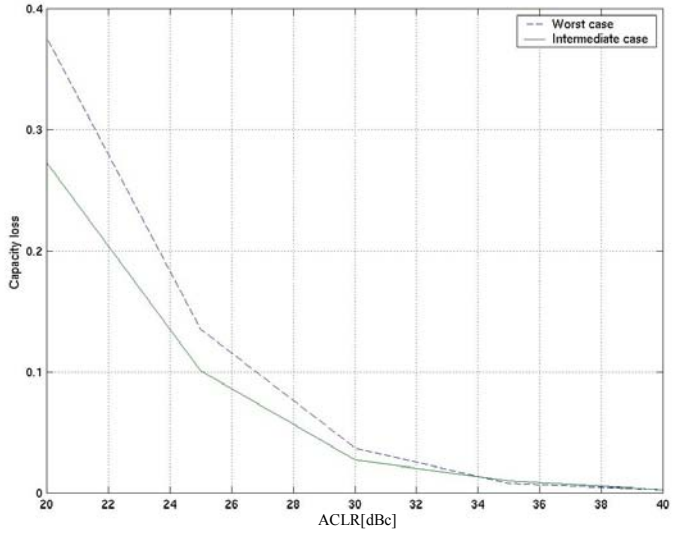

FIGURE 3.3-11. Capacity loss for 8 kbps service with worst-case cell layout (dotted line) and intermediate case cell layout (solid line).

In FIGURE 3.3-11 the capacity loss due to adjacent channel interference for 8 kbps service is shown. Simulation parameters are shown in TABLE 3.3-5. Simulations are executed with an average noise rise of 6 dB, that is, first a single operator network is loaded until 6 dB noise rise is reached and then the multi-operator capacity is also measured with an average of 6 dB noise rise for different ACLR values. Simulations show a modest capacity loss of 2–3 % for ACLR of 30 dBc or higher, while for high load case capacity loss was 12 %. The capacity loss is also studied for the noise rise criteria of 3 and 10 dB. Simulations show very small differences between results obtained for the studied loadings. This is an unexpected result: a priori it was expected that lower capacity loss would occur for lower loading. The reason for this observation is that when the load is 3–10 dB, the system is still operated in the stable area of CDMA pole curve. However, when simulating the system with 5 % outage, loading is as high as 15–20 dB in terms of noise rise. Then the system is operated in the highly unstable area of the pole curve; therefore, also higher capacity loss can be seen due to adjacent channel interference.

FIGURE 3.3-12 shows simulation results for the previously described *practical* PA *model*. As can be seen now 25 dBc ACLR gives the same capacity loss for the worst-case layout scenario as 30 dBc previously. When using the practical power amplifier model 30 dBc ACLR does not introduce any capacity loss, since the mobile stations seldomly use their maximum power that ACLR at maximum power has a low impact on the capacity. FIGURE 3.3-13 gives an example of mobile station transmission power distribution. As seen the highest mobile station powers are rarely used. It can be concluded that mobile station

ACLR at the highest power levels does not have a significant effect on the system capacity.

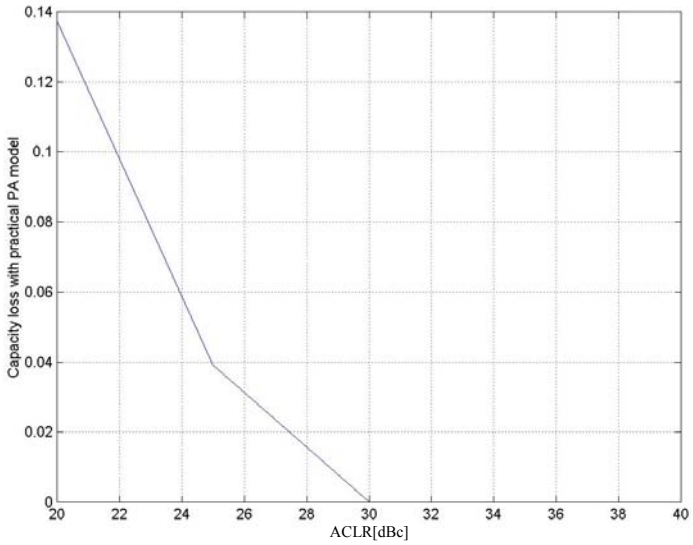

FIGURE 3.3-12. Capacity loss using practical PA model and worst-case layout.

Simulation results in FIGURE 3.3-11 and FIGURE 3.3-12 show that capacity loss is modest on average. However, concern is that some base stations suffer more from adjacent channel interference than others. It could even happen so that some base stations are blocked while others are lightly loaded. Simulations are carried out to find out how much noise rise deviates at different base stations and for different simulation snap-shots. FIGURE 3.3-14 shows the simulation results for the noise rise deviation. The CDF (Cumulative Density Function) of the noise rise shows that with 20 dBc ACLR the observed noise rise deviates significantly. However, when ACLR is 30 dBc, 40 dBc and 1000 dBc noise rise deviation is almost the same. From these simulations it can be concluded that ACLR of 30 dBc causes a similar noise rise behaviour than occurs in a single operator network.

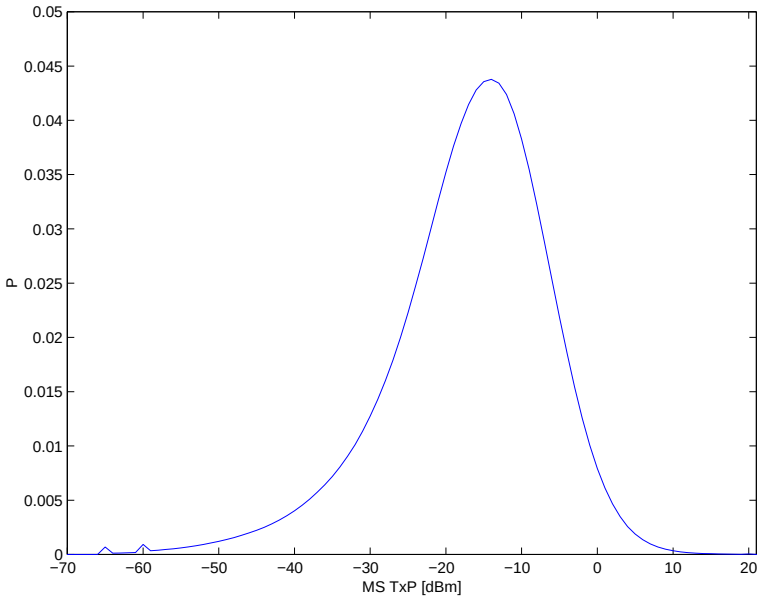

FIGURE 3.3-13. An example of mobile station TxP PDF. Minimum power not limited.

Although simulations do not show a high noise rise it is still possible that such a scenario occurs where the mobile station is transmitting with its full power near the other operator base station. To cope with these "catastrophic" cases it is beneficial to specify the mobile station selectivity so loose that adjacent frequency downlink signal blocks the mobile station before it causes catastrophic problems for adjacent channel in the uplink [Nok98b].

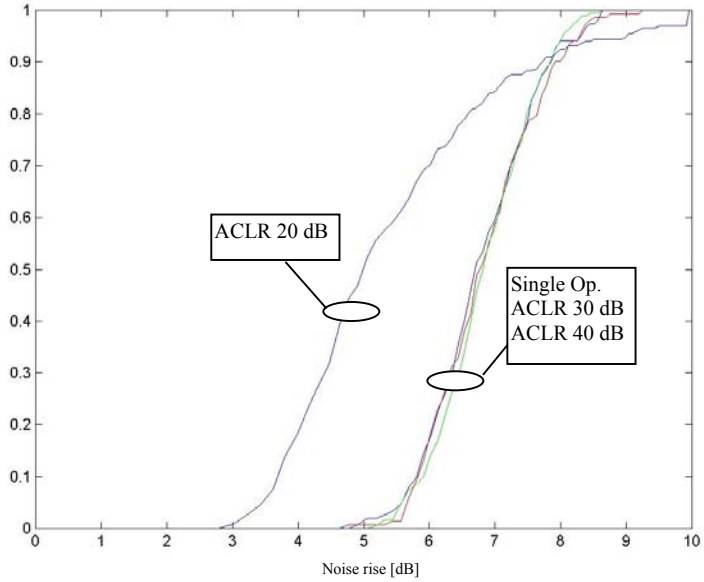

FIGURE 3.3-14. Cumulative density function for ACLR of 20, 30, 40 and 1000 dBc. X-axis represents the noise rise in decibels.

In the downlink adjacent channel interference is mainly due to ACS of the mobile station and ACLR due to the base station power amplifier can be thus

neglected. In the downlink the system capacity loss is simulated with 5% outage criterion. In the downlink it is possible to use higher loading than in the uplink, since base station transmission power can be controlled by the RAN to keep the system stable. FIGURE 3.3-15 shows the simulation results for the system capacity loss in the downlink. Simulations show a small capacity degradation for ACIR 30 dBc or higher.

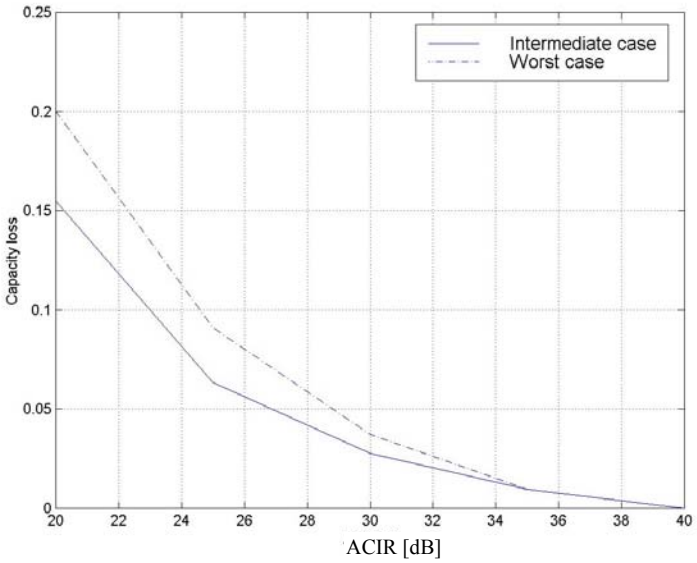

FIGURE 3.3-15. Downlink capacity loss as a function of ACIR.

Unfortunately, too loose ACIR requirement can introduce "outage areas" near the other operator's base station. A possibility to reduce the outage area is to accomplish IFHO (Inter-Frequency HandOver) to other carriers before the call is blocked due to a high power adjacent channel signal. The IFHO procedure can be activated in the following way: the mobile station measures the adjacent channel signal level in the *uplink compressed mode*. When the level of the adjacent channel signal is high enough compared to its own channel signal, the mobile station knows that the call will be dropped if nothing is done. At this point the mobile station signals the network IFHO command or measurement report that triggers the IFHO decision in RNC. For more about the compressed mode and the inter frequency handover see Chapters 4.5 and 4.4.3, respectively.

3.3.3.3 *Hierarchical Cell Structure with Realistic Loading*

Since in the micro-cell scenario the minimum coupling loss can be as low as 53 dB, a single user transmitting with its minimum power[13] near to its own micro-cell base station can cause a noise rise higher than 6 dB. If the admission threshold is 6 dB one user can block the whole cell. To overcome this problem there are three different solutions: 1) higher noise rise has to be allowed, 2) micro-cell base stations are desensitised or 3) higher mobile station power control dynamic range is to be used. As discussed in Chapter 4.1.2 the mobile

---

[13] Here power control range of 65 dB is assumed for uplink power control.

station minimum power has been lowered by 6 dB from –44 dBm to –50 dBm to provide more dynamics to power control. Since micro-cells are more isolated than macro-cells (less interference suffered from neighbouring cells), micro-cells can cope with the higher noise rise. To see CDMA behaviour in different environments, a CDMA pole curve is generated as a function of the number of users for the different frequency re-use factors, *F*. *F* equal to 1 corresponds to a single cell, while *F* is equal to 0.9 corresponds to isolated micro-cells and *F* equal to 0.67 corresponds to typical macro-cells. CDMA loading as a function of users, *n*, is given [Sha94]

$$\eta = \frac{(\frac{n}{F} - 1)d}{G_p / (E_b / N_0)}, \tag{3.3-10}$$

where G_P is the processing gain, and *d* is the voice activity (value 1 used in FIGURE 3.3-16). From Equation (3.3-9) and Equation (3.3-10) we get

$$r = \frac{1}{1 - \frac{(\frac{n}{F} - 1)d}{G_p / (E_b / N_0)}}. \tag{3.3-11}$$

FIGURE 3.3-16 shows the resulting CDMA pole curves for different environments according to Equation (3.3-11). When (3.3-11) is derivated we get

$$r' = \frac{\frac{d}{F} \cdot \frac{G_p}{E_b / N_0}}{(G_p \cdot E_b / N_0)^2 - 2 \cdot (\frac{n}{F} - 1) \cdot d \cdot (G_p \cdot E_b / N_0) + (\frac{n}{F} - 1)^2 \cdot d^2}. \tag{3.3-12}$$

In FIGURE 3.3-17 *r′* is shown as a function of noise rise. *r′* depicts the speed of change in noise rise. As can be clearly seen from FIGURE 3.3-17 higher noise rise can be allowed for micro-cells than for macro-cells.

Typically micro-cells are planned to be interference limited rather than noise limited. Therefore, receiver desensitisation is applicable with micro-cells even though it reduces the cell range. In [TR25.942] 20 dB of noise rise criterion is used for the micro-cells (receiver desensitisation or power control range widening are not considered in this study). Loading for the micro-cell and macro-cell layers was selected so that the mean noise rise reaches pre-defined value: 20 dB for the micro-cell layer and 6 dB for the macro-cell layer. To reach such a condition several iterations have to be done so that proper loading fulfilling the noise rise requirement for both layers is reached. The number of users in the micro-cell layer is significantly higher than in the macro-cell layer. This is because the E_b/N_0 requirement for micro-cells is lower and the number of micro-cell base stations is much higher than the number of macro-cell base stations.

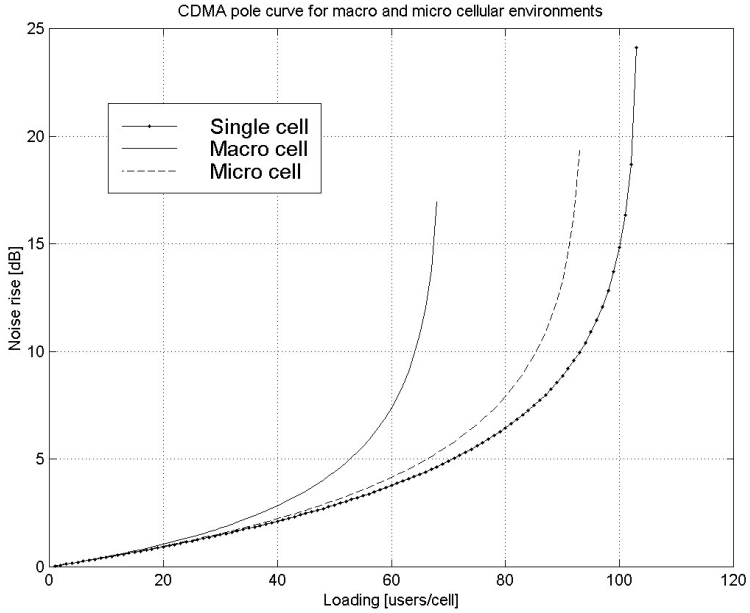

FIGURE 3.3-16. CDMA pole curve for a single cell, for a micro-cell and a macro-cell according to Equation (3.3-11). E_b/N_0 value of 7 dB was used for Equation (3.3-11). Noise rise is drawn in decibels.

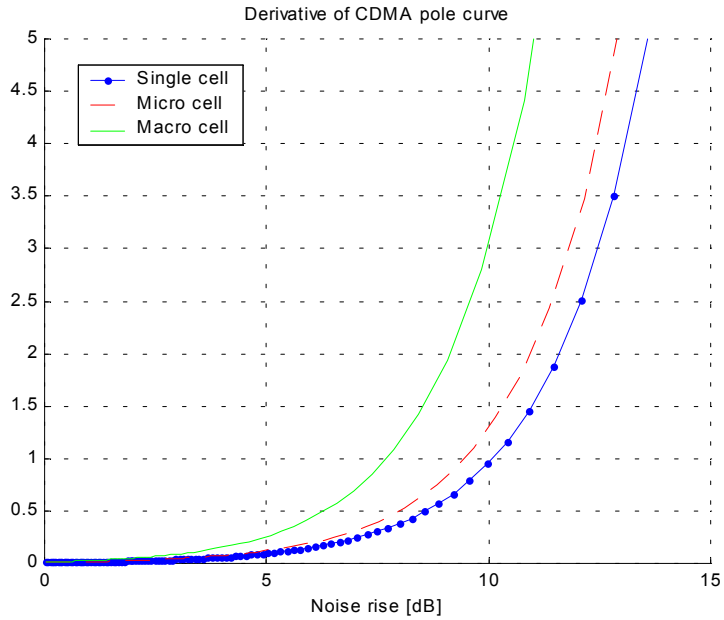

FIGURE 3.3-17. Derivate of noise rise as a function of noise rise.

FIGURE 3.3-18 shows the micro-cell, the macro-cell and the total uplink capacity for 8 kbps service in the HCS scenario. FIGURE 3.3-19 shows the corresponding capacity loss. As seen from the figures, capacity is not very sensitive to ACLR – for ACLR higher than 20 dB capacity loss is very small. Surprisingly the macro-cell capacity is more sensitive for the adjacent channel interference than the micro-cell capacity. It was expected that macro-cell users far away from the serving base station and near to the interfered micro-cell base station are using very high transmission powers and thus causing capacity loss

in the micro-cell layer. Simulations show, however, that the micro-cell capacity remains good while the macro-cell performance suffers more from adjacent channel interference. This is due to the fact that the number of interfering macro-cell users is so small that adjacent channel interference generated by them is negligible. On the other hand, the number of micro-cell users is very high thus they generate high adjacent channel interference for the macro-cell base stations.

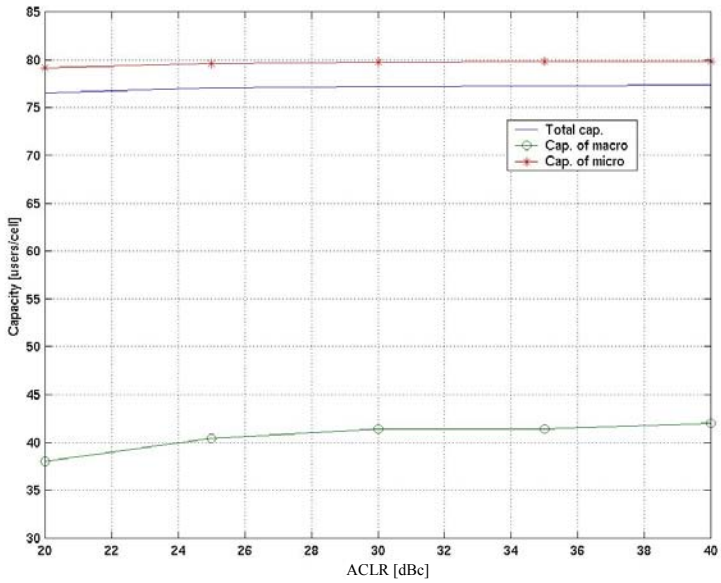

FIGURE 3.3-18. Uplink capacity for the HCS scenario.

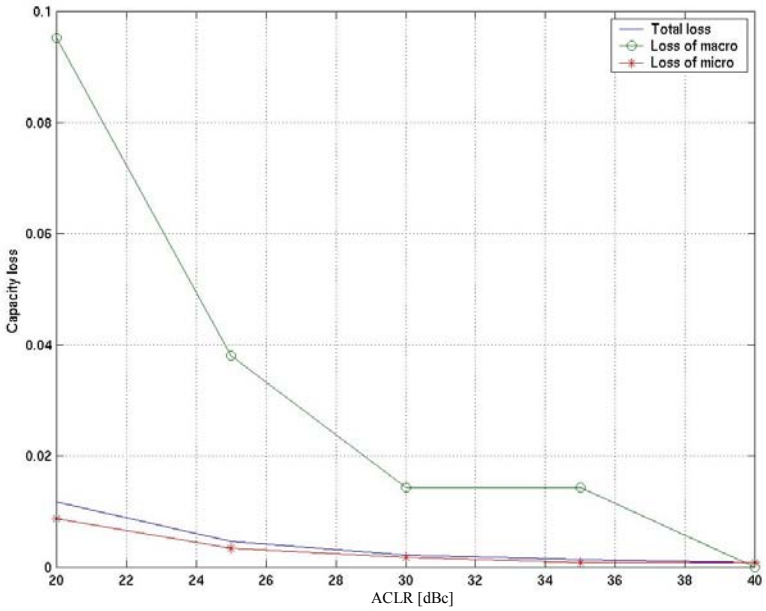

FIGURE 3.3-19. Uplink capacity loss due to ACI for the HCS scenario.

In FIGURE 3.3-20 the relative downlink macro-cell capacity is given as a function of relative micro-cell load. In the figure, loading equal to one can be interpreted as a single operator capacity. The x-axis is the load of the micro-cell layer and y-axis is the load of the macro-cell layer when the outage probability is 5% in both layers. The simulated maximum capacity of the micro-cell layer corresponds to 225 users/cell. In WCDMA only 128 code channels exists in the downlink thus the maximum number of users is limited to 128 per cell. This corresponds to 60% of simulated micro-cell layer capacity. When all code channels of the micro-cell base stations are in use, the macro-cell layer capacity loss is about 17 %, 12 %, 4 % and 1 % for ACIR 33 dBc, 35 dBc, 40 dBc and 45 dBc, correspondingly. When considering these results, one should keep in mind that network planning was not optimised. By placing base stations in better places the performance of a network could be improved. By using inter-frequency handover capacity loss can be lowered to 1 % level, see Chapter 4.4.3.

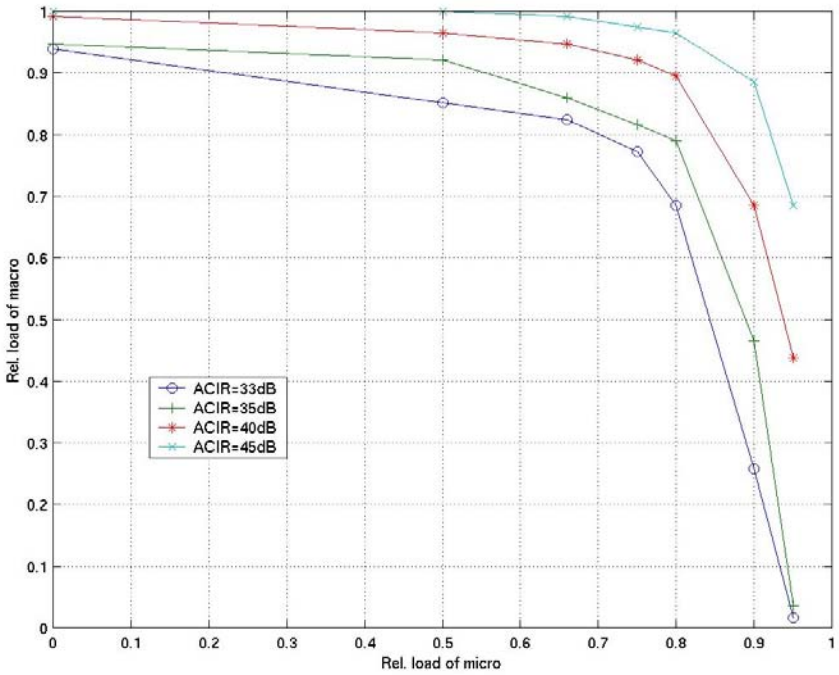

FIGURE 3.3-20. Downlink HCS simulations. Relative macro-cell capacity given as a function of relative micro-cell loading.

3.4 Discussion

In this chapter uplink and downlink capacity and the network effects of adjacent channel interference were studied.

According to this analysis multi-user detection WCDMA system provides considerably higher uplink capacity than a conventional DS-CDMA (Direct Sequence CDMA) RAKE receiver system for both macro- and micro-cellular environments. The capacity gain depends on the ratio of intra-cell interference

to inter-cell interference, and therefore the micro-cellular environment offering high cell isolation gains more from the use of multi-user detection. The simulated capacity gain in the selected operation point from multi-user detection is 3.7 dB and 2.9 dB for the micro-cell and macro-cell environments, respectively. An alternative solution for capacity enhancements is, for example, the use of adaptive antennas, which requires RF hardware, while with the use of multi-user detection for capacity enhancement only baseband hardware is modified. The required baseband processing may be, however, excessive. The spreading code cross-correlations must be updated every time the mutual tap delays change. In an extreme case the whole cross-correlation matrix needed by the multi-user detection has to be updated for every symbol. In addition to cross-correlations, interference estimates need to be computed at symbol rate. As the aggregate symbol rate depends on the cross-correlations and differ each multipath, K x L (K = no of users, L = number of multipath taps per user) interference estimates, each consisting of K x L – 1 additions and multiplications, needs to be calculated [Eri98a]. The given complexity analysis is an example applicable for PIC receiver.

From the downlink studies it can be concluded, that in the macro-cell environment it is important to cancel intra-cell interference that is due to multipath propagation. This can be done by using orthogonal codes or interference cancellation receivers. Cancelling of inter-cell interference provides only a marginal gain from the capacity point of view, although for a single mobile unit the inter-cell interference cancellation can bring large quality improvement as the resistance towards unideal handover conditions increases. The macro diversity, i.e., soft handover is important from the capacity point of view in the micro-cell environment where the number of separable multipaths is small, as in the macro-cell environment several separable multipaths already exist and thus the gain from macro diversity is small. The same applies for the mobile station antenna diversity, as the short delay spread micro-cellular channel offers only limited diversity for the RAKE reception. From the complexity point of view the use of antenna diversity adds additional RF parts to the mobile station while the interference cancellation keeps the RF as it is and adds complexity to the baseband processing. Which is then more economical in terms of cost vs. gain depends on the relative cost between the additional RF parts and the baseband processing power. As was discussed above for the uplink direction, baseband implementation of interference cancellation may be excessive. The simulated soft handover gain is 0.4 dB and 2.0 dB in the macro-cell and micro- cell environments, respectively. Capacity gain due to orthogonalization in the downlink is 0.8 dB and 4.5 dB for the macro-cell and micro-cell environments, respectively. Capacity gain from the inter-cell interference cancellation is less than 0.7 dB in the macro-cell environment and less than 0.2 dB in the micro-cell environment.

System loading has a significant impact on the adjacent channel interference simulations. In this chapter system loading was studied and practical loading was used with simulations. Also a more realistic power amplifier model was presented to model the adjacent channel interference in

the uplink. In 3GPP adjacent channel interference parameters are selected so that in the uplink the mobile station ACLR and in the downlink the mobile station ACS are the same (33 dBc). This ensures that the call drops due to downlink reasons before any severe interference is caused for another operator in the uplink. Possible dead-zones near to other operator base stations are solved by utilizing inter-frequency handovers. According to the simulation results, the adjacent channel interference requirement in the multi-operator scenario should be in the order of 30 dBc for both the uplink and downlink. If the realistic power amplifier model was used even a less stringent adjacent channel requirement could be accepted for the uplink. According to simulations adjacent channel interference requirement of 30 dBc seems to be acceptable also for a hierarchical cell structure scenario.

4 WCDMA RADIO RESOURCE MANAGEMENT PERFORMANCE

4.1 Power Control

In WCDMA three power control loops are used – the open loop power control, the inner fast closed loop power control and the outer quality loop power control. The open loop power control is used when establishing a new call or transmitting packets in the common packet channels. Generally speaking, the open loop power control is needed when there does not exist any dedicated control channels between the base station and the mobile station. Setting the power in case of the open loop power control is based on pathloss estimates made by the mobile station.

When the control channels are setup in dedicated mode between the base station and the mobile station, the fast closed loop power control can be used. In the base station, the quality of the received signal from the mobile station is estimated by using SIR-estimation algorithm and compared together with the quality target provided by the outer loop power control algorithm. If the quality is below the required, transmission power is increased by a fixed step and vice versa. By doing so, it tries to keep the quality of the received signal as close as possible to the target. This ensures sufficient FER, BLER (BLock-Error-Rate) or BER for the connection. Fast closed loop power control frequency is 1500 Hz, thus it is able to cope fast fading if the mobile station speed is low or moderate (up to 50 km/h). In case of faster mobile stations, the closed loop power control is not able to compensate for fast fading, but only slow fading and changes in interference levels. Then the quality loop power control automatically adds a margin for fast fading by increasing the SIR-target.

If the same quality target is assumed for each user, received power from each user should be at about the same level. In case of no power control, received power from near-by users would exceed the received signal power from distant users by several decibels due to different distance attenuation. In practice, those near-by users would block signals from distant users. This is so called near-far problem in CDMA-systems. By employing the fast closed loop

power control received signal levels from each user can be controlled and the near-far effect avoided.

In the downlink direction, when the base station is transmitting to the mobile station, the problem is different; now intra-cell interference propagates via exactly the same paths as the desired signal. In addition, intra-cell interference propagating via the same multi-paths remains orthogonal in the reception. Due to that no closed loop power control is needed even fast fading causes fluctuations to its own signal – interfering signal experiences exactly the same fading process. In the downlink fast closed loop power control is needed to control interference coming from the other cells (inter-cell interference) and ensure sufficient received power level in cell border. In cell border, adjacent-cell interference is more dominant, since shorter distance to the interfering base stations and higher distance to the serving base station. Also the thermal noise level has its impact on cell border since the received power from the serving base station is closer to level of noise and fluctuations in signal level due to fast fading.

The quality of the connection is adjusted with the outer quality loop power control. The outer loop power control is used to set SIR-target for the closed loop power control. Different SIR-targets are needed in different multipath environments and for different speed mobile terminals. A multipath environment and mobile terminal speed can change at any time during the course of the call. A well know algorithm, a so-called jump-algorithm is presented in [Sam97a]. In the jump-algorithm SIR target is increased by step $k \cdot d$ whenever a frame error occurs. If a frame is correctly received, SIR target is decreased by step d. It is shown in [Sam97a] that this algorithm leads to FER of $1 / (k + 1)$.

In the following the fast closed loop power control and the outer loop power control are investigated. First the network effects of the fast closed loop power control and requirements for the power control dynamic range are investigated. Then, the outer loop power control network effects are discussed.

4.1.1 Network Effects of the Closed Loop Power Control

In this chapter the effect of inter-cell interference in different channels with the uplink fast closed loop power control is analysed. Relative cellular capacities with different amounts of diversity are evaluated based on the numerical calculations as well as on network simulations. Fast fading and fast closed loop power control are modelled in the semi-static network simulator presented in Chapter 2.5. It is shown that even if a system employs an ideal fast power control, diversity has a considerable effect on the cellular capacity. This study was first presented in [Hol97]. Later on, thorough investigations of the fast closed loop power control network effects were made in [Sip99a, Sip99b].

In the uplink of a WCDMA cellular system the fast closed loop power control attempts to keep the received power levels equal. This is the optimum case for a single cell performance. Even if the channel experiences fast fading, enough fast power control offers such a link performance that is close to the

performance in AWGN (Additive White Gaussian Noise) channel. In a cellular system, however, fast closed loop power control together with fast fading causes the transmission power to have high peaks. Since the propagation channel from the mobile station to other base stations is uncorrelated with the transmission power levels, the average received interference power at the other base stations is higher than without fading and power control. FIGURE 4.1-1 illustrates the increased interference to the neighbouring base stations.

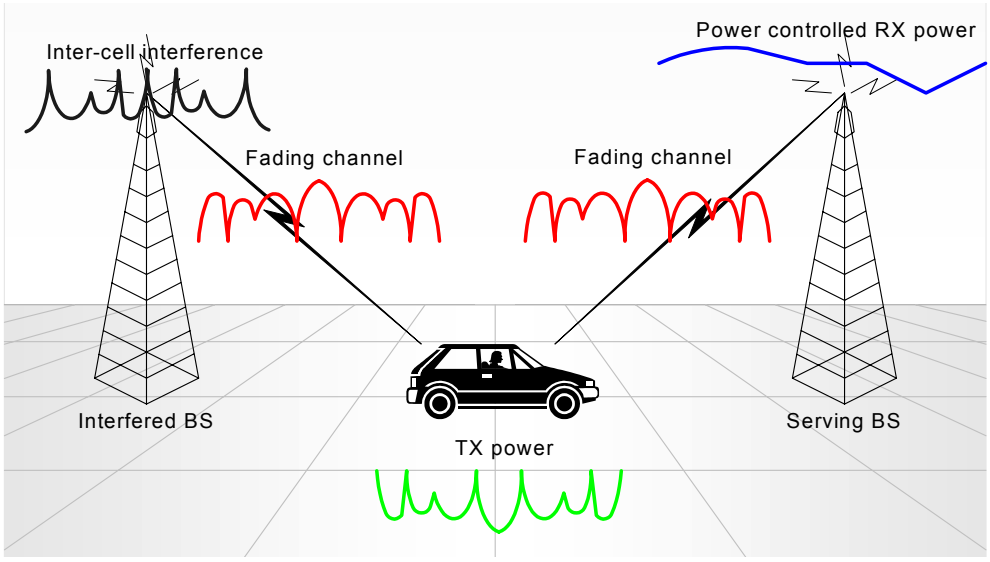

FIGURE 4.1-1. Increased interference from the mobile station to the neighbouring base station due to fading channel and the fast closed loop power control.

4.1.1.1 *Analytical Approach*

In [Hol97] an increase on average inter-cell interference is analysed. It is assumed that fast fading in the uplink is compensated by the WCDMA fast closed loop power control, i.e. the received signal power is constant within the limited dynamics of the power control. For the reception at the own base station, this is the optimum case. Handovers are not considered; instead it is assumed that the mobile station is connected to the closest base station.

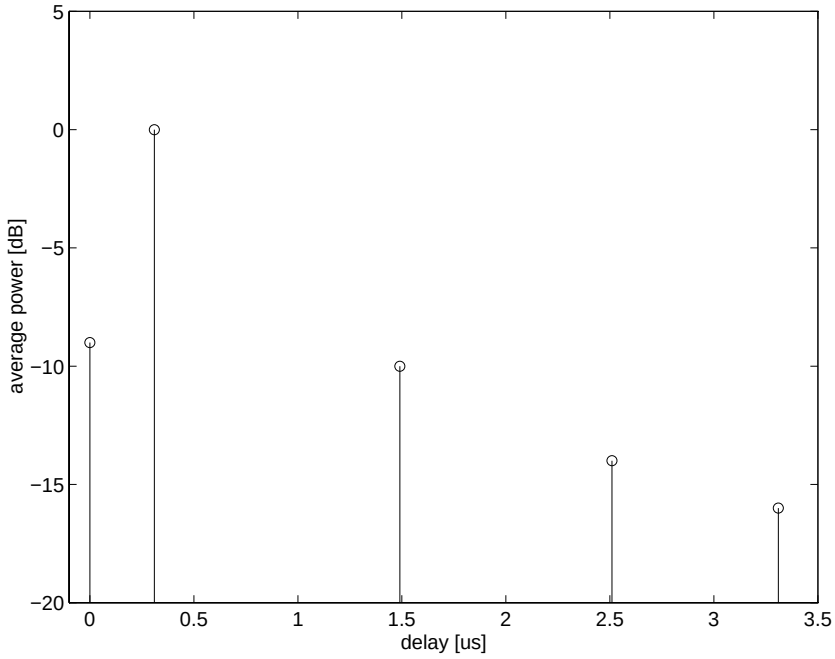

FIGURE 4.1-2. Impulse response of ATDMA macro cell channel.

The average transmission powers are calculated in AWGN channel, in 1-tap Rayleigh fading channel, in 2-tap Rayleigh fading channel (2 equally strong taps on average), in 4-tap Rayleigh fading channel (4 equally strong taps on average) and in ATDMA macro cell channel ([Str93]) with and without base station antenna diversity. The impulse response of the ATDMA macro-cell channel model used is shown in FIGURE 4.1-2. The used bandwidth is so high that all the multipath components in ATDMA macro-cell channel model can be resolved. A maximal ratio combining of multipath components is assumed. The 2-tap and 4-tap Rayleigh fading channels can be considered either as multipath channels or as a case with antenna diversity. The calculated increase in average transmission powers is shown in TABLE 4.1-1.

TABLE 4.1-1. Increase in average transmission power ΔP_{tx} [Hol97].

Channel	Increase in TXP
AWGN channel	0 dB
1-tap Rayleigh fading channel	10.1 dB
2-tap Rayleigh fading channel (equal power taps)	3.0 dB
4-tap Rayleigh fading channel (equal power taps)	1.2 dB
ATDMA macro-cell channel	2.5 dB
ATDMA macro-cell channel with antenna diversity	1.3 dB

Next, the effects of power control on inter-cell interference and system capacity are analysed. The maximum number of simultaneous users N on one carrier in a cellular WCDMA system can be calculated as in Chapter 3.1

$$N = F\left[G_p \left(\frac{E_b}{N_0} \right)^{-1} + 1 \right]. \tag{4.1-1}$$

The increase in inter-cell interference is equal to the increase in the average mobile transmission power ΔP_{tx} shown in TABLE 4.1-1:

$$\frac{I'_{other}}{I_{other}} = \Delta P_{tx}. \tag{4.1-2}$$

Now, we can obtain F' as

$$F' = \frac{1}{1 + \Delta P_{tx}\left(\frac{1}{F} - 1 \right)}. \tag{4.1-3}$$

In this work F' is assumed to be 55 % in AWGN channel with hexagonal base stations. This value is obtained from the system simulator and this is a typical value for the macro-cell environment. The values for F' in different channels are calculated in TABLE 4.1-2. If we assume in Equation (4.1-1) that the processing gain G_p and the E_b/N_0 requirement do not change between different channels, then $N = F \cdot$ constant. Therefore we have

$$\frac{N'}{N} = \frac{F'}{F}, \tag{4.1-4}$$

which is called relative capacity. The relative capacities N'/N are calculated in TABLE 4.1-2.

TABLE 4.1-2. Relative capacities with different channel models with macro cellular distance attenuation.

Channel model, i.e. amount of diversity	Percentage of interference from own cell mobiles F'	Relative capacities N'/N compared to AWGN
AWGN channel	55 %	100 %
1-tap Rayleigh	11 %	19 %
2-tap Rayleigh	38 %	69 %
4-tap Rayleigh	48 %	87 %
ATDMA macro	41 %	74 %
ATDMA macro with antenna diversity	48 %	86 %

4.1.1.2 *Simulation Analysis*

Next the power control capacity effects are studied by simulations. The used simulation tool is the static simulator presented in Chapter 2.5. The used power control dynamics is 80 dB, which is larger than in the 3GPP WCDMA system and in the calculations above. The mobile station speed is set to be 1.5 km/h corresponding to slowly walking pedestrians. The parameters of the capacity simulation are shown in TABLE 4.1-3.

TABLE 4.1-3. Simulation parameters.

Parameter	Value
Power control frequency	1.5 kHz
Power control step size	1.0 dB
Power control dynamics	80 dB
Mobile speed	1.5 km/h
Active set size in soft handover	3
Handover margin in non-ideal handover	5 dB
Log normal shadowing	Mean 0 dB, STD dev 6 dB
User bitrate	10 kbit/s
Voice activity	100 %

The results of network simulations are shown in TABLE 4.1-4 and compared to non-fading AWGN channel case. The calculated and simulated capacities are compared in FIGURE 4.1-3.

The simulated capacities are lower than the calculated capacities except in the 1-tap Rayleigh fading channel. These differences are due to nonidealities in the power control in the network simulation. The power control step size is fixed and the same in different fading channels. In 1-tap Rayleigh fading channel the power control is not able to track the deepest fades and thus the generated inter-cell interference does not increase as much as with analytical calculations. It should be noted that the SIR target is set to be the same for all capacity simulations and in practice the 1-tap Rayleigh type channel with power control imperfections would require the highest SIR target for power control to achieve a comparable link quality with other cases. In other channels, the power control step size is too large and thus unnecessary power fluctuations increase the interference and resulted into lower capacities.

Increased inter-cell interference needs to be taken into account in the link budget. Headroom for a power increase has to be arranged due to the increased inter-cell interference. Headroom reduces the cell range, thus more base stations are needed to cover the planned area.

TABLE 4.1-4. Simulated relative capacities with different channel models.

Parameter	Value
Channel model	Relative capacities compared to AWGN channel
AWGN channel	100 %
1-tap Rayleigh, hard handover	25 %
1-tap Rayleigh, soft handover	43 %
2-tap Rayleigh	57 %
4-tap Rayleigh	78 %
ATDMA macro	60 %
ATDMA macro with antenna diversity	79 %

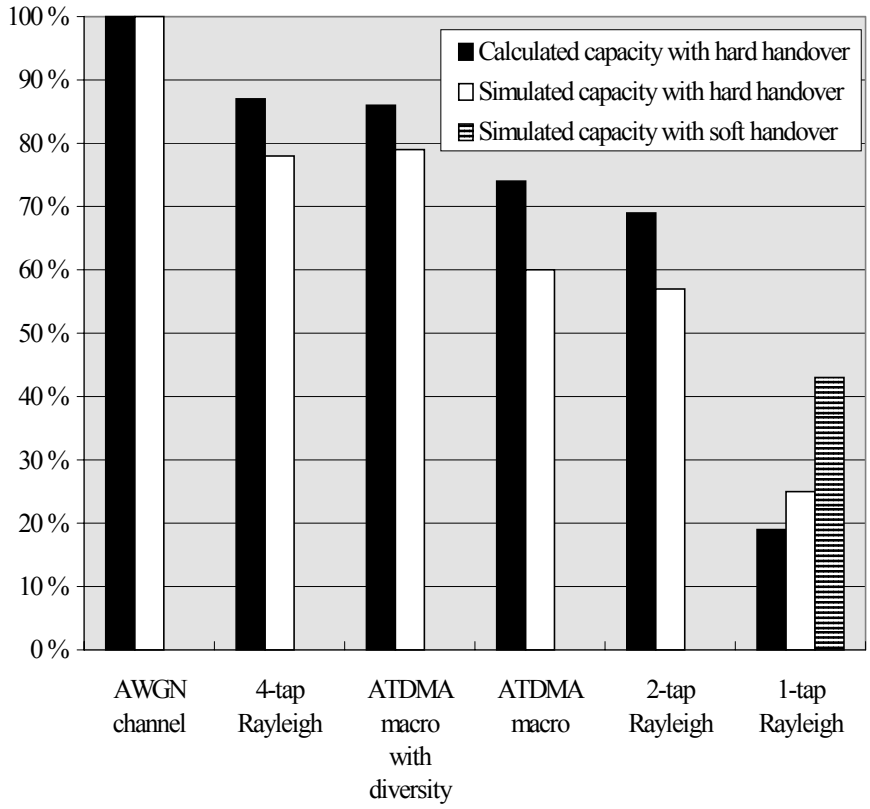

FIGURE 4.1-3. Calculated and simulated relative capacities with different channel models.

4.1.2 Dynamic Range of Closed Loop Power Control

The maximum power for the class-4 mobile station is 21 dBm [TS25.101]. The minimum power was originally -44 dBm leading to 65 dB power control dynamic range. However, from simulations it was noticed that the mobile station minimum power should be even smaller when the mobile station is situated close to the serving base station. Otherwise unnecessary interference could be caused in the base station. Such situations can occur especially in micro-cellular networks where minimum coupling loss can be low. This problem is depicted in FIGURE 4.1-4.

As small mobile station minimum power as possible would be desired from the network performance point of view. Implementation of the mobile

station sets, however, limits for the lowest power levels. In practice minimum power cannot be below -50 dBm, since otherwise the implementation costs would be excessive. Very low minimum output power can be implemented only by using an additional attenuator to limit output power. The attenuator is needed as the oscillating circuit needs a certain minimum currency in order to be stabile.

This chapter investigates the effects of the mobile station minimum power to the system performance. Based on this analysis given originally in [Nok99a, Nok00a and Nok00d] the minimum power requirement was changed in 3GPP.

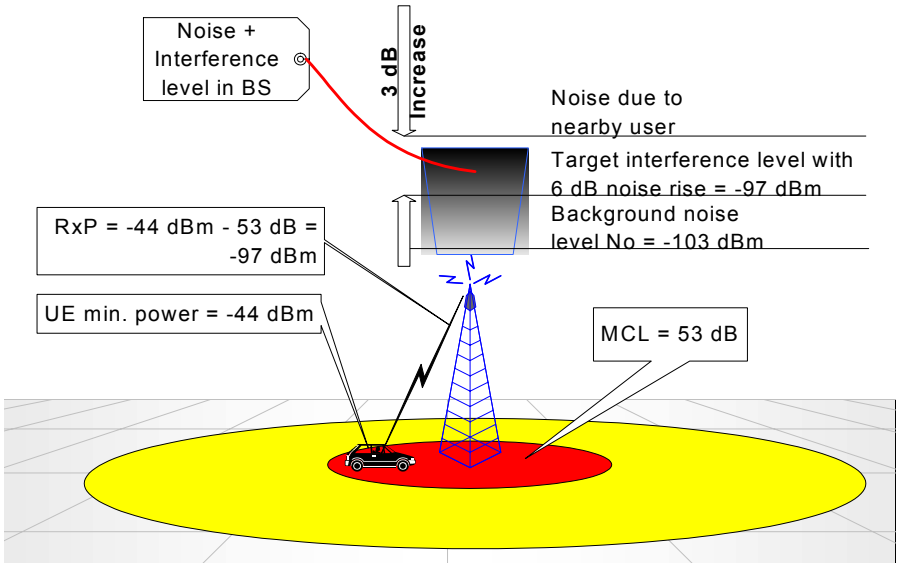

FIGURE 4.1-4. Example depicting how too high mobile station minimum power increases base station interference level.

4.1.2.1 *Minimum Transmission Power Simulations*

Simulation studies are executed in the Manhattan environment with the static simulator presented in Chapter 2.5. Two minimum coupling loss values are used, 53 dB and 70 dB. If the mobile station minimum power can be low enough, the capacity will be higher for lower MCL, see FIGURE 4.1-5. The reason for that is obvious - when MCL is large users near the base station transmit with higher power and can cause larger inter-cell interference.

The simulation results for 70 dB minimum coupling loss are shown in FIGURE 4.1-6 and for 53 dB minimum coupling loss in FIGURE 4.1-7. Both simulations show that the difference in noise rise is negligible with high loading. This is because near base station users have to increase their transmission power due to the increased interference. Thus, they are not using minimum power, and the effect of minimum coupling loss and minimum power is not valid anymore.

If minimum transmission power is set very high, noise rise will also be high. However, the system becomes unstable at the same loading for all minimum transmission power (with loading of 140 users/cell in FIGURE 4.1-7).

This indicates that in micro-cells the noise rise target should be set higher – in case of –44 dBm minimum power, as high as 30 dB. However, if the network was planned to be range limited rather than capacity limited, some problems can been seen; high minimum transmission power causes high background noise rise that is seen directly in the link budget as shorter cell range.

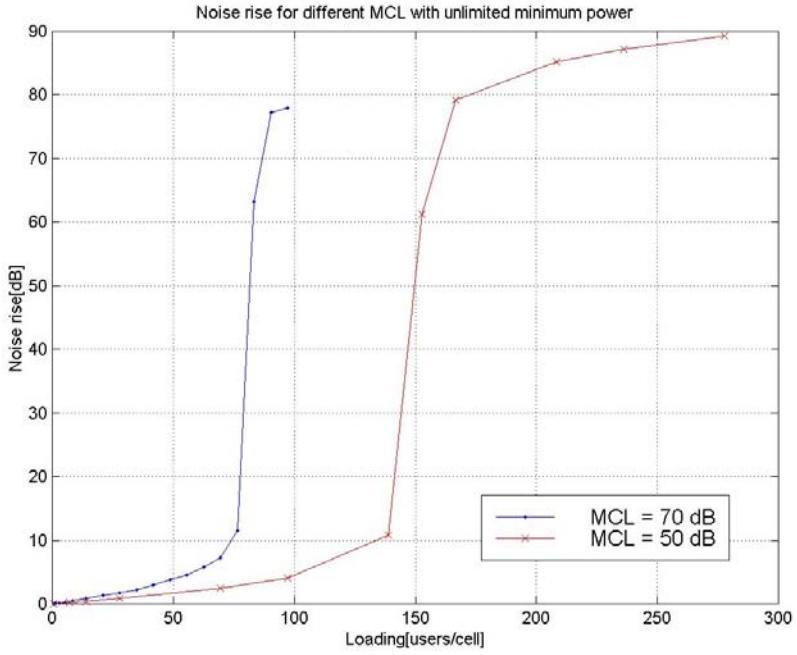

FIGURE 4.1-5. Noise rise vs. loading with unlimited minimum power and 50 dB and 70 dB minimum coupling loss.

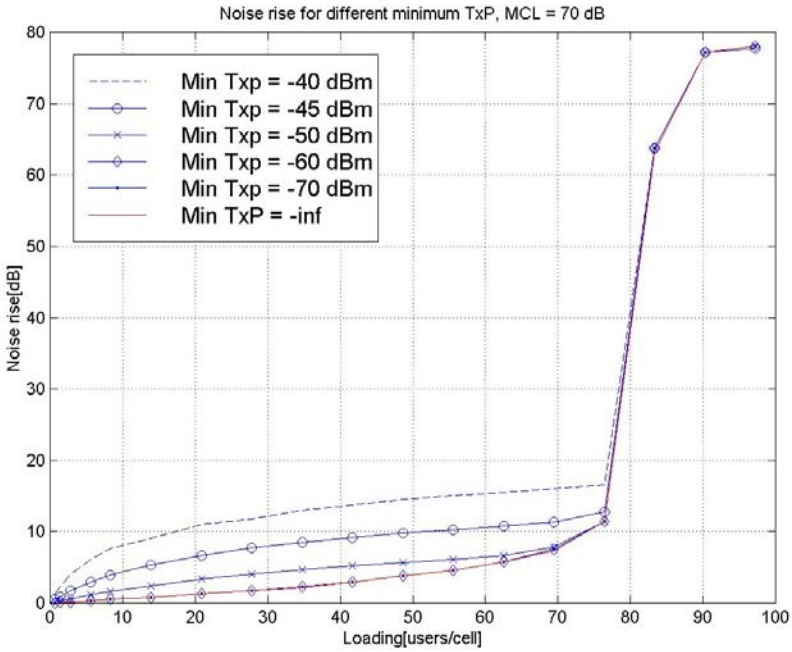

FIGURE 4.1-6. Noise rise vs. loading for different minimum TX power levels with 70 dB minimum coupling loss.

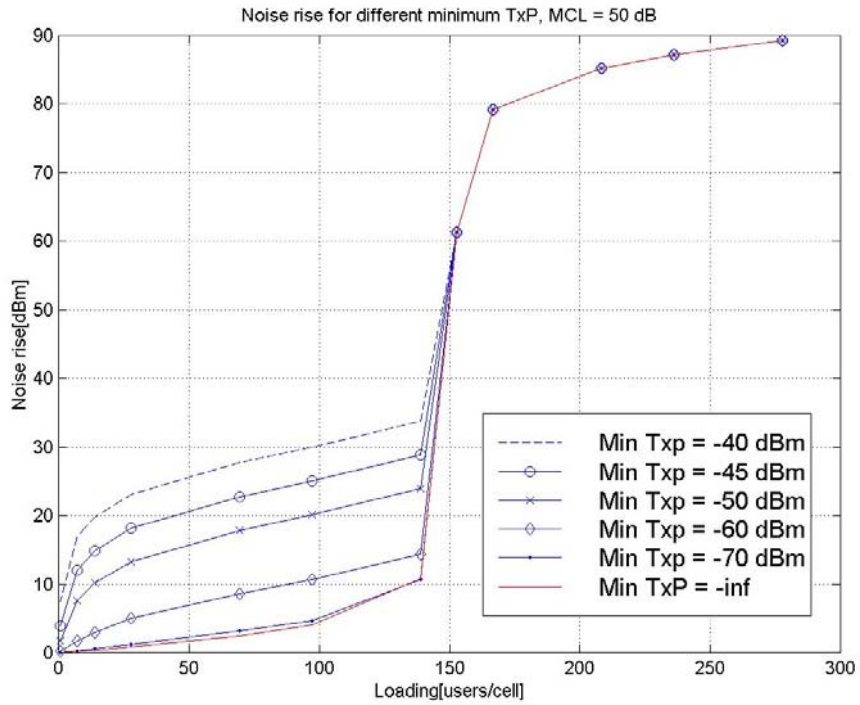

FIGURE 4.1-7. Noise rise vs. loading for different minimum TX power levels with 50 dB minimum coupling loss.

If it is assumed that micro-cells are of planned capacity, not coverage limited, -44 dBm minimum transmission power is applicable. Then the micro-cell base stations should be desensitised or noise rise planning criteria should be much higher than for macro-cells. On the other hand when considering a range limited macro-cell case noise rise due to nearby terminals will impact on the link budget. Hence it should be considered lower values than –44 dBm as a minimum power. Based on the curve in the macro-cell case in FIGURE 4.1-6, it can be observed that by changing the minimum power from –45 dBm to –50 dBm noise rise enhances noticeably. After this point there is not much to gain, but the implementation will become very demanding.

For example, assume the minimum output power of -50 dBm. The received signal power from a mobile station having a minimum coupling loss of 70 dB to the base station would be -120 dBm. This is at the similar received power level as all the other mobiles served by the same base station, even if the base station is planned for high coverage and operates at the noise rise of over thermal noise floor of 3–4 dB. Consequently, the coverage of the cell is not affected.

To avoid high noise rise due to excessive mobile station minimum transmission power, desensitisation could be a used. Desensitisation, however, is not applicable in all cases:

- Micro-cells are needed for providing high bitrate indoor coverage and therefore good sensitivity is needed and desensitisation should be avoided. Typically, when link budgets are made 15–20 dB is reserved for indoor coverage.

- Desensitisation leads to increased mobile station transmission power. This increases the interference to other cells on the same frequency.

4.1.2.2 *Minimum Mobile Station Transmission Power and Adjacent Channel Interference*

Earlier it has been claimed that the effect due to excessive mobile station minimum transmission power is minor if compared to the effect of uncoordinated interference (adjacent channel interference). The following section presents calculations that show that adjacent channel interference is a less serious problem as excessive minimum power.

First the capacity effect of mobile station minimum power is analysed. In this analysis it is assumed that the maximum received power in the mobile station is –25 dBm which is the blocking limit of the mobile station, see [TS25.101]. Micro-cell base station output power is assumed to be 28dBm and noise level -103dBm. The assumed noise rise is 6 dB leading to interference power of –97 dBm in the base station receiver.

The call will drop in the downlink direction when the received power from the serving base station exceeds the dropping level. From the blocking level and the base station maximum power minimum allowed coupling loss can be calculated as

$$MCL = TxP_{BS} - Th_{Blocking} = 28dBm - (-25dBm) = 53dB. \quad (4.1\text{-}5)$$

When minimum coupling loss is 53 dB interference generated by the mobile station is -44dBm –53 dB = -97dBm. This leads to a situation in which the mobile station can cause 3 dB additional noise rise in the base station before the call is dropped in the downlink direction. If the minimum power is -50 dBm as suggested, only 1 dB additional noise rise is caused.

Next adjacent channel interference is analysed. It is assumed that the micro-cell base station output power is 28dBm and noise level –103 dBm. The assumed noise rise is 6 dB, and hence the interference level in the base station receiver is -97 dBm. The mobile station output power is 21dBm and noise level -99dBm at the receiver. Both, mobile station ACLR and ACS receive the value of 33 dBc.

If it is assumed that 3 dB degradation in downlink SIR can be tolerated at the cell border (interference is equal to the noise level) minimum coupling loss to the adjacent operator base station can be

$$MCL = TxP_{BS} - ACS_{UE} - N_0 = 28dBm - 33dBc - (-99dBm) = 94dB. \quad (4.1\text{-}6)$$

Then the received power in the uplink is

$$RxP = TxP_{UE} - ACLR_{UE} - MCL = 21dBm - 33dBc - 94dB = -106dBm. \quad (4.1\text{-}7)$$

The received power is 9 dB below the interference level and only 0.1 dB more interference is generated.

As above the calculations show adjacent channel interference is less harmful than co-channel interference if we take into account the downlink dead zones. In the above calculations the ACLR value of 33c dB was used. Inter-frequency handover is an escape mechanism to adjacent channel interference (see Chapter 3.3), when the mobile station ACLR and ACS get value 43 dBc. Then adjacent channel interference has an even smaller effect. In the above calculations it is assumed that two operators have their base stations in the worst-case scenario. If the base stations are not in a cell border of another operator's cells, adjacent channel interference situation becomes easier. This, however, does not help with the mobile station minimum transmission power. Further, if base stations of the two operators are co-sited, adjacent channel interference is not a problem at all, while the minimum transmission power problems still persists.

Simulations are carried out to see the joint capacity effect of adjacent channel interference and excessive minimum mobile station transmission power. Two scenarios have been considered: two operators having their base stations in a macro-cellular hexagonal grid in the worst-case scenario and two operators having their base stations in a micro-cellular Manhattan grid. In the latter case, the base stations of the two operators has been shifted by two blocks. In both cases minimum coupling loss is set to –53 dB, Simulations are executed for single operator and multioperator case and for -44 dBm, -50 dBm and –1e9 dBm (-∞) minimum mobile station transmission power.

The simulation results for the hexagonal layout and for the Manhattan layout are shown in FIGURE 4.1-8 and FIGURE 4.1-9, respectively. In the single operator case capacity loss for –50 dBm minimum mobile station transmission power is 8 % and for –44 dBm 24 % if compared to -∞ dBm minimum mobile station transmission power. In the multi-operator case the corresponding capacity loss for –50 dBm minimum mobile station transmission power is 8 % and for –44 dBm 21 %. From the simulations it can be seen that adjacent channel interference does not remove capacity loss caused by excessive mobile station transmission minimum power. Adjacent channel interference and excessive minimum mobile station transmission power has the combined effect that can be reduced by selecting a feasible minimum mobile station transmission power requirement. In the Manhattan environment with the mobile station minimum power of –44 dB 6 dB noise rise is obtained with loading around 4 users/cell and 20 dB noise rise with around 56 users/cell. For –50 dBm the mobile station minimum transmission power corresponding to the loading is 13 and 113 users/cell. This means, that with –50 dBm minimum mobile station transmission power around 2 times higher capacity is obtained if compared to –44 dBm minimum power.

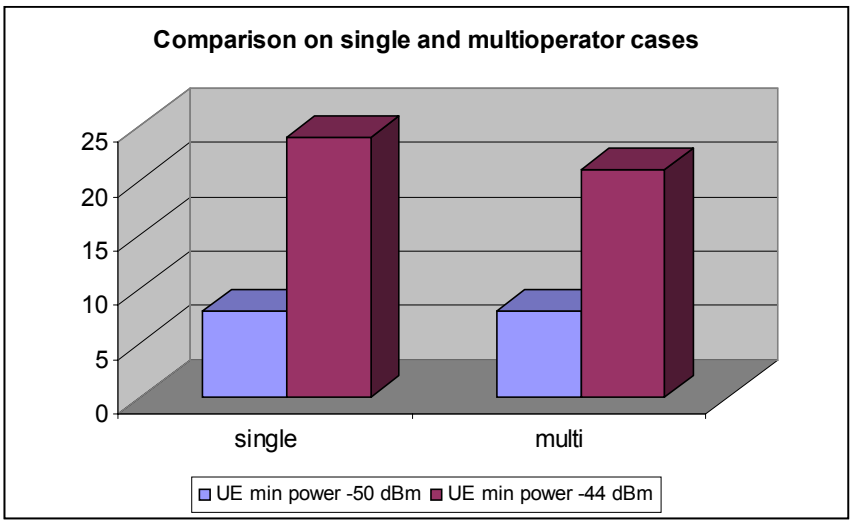

FIGURE 4.1-8. Simulation results for two mobile station minimum power levels in single and multi operator environments. Hexagonal layout.

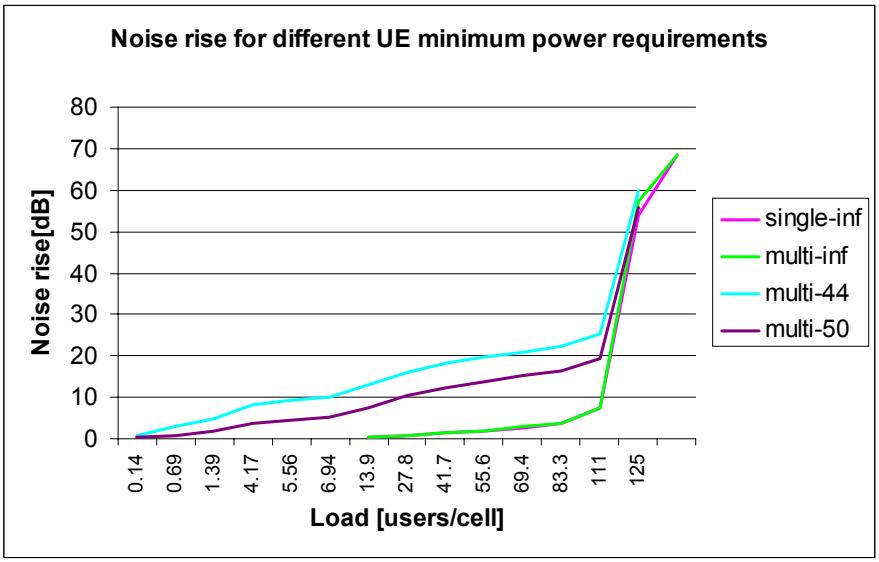

FIGURE 4.1-9. Simulation results for two mobile station minimum power levels in single and multi operator environments. Manhattan layout.

4.1.2.3 *Minimum Power Requirement and EVM*

Simulations for EVM (Error Vector Magnitude) capacity effects has been executed as it may be possible that with very low power EVM starts to dictate transmission power through worse SNR performance.

Simulation methodology used here is as follows. First the mobile station transmission power is identified. The mobile station transmission power is then mapped to EVM SNR by using the lookup table given in TABLE 4.1-5. Next the mobile station's received power in the base station is identified. Noise due to EVM can be calculated from the received power in the base station and SNR due to EVM

$$SNR = \frac{RXP}{N_{EVM}} \Rightarrow N_{EVM} = \frac{RXP}{SNR} \quad (4.1\text{-}8)$$

Finally SIR for a user can be calculated as

$$SIR = \frac{RXP \cdot GP}{I_{total} + N_0 + N_{EVM}} \quad (4.1\text{-}9)$$

TABLE 4.1-5. TXP to EVM mapping.

TXP	EVM SNR – assumption 1	EVM SNR – assumption 2
+21 .. –20	15	15
-20 .. –30	15	10
-30 .. –40	10	5
-40 .. –50	5	0

When the effect of EVM is simulated with the models given above, it can be observed that EVM has only a marginal effect on the noise rise and capacity in the system. Noise due to EVM reduces SIR of the mobile stations uplink by three decibels in maximum or, in other words mobile station have to increase its transmission power by a maximum of 3 dB to keep SIR as required for the service.

In FIGURE 4.1-9 simulation results for the case in which two operators run their network in a micro-cell scenario are shown. As seen in FIGURE 4.1-9, even if the mobile station minimum power is –50 dBm interference in the base station increases due to too high minimum power. Consequently the result SIR for the nearby mobile station is better than required for the service. The minimum transmission power of the nearby mobile stations could be reduced by more than the power should be increased due to EVM. Thus EVM does not have effect on the capacity. For example, assume the system that serves 1 user/cell and the served mobile station is located close to the base station. Then the noise rise caused by the user is 3 dB[14] (2 as absolute value). We get

$$1 \cdot RXP + N_0 = 2 \cdot N_0 \Rightarrow RXP = N_0 . \quad (4.1\text{-}10)$$

PRX is the received power from the observed mobile station, and N_0 is the receiver noise in the base station. Assume EVM SNR = 0dB. Then noise due to EVM is

$$N_{EVM} = \frac{RXP}{1} = N_0 . \quad (4.1\text{-}11)$$

[14] RXP= -50 dBm-53dB = -103dBm. Since thermal noise is –103 dB, received power cause 3 dB noise rise

Then the total interference is

$$I_{total} = 2 \cdot N_0 + N_0 = 3.0 \cdot N_0, \Delta TXP = \frac{3.0}{2.0} = 1.5 \Rightarrow \Delta TXP = 1.76dB \quad (4.1\text{-}12)$$

.

This means that the mobile station should increase its power by 1.76 dB in order to maintain SIR obtained without EVM modelling. However, in this scenario the mobile station near to the serving base station has much better SIR than required for the service. Power could be reduced much more than is the performance degradation due to EVM – how much exactly depends on the SIR requirement and processing gain for the service, because of that noise due to EVM does not affect the capacity. For users further away from the serving base station EVM has only a small impact since they do not operate with the minimum power.

4.1.3 Outer Loop Power Control in the Downlink

This chapter discusses some aspects of the OL (Outer Loop) power control function in the downlink illustrated by examples. This study was shown in 3GPP [Nok99b] to illustrate the reasons why the downlink outer loop power control algorithm should be implemented in the mobile station instead of the UTRAN.

The role of the downlink outer loop power control function is to ensure constant quality (FER/BLER/BER) of the radio link against the background of the changing propagation conditions. The outer loop power control operation is typically achieved by frequently updating of the E_b/I_0_target value (or target SIR) which is used during the downlink closed loop power control operation in deriving the appropriate power control commands for the base station by means of a threshold comparison of the measured E_b/I_0 against this E_b/I_0_target.

An increase of E_b/I_0_target is typically triggered when the mobile station receives one or more erroneous frames. The E_b/I_0_target value can be decreased when no frame errors have occurred for a specified amount of time, depending on the targeted FER. It is assumed that the mobile station updates E_b/I_0_target value in accordance with the measured frame errors (or other relevant metrics) *without* involvement of the UTRAN. However the UTRAN may specify during the connection setup certain parameters related to the outer loop power control operation such as minimum and maximum values for the E_b/I_0_target the mobile station may use. There are a couple of reasons why it appears desirable to have the mobile station update the E_b/I_0_target without direct involvement of the UTRAN, in particular without the need for a L3 (Layer 3) signalling transaction in order to do so.

Let us look at the following examples wherein the mobile station needs to change its E_b/I_0_target value:

- Occurrence of one or more frame errors during steady state outer loop power control operation. The basic outer loop power control behaviour in this case is to

increase the E_b/I_0_target (see above). Similarly, occurrence of a longer period or frame error free reception, the outer loop power control shall lower the E_b/I_0_target. The likelihood of these events is proportional to the specified target FER.

- Changes in the mobile station speed leading to an increase or decrease of the required E_b/I_0
- Changes in the multipath delay profile and thus the amount of available diversity presented to the mobile station RAKE receiver.
- Modifications of the soft/softer handover configuration (i.e. updating the active set in handover) and thus the amount of available diversity presented to the mobile station RAKE receiver together with a modified transmission power control behaviour. It has been observed that the E_b/I_0_target needs to be updated by up to 3 dB depending on the channel conditions.
- Modifications in the physical layer bearer parameters (services, data rates, encoding and so on)
- In general activation/deactivation of the downlink compressed mode (see Chapter 4.5). In here one special case is where the mobile station would half the spreading factor and possibly have to revert to a non-orthogonal spreading code and thus loosing orthogonality with the possible result of large change in the required E_b/I_0_target value.

However, if the outer loop power control is made in UTRAN, the following problems are faced:

- Significantly increased signalling load in I_{ub} (Node-B[15] to RNC) interface
- Significantly increased delays in E_b/I_0_target decision
- Significantly increased processing load in the radio network controller

By using simulation examples outer loop power control operations are illustrated. FIGURE 4.1-10 and FIGURE 4.1-11 show an example obtained from a dynamic simulation presented in Chapter 2.4. In the following figures, three simulations are made with different parameters, so that handover occurs at different times. In FIGURE 4.1-10 and FIGURE 4.1-11, E_b/I_0 and E_b/I_0_target correspond to each other since they are taken from the same simulation and the same mobile station.

FIGURE 4.1-10 shows realized E_b/I_0 for a mobile station when different simulation parameters are used. During time ~55 seconds to ~59 seconds (the lowest figure) active set size for the mobile station is one. Then the mobile station has only little diversity from the channel. When handover occurs more diversity is obtained and the variance of the realized E_b/I_0 becomes significantly lower. Similar improvement in variance of E_b/I_0 can be seen when getting more diversity from appearing new channel taps or when the mobile station speed becomes lower and the closed loop power control is able to compensate the channel. When variance of E_b/I_0 changes, also the closed loop target set by the outer loop power control should change.

---

15 Same as base station

FIGURE 4.1-11 shows corresponding E_b/I_0 thresholds for the user. The used outer loop algorithm is similar to that of used in some CDMA systems [Sam97a]. In figure the E_b/I_0_target starts to decrease immediately when handover is made and the variance of E_b/I_0 becomes smaller.

Let's next consider the example situations in which fast reaction of the outer loop power control is needed. First a situation is described in which the amount of diversity is first small, then becomes higher and finally becomes poor again. The amount of diversity can change because of handovers, change in the mobile station speed, the changing number of channel taps and so on. When the amount of diversity increases the outer loop power control algorithm made in the mobile station immediately lowers E_b/I_0_target. Then also DCH (Dedicated CHannel) powers starts to decrease and less interference is generated to the network. If the outer loop power control is implemented in the UTRAN, a delay of possibly hundreds of milliseconds would be experienced before the outer loop power control could react to the changing conditions. Then used DCH powers would be unnecessarilly high for hundreds of milliseconds and interference was generated to the network. When the amount of diversity again decreases, the outer loop power control in the mobile station immediately increases E_b/I_0_target and quality of the user is maintained. If the outer loop power control was made in network delay would be experienced and quality of the connection would worsen for a time that can last for over hundreds of milliseconds.

The second example presents a case in which diversity improves over a very short period. If the outer loop power control is made in the UTRAN change in diversity is not seen by it or the actions are made when already returned to the initial situation. This would cause a short-term poor signal quality for the connection.

The third example is the case in which diversity becomes smaller for a very short period. If the outer loop power control is made in the UTRAN, it is not able to raise the E_b/I_0_target, and too low powers are used. Then the quality of the link may be poor and several erroneous frames are possibly received. A user possibly notices this as a click sound. As shown in simulation example in FIGURE 4.1-10, diversity can change frequently. A user notices this possibly as frequent clicks in the voice.

Based on this study it is proposed to have the mobile station update the E_b/I_0_target autonomously based on measurements directly available to the mobile station (such as e.g. FER).

In 3GPP the outer loop power control is defined so that the UTRA may control key parameters related to the outer loop power control operation [TS25.331]. Moreover the UTRAN always has control over the downlink power allocated to a mobile station by means of a downlink power control in the base station, regardless the outer loop actions within the mobile station.

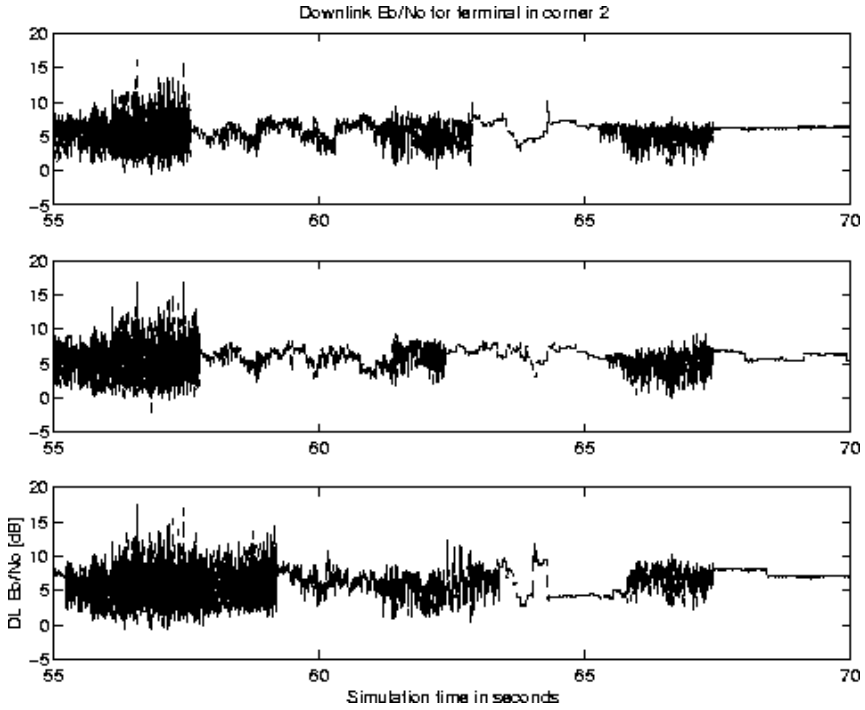

FIGURE 4.1-10. E_b/I_0 as a function of time.

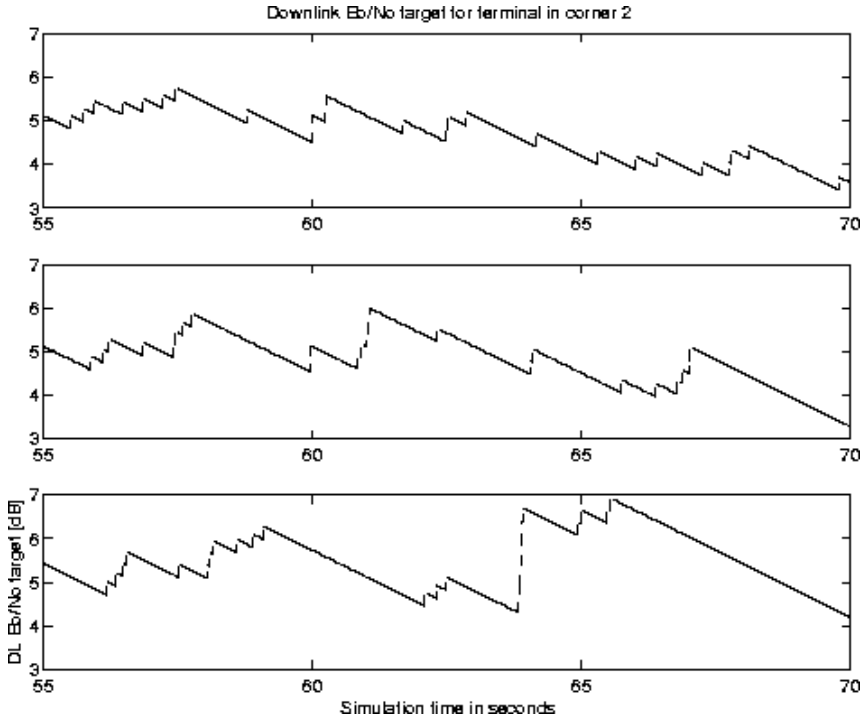

FIGURE 4.1-11. E_b/I_0_target for the closed loop power control provided by the outer loop power control.

4.2 Random Access

Prior negotiations with UTRAN a limited set of data can be sent by using the RACH. Such data may be for example a connection setup related information or a small amount of data. The random access channel is mapped to the PRACH (Physical Random Access CHannel). The cell planning has to be made so that the physical random access channel can be received throughout the entire cell. Transmission of the random access is based on slotted Aloha with fast acquisition indication. Slotted Aloha is in turn based on the Aloha system presented by Abrahamson in 1970 [Abr70]. In the original Aloha system, if a collision among packets occurs, those packets are discarded. In slotted Aloha, random access messages can be sent at different times during access slots [Rob75]. This reduces the probability of collision. In WCDMA the mobile stations first send preamble to the base station. If the base station is able to receive preamble and it has resources available for the mobile station it will acknowledge the random access by sending acquisition indication. The mobile station may send its data after it has received acquisition indication through an acquisition indication channel. By doing so collisions between random access attempts can be reduced. It has been analysed in [Shi01] that this improves a system's performance considerably if compared to pure slotted-Aloha approach.

The mobile station can start the random access transmission at the beginning of time intervals that are called access slots. Timing of AICH is made relative to the uplink access slots. The random access transmission consists of the preamble sending part and the message part. Each preamble is of length of 4096 chips and consists of 256 repetitions of a signature of length 16 chips ($256 \bullet 16 = 4096$ chips). The maximum number of signatures is 16. The message part length is a 1 or 2 frames that corresponds to 10 or 20 ms time. The 10 ms message part radio frame is split into 15 slots, each length of 2560 chips. Each slot consists of data and control parts that are transmitted in parallel. The message part length is equal to the Transmission Time Interval (TTI, same as the interleaving period) of the random access transport channel in use. Length of TTI is configured by the higher layers. The data part consists of $10 \bullet 2^k$ bits, where k gets values from zero to three. Values of k correspond to the spreading factor of 256, 128, 64 and 32 respectively. The control part consists of 8 known pilot bits used for channel estimation and coherent detection and 2 TFCI bits per slot. Spreading factor for control part is fixed to 256.

The physical random access procedure is initiated upon request from the MAC (Medium Access Control) sub-layer. Before the actual random access procedure can be performed certain information is received from RRC (Radio Resource Control), such as power ramping factors and scrambling codes. When the random access procedure is started, the available uplink access slot, used sub-channel and signatures are identified. An access slot and signature are selected randomly from the available ones. Then the first random access preamble is sent with the initial power. The random access procedure in

WCDMA has to cope with a near-far problem when selecting used transmission power and having no prior information of power levels needed [Hol00]. Required power levels depend on interference levels in the target base station and signal attenuation and fading. The initial transmission power level in the mobile station is defined by using the open loop power control. Since there is significant uncertainty involved with the open loop power control due to measurement accuracy[16], low transmission power level is first used. If the mobile station does not receive an acquisition indication as a response to the random access, a new random access signature is randomly selected and a new preamble sent with higher power. The transmission power is increased by a step called "power ramping step" and defined by RRC. If the mobile station receives a negative acquisition indicator the random access is exited and MAC layer notified failure in random access. If the mobile station receives a positive acquisition indicator it starts transmission of the message part. [TS25.211, TS25.214]

It is also possible that the mobile station is not able to receive AICH ACK message. The detection error probability (the probability that a preamble is not detected) is referred to as 1- P_d described in [Nok00e]. It may also happen so that the mobile station erroneously decodes AICH ACK even no such message is sent. This is called false detection and the probability of false detection (the probability that an ACK is falsely detected) is called P_{fa} in [Nok00e]. FIGURE 4.2-1 illustrates the power ramping procedure and FIGURE 4.2-2 clarifies the false detection possibility.

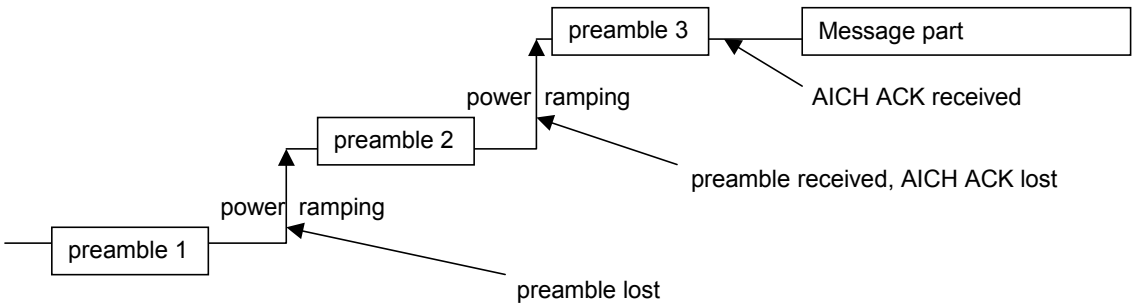

FIGURE 4.2-1. Schematic example of a preamble sequence.

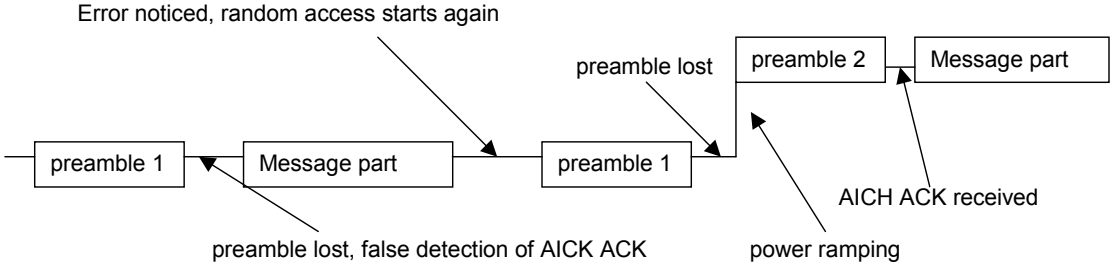

FIGURE 4.2-2. Schematic example of a preamble – sequence that contains a false detection of ACK.

---

16 Outer loop accuracy requirement is ±9 dB with 90 % probability [TS25.101].

4.2.1 Random Access Performance Analysis

This chapter presents simulations studying network level effects of random access algorithm. The used tool is the dynamic system simulator presented in Chapter 2.4. This study was originally presented in [Hen01].

Simulations are performed for random access assuming ideal acquisition indication performance to see the impact of random access on the systems capacity and determine the parameter values for the random access algorithm in an ideal case. Next, the parameters identified were used and acquisition indication parameters varied to identify the system impact due to acquisition indication algorithm, see Chapter 4.3. TABLE 4.2-1 shows constant parameters common for both random access and acquisition indication simulations.

The main goal of the simulations is to evaluate the effect of random access with different parameter values and to check whether random access defined in 3GPP works in a robust manner in the system level. The parameter values are selected to be such that they conform to the specifications and are otherwise reasonable. The values of most important parameters in the simulations are given in TABLE 4.2-2.

TABLE 4.2-1. Common parameters for RACH and AICH simulations.

Parameter	Value
Mean mobile speed	13.9 m/s
Data rate	12.2 kbps
Scenario	Macro cell, ETSI Vehicular-A Channel
Cell radius	333 meters
Delay between two preambles	6 slots
Delay between successful preamble and start of message part	4 slots
Maximum number of preambles to be sent in row	20
SIR threshold value used in open loop	-35 dB
Delay between a failed random access and start of another one	15 slots
Deviation for error in the open loop power control	4.5 dB[17]
Maximum allowed random access length	1500 slots
The percentage of random access users in simulations	10%

TABLE 4.2-2. Parameters varied with RACH simulations.

Parameter	Value
C/I – Threshold determines the signal strength preambles must have to be successfully detected by BS.	-30 dB,-25 dB,-20 dB and -15 dB
Length of sent message part (messagePartLength)	15 or 30 slots
Power ramping factors used	1, 3 and 8 dB
Probability of error in receiving AICH ACK, 1- P_d	0.0
Probability of a false detection of AICH ACK, P_{fa}	0.0

[17] This value implies that roughly 95% of errors are in the interval [-9 dB, 9 dB], because if $\mathbf{X} \sim \mathbf{N}(0, \delta)$ then $\mathbf{P}(|\mathbf{X}| \leq 2\delta) \approx 95\%$.

TABLE 4.2-3 shows the results from the simulations where the duration of the message part was 2 frames, i.e., 30 slots. Two C/I threshold values (-25 dB and –20 dB) for detecting random access preamble are used. The results from the cases where the random access message part is 1 frame long are omitted because, except for a 15 slots shift in the duration, they were virtually identical to the 2 frame results.

The average duration in TABLE 4.2-3 is formed from the length of the message part (30 slots) + duration between the last preamble and the message part (4 slots) + number of required preambles *n* times preamble duration (1.3 • n) + delay between preambles ((n - 1) • 6 slots). As seen from FIGURE 4.2-4 almost 90 % of users receive random access through with the first preamble. However, there exist a low percentage of users that require more than 20 slots to receive random access through. Then an additional 15 slots is added between two random access attempts.

TABLE 4.2-3. Statistics of random access duration and number of sent preambles. Mean delay consists of fixed length message part (30 slots) and varying number of preambles (1 ms each).

PowerStep	Average duration in slots	STD of duration in slots	Average # of preambles	STD of sent preambles
-25 dB C/I Threshold:				
1	42.09	9.04	1.26	1.13
3	41.17	4.48	1.15	0.56
8	40.78	2.86	1.10	0.36
-20 dB C/I Threshold:				
1	49.00	20.13	2.13	2.52
3	44.65	9.11	1.58	1.14
8	42.99	5.46	1.62	1.37

These results show that the larger the power ramping step, the shorter the duration is. However, the change is very small, measured in a few slots. From TABLE 4.2-4 below it can be seen that the load change is also minor for different cases. The mean number of sent preambles is in order of one to three, which partly explains why the lengths and interference do not differ much: The scale is too small to allow for large differences. The main differences of 3 dB and 8 dB power ramping factors are in the deviations: They are clearly smaller than in case of 1 dB ramping factor. TABLE 4.2-4 also shows that while random access has a small effect on the load, it is at most 0.5 dB in magnitude with all power ramping factors.

TABLE 4.2-4. Load change statistics. In the reference case all the users are using dedicated channel.

PowerStep	NR mean	Load, mean	Load change factor	Load change factor [dB]
Reference case:	2.41	0.43	1	0
-25 dB C/I Threshold:				
1	2.98	0.50	1.17	0.67
3	2.96	0.49	1.16	0.65
8	2.96	0.49	1.16	0.65
-20 dB C/I Threshold:				
1	3.0	0.50	1.17	0.69
3	3.05	0.50	1.18	0.74
8	3.06	0.51	1.19	0.75

FIGURE 4.2-3 and FIGURE 4.2-4 show the reason as to why random access durations are so similar with all the simulated power ramping factors. FIGURE 4.2-4 shows that roughly 80%[18] of users succeed with the very first preamble sent; this creates a large "probability mass" for the smallest possible duration, and even though the rest of the users may experience significantly longer durations, the mean changes only little. These long durations are seen only in the deviation. FIGURE 4.2-3 shows that while a 3 dB power ramping step helps a great deal when compared to a 1 dB step, the difference between 3 dB step and 8 dB step is smaller.

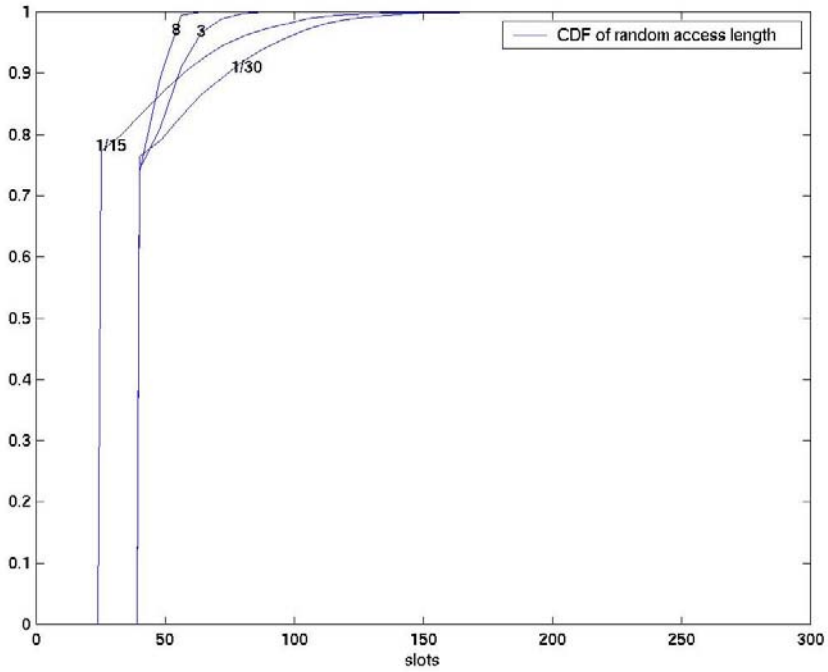

FIGURE 4.2-3. Random access duration distributions for cases with -20 dB C/I-threshold. Simulated step sizes are 1, 3 and 8 dB. Message part length is 30 slots. For 1dB step size result also for 15 slots message part is shown.

[18] With –25 dB C/I threshold the results are very similar. The only difference is that roughly *90%* succeed with first preamble. The same reasoning applies to both cases.

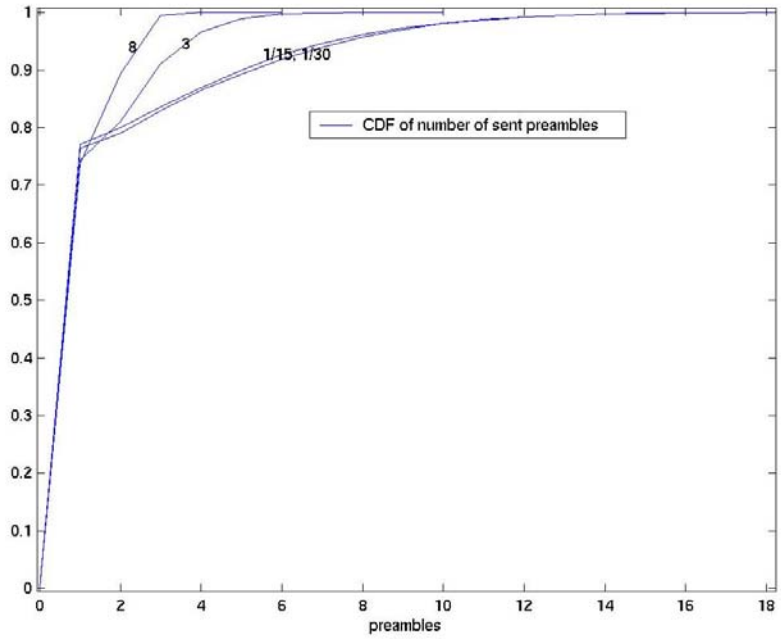

FIGURE 4.2-4. Distribution of the number of sent preambles for cases with –20 dB C/I-threshold.

Random access simulations show that random access has very small impact to the system. The loss is small enough to be considered almost negligible from the network point of view. Also it would seem that having 3 dB power ramping step helps the preambles get acknowledged somewhat faster with almost no effect on the network load. An 8 dB step was also simulated, but it seems not to give a significant gain over 3 dB. This is because the noise rise is somewhat higher and preambles are not acknowledged significantly faster. It can be concluded that the random access algorithm selected in 3GPP provides good performance.

4.2.2 Macro Diversity and Random Access

Both WCDMA and cdma2000 systems use random access method that is here called *diversity random access*. Diversity random access facilitates macro diversity during random access or immediately after random access has been finalized. Diversity random access was first introduced in [Häk96].

4.2.2.1 *Diversity Random Access Principle*

The objective of the diversity random access is to accomplish a solution, which diminishes interference relating especially to the initial stage of the connection. It also enables the use of macro diversity for a packet-mode connection when using common packet channels. This is achieved by forming a random access type connection to more than one base station or sector.

When the mobile station initiates connection establishment, it sends on the random access channel a connection request relating to several base stations or

sectors to the strongest base station (lowest pathloss, highest pilot quality or corresponding) from which the request is forwarded to the radio network controller. Before the mobile station sends the connection establishment request, it selects from the base stations or sectors the ones where the quality of the connection is presumably the best. Those base stations are also the ones to which the mobile station would most preferably be connected. The set of base stations is selected based on the mobile station measurements.

The base station responds to the request from the mobile station by using an acquisition indicator channel (see Chapter 4.3), paging channel or corresponding – depending system architecture. The radio network controller selects from the list of base stations selected by the mobile station those to which connection may be created. The reason why the base station controller may restrict the number of the base station or sectors may be for example the heavy loading of the system at that moment.

After the mobile station receives a response from the radio network controller via the accessed base station the mobile station makes a synchronization with the selected base stations. When the synchronization is ready, the mobile station may continue in a traffic channel with several active base stations. The synchronization process can be started already when waiting for a response from the radio network controller.

This procedure makes it possible to include several base stations or sectors to the active set right from the beginning of connected mode traffic.

In [Häk96] there is also a modified approach presented in which all those base stations selected by the mobile station and granted by the radio network controller sends a response to the mobile station in their acquisition indicator, paging or corresponding channel. This accelerates the random access execution. This method is used with cdma2000 reservation access mode, see Chapter 4.2.2.3.

In an alternative procedure, the mobile station also sends a transmission request to several base stations or sectors. This procedure may have several purposes. At its simplest, connection establishment is initiated along with several base stations (RACH message sent to several base stations) but the actual connection will be established with only one base station or sector. The connection that has been established with the base station responds first to the mobile station's request. That base station is thus also the best base station at that moment. In a more advanced alternative, the connection establishment message may also proceed via several base station transceivers. In the third alternative the message proceeds along one route but the other base stations are synchronized with the connection request of the mobile station without being able to interpret the message correctly. This will also accelerate the generation of the actual macro diversity connection.

In case of packet data in common channels, by using the solution presented here also in packet-mode data transmission, several base stations or sectors can be used and macro diversity will be attained, whereby changes in the quality of the connection are less significant than when in connection to only one base station or base station transceiver unit.

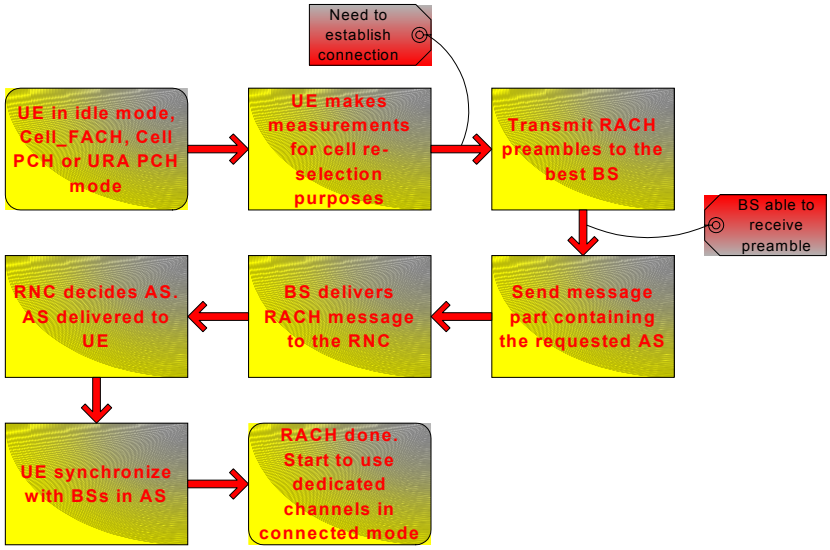

FIGURE 4.2-5. Block diagram describing an example of diversity random access principle.

4.2.2.2 *Diversity Random Access in WCDMA*

When the mobile station starts connection setup the first RRC connection message sent is the RRC Connection Request. The RRC Connection Request message contains among other things measurement report of all requested reporting quantities for cells for which measurements are reported.

Upon receiving an RRC Connection Request message, radio access network should either submit an RRC Connection Setup message or an RRC Connection Reject message on the downlink CCCH (Common Control CHannel). In the RRC Connection Reject message, the radio access network may direct the mobile station to another UTRA carrier or to another system. After the RRC Connection Reject message has been sent, all context information for the mobile station may be deleted in the radio access network. If radio access network decides to proceed with connection setup, connection will be created to the reported base stations or sectors, thus macro diversity is created from the beginning of dedicated mode.

Measured results are transmitted by the mobile station to the base station on RACH message. It contains measured results of the quantity indicated optionally by Reporting Quantity in the system information broadcast on BCH (Broadcast Channel). The list of measurements is in the order of the value of the measurement quality (the first cell should be the best cell). The best FDD cell has the largest value when the measurement quantity is E_c/I_0 or RSCP. On the other hand, the best cell has the smallest value when the measurement quantity is pathloss between the mobile station and the measured base station. The best TDD cell has the largest value when the measurement quantity is RSCP of CCPCH (Primary Common Control Physical CHannel). [TS25.331]

4.2.2.3 *Diversity Random Access in cdma2000*

In 3GPP2 documents [C.S0003-A and C.S0004-A] the access attempt that corresponds to the diversity random access discussed here is described. In cdma2000, an access attempt consists of one transmission and several re-transmissions of the same PDU (Packet Data Unit). Each transmission within an access attempt is called an access probe. When the mobile station stops transmitting an access attempt to one base station and starts transmitting to another base station, an access probe handoff[19] is made. A portion of the access probes sent to a base station is called a sub-attempt. Each sub-attempt contains a sequence of access probes. The maximum number of access probes within a sub-attempt is a system parameter. This method of sending access probes to several base stations during an access attempt conforms the idea behind the diversity random access. An example of diversity random access in cdma2000 is given in FIGURE 4.2-6.

3GPP2 document [C.S0003-A] describes *Enhanced Access Channel Procedures*. Enhanced access mode can be in two modes – basic access or reservation access. The mobile station selects the access mode depending on the amount of transmitted data. The basic access mode is used for a low amount of data while the reservation access mode is better suited for larger amounts of data [Ete01]. When operating in Reservation Access mode, diversity random access in which several base stations receive mobile stations random access as described in Chapter 4.2.2.1 is possible. The mobile station measures the pilot E_c/I_0 value for the candidate base stations. If a candidate base station pilot E_c/I_0 is strong enough (relative to the active pilot), the mobile station can request a reservation channel with soft handover. The mobile station indicates the request of soft handover in Reservation Access Enhanced Access Header that is followed transmit of Reservation Access Enhanced Access Probe (similar to preamble in WCDMA). After the header has been sent the mobile station starts to monitor a Forward-Common Assignment Channel Channel (F-CACH). From F-CACH channel the mobile station receives necessary data to be able to receive power control bits transmitted by one or more base stations in their CPCCH (Common Power Control CHannel) channels. Those active base stations are able to receive random access messages sent by the mobile station, and make power control according to the quality of the reception. An example of Reservation Access Mode with diversity random access is presented in FIGURE 4.2-7. In FIGURE 4.2-7 EACAM (Early Acknowledgement Channel Assignment Message) is used to inform the mobile station that the base station has received the probe and header successfully and PCCAM (Power Control Channel Assignment Message) to identify that power control is used with the message part.

---

[19] Handoff is same as handover in 3GPP2 terminology

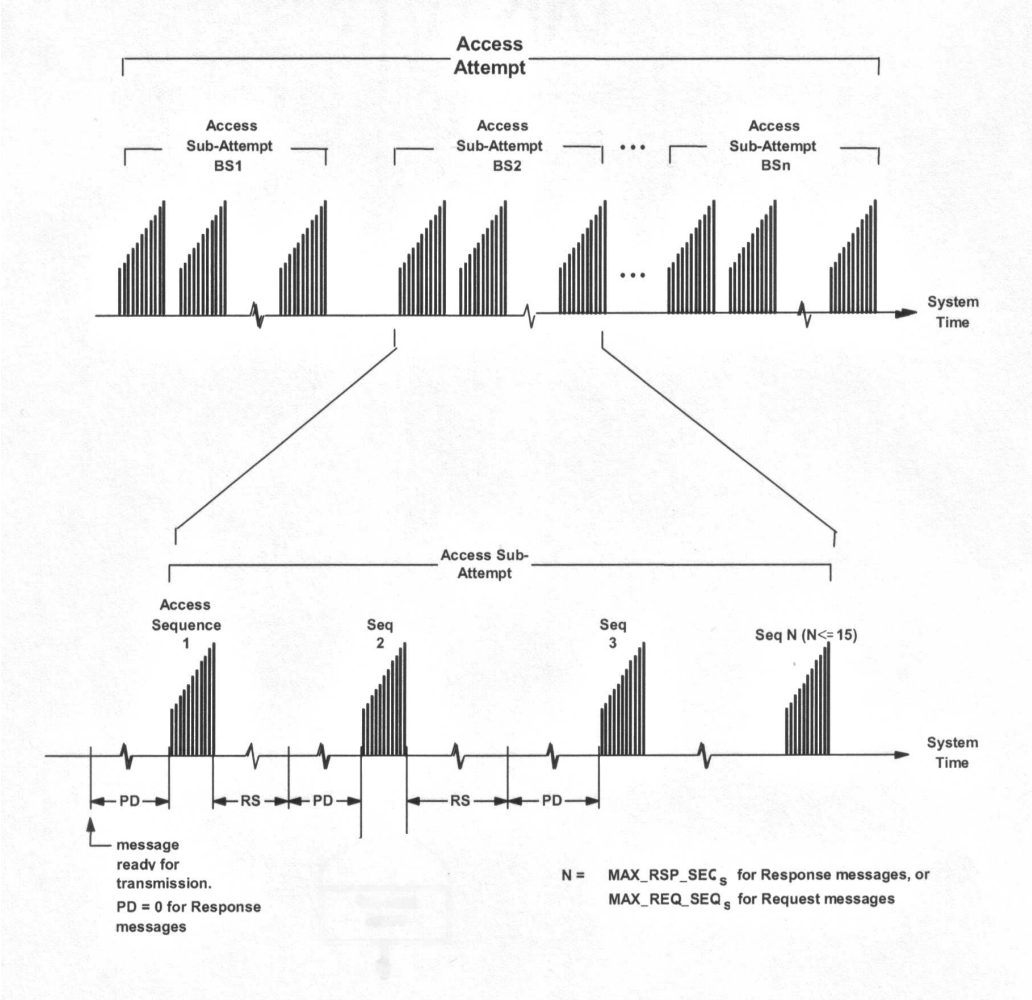

FIGURE 4.2-6. Access attempt to several base stations [C.S0003-A].

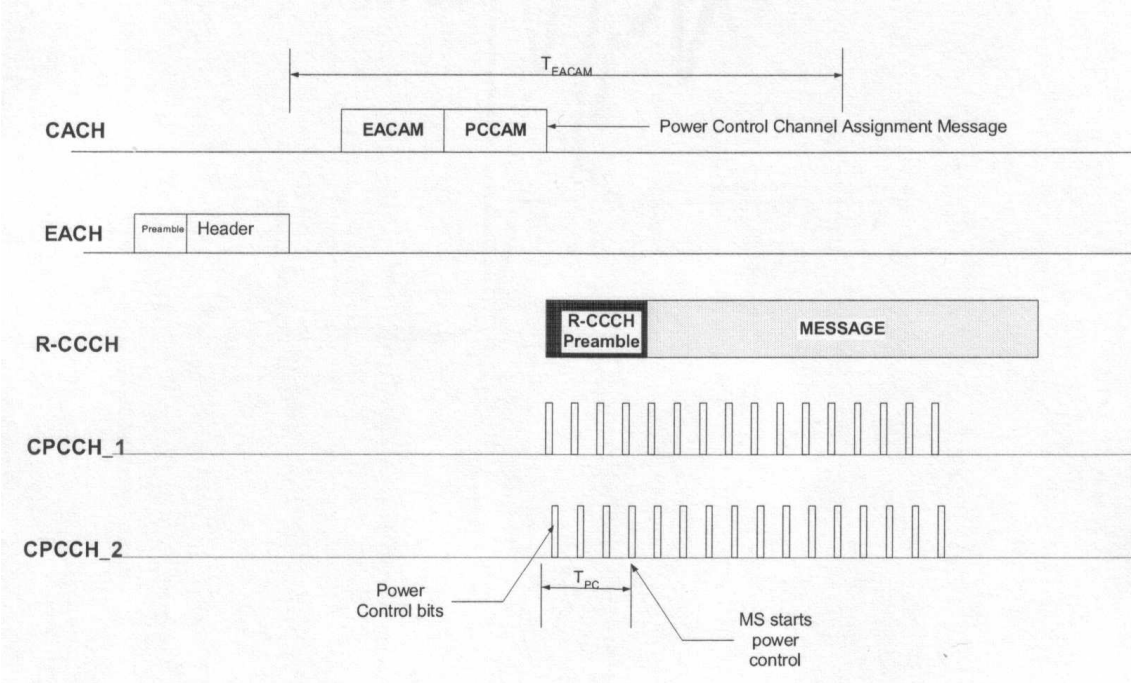

FIGURE 4.2-7. An example of Reservation Mode with diversity random access. [C.S0003-A].

4.2.2.4 *Gains from Diversity Random Access*

Usually, when radio network planning is made, gain from macro diversity is included to the link budget. For example, in [Hol00] it is assumed 2–3 dB gain from macro diversity in the shown link budgets. Macro diversity gain extends the cell range correspondingly. If the random access is made to only one base station or sector there does not exist any macro diversity at the beginning of the call. Then the maximum pathloss that is tolerated for the connection is 2–3 dB lower than the maximum pathloss existing in the system. This leads to the fact, that at the beginning of the call the quality may be poor and can lead to call drop if the mobile station is located in the cell border. This problem is depicted in FIGURE 4.2-8. By using diversity random access this is avoided, since the macro diversity state is utilized from the beginning of the connection.

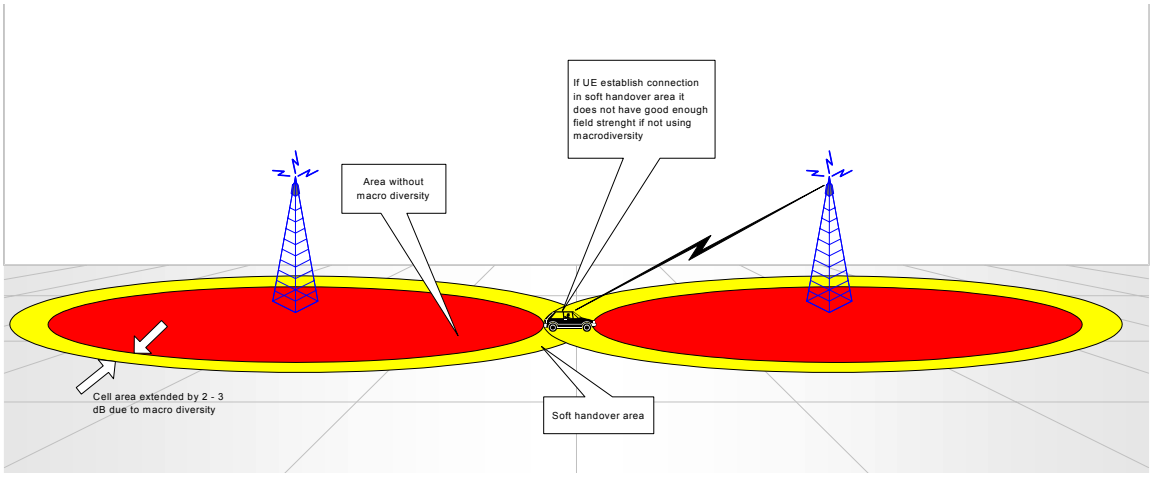

FIGURE 4.2-8. The problem for the user without macro diversity in the beginning of the call.

If the random access is made to only one base station, the delay in forming the diversity handover corresponds to the delay in the handover execution. After the connection has been established with the random access, the mobile station sends an active set update message to the radio network controller via the serving base station. After receiving the mobile station's message, the radio network initiates the required actions to add the requested base stations to the active set of the mobile station. This may, however, last over tens or hundreds milliseconds. During that time the quality of the mobile station may be insufficient. In addition, more signalling is involved since random access and handover signalling has to be made separately.

Consider link budget example in [Hol00]. Allowed propagation loss in cell border is 141.9 dB with macro diversity. If macro diversity is neglected the maximum propagation loss reduces to 138.9 dB. By using Okumura-Hata propagation model, size of soft handover area can be analysed. Okumura-Hata propagation model for an urban macro cell with base station antenna height of

30 meters, mobile antenna height of 1.5 meters and carrier frequency of 1950 MHz is [Wan00]:

$$L = 137.4 + 35.2 \log10(R), \quad (4.2\text{-}1)$$

where R given in kilometres.

By using Equation (4.2-1) the maximum cell radius can be calculated. For case with macro diversity maximum cell radius is 1.34 km and for case without macro diversity 1.1 km. If we assume the cell area as a circle, the maximum cell area for the macro diversity case is 1.69 km^2 and for non-macro diversity case 1.21 km^2. Thus, the size of the soft handover area is 1.69 / 1.21 ~ 30 % of total cell area. In this 30 % of the total cell area call quality may be poor at the beginning of the connection if diversity random access is not used.

Even if the quality was sufficient for random access without macro diversity, the mobile station would need to use higher transmission powers in both uplink and downlink directions due to 2–3 dB higher pathloss. This means that higher interference is also generated to the network and thus the capacity reduced.

When using diversity random access, macro diversity state will also be created directly for the packet data connection using common channels. The macro diversity state continues for the duration of the whole packet in which case the quality will worsen less probably during the packet. Since it is difficult to carry out soft handover during the common channel access the use of macro diversity on a packet-mode connection is possible only by using the presented method.

4.3 Acquisition

As a response to random access the preamble received from a mobile station the base station sends AI (Acquisition Indicator) to the mobile station by using AICH. The Acquisition Indicator is sent by using the same signature as was used by the mobile station on the physical random access channel [TS25.211].

Acquisition indicators are transmitted in downlink access slots that the timing is such that they are sent $\tau_{p\text{-}a}$ chips after uplink access slot. The spreading factor used for channelisation is fixed to 256.

When the mobile station receives the acquisition indicator channel there exists the possibility of a false alarm and detection error. A false alarm occurs, when the mobile station erroneously decodes the acquisition indicator even though no indicators were sent by the base station. Detection error occurs when the mobile station is not able to decode the acquisition indicator sent by the base station. To be able to recover from false detection, a RRC layer timer T300 is started in the beginning of random access. If timer T300 expires before the mobile station receives RRC connection setup, random access is started again.

4.3.1 Performance of Acquisition Indicator Procedures

Since the random access performance has now been investigated in Chapter 4.2.1 for an ideal acquisition indicator procedure, we can start to study the performance effects of the acquisition indicator procedure. The used simulator is the dynamic simulator presented in Chapter 2.4. The parameters for acquisition indicator simulations are shown in TABLE 4.3-1. This study was originally given in [Hen01].

As explained in Chapter 2.4.4.1, detection error is modelled with probability 1-P_d and false alarm with probability of P_{fa}. Here three main cases were simulated: The effects of P_d, P_{fa} and joint P_d / P_{fa}. The results are shown in TABLE 4.3-2. These results show that P_{fa} clearly causes more delay than P_d. However, the mean duration changes surprisingly little, while the deviation explodes. The explanation for this is subtle: As FIGURE 4.2-3 shows, around 80% of all users in random access can be received with the first preamble. This means that only 20% of users even have a chance of false detection happening. Thus when $P_{fa} = 0.1$, only $0.1 \bullet 0.2 = 0.02$ or 2% of users actually experience false detection.

TABLE 4.3-1 Parameters for AICH simulation.

Parameter	Value
Varied AICH parameters	
P_d ($P_{fa} = 0$)	1, 0.99, 0.95 and 0.9
P_{fa} ($P_d = 1$)	0, 0.01, 0.05 and 0.1
(Pd, Pfa)	(0.99, 0.01), (0.95, 0.05), (0.90, 0.10)
Constant parameters	
SIR threshold value used in open loop	-35 dB
C/I threshold for RACH preamble detection	-25 dB
Power ramping factor	3 dB
The maximum number of RACH messages UE can send before random access is terminated	3
Timer T300	200 ms

TABLE 4.3-2. Random access statistics.

P_d	P_{fa}	Average duration in slots	STD of duration in slots	Average # of preambles	STD of sent preambles
1	0	41.79	5.54	1.24	0.69
1	0.01	42.19	14.24	1.21	0.67
1	0.05	44.63	31.67	1.22	0.69
1	0.1	46.99	42.59	1.21	0.70
0.99	0	41.79	5.41	1.22	0.68
0.95	0	42.17	5.76	1.27	0.72
0.9	0	42.62	6.09	1.33	0.76
0.99	0.01	42.53	15.48	1.24	0.71
0.95	0.5	45.09	31.71	1.27	0.74
0.9	0.1	47.65	42.02	1.31	0.77

TABLE 4.3-3. System capacity, TX and SIR target statistics.

P_d	P_{fa}	NR[20] mean	NR STD	Load, mean	Load change factor	Load change factor in dBs
1	0	2.57	1.29	0.45	1	0
1	0.01	2.66	1.36	0.46	1.03	0.11
1	0.05	2.54	1.33	0.44	0.99	-0.04
1	0.1	2.56	1.22	0.45	1.00	-0.01
0.99	0	2.58	1.31	0.45	1.00	0.01
0.95	0	2.62	1.37	0.45	1.01	0.06
0.9	0	2.65	1.39	0.46	1.02	0.10
0.99	0.01	2.69	1.40	0.46	1.03	0.14
0.95	0.5	2.58	1.29	0.45	1.00	0.01
0.9	0.1	2.53	1.38	0.44	0.99	-0.05

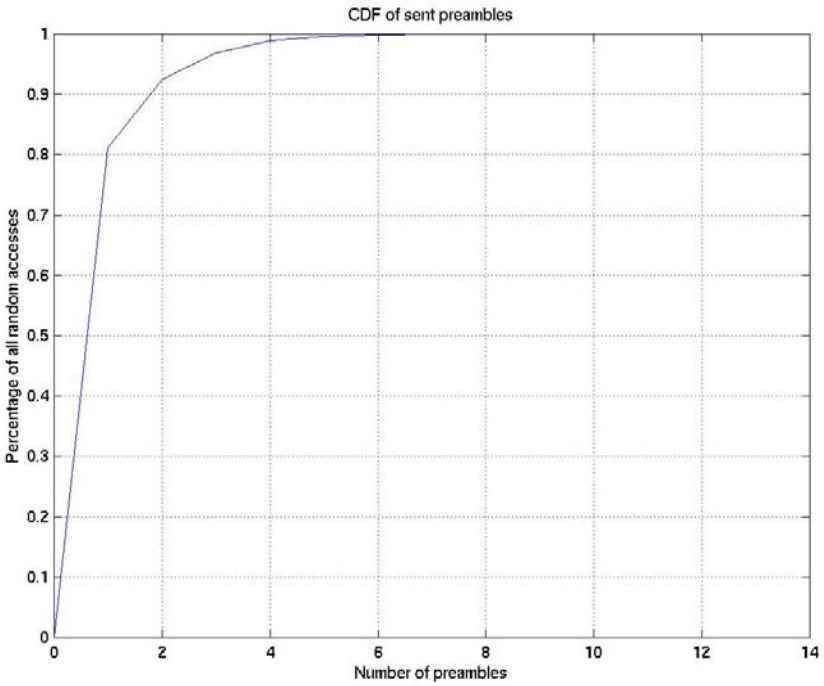

FIGURE 4.3-1. Distribution of the number of sent preambles for the case P_{fa} =10%, P_d =90%.

[20] Noise rise

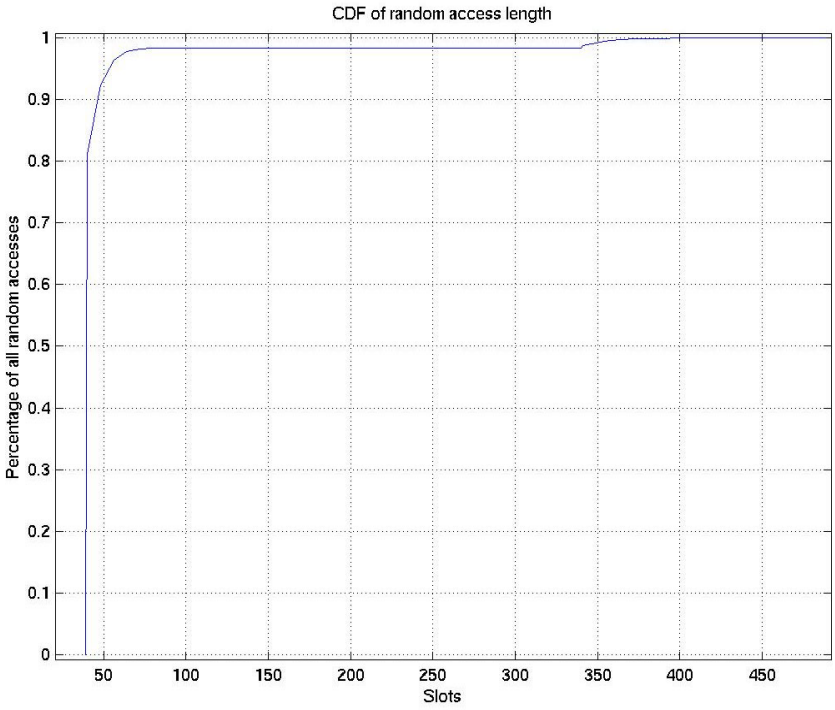

FIGURE 4.3-2. Random access duration distribution for the case P_{fa} = 10%, P_d = 90%.

The effect due to P_d is not been seen since an unsuccessful detection of a preamble caused only a short delay in random access. If a detection error occurs a delay of 5 slots is generated. This leads to maximum delays of in order of 10–15 slots (in case P_d = 0.1, probability of 15 slot delay is 0.001), i.e. one frame. If this is compared to a delay caused by a single false detection that causes a delay of tens of frames it is obvious that P_{fa} has a bigger impact on the performance than P_d.

The results show that the acquisition indicator channel errors do not have a significant effect on noise rise and hence, on the system capacity. In fact, a noise rise is even lower in some cases, but this can be attributed to a statistical phenomena and the fact that with high P_{fa} probabilities, the mobile station suffering from P_{fa} will have fairly long silent periods.

The acquisition indicator channel simulations show that the P_{fa} value has more of an impact on random access delay than the P_d value. This is because of the delay caused by a single false alarm is completely determined by the value of the timer T300 at the time the false alarm occurs. The magnitude of this timer is measured in hundreds of milliseconds while the length of a single preamble is just one millisecond and the length that is needed to send (and listen to acknowledgement for) a preamble is in order of 5 ms. Therefore, a false alarm can cause ten times more delay than a preamble that was not detected.

The effect of an acquisition indicator channel on the overall performance of the network is negligible in most cases. The highest simulated increase in noise rise is 0.12 dB. From this it can be concluded that the parameters selected for the acquisition indicator algorithm provide good performance to the network.

4.4 Handover

WCDMA handover takes advantage from the soft handover and macro diversity. New base stations can be added to the active set before they are employed by the mobile station. Gradually they become stronger and more and more of the information is conveyed through them. When the mobile station leaves the cell area of a base station less and less information is conveyed through that base station until it is finally removed from the active set. Thus, addition and removing a base station to/from the active set is done softly. Therefore, WCDMA handover is called soft handover. If there exists several almost equally strong base stations in the active set, signal paths from them can be received simultaneously. This increases the signal path diversity and thus improves the quality. Improvement can be exploited by reducing transmission power. This further leads to less interference on the system and higher capacity. In WCDMA handover is mobile station assisted handover, i.e. the mobile station performs measurements that are signalled to the radio network controller that makes actual handover decisions based on mobile stations measurements. The idea of a soft handover was first presented in [Gil89].

An example of WCDMA handover is given in [TR25.922]. Execution of example handover is shown in FIGURE 4.4-1. Algorithm consists of a number of functions: measurements, filtering of measurements, reporting of measurement results, the soft handover algorithm and execution of the handover.

The measured value for handover purposes is e.g. wideband pilot E_c/I_0[21]or narrowband pilot SIR[22]. Due to the fact of the fading channel and errors in the measurement samples the mobile station needs to filter the handover measurements before sending them to the network. The way filtering is made has its impacts on the system's performance. Filtering of measurements in layer 1 can be made in several ways in the mobile station. Two examples of filtering are sliding window and block wise filtering. Sliding window filter is a FIFO (First-In-First-Out) buffer, which provides an average value for n last samples after every measurement. Parameter n defines the length of the filter. Block wise filtering takes n measurement samples to the buffer after which an average value of n samples is provided. Thus, the average value is provided after n samples. An advantage of the latter method is less processing. Its disadvantage is increased delay in detecting changes in the relative strengths of the base stations. In addition to layer 1 filtering in the mobile station, more filtering can be obtained by using layer 3 filtering in the network.

Filtered measurements can be sent to the network whenever the relative strength of base stations change, i.e. an event occurs, or periodically after certain fixed time intervals. In case of event-triggered reporting, events in the example shown in FIGURE 4.4-1 may happen. Event 1A occurs when a new cell

---

21 E_c/I_0 = CPICH RSCP / RSSI

22 SIR = CPICH RSCP / ISCP

that was not in the current active set becomes sufficiently strong and is added to the active set. A new cell is sufficiently strong if its relative strength is higher than *Best_Ss - AS_th + AS_th_Hyst*. Best_Ss is the strength of the currently strongest cell in the active set, AS_th is threshold for macro diversity and AS_th_hyst is addition or removing hysteresis preventing ping-ponging. Event 1C occurs when a new cell that was not in the current active set becomes stronger than the weakest cell in the active set and replaces the weakest cell. The relative strength of the new cell has to be higher than the strength of the weakest cell in the active set by AS_Rep_Hyst. Event 1C occurs only if the number of cells in the active set is equal to the maximum value defined. Event 1B occurs when a cell in the active set becomes weak and is removed from the active set. The strength of the removed cell has to be below Best_Ss - AS_Th - AS_Th_Hyst. To every event timer Δt is involved.

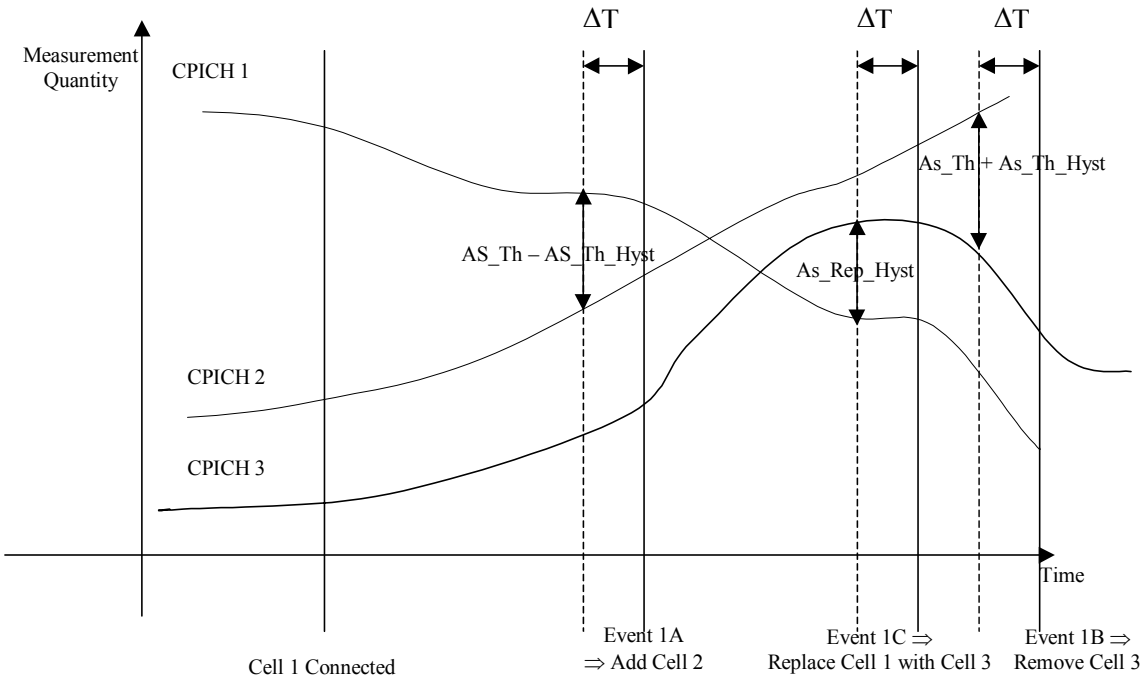

FIGURE 4.4-1. An example of WCDMA handover algorithm [TR25.922].

If the radio network controller decides to modify the active set based on the reported measurements some delay is experienced before the actual change of serving branch (base station or sector) happens. This is due to processing and signalling delays in the network and in the radio network controller.

4.4.1 Handover Measurements

In this chapter two handover evaluation criteria for WCDMA handover are compared. Two approaches for handover measurements have been proposed [Tel99] – narrow band SIR in which CPICH SIR is measured as a ratio of RSCP and narrowband ISCP (Interference Signal Code Power) and wideband SIR in

which SIR is measured as a ratio of RSCP and wideband interference measurement, RSSI (Received Signal Strength Identifier). Also other criteria exist, such as uplink SIR-based handover presented in [Gra95].

Based on the study shown in the following chapter it is proposed to use only the wideband estimate with WCDMA handover measurements in order to maximize the system performance. This study was first presented in [Kor01].

4.4.1.1 *Narrow Band and Wide Band Pilot SIR Based Handovers*

Here two measurement quantities proposed for handover evaluation are compared, namely CPICH E_c/I_0 = CPICH RSCP/RSSI, that is referred as the wideband criterion and CPICH SIR = CPICH RSCP/ISCP that is referred as the narrowband criterion.

The definitions of the measurements are discussed here are as follows: RSCP is the received code power measured on the Primary CPICH. RSSI is the wide-band received power within the relevant channel bandwidth. ISCP is the measured interference after despreading on a reserved orthogonal code, which has the same spreading factor as the Primary CPICH.

If the narrowband criterion is used for handover evaluation, the mobile station tends to propose that a handover is made to higher loaded cell due to orthogonality. Ideally narrowband criterion minimizes locally the required downlink power for an individual radio link if secondary effects are not taken into account. Thus, theoretically narrowband criterion could minimize the total downlink interference and thereby maximize downlink capacity.

In [Kor01] measurement accuracies of the two handover evaluation quantities were analysed by comparing the probability density functions (PDFs) of RSSI and ISCP in AWGN channel. Differences in the measurement accuracies were illustrated by an example where the averaging period of the measurements was 4 symbols and E_s/N_0 in the channel 7 dB. Calculations show that in this case the RSSI estimation performs approximately 250 (almost the spreading factor of CPICH) times better than the ISCP estimation. TABLE 4.4-1 shows that the performance of ISCP estimate is significantly worse than the performance of RSSI and RSCP estimates.

TABLE 4.4-1. RSCP, RSSI and ISCP measurement accuracy [Kor01].

Measurement	Channel	Mean	Variance
RSSI	AWGN	52.1	2.65
ISCP	AWGN	51.1	654.0
RSCP	AWGN	1.1	0.1
E_c/I_0	AWGN	0.02	0.00004
SIR	AWGN	0.03	0.0005
RSSI	1-tap Rayleigh	52.1	3.7
ISCP	1-tap Rayleigh	51.1	652.1
RSCP	1-tap Rayleigh	1.1	1.1
E_c/I_0	1-tap Rayleigh	0.02	0.0004
SIR	1-tap Rayleigh	0.03	0.002

In FIGURE 4.4-2 PDFs for E_c/I_0 and SIR are shown. The PDF of E_c/I_0 is the joint probability density function of RSCP and RSSI and correspondingly the PDF of SIR is the joint probability function of RSCP and ISCP. In both of the measurements the numerator is the same and only the denominators differ from each other. Since the performance of the ISCP estimate is clearly worse than the performance of the RSSI estimate, the SIR is always worse than E_c/I_0. However, the performance difference between RSCP/RSSI estimate and RSCP/ISCP estimates is not as straightforward as the difference of the denominators since the quality of RSCP estimate e.g. due to fading and SNR also influence the total estimation performance. [Kor01]

RSCP, RSSI, ISCP, E_c/I_0 and SIR results for 1-tap Rayleigh fading channel with a vehicle speed of 50km/h were also analysed. The results are shown in TABLE 4.4-1. The performance difference between RSSI and ISCP and further E_c/I_0 and SIR can also be clearly seen in this case although fading and too short averaging period (4 symbols) has caused significant variation into RSCP level. [Kor01]

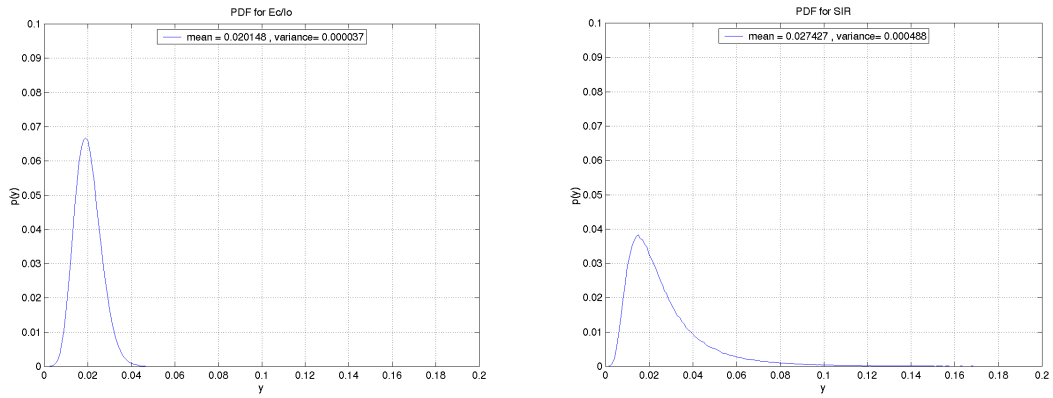

FIGURE 4.4-2. PDFs of E_c/I_0 and SIR in AWGN channel.

4.4.1.2 *Simulation Tool*

The used simulation tool is a static Monte Carlo type system simulator as described in Chapter 2.5. During a simulation step mobile stations are put to random positions in the simulated area, after which they connect to the serving base station(s) according to the handover criteria. After the handover, several power control iterations are made. Finally, the quality of the mobile stations is checked and outage calculated.

With this study the parameters and models used in the simulations are as in [TR25.942], except the handover models have changed. When selecting serving base stations in case of the wideband criteria, an error is added to the pathloss measurement. The error is generated from a log-normal distribution with zero mean and a given standard deviation.

In case of narrow band criteria, the mobile station selects an initial active set by using pathloss as a criterion. Then the downlink SIR of the pilot is calculated by taking orthogonality into account. It is assumed that the downlink is not perfectly orthogonal: the orthogonality factor 0.6 specified in [TR25.942]

for the used scenarios. Next the mobile station re-selects the serving base stations by using the narrowband handover criteria. Pilot SIR calculations and handovers are iterated a few times (20 were used in the simulations) so that the system converges. When the pilot SIR is calculated a log-normal error is added as is done with the wideband estimate.

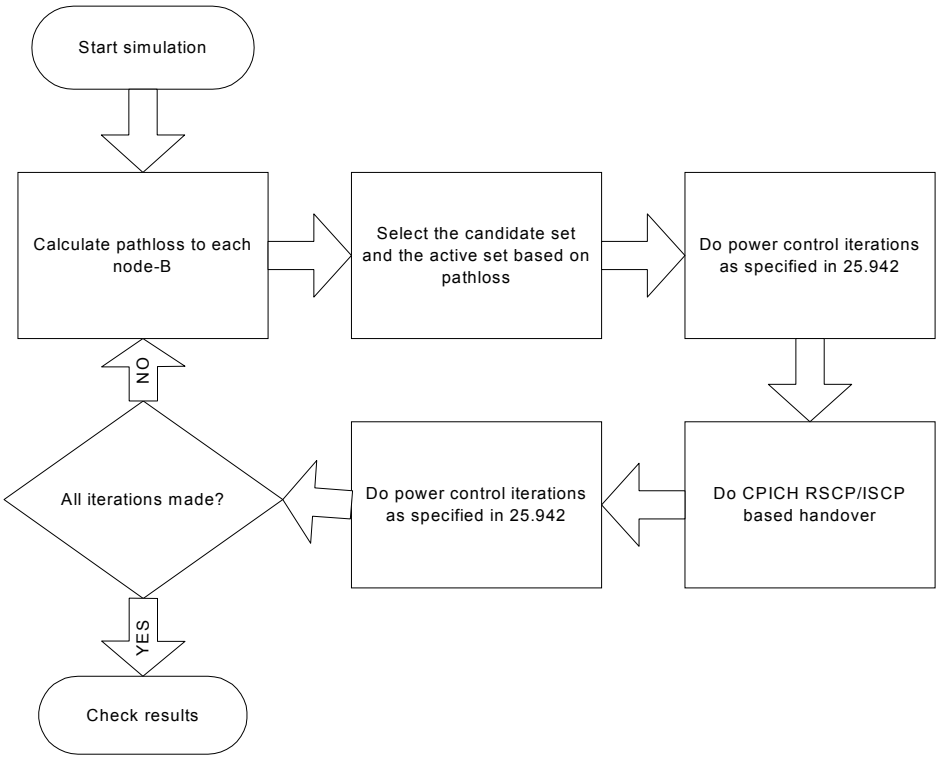

FIGURE 4.4-3. Simulation model for CPICH RSCP/ISCP handover.

4.4.1.3 *Effect of Measurement Error*

In FIGURE 4.4-4 capacity as a function of measurement error for downlink and uplink is shown. If it is assumed that CPICH SIR estimation and CPICH E_c/I_0 estimation performs equally well, it can be seen that with the narrowband criteria slightly higher capacity is obtained. However, as discussed in Chapter 4.4.1.1, the CPICH SIR estimation performs worse than the CPICH E_c/I_0 estimation. The measurement error of the CPICH E_c/I_0estimate is typically in the order of 2–4 dB (accuracy requirement in [TS25.133] ±3 dB), which implies that the capacity for the wideband handover criterion is 45–65 users/cell in the downlink and 43–54 users/cell in the uplink. There is no measurement accuracy requirement defined for CPICH SIR in 3GPP. Based on analysis in [Kor01] the measurement error of the CPICH SIR estimate is in the order of 7–10 dB. Then the capacity is 5–28 users/cell in the downlink and 3–26 users/cell in the uplink. As we can see from these figures measurement accuracy has a very high impact on capacity. Furthermore, FIGURE 4.4-4 show that the capacity of the narrowband criteria based handover is significantly worse than the capacity of

the wideband criteria based handover when measurement accuracies are taken into account.

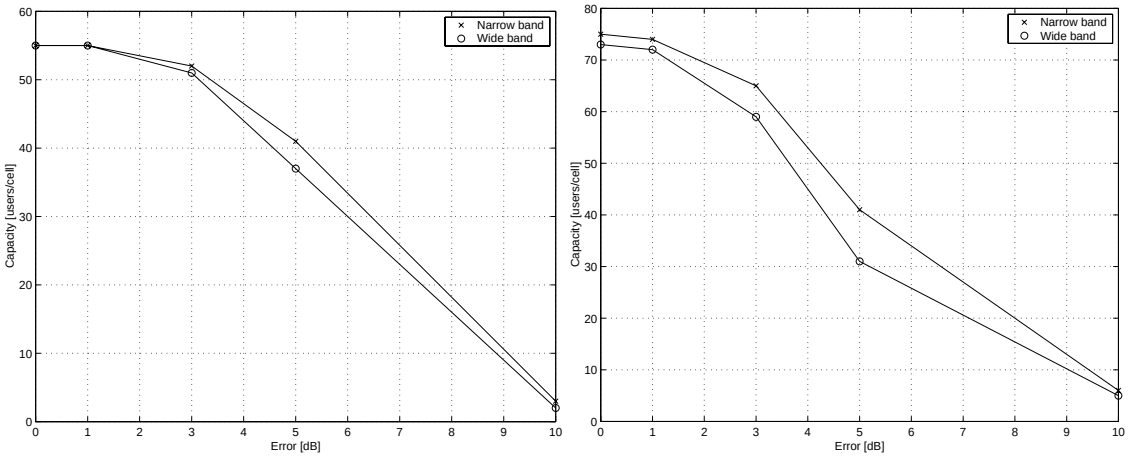

FIGURE 4.4-4. Uplink and downlink capacity as a function of measurement error. Wideband and narrowband handover criteria.

4.4.1.4 *Size of Handover Zone*

The size of the handover zone is not exactly the same for both handover criteria when the handover thresholds have the same value. It is expected that the handover area would be smaller for the narrowband criteria. It is crucial to keep the size of the handover zones the same, since otherwise ping-ponging is increased and handover reliability decreased. This can be further seen as degradation in call quality or even increased probability for call dropping. Also, in order to make a fair comparison, with the same quality of service and the same mobility supported, the sizes of handover zones should be chosen to be equal.

In static simulation methods the best capacity is obtained by having ideal hard handover since mobility is not modelled and handover zones can be infinitely small. Handover margins are added only to model hysteresis in real handover algorithms – not to provide capacity gain.

The simulations results show that the narrowband criterion gives significantly smaller handover probability and handover zone. According to statistics of soft handover overhead, with wideband criterion soft handover overhead is 24 %, while for narrowband criterion it is only 17 %. From this, it is obvious that narrowband criterion provides smaller handover zones. Further, this is the main reason why narrowband criterion seems to give better capacity with ideal measurement accuracy.

It should be noted that the size of the handover zone for narrowband criterion is highly affected by the orthogonality of the cell. Handover zones for wideband and narrowband criterion can be also examined with a simplified example, where only two cells are present. In this case the handover evaluation quantities are as follows:

$$(E_c / I_o)_1 = \frac{TXP_{CPICH1} / L_1}{P_{tot1} / L_1 + P_{tot2} / L_2 + N}, \tag{4.4-1}$$

$$(SIR)_1 = \frac{TXP_{CPICH1} / L_1}{(1-\alpha) P_{tot1} / L_1 + P_{tot2} / L_2 + N}. \tag{4.4-2}$$

If we assume perfect orthogonality in the channel i.e. the orthogonality factor α is 1, cell 1 and cell 2 have the same pilot and total powers and system noise N approaches zero, we can easily demonstrate smaller handover zones for narrowband criterion. In this example CPICH E_c/I_0 difference between two cells becomes

$$\left.\begin{aligned} (E_c/I_0)_1 &= \frac{TXP_{CPICH} / L_1}{TXP_{tot} / L_1 + TXP_{tot} / L_2} \\ (E_c/I_0)_2 &= \frac{TXP_{CPICH} / L_2}{TXP_{tot} / L_1 + TXP_{tot} / L_2} \end{aligned}\right\} \Rightarrow \Delta = \frac{(E_c/I_0)_1}{(E_c/I_0)_2} = \frac{L_2}{L_1} \tag{4.4-3}$$

,

and CPICH SIR difference between the same two cells in then

$$\left.\begin{aligned} SIR_1 &= \frac{TXP_{CPICH} / L_1}{TXP_{tot} / L_2} \\ SIR_2 &= \frac{TXP_{CPICH} / L_2}{TXP_{tot} / L_1} \end{aligned}\right\} \Rightarrow \Delta = \frac{SIR_1}{SIR_2} = \frac{L_2^2}{L_1^2} \tag{4.4-4}$$

.

CPICH E_c/I_0 difference between two cells, which is used for handover evaluation, reduces to a form in which pathlosses from two base stations are compared. For CPICH SIR difference reduces to a form in which squares of pathlosses from two base stations are compared. For example, if difference Δ in Equation (4.4-3) was 3 dB, it would be 6 dB in Equation (4.4-4).

Next we adjust the handover thresholds so that the handover probability becomes equal to that of a wideband criterion case. Capacity as a function of error is then simulated. The simulated scenario is a macro cell scenario with an evenly distributed load that is symmetric in uplink and downlink. The results from simulation can be seen in FIGURE 4.4-5. Originally, the handover threshold was 3 dB for both criteria. In order to obtain an equal handover probability the handover threshold has to be increased to 5.4 dB in case of narrowband criterion.

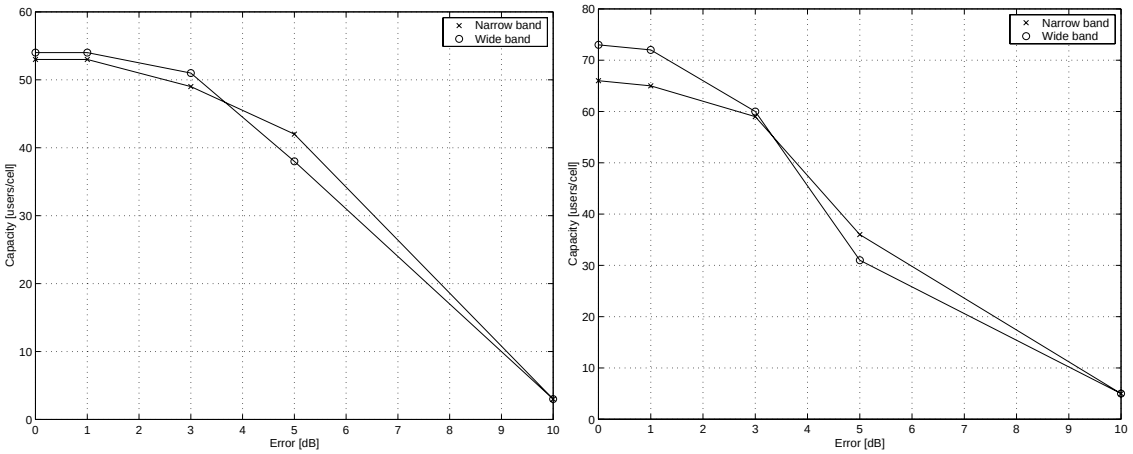

FIGURE 4.4-5. Uplink and downlink capacity as a function of measurement error. Handover zones are selected to be same for wideband and narrowband criterion.

The simulation results in FIGURE 4.4-5 show slightly better performance for the wideband criterion than for the narrowband criterion when assuming equal error performance. With a small error number of users is large and the simulation results are more reliable i.e. the standard deviation is smaller. In case of a large error the same capacity can be obtained with two criteria. The curves differ a bit from each other but this is due to the fact that the deviation of the results is quite high due to the low number of users in the simulation.

4.4.1.5 *Manhattan Hot Spots*

Since it is expected that the narrowband criteria performs better in case of non-uniform loading in the network, also a hot-spot scenario is simulated in a Manhattan environment. Manhattan hot spots are modelled so that some streets and corners are defined as hot spot positions. Some terminals are then named as hot spot terminals, which are always placed in a hot spot area. Thus, the load in the hot spot area can be increased by setting the hot spot probability p. The modelling is such that $(100 \cdot p)$% of users are hot spot terminals and are put randomly to the hot spot area. In addition to the hot spot terminals, there can also be other terminals in the area, because other terminals' positions are decided randomly from the whole simulations area. In the simulations p was set so that the load is about 20 % higher in the hot spot zones than elsewhere.

The simulation results of the Manhattan scenario with hotspots are given in FIGURE 4.4-6 as a function of measurement error. It should be noted that in these simulations the same handover thresholds are used for both criteria, i.e. handover zone becomes smaller for narrowband criterion. Since in the Manhattan scenario the orthogonality is high ($\alpha = 0.94$), the difference in the handover zone sizes is expected to become significant. However, since the scenario and the shape of the cells are different from the macro cell scenario, the iteration of the correct threshold values has to be determined independently from the macro scenario. Simulation results show that the handover threshold

of the narrowband criterion is between 4.5 dB and 5 dB when 3 dB handover threshold is used for wideband criterion.

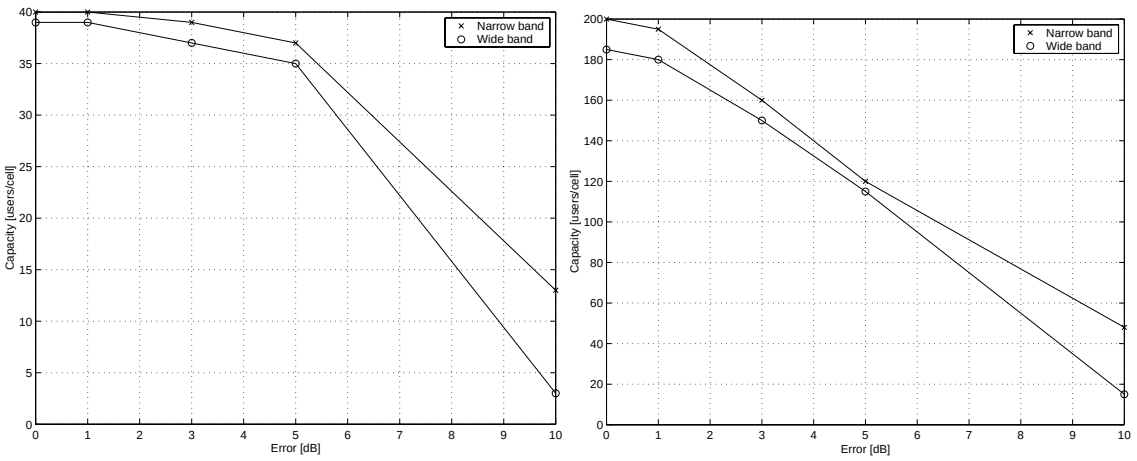

FIGURE 4.4-6. Simulation results for uplink and downlink in Manhattan environment with hot spots when equal handover thresholds are used.

When the same measurement error is assumed for both of the criteria, narrowband criterion gives a minor capacity gain. This, however, is the result of a smaller handover zone for narrowband criterion than for wideband criterion. If realistic measurement performance is considered, the wideband criterion gives 1.4 to 3.7 times better capacity than the narrowband criterion, assuming 2–4 dB measurement error for wideband measurement and 7–10 dB measurement error for narrowband measurement. When the simulations are repeated with the correct handover threshold (4.5–5 dB), the capacity of the narrowband criterion is expected to degrade.

4.4.1.6 *Asymmetric Loading*

A case with asymmetric loading in uplink and downlink is also simulated. The selected bitrates in the uplink and downlink are 12 kbps and 64 kpbs, respectively. It should also be noted that in these simulations the same handover threshold (3 dB) is used in both of the models, i.e. smaller handover zones are assumed for the narrow band criterion simulation. Due to difference in the sizes of handover zones the narrow band criterion gives a slightly better capacity if the same measurement error is assumed for both of the criteria. Results with adjusted handover zones show that the uplink capacity becomes 67.9 users/cell for the wideband criterion and 65.4 users/ cell for the narrowband criterion when 0 dB measurement error is considered for both of the criteria, see FIGURE 4.4-7.

When realistic measurement performance is considered, the wideband criterion gives better capacity even without handover zone adjustment. If we assume 2–4 dB measurement error for the wideband criterion and 7–10 dB measurement error for the narrowband criterion, 1.7–13 times better capacity is obtained with the wideband criterion than with the narrowband criterion.

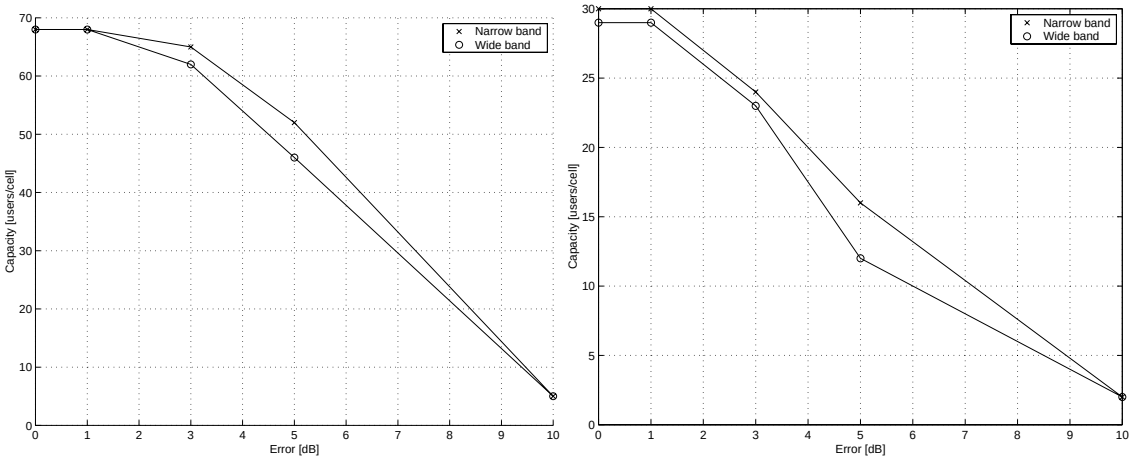

FIGURE 4.4-7. Simulation results for uplink and downlink for asymmetric traffic when equal handover thresholds are used.

Results in this study indicate that handover with CPICH E_c/I_0 measurement provides a higher capacity than CPICH SIR measurements when soft handover is properly modelled. When realistic measurement accuracy is considered, the CPICH E_c/I_0 measurement based handover criterion clearly outperforms the CPICH RSCP/ISCP measurement based criterion.

4.4.2 Handover Delay Effects

In this chapter delay effects due to filtering and different reporting schemes are investigated. The selected filtering schemes are sliding window and block wise filtering. It is assumed that the block wise filtering introduces such additional delay to handover decisions that may deduct handover performance. In the worst-case additional delay may be up to the length of the filter. Even though block wise filtering introduces additional delay, it may be preferred choice for a practical implementation due to lower processing needs. The purpose of this study is to show performance difference between sliding window and block wise filtering schemes. The selection of filtering scheme is a trade-off between worse radio network performance and higher complexity.

In addition to filtering, reporting schemes are investigated. Studied schemes are event-triggered and periodic reporting. Similar effects are expected to appear from the periodic reporting as from block wise filtering; in the worst-case additional delay to handover execution maybe up to the length of the reporting period. Benefit of periodic signalling is less signalling traffic in the air-interface.

Simulations are executed by using dynamic simulator presented in Chapter 2.4. Simulations are carried out in Manhattan type micro-cellular and hexagonal macro-cellular networks. As the outcome of this study some guidelines for proper filtering and reporting schemes are given. This study was first presented in [Häm02].

4.4.2.1 *Comparison of Sliding Window and Block Wise Filtering Schemes*

In these simulations the L1 filtering length in the mobile station is 200 ms. With the sliding window approach, a filtered value is obtained every 10 ms. With the block wise filtering, a filtered value is obtained every 200 ms. With both methods, the filtered value is an average over 20 measurement samples. Some of the parameters used with the simulations are gathered in TABLE 4.4-2.

TABLE 4.4-2. Simulation parameters.

Parameter	Value
General parameters	
Service	Speech
Data rate	12 kbps
Voice activity	50 %
Micro-cell environment	
Mobile speed	3, 5, 30, 50 km/h
Load	32 subscribers/cell
Cell Size	11x12 Micro scenario, buildings 200mx200m, 72 BSs
Channel model	In-to-Out A with 2 taps
Macro-cell environment	
Mobile speed	50, 120 km/h
Load	28 Subscribers/cell
Cell Size, number of BSs	5x4 Macro scenario, 666 m cell radius, 18 BSs
Channel model	Vehicular-A with 5 taps

Simulation results in the Manhattan environment are shown in TABLE 4.4-3. From the results a clear increase in noise rise can be seen if block wise filtering is used instead of the sliding window. With the sliding window the mean noise rise is 3.4 dB for both 5 km/h mobile speed and 30 km/h mobile speed. The corresponding values for the block wise filtering are 4.0 dB for both cases.

In addition to an increase in the noise rise, deviation of noise rise also increases significantly. An increase in deviation may be even more of a severe problem than the increase in the mean value. If load and admission control algorithms are based on noise rise thresholds as presented in [Hol00] fluctuations in noise rise may cause problems for those algorithms. Even though the mean noise rise remains well below the target value (e.g. 6 dB), fluctuations in noise rise may force a rejection of new users or drop existing users if high and lengthy noise rise peaks are experienced. In this kind of situation, the only way to overcome this problem is to reduce loading on such a level that noise peaks have no impacts on load or admission control.

In the downlink the mechanism is a bit different – when a mobile station performs the handover too late and is connected to the wrong base station, high interference for that user is generated by the stronger base station not yet included in the active set. Unlike in the uplink, only the observed user suffers delayed handover. Simulations show the impact on bad quality percentage that increases from 0.6 % to 3.1 % when the block wise filtering is used instead of the sliding window.

TABLE 4.4-3. Simulation results in Manhattan environment.

UPLINK				
Mobile speed	Mean noise rise [dB]	STD of noise rise [dB]	Mean load [%]	Uplink bad quality %
Sliding window				
5 km/h	3.4 dB	2.2 dB	54 %	1.6%
30 km/	3.4 dB	2.2 dB	54 %	1.6%
Block wise				
5 km/h	4.0 dB	3.5 dB	60 %	2.5%
30 km/	4.0 dB	3.5 dB	60 %	2.5%
DOWNLINK				
Sliding window				
Mobile speed	Mean total TxP [W]	STD of TxP [W]	Mean load [%][23]	Downlink bad quality %
5 km/h	1.01	0.062	5.064	0.62%
30 km/h	1.01	0.064	5.064	0.57%
Block wise				
5 km/h	1.03	0.072	5.161	3.14%
30 km/h	1.03	0.007	5.1595	3.18%

TABLE 4.4-4. Simulation results in macro cell environment.

UPLINK				
Mobile speed	Mean noise rise [dB]	STD of noise rise [dB]	Mean load [%]	Uplink bad quality %
Sliding window				
50 km/h	2.53	1.03	44.2%	1.0
120 km/h	2.18	0.85	39.5%	0.6
Block wise				
50 km/h	2.76	1.23	47.0%	1.0
120 km/h	2.30	0.92	41.1%	0.6
DOWNLINK				
Sliding window				
Mobile speed	Mean total TxP [W]	STD of TxP [W]	Mean load [%]	Downlink bad quality %
50 km/h	5.63	2.72	28.15%	6.0
120 km/h	3.93	1.66	19.65	2.3
Block wise				
50 km/h	17.72	3.08	88.6%	60.5
120 km/h	13.69	3.85	68.45%	34.9

In TABLE 4.4-4, corresponding simulations are shown for the macro-cell environment. It was expected that the macro-cell environment is less demanding for handover and handover measurements. Simulations confirm this conjecture in the uplink; an increase in noise rise and loading is rather

[23] In downlink mean load is given as a fraction of mean total TxP and maximum TxP of the base station

modest. In the case of 50 km/h, mean noise rise for the sliding window is 2.53 dB and for the block wise method 2.76 dB. This shows only an 8 % increase in loading, while in the Manhattan environment an increase in load was about 17 %. In the case of 120 km/h, difference between the sliding window method and the block wise methods is even less. Standard deviation of noise rise increases from 1.03 dB to 1.23 dB in case of 50 km/h and from 0.85 dB to 0.92 dB in case of 120 km/h. The change in standard deviation is much smaller than in case of Manhattan simulation.

However, simulations show a very large effect in the downlink. The mean total downlink transmission power increases 215 % for 50 km/h case and 249 % for 120 km/h case. Increase in transmission powers is seen as a drastic drop in call quality. For the sliding window 6 % of users suffered poor call quality (in case of 50 km/h). For block wise filtering the poor quality percentage increases to over 60 % for the same simulation setup.

In FIGURE 4.4-8, histograms of noise rise are shown. From the figure, it can be seen that with the block wise filtering a higher mean and larger deviation is suffered. A major reason for the higher mean and deviation is the delay in handover execution: since the block wise filter produces a mean value in 200 ms intervals, it may take almost 200 ms to notice a new cell becoming stronger. Due to that, a mobile station may be connected to weaker base stations than the new base station not yet added in the active set. This may happen especially in the micro-cellular environment when a mobile station is turning over the corner. If a mobile station is not connected to the strongest base station, it uses high powers and generates high interference to that base station.

In FIGURE 4.4-9 an example of noise rise is shown as a function of time. The simulated mobile station travels along the same route in both of the shown curves. The sliding window is used in the upper curve and the block wise filtering in the lower curve. The simulated case is such that a user turns over a corner and enters into the area of the observed base station. The approximate time when the user turns over a corner is circled to better show the effect. Due to delays in the handover, the mobile station is connected to the wrong base station and causes high interference to the observed base station. In these simulations it is assumed that the mobile speed does not change when the mobile station turns around the corner. Lower speed would lead to shorter duration of noise rise peak in both sliding window and block wise filtering case.

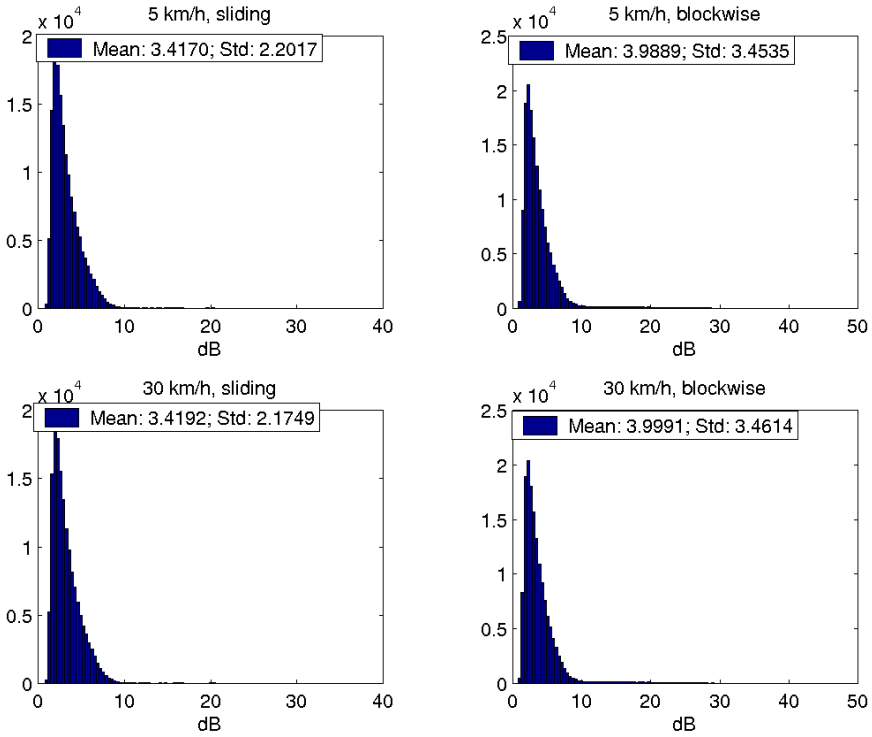

FIGURE 4.4-8. Noise rise histogram measured in the base station. Manhattan cell environment.

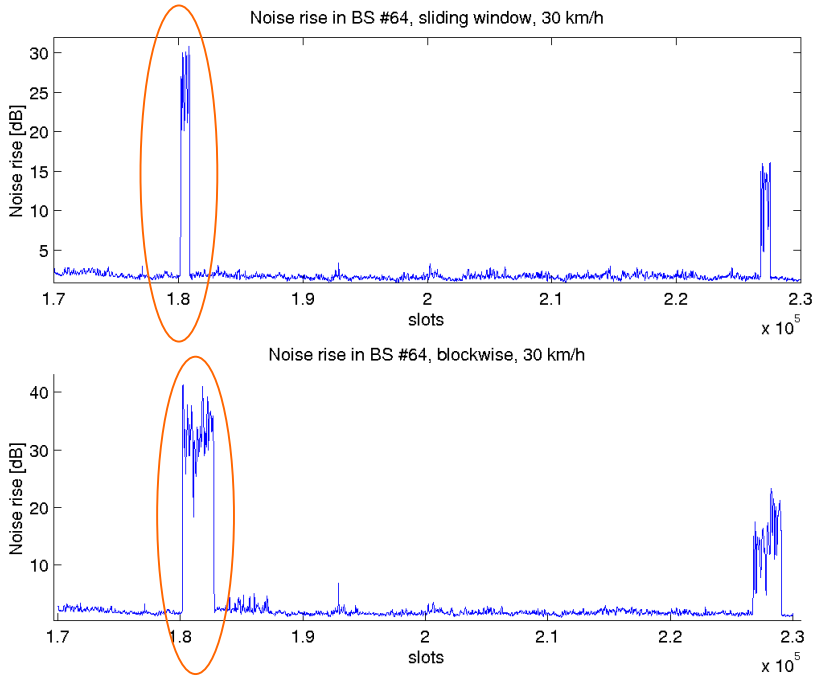

FIGURE 4.4-9. An example of noise rise when a mobile station turns around a corner and approaches base station that is not yet included in the active set. Simulation in Manhattan environment, mobile speed 30 km/h.

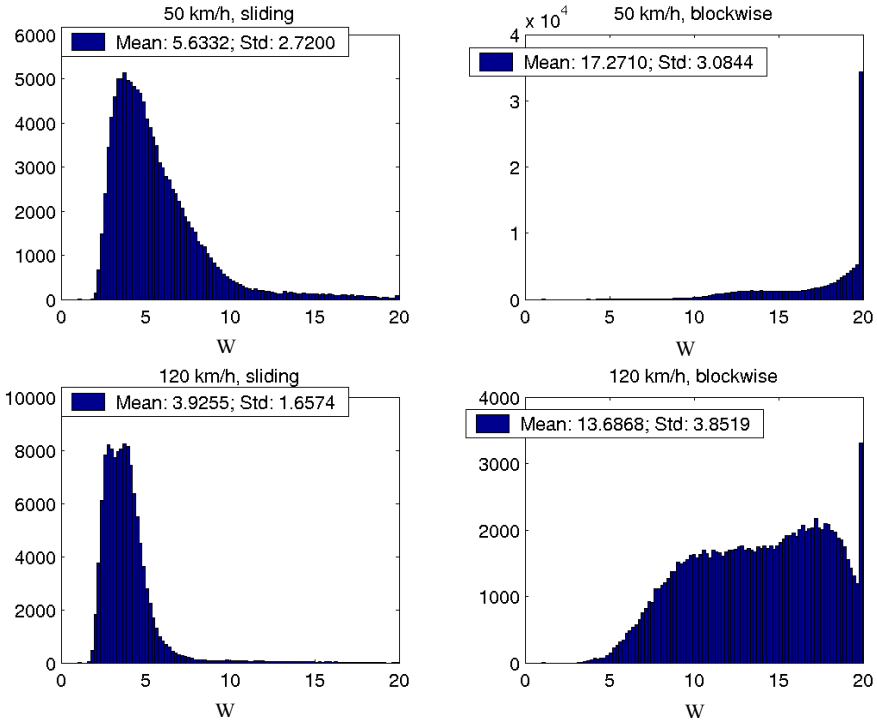

FIGURE 4.4-10. Downlink transmission power histogram. Simulations in macro cell environment.

In FIGURE 4.4-10 histograms of downlink transmission powers are shown in the macro cell environment. Histograms are given for 50 and 120 km/h cases with equal loading. For example, in case of 50 km/h, used transmission powers are rather low for the sliding window. When the filtering scheme is changed to the block wise filtering, very high powers are used. A very high number of samples is recorded with the maximum base station power (20 Watts). The limited maximum power also limits deviation, which would be very high for the block wise filtering if the transmission power was not limited. In case of 120 km/h used powers are lower, but deviation due to block wise filtering is very high.

4.4.2.2 *Comparison of Event-Triggered and Periodic Handover Reporting*

In [Hil00b] the event-triggered and the periodic handover reporting schemes were compared. A conclusion in [Hil00b] was that the periodic measurement reporting over performs the event-triggered reporting in the macro-cellular environment if the increased signalling load is not considered. Here the event-triggered and the periodic reporting schemes are simulated in Manhattan micro-cellular and in hexagonal macro-cellular environment.

TABLE 4.4-5. Simulation results in micro cell environment.

UPLINK				
Mobile speed	Mean noise rise [dB]	STD of noise rise [dB]	Mean load [%]	Uplink bad quality %
Event-triggered				
3 km/h	3.42	2.20	0.54	1.57
50 km/	3.43	2.19	0.55	1.57
Periodic				
3 km/h	6.26	5.35	0.76	2.90
50 km/	6.98	6.43	0.80	2.91
DOWNLINK				
Event-triggered				
Mobile speed	Mean total TxP [W]	STD of TxP [W]	Mean load [%]	Downlink bad quality %
3 km/h	1.012	0.062	5.061	0.47%
50 km/h	1.014	0.063	5.068	0.52%
Periodic				
3 km/h	1.106	0.122	5.528	12.4%
50 km/h	1.137	0.133	5.683	12.7%

TABLE 4.4-6. Simulation results in macro cell environment.

UPLINK				
Mobile speed	Mean noise rise [dB]	STD of noise rise [dB]	Mean load [%]	Uplink bad quality %
Event-triggered				
50 km/h	2.53	1.03	0.44	1.0
120 km/	2.18	0.85	0.40	0.6
Periodic				
50 km/h	2.64	1.17	0.46	1.2
120 km/	2.33	1.29	0.41	0.6
DOWNLINK				
Event-triggered				
Mobile speed	Mean total TxP [W]	STD of TxP [W]	Mean load [%]	Downlink bad quality %
50 km/h	5.63	2.72	28.17	6.0
120 km/h	3.93	1.66	19.63	2.3
Periodic				
50 km/h	7.07	3.19	35.36	27.7
120 km/h	4.51	2.19	22.57	9.1

Simulation results show that in the Manhattan environment noise rise increases from around 3.4 dB to over 6 dB if the periodic handover reporting is used instead of the event-triggered, see TABLE 4.4-5. In the downlink, transmission powers remain on a similar level for both reporting schemes but the poor quality percentage increases from 0.5 % to over 12 %.

In the macro-cell environment the impact is smaller, see TABLE 4.4-6. Uplink noise rise increases only a little, but downlink bad quality increases from 6 % to 27.7 % in case of 50 km/h and from 2.3 % to 9.1 % in case of 120 km/h.

Conclusions based on the results shown here differ from the conclusions given in [Hil00b]. These results show that the event-triggered reporting scheme clearly over-performs the periodical reporting. In these simulations, the periodic reporting frequency used was 1 report/s. The reporting frequency in the event-triggered case was approximately 2.3 reports/s. The high reporting rate partly explains the better performance of the event-triggered reporting. However, if compared to [Hil00b] with these reporting rates the performance of two methods should be similar.

The major reason why the event-triggered method performs better than the periodic is that the event-triggered method can more quickly observe changes in relative pilot strengths. There is always a one second delay in-built to the periodic method.

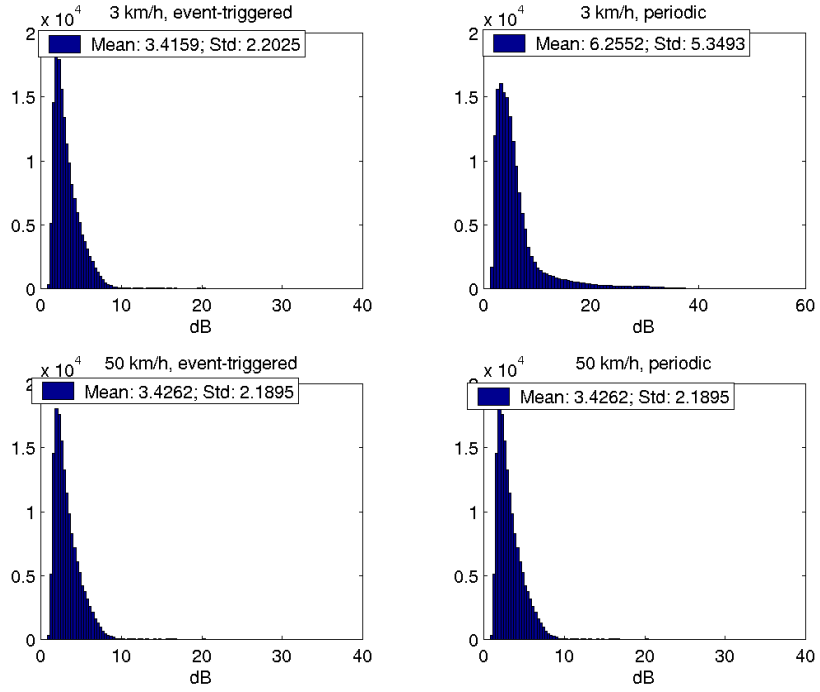

FIGURE 4.4-11. Example noise rise histograms from event-triggered vs. periodic reporting in micro cell environment.

4.4.3 Inter-Frequency Handover

Hierarchical cell structures can be arranged by using different frequencies in different cell layers or with spatial isolation as discussed in [Sha92 and Sha94]. If different frequencies are utilized, issues such as inter-frequency interference and inter-frequency handovers need to be considered. In case of spatial isolation they can be omitted, but then other problems are generated as discussed below. In this chapter, two approaches for hierarchical cell structure design in CDMA are described, and the advantages and disadvantages of the two methods are discussed. In the first approach, co-existing hierarchy layers operate on the same frequency band. Users operating on different layers are separated by handovers and signal fading. In the second approach, different

hierarchy levels are separated in the frequency domain. The aspects related to hierarchical cell structures are also relevant in a multi operator environment where an operator has to consider interference from the adjacent frequencies belonging to another operator. This discussion was originally given in [Häm98].

4.4.3.1 *Spatial Isolation*

In the case of micro- and macro-cells operating at the same frequency, frequency reuse is set to one and spatial isolation is used for separating micro- and macro-cell layers [Sha92, Sha94]. Reuse one can be offered since the processing gain allows users to experience interference originating from any cell layer. Intra-layer interference is controlled by power control and inter-layer interference by spatial isolation. In a generic flat-Earth model, the average transmission loss follows R^{-2} until a breakpoint that marks the separation between two segments. After the breakpoint, R^{-4} is followed. The location of the breakpoint depends on the receiver and transmitter heights. As the base station is installed lower, the breakpoint occurs nearer the base station. Thus, the signal from a micro cell base station attenuates faster than the signal from a macro cell base station. In FIGURE 4.4-12, spatial isolation is depicted for both, the hot spot case and for the continuous coverage of micro cells.

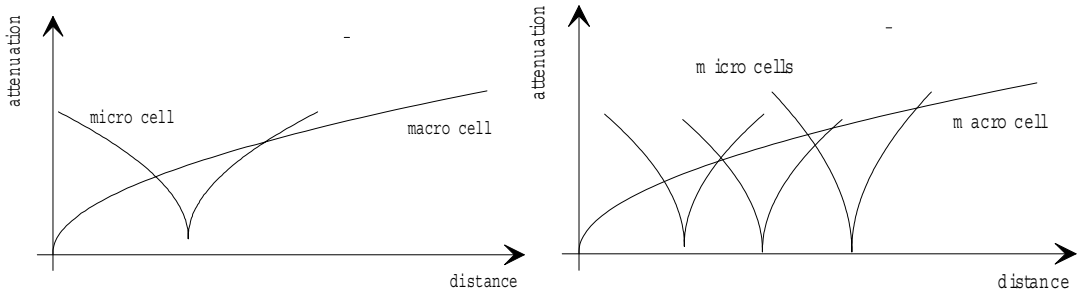

FIGURE 4.4-12. Spatial separation of umbrella cells and underlay micro cells along [Sha92]. The figure in the left depicts hot spot case covered by one micro-cell base stations, and the figure in the right depicts the full coverage of micro-cells.

The problem with the presented method is that the mobile station should be instantly handed to the corresponding cell-layer when it arrives at the intersection of micro- and macro-cell attenuation curves. Soft handover eases the problem, but if the mobile station arrives in the micro-cell area, it is for most of the time connected to both micro- and macro-cell base stations. This occurs since the handover region has to be rather large in order to avoid ping-ponging between cells (or cell layers). This is the case especially if the mobile stations are fast moving. Thus, the area where mobile stations are in a soft handover state is rather wide compared to the area of micro-cell.

Handover can never be very fast. If the number of candidate base stations is high, the pilot signal of a candidate base station can be measured only after some delay. In addition, this pilot has to be measured for a rather long period in order to filter fast fading. Handover cannot be performed when the mobile station encounters a fading dip due to fast fading. After the handover decision has been taken, signalling between the mobile station and the base station takes

place. Before both the network side and the mobile side receive all the handover related parameters, some delay has been experienced. The total delay due to pilot measurement, filtering and handover signalling may be in the order of several hundred milliseconds. If the mobile station runs with a 120 km/h speed, it moves over 33 meters during one second. If the size of a micro cell is 100 meters, only a 3 second delay on handover is needed to go to the centre of the cell.

4.4.3.2 *Cell Hierarchies Having Different Frequencies*

A system with different cell layers at different frequencies is easier to manage since cell layers do not interfere with each other as much as when they are on the same frequency. The main interference comes from the adjacent channel spill-over which is related to power amplifier linearity and receiver selectivity. A drawback to this approach is large spectrum requirements since each cell layer requires its own frequency. In Chapter 3.3, interference between adjacent frequencies and hierarchy layers are discussed together with capacity loss caused by adjacent frequency interference. In Chapter 3.3, it is shown that with the selected ACIR value of 33 dBc capacity loss is minor. However by doing the MCL calculation, it can be seen that there exists the possibility for a user to block an entire cell of the neighbouring operator when locating the immediate proximity of the base station, see TABLE 4.4-7.

TABLE 4.4-7. Worst case calculation of adjacent channel interference when the interfering another operator mobile station locates immediate proximity of the base station.

Parameter	Value
UE maximum TxP	21 dBm
- MCL	70 dB
= received power in the desired band	-49 dBm
- ACLR	33 dBc
= ACI	-82 dBm
- thermal noise (3.84 MHz band)	-108 dBm
- Noise figure	5 dB
= ACI over system noise	21 dB[24]

A mechanism for combating against this kind of situation is the inter-frequency handover. Inter-frequency handover can be triggered by many reasons, but the most relevant one in this case is loss of coverage in the downlink. In 3GPP ACIR parameters are selected so that the downlink quality goes below the minimum tolerated before the mobile station transmission power causes too much interference to the neighbouring operator base station. The handover decision can also be based on interference measurements in adjacent frequencies as described in [Lil99b]. In Chapter 4.5, inter frequency/mode/system handovers

[24] For normal cell planning noise rise gets values in range of 3 to 6 dB

are discussed together with compressed mode. The method presented in [Lil99b] requires measurements in the compressed mode. In [Häm00] further modifications to the idea is presented so that the time used in the compressed mode can be minimized.

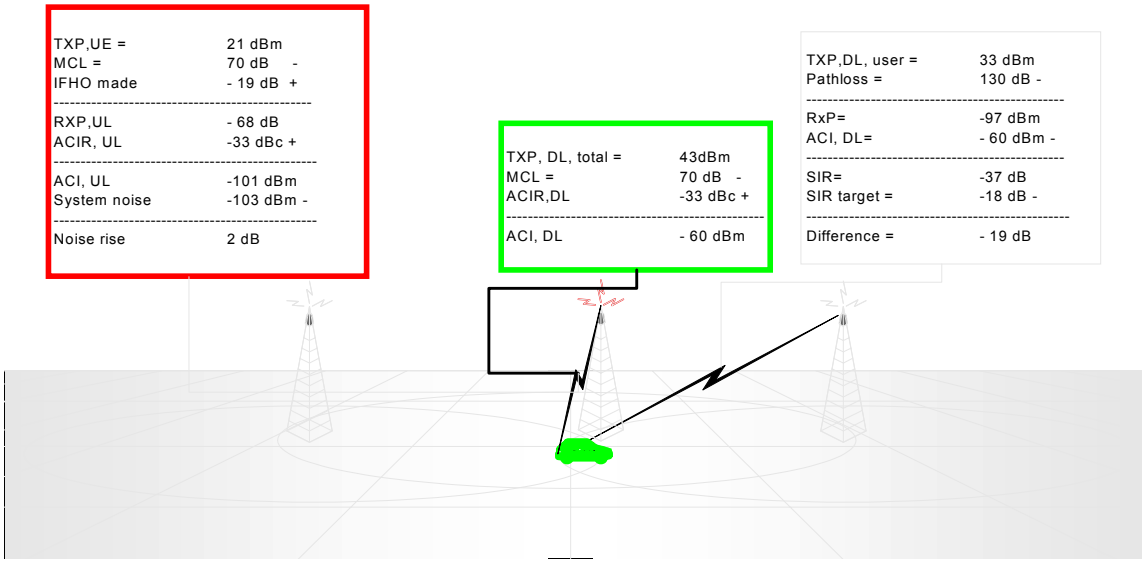

FIGURE 4.4-13. Relationship between the downlink blocking and caused interference in the uplink. Also inter-frequency handover is presented. The downlink ACI at MCL is –60 dBm. However to maintain downlink quality IFHO has to be done when coupling loss is 19 dB more than the MCL.

The effect of the inter-frequency handover to the outage and noise rise is investigated by using the static simulator presented in Chapter 2.5. The simulator contains simple models for inter-frequency handover so that users making inter-frequency handover will have 10 dB higher ACLR. This models inter-frequency handover from the 1st adjacent channel to the 2nd adjacent channel. A user makes inter-frequency handover if its downlink SIR after power control iterations is below a pre-defined threshold. Thus, simulation is first done for the downlink and for the uplink ACLR2 is used for those users that made inter-frequency handover due to bad downlink. After inter-frequency handover is performed the additional attenuation is taken into account when the power control iteration is made again. SIR threshold for inter-frequency handover was selected 7.2 dB (SIR criteria for bad quality was 7.9 dB).

Simulations in Chapter 3.3 show that with 33 dBc ACLR capacity loss is small for both, uplink and downlink. It is also seen, that in the downlink poor quality users are not clearly concentrated into certain geographical positions as it was expected. Due to these reasons, a very pessimistic ACLR value of 25 dBc is selected for the simulations, so that the effect of the inter-frequency handover can be clearly seen due to increased probability.

The system is simulated with two operators with the worst-case layout. In FIGURE 4.4-14, geographical positions of bad quality users in the downlink direction are shown. As can be seen, with 25 dBc ACLR, users that call quality is

poor due to adjacent channel interference are concentrated to the proximity of another operator base stations. Outage with 25 dBc ACLR is 5 % for the selected loading. In FIGURE 4.4-15, the corresponding plot is made when the inter-frequency handover is modelled. As can be seen, dead-zones are clearly vanished. In addition, quality outage is now only 0.1 %. About 2 % of all users perform inter-frequency handover.

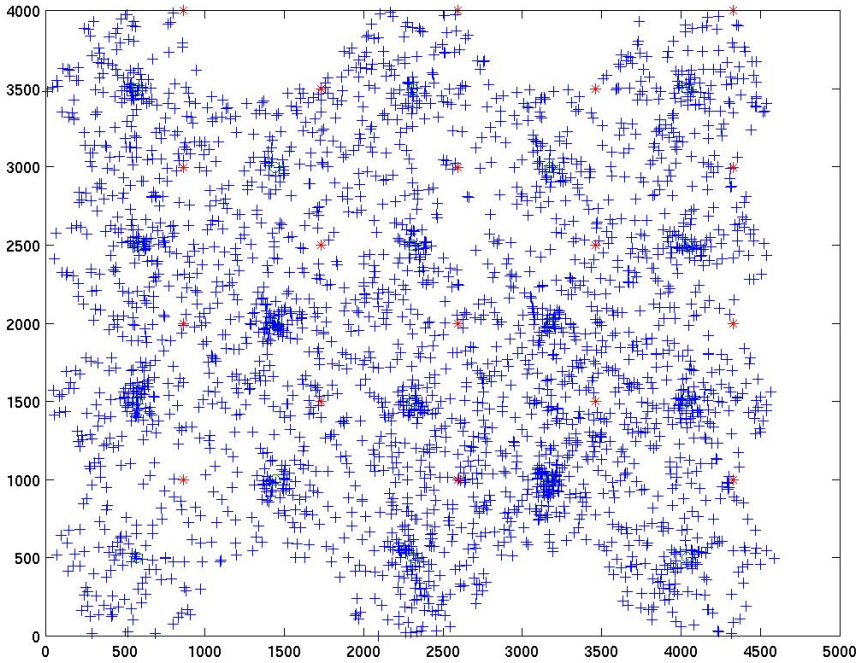

FIGURE 4.4-14. Geographical positions of bad quality calls in downlink when inter frequency handover is not used and ACLR is 25 dBc.

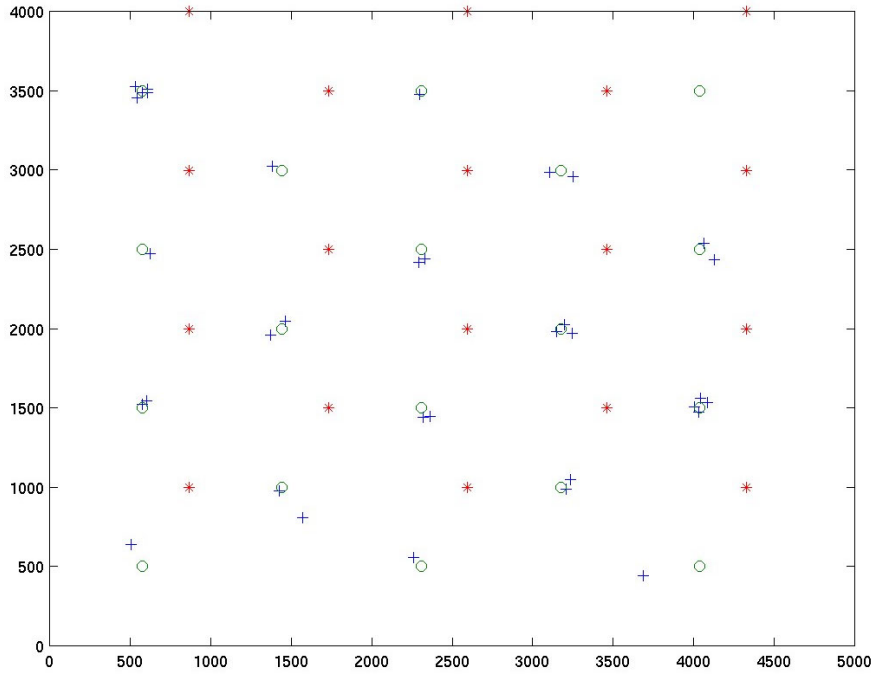

FIGURE 4.4-15. Geographical positions of bad quality calls in downlink when inter frequency handover is used and ACLR is 25 dBc.

In the uplink loading criteria is such that the number of poor quality users is close to zero. Due to that, the corresponding plots of geographical positions of poor quality users cannot be done for the uplink. Instead, noise rise is studied when the inter-frequency handover is on or off. For the selected loading noise rise is 29.3 dB for 25 dBc ACLR if the inter-frequency handover is not used. If the inter-frequency handover is used, noise rise is only 10.6 dB. These are both high values and selected on purpose so that the effect of the inter-frequency handover can be demonstrated.

According to the simulations, outage due to adjacent channel interference becomes small. On the downlink outage degrades from 5 % to 0.1 % with 25 dBc ACLR, and in the uplink noise rise degrades from 29.3 dB to 10.6 dB. In the downlink dead-zones due to adjacent channel interference vanish. It should also be noted that the parameters used in simulations are not according to the current requirements, and hence can be concluded this phenomena to be even improved with the real specified values. These simulations show inter-frequency handover as a robust mechanism against catastrophic cases due to adjacent channel interference.

4.5 Compressed Mode

This chapter presents network performance effects due to compressed mode of WCDMA. This chapter is based on [Häm03] where it was originally presented.

The compressed mode (CM) functionality has been discussed from the beginning of 3GPP standardization work [3GPP], and before in research projects such as CODIT project ([And95]) and CDMA project by Nokia ([Oja96a) focusing on 3rd generation access technologies. In those days it was identified that existing CDMA systems were lacking in well-defined inter-frequency measurement capabilities. Based on this discontinuous reception and transmission ideas were introduced. The compressed mode is an essential part of WCDMA allowing inter-frequency, inter-mode and inter-system measurements and handovers. The compressed mode means a mode in which a gap is arranged to the mobile station's transmission and reception. Naturally this cannot be done without some losses in performance of the network.

As in any CDMA system WCDMA users transmit and receive continuously. Thus, measurements in a basic mode cannot be made in adjacent frequencies. To be able to perform inter-frequency, inter-mode (TDD mode) and inter-system (GSM system) measurements gaps in transmission and reception of the mobile station needs to be arranged by using a so-called compressed mode. In order to avoid any losses of data, there are two ways to arrange gaps: spreading factor halving (SF/2) and the puncturing methods. In both methods data that was supposed to be transmitted during the gap is transmitted during the non-gap part of the frame with a higher data rate. In the SF/2 method higher data rate can be achieved by reducing the spreading factor. This method can be used in both transmission directions. In the downlink the puncturing method can also be used, in which the spreading factor remains constant. Room for additional bits is arranged by puncturing coding bits.

An alternative way for the compressed mode is a dual receiver in which part of the receiver is duplicated. This allows easy measurements in adjacent frequency/mode/ system. A drawback of this approach is considerably higher implementation cost of the mobile station receiver. Besides, the dual receiver does not remove the need for the compressed mode – the compressed mode is needed when performing inter-system measurements in GSM1800 (GSM in 1800 MHz frequency band) band since otherwise own WCDMA transmission would interfere GSM1800 measurements.

4.5.1 Compressed Mode Principle

A WCDMA mobile station has to be able to perform inter-frequency, inter-mode and inter-system measurements depending on the mobile station capabilities given in [TS25.306]. The mobile station monitors cell on other FDD frequencies, on other modes and radio access technologies supported by the mobile station based on commands from the UTRAN. Depending on the mobile station capabilities the compressed mode may be needed to perform those measurements. The UTRAN commands the mobile station to the compressed mode when inter-frequency/mode/system measurements need to be done. [TS25.215]

As a response to a request sent by higher layers, the UTRAN signals compressed mode parameters to the mobile station. A transmission gap is

characterized by the following parameters [TS25.215]: Transmission Gap Starting Slot Number (TGSN), Transmission Gap Length 1 (TGL1), Transmission Gap Length 2 (TGL2), Transmission Gap start Distance (TGD), Transmission Gap Pattern Length 1 (TGPL1), Transmission Gap Pattern Length 2 (TGPL2), Transmission Gap Pattern Repetition Count (TGPRC) and Transmission Gap Connection Frame Number (TGCFN). The relationship between parameters is depicted in FIGURE 4.5-1. In addition, the compressed mode can be active in the uplink or downlink only or in both directions at the same time. If active in the uplink, the compressed mode method (SF/2 method or higher layer scheduling) needs to be signalled to the mobile station. If active in the downlink, possible compressed mode schemes are SF/2, puncturing or higher layer scheduling. [TS25.215] Higher layer scheduling can be used especially with non-real time services since non-real time traffic allows to post-pone data transmission.

With a single compressed mode pattern only one type of measurement can be made. The mobile station may have several concurrent types of measurements when several patterns are used.

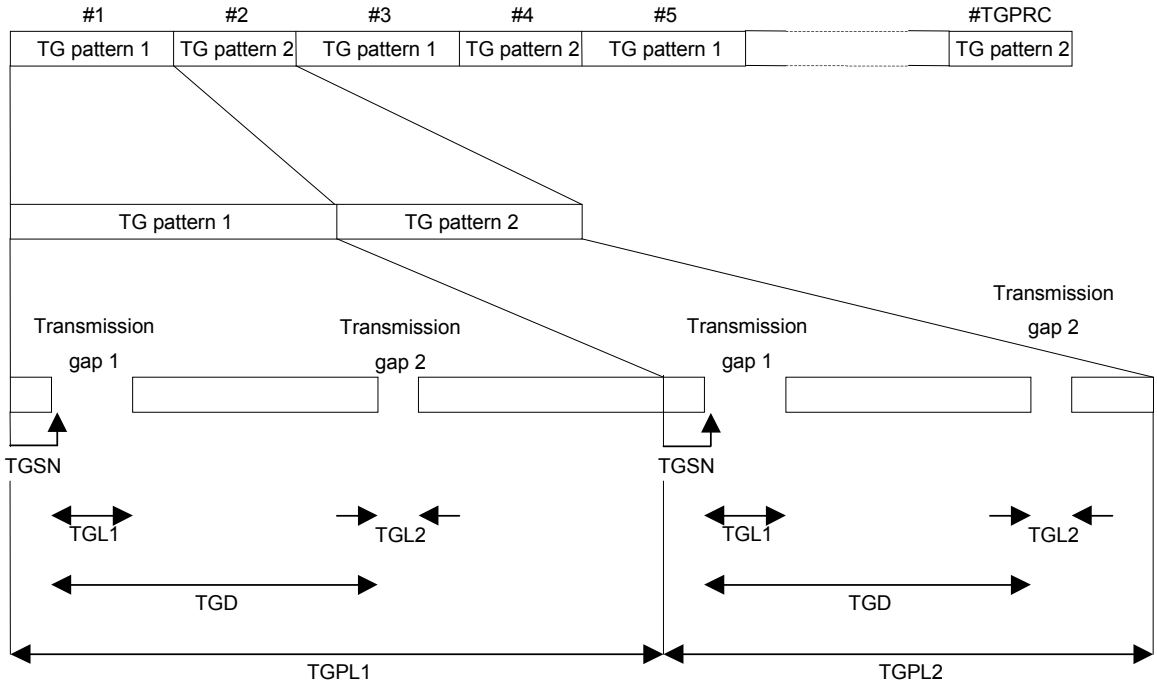

FIGURE 4.5-1. Compressed mode pattern parameters illustrated [TS25.215].

In the compressed mode, slots from N_{first} to N_{last} in FIGURE 4.5-2 are not used for the transmission of data. As illustrated in FIGURE 4.5-2, the instantaneous transmit power is increased in the compressed frame in order to keep the quality (BER, FER, etc.) unaffected by the reduced processing gain (in case of SF/2) or reduced coding gain (in case of puncturing method). The amount of power increase depends upon which method - SF/2, puncturing or higher layer

scheduling – is used. [TS25.212] In case of puncturing, rate matching is used, i.e. part of the coding bits are punctured so that data for transmission can fit into shorter transmission times. In case of SF/2 information bits of the gap period are sent during the rest of the frame. This is done by increasing the data rate and reducing the spreading factor. In case of higher layer scheduling only a subset of the allowed Transport Format Combinations (TFCs) is used in a compressed frame. The maximum number of bits that the physical layer can deliver during the compressed radio frame is then known. In other words, bitrate is reduced during the compressed mode.

When in compressed mode, compressed frames can occur periodically, as illustrated in FIGURE 4.5-2, or requested on demand. The rate and type of compressed frames is variable and depends on the environment and the measurement requirements.

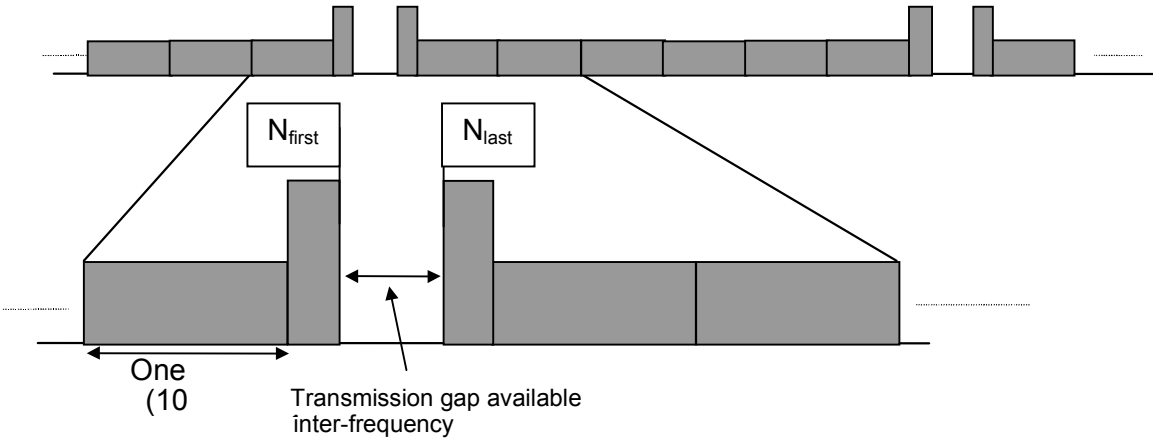

FIGURE 4.5-2. Compressed mode transmission [TS25.212].

4.5.2 GSM Measurements

The requirements for GSM measurements are listed in [TS25.133]. In this section it is presented how these requirements will reflect the whole RRM behaviour in WCDMA system, and based on this present the estimation of impact on the system itself.

For the sake of simplicity measurement times are here based on the following patterns:

- Pattern 1: 7 slot gap every 3rd frame.
- Pattern 5: 14 slot gap every 8th frame.

GSM measurements are divided into three different types: GSM carrier RSSI measurement, GSM carrier BSIC (Base Station Identity Code) search (initial BSIC identification) and BSIC re-confirmation (after the initial synchronization has been found). Details of the requirements are defined in section 8.1.2.5 in [TS25.133]. Based on these requirements the Radio Network Controller can build up a suitable compressed mode pattern sequences for the mobile station

to perform measurements necessary for the preparation of WCDMA-GSM handover.

4.5.2.1 *GSM RSSI Measurement Time*

GSM measurement and handover evaluation procedures are defined in [TS25.133] so that GSM carrier RSSI measurements have to be made prior to BSIC identification in order to set GSM cells in signal strength order. BSIC identification is performed in decreasing signal strength order. This means that depending on the reporting mode and criteria, the strongest GSM cell(s) with successful BSIC verification can be reported to the network significantly sooner than weaker GSM cells. Time required for RSSI measurements can be estimated based on the requirement stated in Table 8.4 in [TS25.133]. Time needed for GSM RSSI measurements is:

$$T_{RSSI} = \frac{S \cdot C}{G} \cdot TGD \tag{4.5-1}$$

where

S = number of needed measurement samples per RSSI

C = carriers to be measured

G = number of GSM carrier RSSI samples measured in each gap

TGD = time between gaps

In TABLE 4.5-1 the required time to perform an RSSI measurement is shown when assuming the maximum 32 carriers in GSM neighbour list. Naturally, it is possible to use other types of compressed mode patterns if different kind of averaging of fading is needed.

TABLE 4.5-1. GSM RSSI measurement time. S = 3, C= 32, G = 6 and TGD = 30 ms for pattern 1 and G = 15 and TGD = 80 ms for pattern 2.

CM Pattern	Measurement time
Pattern 1	480 ms (16 meas. gaps).
Pattern 5	512 ms (7 meas. gaps).

4.5.2.2 *GSM BSIC Identification*

Based on the RSSI measurement the mobile station will select the strongest carrier to start the BSIC identification procedure with. The requirement in [TS25.133] is based on the assumption that the mobile station has to make two attempts to verify BSIC. However in real life this is not necessary in all cases, since the probability to find the BSIC at the first attempt is naturally quite possible. Based on Table 8.7 in [TS25.133] the required time for BSIC identification based on two decoding attempts can be concluded. The worst-

case time for identifying a single BSIC is 1.53 seconds and 1.76 seconds for pattern 1 and pattern 5, respectively. The worst-case time for identifying multiple BSIC is

$$T = N_{BSIC} \cdot T_{pattern-x} \quad (4.5\text{-}2)$$

where N_{BSIC} is number of BSICs to be identified and $T_{pattern\text{-}x}$ is the BSIC identification time for the compressed mode pattern used. Worst-case identification times for different number of BSICs are shown inTABLE 4.5-2.

TABLE 4.5-2. BSIC verification time.

#BSIC	PATTERN 1 Worst case BSIC identification time/s	PATTERN 5 Worst case BSIC identification time/s
1	1.53	1.76
2	3.06	3.52
3	4.59	5.28
6	9.18	10.56
8	12.24	14.08

4.5.2.3 *GSM BSIC Reconfirmation*

The performance of BSIC reconfirmation is indicated in Table 8.8 and 8.6 of [TS25.133], and it is faster than the initial BSIC identification. This is due to the fact that the mobile station is able to internally determine a suitable gap for decoding each BSIC with the given pattern. The emphasis in this analysis is on the BSIC identification since after the first BSIC verification result(s) are reported to the network, the network can start to evaluate any possible handover candidates. Typically it can also make an actual inter-system handover decision. The reason for this is that it is seen that GSM measurements are needed only when there is a need to transfer the user to the GSM system, mainly due to coverage reasons. The BSIC reconfirmation process will have a similar impact on system capacity as inter FDD measurements.

4.5.3 FDD Inter-Frequency Measurements

In order for the mobile station to provide information about neighbour cells on an adjacent frequency, the mobile station needs to be able to make inter-frequency measurements. The same compressed mode patterns as presented earlier can also be used for making inter-frequency measurements.

In WCDMA system, in which there are several cells on the same frequency, neighbour cell search and measurements are performed in reverse order compared to GSM. First the mobile station has to search new cell(s) and after identifying a cell the CPICH E_c/I_0 or RSCP level of the cell can be measured. The situation becomes a little more complicated since before

synchronizing to any of the cells on an adjacent frequency, the mobile station cannot differentiate the multi paths of different cells. In order to identify all cells on that frequency the mobile station has to identify all detectable multi paths. Below are the different issues, which affect the identification time of a new cell are listed

- Number of cells within detection range
- Propagation conditions (e.g. the number of multi paths for a cell)
- Size of the neighbour list (minor impact compared to GSM)

The requirements in Section 8.1 of [TS25.133] are written based on the worst-case scenario and therefore in a real network environment with good cell planning significantly better performance can be achieved.

The worst-case performance is calculated for one FDD inter-frequency carrier with 32 neighbour cells indicated on that carrier. These worst-case figures in [TS25.133] assume a multipath fading environment with several cells in a detection range. The worst-case value is calculated by using a slot format, which gives the shortest effective measurement time. Time for identifying a new FDD cell with patterns 1 and 5 become 9 and 8.7 seconds, respectively.

As stated earlier normal search performance in easier propagation conditions would give significantly better identifying times. As a conclusion it is reminded that it is not possible to state an identification time of a new cell exactly due to the nature of the identification procedure and radio environment. Hence the compressed mode time for making FDD inter-frequency measurements can vary a lot due to the different propagation conditions. The system needs to be prepared for larger variations in compressed mode times.

4.5.4 Compressed Mode Simulations

This chapter presents simulations describing network level effects of the compressed mode. The used tool is the dynamic system simulator presented in Chapter 2.4. With the selected parameters and assumptions very small effect in downlink capacity was seen. Thus we concentrate here on the uplink simulations only. The used compressed mode method is SF/2.

4.5.4.1 *Impact on the Simulation Assumptions*

Based on the discussions in Chapter 4.5.2 some parameters have to be defined to study the system level performance and capacity impacts of GSM and FDD inter-frequency measurements. The trigger of making measurements is based on events in the physical layer. In this study the chosen trigger is the mobile station transmitted power. This is for re-constructing the situation where the WCDMA coverage is ending, and GSM measurements need to be initiated to find GSM cells to make the handover. The used transmission power triggers have been 16 dBm and 0 dBm indicating the different probability for compressed mode measurements due to the coverage reason.

In case of GSM measurements, the number of BSICs to be verified has an impact on the performance. Here the chosen number of BSICs to be verified is

three. After 3 BSICs has been verified, the GSM BSIC identification procedure can be terminated by the radio network controller. Naturally the mobile station can continue the BSIC verification procedure after this point, but this study does not cover this case. The reasoning behind the proposed number is that if the GSM-GSM handover case is considered the probability to make the handover to 4^{th} to 8^{th} strongest BSIC is quite low, and hence the system performance is studied with a value of three.

The time needed for measuring 32 GSM RSSI measurements, and making three BSIC measurements assuming pattern number 1 in total equals to:

$$T = \text{RSSI } \textit{measurement time} + \textit{filtering} + \text{BSIC } \textit{identifying time}$$
$$= 480ms + 500\ ms + 4.5s \approx 5.5\text{s}.$$

It has been assumed an extra 500 ms for different RSSI measurement time for different fading averaging purposes.

The third assumption has been that the WCDMA coverage is not sparse in the area where service is deployed. Hence the GSM measurements are done only when needed. Indoor coverage is assumed to be implemented mainly with GSM.

The fourth assumption that has been studied is the TFC behaviour in the uplink during the compressed mode sequence. With some services the bitrate can be temporally reduced during the measurement sequence, and recovered back after this. This would allow the mobile station to generate minimal interference on the system. In case of voice service the impact of DTX (Discontinuous transmission) will further reduce the output power, but this was not studied in these simulations.

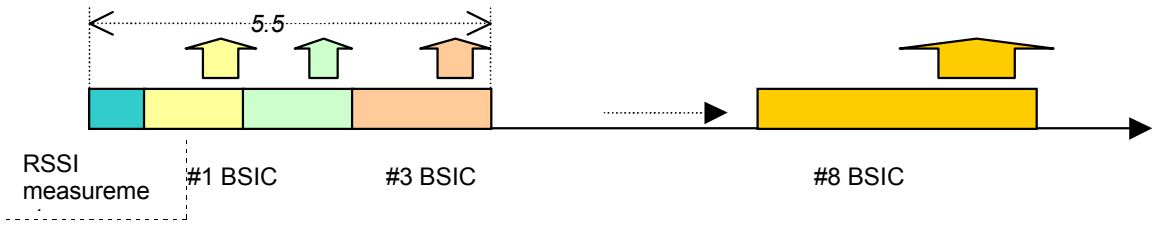

FIGURE 4.5-3. BSIC measurements.

The used simulator is a dynamic system level simulator. In this type of simulator users can be controlled to move with desired routes and the behaviour of each user and the system can be monitored. Hence it is possible to set some radio related triggers to launch radio resource management procedures for maintaining service continuity. In this study simulations are divided into four main cases:

1. *Periodic inter-frequency measurement*. In these simulations mobile stations enter compressed mode randomly, i.e. according to the Poisson process. After completing the compressed mode, mobile stations resume normal operations. This simulates a periodic compressed mode usage. A mobile station may have several compressed mode patterns during a call. In this case mobile stations do not make inter-frequency

or inter-system handovers after the compressed mode pattern. This can be considered quite a pessimistic case. Several different sub-cases were defined for this case. For example, the effect of gap length, the mobile station speed and power control margins after a gap were studied.

2. *Periodic inter-frequency measurement followed by inter-frequency handover*. In this case mobile stations enter the compressed mode randomly, i.e. according to the Poisson process. After the mobile station has performed compressed mode, it is assumed to have made a successful GSM/inter-frequency handover and is removed from the studied WCDMA system. This simulates compressed mode usage where the mobile station always leaves the system (makes a handover) after having finished the compressed mode. Only a few cases were made in order to see the differences between case 1 and case 2.
3. *Inter-frequency measurement triggered by the coverage reason.* In these simulations a mobile station enters the compressed mode when its filtered transmission powers reach a predefined limit. After the mobile station has performed the compressed mode, it is assumed to have made a successful GSM/inter-frequency handover and is removed from the WCDMA system in case of GSM measurements, and removed from the current frequency in case of inter-frequency handover. The filter length and event-trigger transmitted power level are varied in these simulations. Also it is simulated on how the TFC selection in the uplink would impact on the system performance. Hence cases where the bitrate is reduced to lower than normal during the compressed frames is simulated for each of these sub-cases. This simulation is not intended to derive the requirement for TFC, just to study the impact of a reduced bitrate.
4. *The mobile station performing handovers from the outdoor system to the indoor system.* Mixed indoor and outdoor cases in which mobile stations are initiated on streets and may move indoors have been used with these simulations. When a mobile station enters indoors, coverage is naturally reduced and compressed mode measurements are initiated. The simulated scenario is presented in Chapter 2.3.9. This case is as case 3, except the cellular scenario is different. TABLE 4.5-3 presents parameters used in of all the cases.

TABLE 4.5-3. Simulation parameters.

Parameter	Value
Mobile station speed	50 km/h
Channel Model	ETSI indoor-to-outdoor-A, With 2 taps
Compressed mode method in UL	SF/2
Compressed mode duration	480 ms for cases 1-2, 5.5 s for cases 3-4
Service type	Circuit-switched service, No DTX was used
Simulation environment	Macro cell, 5x5 cells for case 3 and 5x4 cells for cases 1-2, mixed indoor and outdoor scenario with 4 outdoor base stations for case 4
Event-triggered compressed mode mobile station transmission power filter length	2 frames or 10 frames, Varied in different simulations, only relevant in cases 3 and 4
Mobile station bitrate	12 kbps
BSIC to be identified	3
Filtering length for CM trigger	500 ms

For cases 2–4, reference simulations where the compressed mode is not used are made so that calls ended as if compressed mode was used. This means that the simulator tracks when the mobile stations would enter the compressed mode, and after a time equal to the compressed mode total length passed, those mobile stations are then removed from the system. This is done in order to keep loading in the same level in compressed mode simulations and in reference simulations. It should also be noted that in the reference case and in the compressed mode case mobile stations generate calls at exactly the same time and move exactly on the same routes.

A diagram of the simulation setup (base stations, antenna directions and cell layout) for the macro-cell scenario is shown in FIGURE 4.5-4.

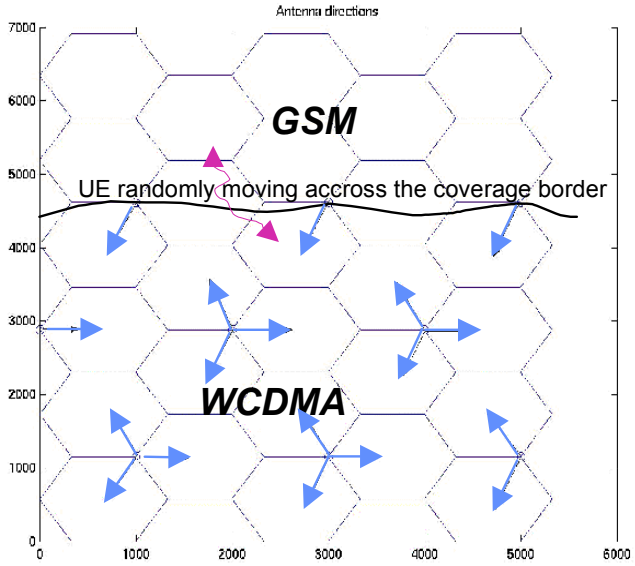

FIGURE 4.5-4 Simulation scenario.

4.5.4.2 *Results and Observations from Case 1*

In TABLE 4.5-4, the impact of the compressed mode is simulated with 10% and 50% of users in the compressed mode. TABLE 4.5-5 shows the effect of mobile station speed during the compressed mode operation active.

TABLE 4.5-4. Main results from case 1 simulations.

CM load	NR mean [dB]	NR STD [dB]	Load change in dBs [dB]	UL SIR target mean [dB]	Difference in mean SIR [dB]
Reference case: No CM	2.3	1.3	0	7.0	0
10% CM load	2.9	1.4	0.7	7.7	0.7
50% CM load	4.2	2.0	1.8	8.4	1.4

This case can be regarded as a case where the compressed mode is done only for measurement purposes without moving the user to the other UTRAN frequency or to GSM.

In results change in load due to the compressed mode is calculated from the change in noise rise as defined in Chapter 2.6. The load change factors and uplink SIR target changes due to the outer loop power control seem to behave in a similar way. This suggests that the cause for load increase is the increase in uplink SIR targets. SIR targets increase because mobile stations in the compressed mode have frame errors during the compressed frame: the outer loop power control increases the uplink SIR target values, which causes higher uplink transmission powers and therefore higher uplink interference and a higher uplink load. An increase in frame errors is due to weakened closed loop power control algorithm performance. From TABLE 4.5-5 it can be clearly seen that the capacity effect of the compressed mode is larger for slower moving mobile stations. The reason for this is the inner loop power control: the slower the mobile station speed is, the more important it is to have an efficient inner loop power control. The gap in the frame distorts the power control performance that can be seen in the loss in the total performance.

TABLE 4.5-5. Results of simulations for mobile station speed effect on compressed mode performance.

Statistics / Simulation	Noise Rise mean [dB]	UL SIR target mean [dB]	load change [dB]	difference in mean SIR [dB]
3km/h, reference simulation	4.8	6.9	0	0
3km/h, simulation with CM	7.0	8.1	0.8	1.2
20km/h, reference simulation	3.0	7.7	0	0
20km/h, simulation with CM	3.9	8.5	0.7	0.9
50km/h, reference simulation	3.9	8.6	0	0
50km/h, simulation with CM	5.1	9.4	0.7	0.8
120km/h, reference simulation	6.7	9.8	0	0
120km/h, simulation with CM	7.7	10.4	0.2	0.6

To better understand the joint effect of the compressed mode and the power control, simulations in which the compressed mode gap length is varied are carried out. The simulation results are shown in TABLE 4.5-6. Simulations show that if the compressed mode gap is very short SIR targets are only slightly increased (0.03 dB). This indicates that a two slot gap does not harm the inner loop power control. In this case, when in a gapped frame the processing gain is decreased and power increased only a little (0.6 dB); thus increased power does not cause any loss to the system. If the gap length is 5 slots SIR targets are increased by 0.5 dB. This indicates some loss in the inner loop power control.

Similar behaviour can be seen for 7 slots case where SIR targets increase by 0.8 dB.

Typically the distance between fast fading dips is equal to λ/2, where λ is wavelength. When operating 2 GHz frequency λ is

$$\lambda = \frac{v}{f} = \frac{3e8\,{}^{m}/_{s}}{2e9\,{}^{1}/_{s}} = 0.15m \quad , \tag{4.5-3}$$

where v is the speed of light and f operating frequency. If the mobile station speed is 50 km/h distance between fading dips is 5 ms, i.e., there will be ~ 2 fading dips per WCDMA radio frame. Further, this means, that if the gap length is 7 slots there can be one dip during the gap, when correlation in the channel between the beginning of the gap and the end of the gap is small. In the case of a 5 slot gap, there can be 0.66 fading dips during the gap. In the case of a 2 slot gap there can be 0.27 dips during the gap, when correlation in the channel between the beginning and the end of the gap is rather high. This partly explains a higher capacity loss for longer gaps.

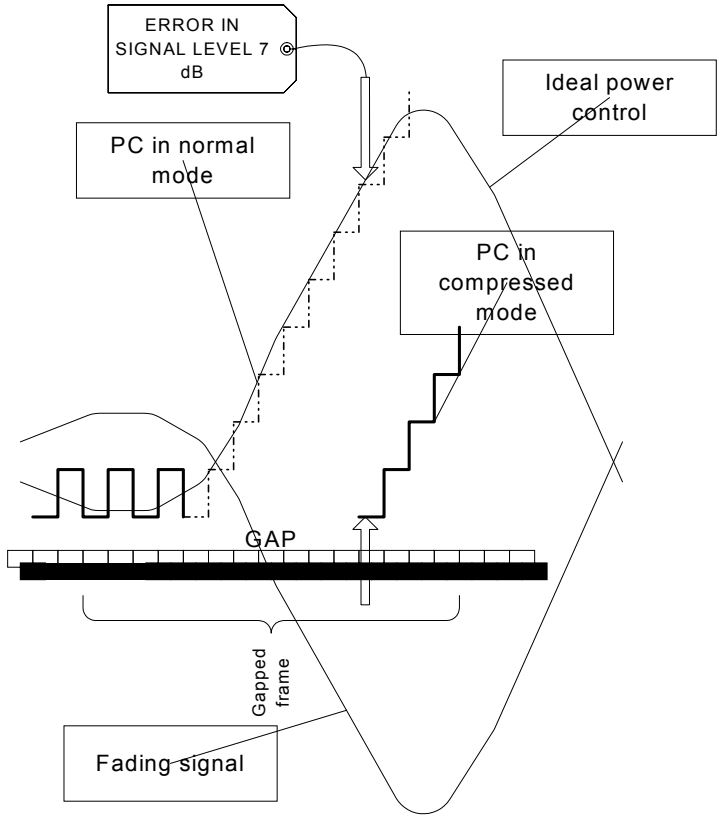

FIGURE 4.5-5. Example of power control error due to compressed mode.

TABLE 4.5-6. Results of simulations with different gap lengths.

Gap length	Increase in PC during active part	Noise rise mean [dB]	SIR target, mean [dB]	load change [dB]	difference in mean SIR [dB]
Ref	NA	3.95	8.56	0	0
2 slots	0.6 dB	3.99	8.59	0.03	0.03
5 slots	2 dB	4.62	9.06	0.40	0.50
7 slots	3 dB	5.11	9.36	0.64	0.80

In FIGURE 4.5-5 an example of a compressed mode effect on the power control is depicted. The power level during the latter non-gap part of the gapped frame deviates up-to 7 dB from the needed level. In this example bit-error-ratio of the latter non-gap part is most likely to be so high that it is very likely that the error correction is not able to fix bit errors and a block error occurs.

4.5.4.3 *Main Results of Case 2*

The results change quite a bit when mobile stations are removed from the system after the compressed mode. Since the users "disappear" from the system after the compressed mode, the noise rise due to increased uplink SIR targets is not as severe.

TABLE 4.5-7. Main results from case 2 simulations.

Statistics / Simulation	Noise Rise Mean (dB)	Noise Rise STD	Load change factor in dBs	UL SIR target mean	UL SIR difference
Reference simulation	2.76	0.60	0	3.69	0
With CM	2.87	0.65	0.12	3.71	0.02
With CM, lower bitrate during CM	2.78	0.64	0.02	3.70	0.01

In these cases the loss in the system performance is negligible, especially when considering the noise rise and load change factor, less than 3 %. In the lowest row the loss is further reduced due to a lower bitrate in the compressed mode operation.

4.5.4.4 *Main Results of Case 3*

The event-triggered cases show similar results as case 2 simulations. Noise rise increase is very low. These results also show the expected effect of the different filter lengths and event-triggers: noise rise in the system depends on a number of users in the compressed mode and mobile station transmission power. The used event-triggered compressed mode mechanism that is based on the mobile station transmission power, can be thought of as a sort of load control: It removes users who have high enough transmission powers from the system

after a constant delay of 5.5 seconds (i.e., the total compressed mode duration). It should be noted that the filtering length of transmission power impacts on the number of users in the compressed mode. The shorter the filter is, the more easily mobile stations start the compressed mode and thus, the more mobile stations there are in the compressed mode on average.

TABLE 4.5-8. Main results from case 3 simulations.

Statistics Simulation	Noise Rise Mean (dB)	UL Load change factor [dB]
0 dBm trigger, 10 frames filter, Reference case	2.8	-
0 dBm trigger, 10 frames filter, CM case	2.9	0.11
0 dBm trigger, 2 frames filter, Reference case	2.8	-
0 dBm trigger, 2 frames filter, CM case	3.0	0.21
16 dBm trigger, 2 frames filter, Reference case	3.2	-
16 dBm trigger, 2 frames filter, CM case	3.3	0.09

TABLE 4.5-9 shows the percentages of users in the compressed mode in the simulations. The first row shows the percentage calculated as the number of compressed mode users divided by the number of all users in the simulation. The second row shows the percentage calculated as the number of compressed mode users divided by the number of users in the border cells, where the most of the compressed mode users are likely to be.

The level of the triggering criteria and the filtering length will have a great impact on the system's performance. Too low a level trigger or short filtering results in unnecessary high amounts of compressed mode users.

TABLE 4.5-9. Number of users in compressed mode in different simulations.

Event-trigger transmission power level [dBm] Filter length [frames]	0dBm event-trigger 10frames filter	0 dBm event-trigger 2 frames filter	16 dBm event-trigger 2 frames filter
Mean number of CM users vs. all users, [%]	7.9	11.6	0.5
Mean number of CM users vs. border cell users, [%]	57.7	82.1	3.3

4.5.4.5 *Main Results of Case 4*

Case 4 is such that the four outdoor base stations provide coverage mainly outdoors. When a mobile station enters indoors, it suffers from the lack of coverage and this initiates the compressed mode measurements. After that inter-system handover to GSM or inter-frequency handover to another frequency is executed. Simulations are performed for two transmission power

level trigger thresholds (16 and 0dBm) leading to 2.5 % and 7.7 % compressed mode load. In 16 dBm transmission power threshold case noise rise without the compressed mode is 9.4 dB and in 0 dBm case 10.4 dB. In both cases the compressed mode causes 0.2 dB increase in noise rise, leading to 9.6 and 10.6 dB noise rise.

These results indicate a very minor impact on the system's performance.

4.6 Site Selection Diversity Transmit

The SSDT method was first introduced in [Keu95]. SSDT is a method in which the mobile terminal switches on and off transmission from base stations in the active set. In [TS25.214] SSDT is described as a power control while in [Keu95] SSDT is described as a handover method. Both [TS25.214] and [Keu95], however, describe exactly the same method.

Similar approach as Site Selection Diversity is used also with cdma2000 [C.S0024] with 1xEV-DO. Fast cell selection approach described in [C.S0024] is first presented in [Keu95].

4.6.1 The Problem Site Selection Diversity Transmit Copes

When a mobile station moves from one cell to another, a handover is performed. Handover can be either a hard handover or a more flexible soft handover. The drawback of the hard handover is that the old connection is broken before a new one is set up. The problem becomes even more severe due to the ping-ponging effect wherein a channel keeps changing back and forth between different channels. This can be diminished by using a handover margin. However, a connection to the best base station cannot be utilized due to the handover margin and the delay of the handover procedure. Therefore an unnecessarily high transmit power must be used and the interference is thereby increased.

Soft handover also employs updating margins. Base stations within the margins are all transmitting (and receiving) to (from) the mobile station. A RAKE receiver used with the WCDMA system comprises of several branches. Each of them may be synchronized with a different signal component and the receiver can therefore receive several signals simultaneously. The RAKE receiver can also receive signals that arrive along different propagation paths and from different base stations. The RAKE receiver adapts to the attenuation changes over the different connections considerably faster than the active set is updated. This leads to soft handover gain in the system. However, the number of fingers in the RAKE receiver is limited – for example four. Furthermore, some of the fingers may be allocated to cell search, acquisition or other tasks. Thus only a limited number of signal paths arriving to the receiver can be received. This may lead to a situation in which only a small portion of arriving signals or even none can be received from a base station transmitting to the mobile station. The mobile station receives only base stations with the best

quality. Thus all transmissions directed to the mobile station cannot be utilized. This is seen as increased interference to the system. In this case transmission by a base station does not improve the signal quality but only increases interference to the system. Even though the best signal can be selected and the power of signals which have propagated along different paths can be compiled when a RAKE receiver is used in the mobile station, the number of the RAKE branches is limited by the power consumption and the manufacturing costs, and therefore the rake receiver cannot utilize, however, more than a few transmissions at a time.

Soft handover has undisputable advantages together with the RAKE receiver. Problems depicted above can be alleviated by using SSDT.

4.6.2 Site Selection Diversity Transmit Concept

The Site Selection Diversity Transmit is described in [Keu95 and TS25.214]. The idea behind SSDT is to avoid the problems depicted in the previous chapter and to implement a soft handover in the manner of hard handover with a very small effective handover margin, and to decrease the interference of the base station when the mobile terminal communicates with several base stations.

This is achieved with the method in which the mobile station controls the downlink transmission of one or several base stations of the active set in such a way that each base station switches its transmission to the mobile station on or off. By doing so, the number of signals transmitted by the base stations can be decreased, and the interference level caused by the base stations can thereby be reduced. This in turn increases the capacity of the system and improves the quality of the connections. Handover also becomes faster. The updating of the active set is slow and requires a great deal of signalling. By using SSDT, a base station can be activated by means of the internal signalling of the radio interface. A mobile station has only to keep active one base station providing the best connection, and to update the active base station rapidly by means of the physical link signalling. The result is a process, similar to a hard handover, from the base station to the mobile station with a very small effective handover margin.

In [TS25.214] an active base station is called a ‘primary’ base station while non-active base stations are called a ‘non-primary’ base stations. In order to select a primary cell, each cell is assigned a unique temporary identification (ID). The mobile station periodically informs a primary cell ID to the connecting cells. The non-primary cells selected by the mobile station switch off their transmission to the mobile station. SSDT is activated, terminated and ID assigned by using higher layer signalling. Transmitting the command signal regularly provides the advantage that the transmit power of the base stations can be adjusted at precise intervals, and when the interval between the adjustments is short, for example one frame, the adjustment is performed rapidly enough to observe even fast changes in the attenuation over the connection.

The primary cell ID is delivered to the base stations by using FBI (Feedback Information) field in the uplink DPCCH channel. The FBI bits are used to support techniques requiring feedback from the mobile station. FBI is used with closed loop mode transmit diversity and site selection diversity transmission. The structure of the FBI field is shown in FIGURE 4.6-1. [TS25.211]

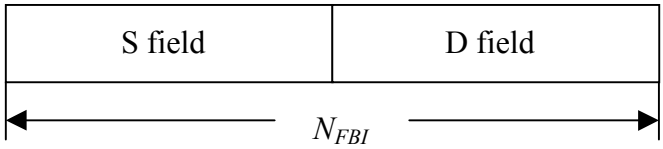

FIGURE 4.6-1. Details of FBI field [TS25.211].

The S field of FBI field is used for SSDT signalling, while the D field is used for closed loop mode transmit diversity signalling. The S field consists of 0, 1 or 2 bits depending length of ID. [TS25.211]

When using SSDT the fixed network may operate in the same manner as in a conventional macro diversity system, and the method does not have the impact to radio access network and signalling – only the radio interface is affected. The method enables the size of the active set and the selection margin to be increased without increasing the interference. This facilitates the maintenance of the best connection especially under difficult circumstances in a micro-cell environment.

The mobile station can change the transmission of the base stations according to the downlink measurements. The mobile station selects the primary cell periodically based on CPICH RSCP measurements. A cell recognizes its state as a non-primary if the received ID code from the mobile station is different than the ID code allocated for the base station and the quality of the uplink reception is sufficient. If the compressed mode is used no more than one third of bits in ID is allowed to be missing. If these three conditions hold, the base station recognizes itself as a non-primary base station. Otherwise the base station recognized itself as a primary base station. [TS25.214].

In [Keu95] an alternative approach is shown in which the base stations which cannot receive the signal of the mobile station observe transmission error and terminate the transmission to the mobile station. The transmission is terminated most preferably by decreasing the transmit power slowly within a predetermined period of time or by disconnecting the transmission after a predetermined delay. When the base station terminates the transmission after it has lost the connection, i.e. after the connection has deteriorated below a predetermined level, the advantage is that the number of the base stations communicating with the mobile station can be restricted to the smallest possible. The base station restarts transmitting when it can receive the command signal of the subscriber terminal switching on the base station.

In another alternative approach given in [Keu95] the mobile station transmits a command signal by means of which the transmission of each base

station of the active set is separately adjusted. Each of the base stations can separately receive the command signal, so that each base station adjusts its own transmit power according to what the command signal determines. The base stations that do not receive the control signal terminate the transmission to the mobile station in the same manner as in the previous approach. The advantage of transmitting the command signal separately for each base station is that the method is then more controlled and the power level of each base station can be separately adjusted to the desired value. The command signal can also be assembled of signals received by several base stations. The control signal is then assembled in some part of the network, for example in the radio network controller, and the control signals are signalled separately to each base station.

The SSDT method is applicable in all interference-limited cellular radio systems, which include for example different spread spectrum systems, including CDMA and OFDMA systems

4.6.3 Fast Cell Selection in cdma2000

In 1xEV-DO system the mobile station estimates the strength of the Forward Channel transmitted by each sector in its neighbourhood based on measuring the strength of the Forward Pilot Channel. Based on the measurement the mobile station selects the best serving sector amongst the base stations in the active set. The mobile station reports the selected base station and requested data rate to the network. The network will transmit data to the mobile station only from the selected sector with the highest data rate that can be achieved with the current quality for the mobile station. [C.S0024, Qua01]

In the Variable Rate State, the network transmits at the rate dictated by the DRC (Data Rate Control) channel transmitted by the mobile station. The mobile station shall use either a DRC cover index 0 or the DRC Cover index associated with a sector in its active set. The DRC cover index 0 is called the “null cover”. A DRC cover that corresponds to a sector in the mobile station’s active set is called a “sector cover”. The mobile station is said to be pointing the DRC at a sector in its active set if the mobile station is using the DRC cover corresponding to that sector. The DRC cover is the means for deciding to switch on or off a sector in the active set. [C.S0024]

4.6.4 Advantages from Site Selection Diversity Transmit

The advantages of SSDT are depicted in FIGURE 4.6-2 and FIGURE 4.6-3. In FIGURE 4.6-2 it is assumed that the mobile station is able to receive two base stations having on average an equal received signal level. Occasionally the signal level received from one of the base stations fades so, that its contribution to the received signal becomes low. Despite that, the base station uses as high a transmission power as another, stronger, base station. Then unnecessary interference is generated to the system by the weaker base station. When using SSDT, a better base station is always selected for communication when interference generated is lowered.

In FIGURE 4.6-3 another example is given in which a number of resolvable multipaths is higher than branches in the mobile station RAKE receiver. In this example, if SSDT is used and three paths received from one base station, transmission power of the active base station has to be increased by 0.32 dB if compared to an ordinary soft handover case. This happens since the third path from the first base station is weaker than the strongest path from the second base station. However, now only one base station causes interference to the system instead of two. In case of a soft handover 2.68 dB higher interference would be caused due to multiple base station transmission. In TABLE 4.6-1, calculations are shown. The problem depicted here can also be alleviated with an optimised handover parameter setting.

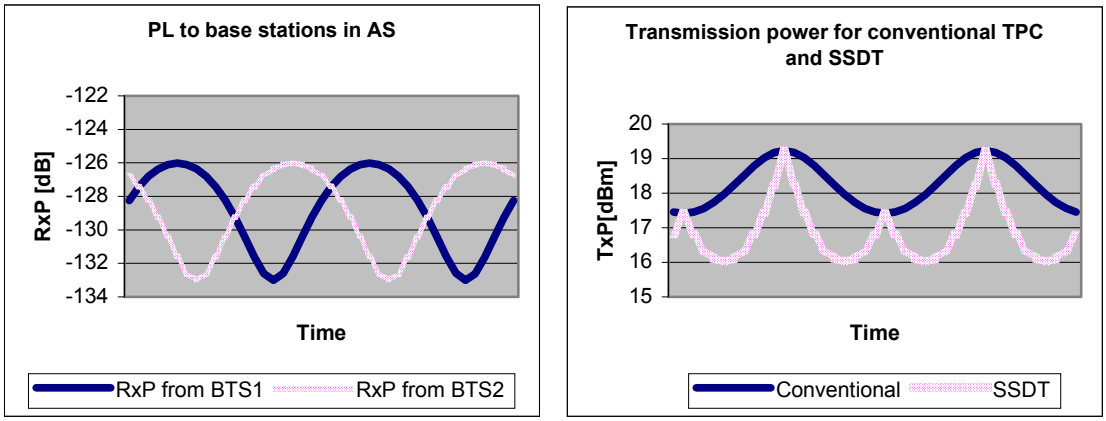

FIGURE 4.6-2. Example in which two equally strong base stations are received (left) by the mobile station and interference caused to the system (right). In case of conventional TPC (Transmit Power Control) it is assumed the caused interference is two times transmission power of one base station.

TABLE 4.6-1. Calculations for transmitted interference in case of soft handover and SSDT.

Tap	Soft handover	SSDT
1	0 dB	0 dB
2	-7.5 dB	-2.5 dB
3	-2.5 dB	-12.5 dB
Sum signal	2.4 dB	2.08 dB
No of BSs [dB]	3 dB	0 dB
Difference	2.68 dB	

In [Fur00] yet another scenario is presented. Due to the errors in power control, power levels to the mobile station may drift between base stations in the active set. Due to errors, in some base stations excessively high transmission powers may be used and thus interference is increased. With SSDT power drift cannot happen as only one base station is active at a time.

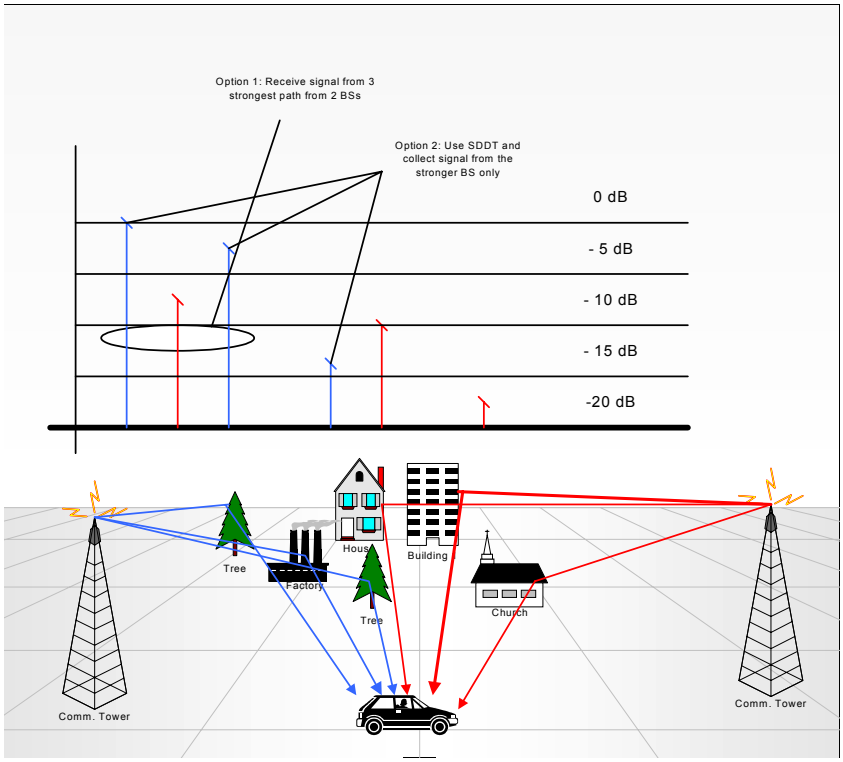

FIGURE 4.6-3. Example in which number of active base stations (three) and multipath components (three per base station) exceed number of RAKE branches in the mobile station (three).

Since SSDT is able to reduce interference generated by the active set base stations and improve the path capture effect, a bigger handover margin can be used and thus more base stations can be added to the active set. Due to that more gain from a soft handover can be gained.

The performance of SSDT has been analysed in [Fur00]. In [Fur00] the uplink signal to interference (SINR) versus ID reception error performance is analysed for different length code words. Longer code words have a longer minimum Hamming distance and thus better performance. Since it is assumed that only one FBI bit is transmitted per WCDMA slot, for longer code words slower SSDT is realized. In addition, capacity gain of SSDT compared to conventional power control is given as a function of maximum Doppler speed. From analysis it is seen that SSDT performance is poor for 2-bit code word, but it gives a gain for longer code words. Highest capacity improvement is simulated for pedestrian speeds. It is also shown that the same path capture collection efficiency is obtained with less RAKE fingers if compared to conventional power control. The simulated capacity gain from SSDT is shown to be 55 % for pedestrian speed mobile station having 6 RAKE fingers and reception diversity. In case of infinite number of RAKE fingers capacity gain is still 36 %.

4.7 Discussion

In this chapter the performance of 3GPP random access algorithm and acquisition indicator channel was validated by simulations. Simulations show almost negligible capacity loss due to 3GPP random access algorithm with the selected AICH false alarm and detection error probabilities. In addition, delays suffered by the user are small enough to be considered negligible. Different power ramping step sizes give almost equal performance. Based on simulations AICH false alarm has a bigger impact than detection error to the system's performance. This is mainly due to T300 timer of RRC protocol layer that causes 200 ms delay in case of a false alarm.

Here a so-called diversity random access method has been presented. Diversity random access makes it possible to create a soft handover and macro diversity during random access before entering dedicated channels. This improves coverage and reduces the probability for call drop at the beginning of a call. It also reduces interference and thus improves the system capacity. Diversity random access is used in both WCDMA and cdma2000 systems.

From simulations it was noticed that in case of a lower mobile station speed uplink inter-cell interference would increase. This effect is due to the fast closed loop power control that is able to follow fading well and adjust power accordingly. When in a fade high power is used and high inter-cell interference generated. Assuming equal link level performance for all mobile station speeds and channel profiles capacity loss due to increased interference will be 75 % in a single tap Rayleigh channel and 22 % in 4-tap Rayleigh channel. Fortunately, for lower mobile station speeds link performance is better when the net effect from power control remains positive.

The original mobile station minimum power was noticed as being too high in micro-cell environments. This is seen as high interference due to near-by users. Based on the simulation study shown here the mobile station minimum power requirement was changed from –44 dBm to –50 dBm. Validity of –50 dBm minimum power was checked also in conjunction of EVM and ACI.

In 3GPP it was discussed in which network element – the mobile station or the radio network controller – the outer loop power control algorithm should be made for the downlink. Based on the analysis shown here it was proposed to have the outer loop power control in the mobile station so that it could react to fast changes in propagation and other conditions. In 3GPP outer loop power control for the downlink is now specified so that the operator may select which entity is responsible for the outer loop power control.

Here measurements, filtering and reporting of intra-frequency handover were discussed. Two measurement schemes - narrowband SIR and wideband SIR - were investigated. According to this study, it is obvious that measurements should be based on a wideband estimate. The capacity of both measurement methods were analysed in several different conditions. In each of them wideband estimate over performed narrowband estimate due to better measurement accuracy.

Two filtering schemes and two reporting schemes were also investigated. The block wise filtering and the periodic signalling introduce a delay that postpones active set update decisions. Further, this leads to situations where the mobile station traverses to an area of a strong base station but is not having an active connection to it. This causes an unnecessary noise rise to the new base station in the uplink direction. The effect is particularly large in the Manhattan environment – loading of the system may increase 25 % due to the delay caused by filtering. In addition, the noise rise fluctuation may cause severe problems for the admission and load control algorithms. Although the selected channel models further accentuate the differences between the two filtering schemes, they cannot be the sole causes for the observed phenomena. The effect is weaker in the downlink, as only one user suffers this kind of situation. However, since the victim mobile station requires higher power from the serving base station, other users are more interfered. This causes an accumulated effect on the entire system. In macro-cellular network a very drastic effect is seen, and bad quality percentage may increase from 6 % to 60 % due to delays in the handover processing.

The event-triggered reporting scheme seems to work better than the periodic, especially in the Manhattan environment. In the macro-cell environment the difference is not as big as in the Manhattan environment, but it is still on par with the difference between the block wise and sliding window filtering. The effect of the reporting scheme is also less for the faster moving mobiles, as can be seen from the number of bad quality calls in each case.

In addition to intra-frequency handover, inter-frequency handover was studied and proposed as an escape mechanism against adjacent channel interference. If the mobile station performs an inter-frequency handover to the 2^{nd} adjacent channel due to increased interference in the downlink, the uplink performance can also be maintained. Uplink and downlink ACIR parameters have been selected so that inter-frequency handover is always triggered due to downlink reasons before the uplink is interfered. If inter-frequency handover is not made, the call will drop due to the poor downlink quality before severe effects are seen in the uplink. Simulations show that inter-frequency handover performs well against adjacent channel interference.

In this chapter the compressed mode method was presented and its capacity effects analysed. In the simulations the latest information on GSM and inter-frequency measurement requirements that have been specified in [TS25.133] were used. It was also assumed that GSM measurements are made only when needed. Filtered mobile station transmits the power measurement results were used as a trigger for a network to set the mobile station into the compressed mode.

Simulation results show clearly that capacity impact of GSM measurements is minor. The capacity loss was shown to be in order of 0–4 % when the parameters for the triggering algorithm were properly chosen. The impact could even be mitigated, when considering further advancements like DTX operation with AMR (Adaptive Multi Rate) codec, reduced bitrate during the compressed mode operation and higher layer scheduling in case of packet

services. These results should be compared to those in [Eri01a and Tel00a], which indicated higher capacity losses. The reason for the lower capacity loss shown here is due to the fact that the GSM measurement were done only when needed and that users making GSM measurements were removed from WCDMA technology to GSM technology after they had executed all the needed GSM measurements requested by the network.

In addition, from the results it can be concluded that the impact of the compressed mode is lower for the fast moving mobile stations than slowly moving mobile stations. The reason for this is the inner-loop power control behaviour. Slow moving mobile stations require a well working inner-loop power control that will be disturbed by compressed mode gaps.

In the case of FDD inter-frequency measurements the impacts on the system are not so straightforward as in the case of GSM. One major reason is that the estimated measurement time may vary quite lot, typically more than in GSM.

Based on the above study it is shown that a compressed mode can be used with very reasonable impacts to the system, and for this reason there is no need for mobile station structures operating without compressed mode.

Here a so-called site selection diversity transmit method has been presented. SSDT method makes it possible to change active base stations rapidly through physical layer signalling. Base stations can be changed even according to variations in the channel. By switching weak base stations off, interference caused to the system can be reduced and capacity increased. SSDT method is used with both WCDMA and cdma2000 in 1xEV-DO and 1xEV-DV.

5 HIGH SPEED DOWNLINK PACKET ACCESS

In this chapter, the performance of the WCDMA HSDPA network is investigated with the proposed features. Capacity gains for the multi-code transmission, FHARQ, FCS (Fast Cell Selection) and AMC (Adaptive Modulation and Coding) are investigated by using the dynamic radio network simulator presented in Chapter 2.4. This study was done before HSDPA features were decided, for example 64QAM that performance has been studied here is not a part of standardized WCDMA HSDPA. This study is originally presented in [Häm01, Pou01].

In WCDMA, there are three types of transport channels that can be used to transmit packet data. They are the common, the dedicated, and the shared transport channels, see details in [Hol00 and TS25.211]. The transport channel for the packet data is selected based on the resource requirements of the bearers, the amount of data, the load of the common and shared channels, the interference levels in the air interface, and the radio performance capability of the different transport channels. In the UTRAN the DSCH (Downlink Shared Channel) is a specific transport channel, which is intended to carry packet traffic in the user plane between the UTRAN network and the mobile station. The DSCH is the downlink time-shared channel with effective power control and fast scheduling but without soft handover. Benefits of using the DSCH have been reported [Gho99, Kwa01 and Mat01]. Recently, efforts have been spent to enhance the performance of the DSCH further by incorporating more features to the existing DSCH concept [TR25.848]. This new set of features is termed the High Speed Downlink Packet Access.

HSDPA and has been presented in [TR25.848]. HSDPA is targeted to provide very high-speed downlink packet access by means of HS-DSCH (High-Speed Downlink Shared Channel) transport channel. HS-DSCH concept is based on DSCH concept of release 1999 of WCDMA. In release 1999 DSCH transport channel is time shared amongst several users. This means that a single physical channel i.e. a code channel is shared by several users and thus the limited code space is saved. If a DCH was used, a code according to the maximum bitrate would be used for each user. This would lead to excessive usage of codes. DSCH is meant for users with bursty traffic. Users are idle most of the time, but require a high data rate every now and then. If DCH was used,

a code channel with a low spreading factor would be allocated for them eventhough they would not have anything to transmit most of the time. This would be a waste of codes. Thus DSCH is better suited for better for bursty traffic. DSCH is used together with a dedicated low data rate DCH channel that can carry low rate data and physical channels like power control. In HSDPA DSCH-concept has been modified. For instance no power control is used.

Another target for HSDPA is to have peak data rates significantly above 2 Mbit/s that is a 3G requirement and also the maximum bitrate with release 99. The target peak rate for HSDPA is 10 Mbits/s. Also throughput is significantly increased compared with existing releases.

In HSDPA retransmissions are processed in the base station with physical layer Hybrid-ARQ. By doing so retransmission delay can be significantly reduced if compared to DSCH. In DSCH retransmissions are made in RLC (Radio Link Control) that terminates in the Radio Network Controller. This easily leads to the delay of hundreds of milliseconds. In HS-DSCH delay is 2 ms that is the transmission time interval in HS-DSCH channel. In release 1999, TTI is always 10 ms.

The main technologies used in the HSDPA in the 3GPP proposal are based on applying the four advanced schemes on top of the existing DSCH concept. The proposed schemes are [TR25.848]

- Adaptive Modulation and Coding (AMC)
- Fast Cell Selection
- Fast Hybrid ARQ
- Multiple Input Multiple Output antenna processing (MIMO).
- Fast scheduling is the base station

Adaptive Modulation and Coding provides peak data rates up to 10 Mbps and extends the system adaptation. 10 Mbps peak data rate can be achieved with high order modulation, e.g. by selecting 16QAM with ¾-rate coding. However, the highest data rates can only be offered when in a good channel and interference conditions. The highest data rates cannot be offered in the cell border or otherwise in adverse conditions. Since modulation and a coding scheme can be selected according to the existing channel and interference situation, a system can better adapt to the existing conditions. This extends the system adaptation.

In combination with AMC FHARQ can be used. This leads to the best of both concepts - AMC provides the coarse data rate selection since it is based on erroneous measurements and may involve more delay, while Hybrid ARQ provides for fine data rate adjustment through re-transmissions.

Fast Cell Selection makes it possible to be always connected to the best base station. This leads to optimal macro and micro diversity and thus possibly provides improvement to the throughput. FCS is very similar to SSDT concept presented in Chapter 4.6.

At this moment from the proposed features the AMC and the HARQ are accepted to be specified in UTRA Release 5 and the FCS and the MIMO are study items for UTRA Release 6. As a result of the addition of any of the above features, the term *High Speed Downlink Shared Channel* (HS-DSCH) is used to distinguish it from the previous DSCH.

5.1 Adaptive Modulation and Coding

The principle of adaptive modulation and coding is to change the modulation and coding set in accordance with the variations of the channel conditions. The channel conditions can be estimated or based on the receiver feedback. If a user has a good signal connection with the base station, a higher order modulation with a lower coding rate can be assigned. The reverse is true if a user has a bad channel connection. Then in good channel condition a higher data rate is allocated for the user and worse channel condition lowers the data rate. [Hol00, TR25.848].

Since AMC replaces power control it is required that it is very fast. In HSDPA adaptation rate can even be per TTI basis, e.g. 2.0 ms. Modulation and coding sets are selected by UTRAN based on mobile station's inputs. The mobile station assists AMC decisions by sending SIR measurement reports or MCS requests. Since the power control is not used with HS-DSCH, it is always transmitted with fixed power. This leads to less interference variations in the system.

There are 7 different MCSs proposed in 3GPP of which 4 are expected to be selected. The proposed modulation schemes are QPSK (Quadrature Phase Shift Keying), 8PSK (8-Phase Shift Keying), 16QAM (16-Quadrature Amplitude Modulation) and 64QAM (64-Quadrature Amplitude Modulation).

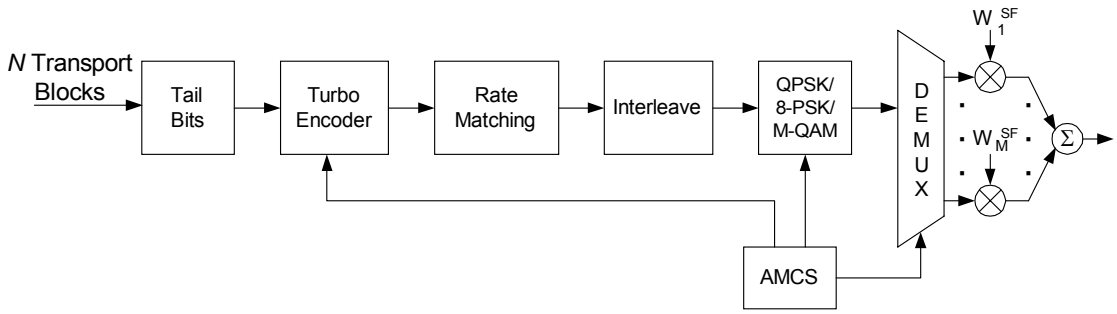

FIGURE 5.1-1. Downlink Shared Channel [TR25.848].

5.2 Multi-code Transmission

Another way to improve granularity of data rates is to use multiple code channels. An arbitrary number of parallel code channels can be selected (between 1 and maximum available codes for certain spreading factor). The

number of codes may be selected by the link adaptation algorithm depending on the existing signal quality or based on the channel condition.

If a variable number of multi-codes is used power per code channel varies. In case of multilevel modulation (like 16QAM or 64QAM) the receiver should know the code power level in the transmitter, since amplitude changes convey the information. Thus the base station should signal the used code power levels or the number of used code channels to the mobile station.

5.3 Fast Cell Selection

When using fast cell selection, the mobile station does not receive simultaneous transmission from multiple cells. Instead, the terminal selects the best cell every frame from the set of base stations in the active set. An uplink DPCH (Dedicated Physical CHannel) is used to make the selection on a frame-by-frame basis. Cell selection is based on fast mobile station measurements. Since cell selection is made frame-by-frame basis FCS can adapt changing channel conditions. For instance, if the currently active base station fades, another base station with a better fading situation can be selected as an active one.

FCS involves interactions with FHARQ and AMC. The new cell needs to know the HARQ state and MCS (Modulation and Coding Set) used in the old cell. There are two types of FCS, inter-Node-B FCS and intra-Node-B FCS. Inter-Node-B FCS is more complex since a mechanism for sending ARQ status information between different Node-Bs is required. This means increased signalling traffic and delays in FCS. Intra-Node-B FCS is less complex since all required information is already available in the base station

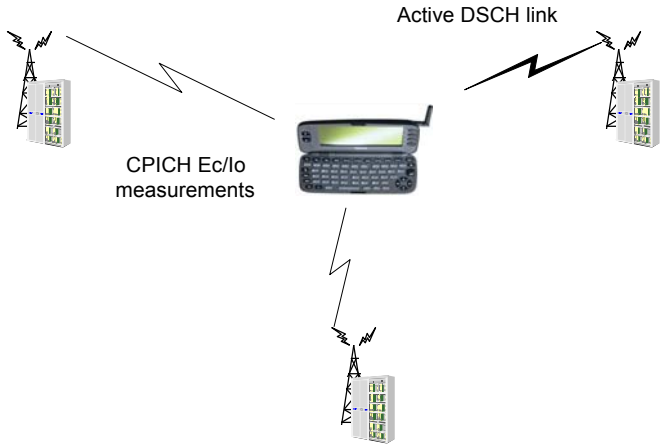

FIGURE 5.3-1. FCS concept.

5.4 Fast Hybrid ARQ

While the AMC takes the feedback from the receiver and adapts the modulation and coding format based on the known channel condition, HARQ is an implicit link adaptation. AMC by itself provides some flexibility to choose the MCS, which matches the channel condition, while HARQ automatically "adapts" to the channel condition by retransmissions. Compared to AMC, HARQ is insensitive to measurement errors and delay. While AMC gives the coarse adaptation, HARQ provides the "fine tuning".

In release 1999 of WCDMA retransmissions are made in Radio Link Control level. Advanced HARQ cannot be added to RLC protocol (for more about RLC protocol see [TS25.322]) since it would require a large data buffer in the mobile station due to the long round-trip delay of the retransmissions. By using a so-called fast HARQ scheme - which is based on an N-channel stop-and-wait protocol - buffering requirements can be considerably decreased. Here N refers to the fact that there may be several re-transmission processes on the process at the same time. Stop-and-wait means that the transmission does not continue until acknowledgement (positive or negative) has been received. FHARQ protocol terminates to the base station and processes retransmissions and acknowledgements in the physical layer [TR25.848]. This allows fast acknowledgements/negative acknowledgements and reduces buffer requirements in the mobile station and network and causes less traffic over Iub interface. N-Channel stop-and-wait protocol can be synchronous (see FIGURE 5.4-1) or asynchronous (see FIGURE 5.4-2). In case of asynchronous scheduling more signalling is required as the timing has to be signalled to the user. However, freedom of scheduling is improved.

The HARQ scheme used with release 1999 DSCH is a so-called type-I HARQ, in which ARQ is used together with error correction and detection. During the specification process in 3GPP several FHARQ methods have been under discussion. In Chase or soft combining (type-I HARQ with soft combining) scheme, if an erroneous packet is received, symbols of packet are stored to the receiver's memory. Retransmissions of the erroneously received packet data are exact copies of the first transmission. The original packet and re-transmitted packet are then maximal ratio combined. This improves the likelihood that the packet is correctly received after re-transmission. For more about Chase combining see [Cha85]. In addition to Chase combining, two incremental redundancy schemes have been under discussion – type-II and type-III HARQ. In type-II HARQ re-transmissions are not self-decodable. This means that the data in re-transmission can be only used together with the original packet. In the first transmission data is sent, and in the following transmissions only redundancy (coding) bits are sent. In type-III HARQ each re-transmission is self-decodable, i.e., a re-transmitted packet can be decoded even if the original packet was lost. In this scheme all packets have the same contents (repetition coding) or in each packet different bits are punctured.

More information of FHARQ can be found in [Hol00 and TR25.848]. Performance of different HARQ techniques have recently been investigated in [Mal01].

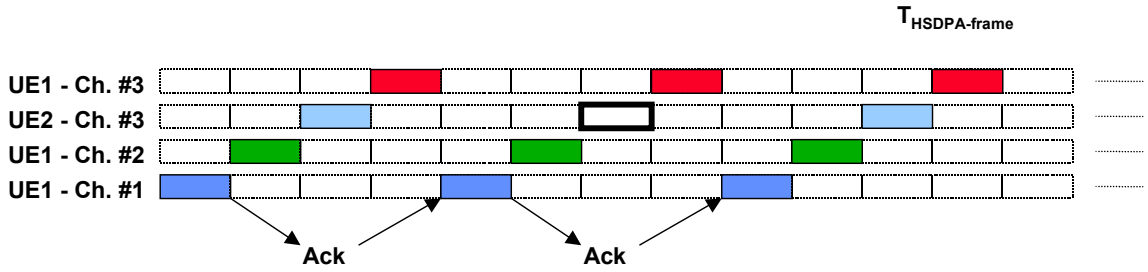

FIGURE 5.4-1. Synchronous N-Channel stop-and-wait structure.

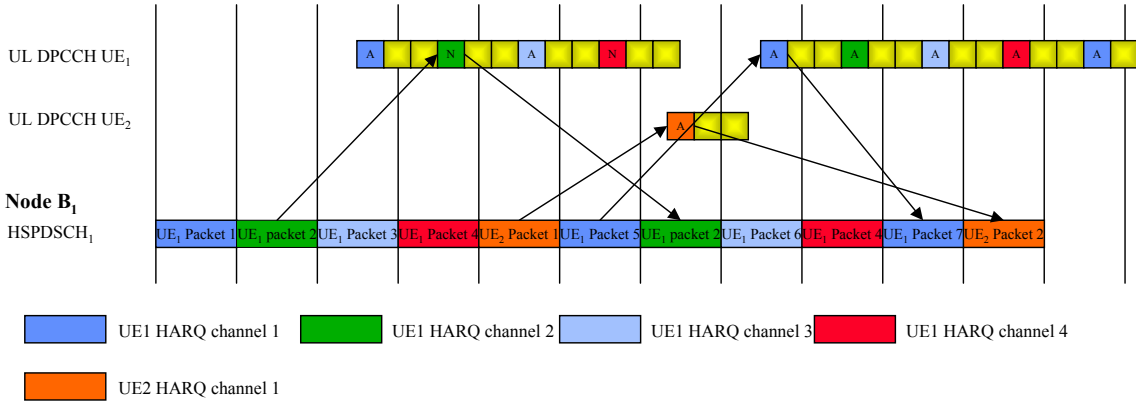

FIGURE 5.4-2. Asynchronous N-Channel stop-and-wait structure [TR25.848].

5.5 Multiple Input Multiple Output Antenna Processing

MIMO processing uses multiple antennas at both the base station transmitter and the terminal receiver. In this scheme, *M* data streams with the same channelization/ scrambling code can be transmitted over the air interface using *M* antennas at the transmitter. These data streams with the same channelization/scrambling code can be distinguished using *M* antennas at the terminal receiver. See [TR25.848].

5.6 Fast Scheduling in Base Station

The scheduling of HS-DSCH users is made in 2 ms basis in the base station. The scheduling can be Round-Robin, C/I-based or a combination of Round-Robin and C/I-scheduling. Since scheduling is made in the base station, resources can be rapidly allocated according to the needs and the quality of the channel.

5.7 Evaluation Criteria for Simulation

Two output parameters are selected as the evaluation criteria, in order to take into account the network performance as well as the user quality of the service.

Average HS-DSCH *bitrate [kbps/cell/MHz]* is used to study the network throughput performance, and is measured as

$$R = \frac{b}{k \cdot T \cdot B}, \tag{5.7-1}$$

where b is the total number of *correctly* received bits by HS-DSCH from all base stations in the simulated system over the whole simulated time, k is the number of cells in the simulation, T is the simulated time and B is the bandwidth 5 MHz.

Transfer delay [ms] is computed for the documents. It is the 95th percentile of the transmission times of the individual packets within the document. The transmission time is the delay from the packet arrival in the device buffer to its correct delivery over the air interface.

5.8 Simulation Cases and Assumptions

Simulations are executed by using the dynamic system level simulator described in Chapter 2.4. The following simulations focus on the effects of multi-code transmission, AMC, FHARQ, and FCS. Also HSDPA overall performance has been studied and compared to release 1999 DSCH. Simulations are made in macro-cell and pico-cell environments. By default, the HS-DSCH allocation period and the HS-DSCH capacity granted period are both 1 HS-DSCH frame (2 ms). The total HS-DSCH power allocation per connection is 40% or 70 % of the total cell power in outdoors and indoors, respectively. This total power allocation was selected since higher power allocations did not significantly increase the throughput when tested. The power level per one code channel can vary depending on the number of multi-codes

The selected maximum number of DCH-channels per sector is 10 or 20, and that of the HS-DSCH is 1. The default DCH bitrate is set to be 1 kbps in order to minimize its effect, and to isolate the effect of the HS-DSCH. The link level performance of different modulation and coding sets is given through the AVI lookup tables. The lookup tables has been generated by using a separate link level simulator. The basic bitrates used in the link level results are tabulated in TABLE 5.8-1. The table shows the peak bitrate, which can be achieved using a single OVSF code with spreading factor of 16 and 32. Higher bitrate per HS-DSCH connection can be achieved when multiple, N, OVSF codes are used in parallel. Hence, the bitrates can be increased by N times.

In the network simulation, the assumption is that the link level behaviour does not change with the multi-code transmission given the same modulation and coding is used.

TABLE 5.8-1. Modulation and Coding Scheme with the corresponding bitrates.

Modulation and Coding Scheme (MCS)	Bitrate [kbps], SF = 16	Bitrate [kbps], SF = 32
QPSK ½	240	120
QPSK ¾	360	180
16 QAM ½	480	240
16 QAM ¾	720	360
64 QAM ¾	1080	540

TABLE 5.8-2. Common simulation parameters.

Parameter	Value
Cell radius	Macro - 933 m ; pico – 50 .. 60 m
Data source	UMTS30.03, 2048 kbps
Air interface data rate	1 kbps (DCH) and 120, 180, 240, 360 or 540 kbps (HS-DSCH in AMC)
UE speed	3 km/h
CPICH power	Macro - 36 dBm; pico – 14 dBm
STD. Deviation of slow fading	Macro - 8 dB; pico – 6 dB
Correlation between sectors	Macro - 1.0, pico –NA
Correlation between sites	Macro - 0.5 ; pico – 0
Correlation distance of slow fading	Macro - 50 m ; pico – 5 dB
Channel model	1 tap Rayleigh
Max. number of re-transmissions	10
HARQ scheme	Type I HARQ with soft combining
BS total Tx power	Macro - 43 dBm ; pico – 24 dBm
Window_add	1 dB
Window_drop	3 dB
t_tdrop	250 ms
branch deletion delay	100 ms
Softer addition delay	140 ms
soft addition delay	280 ms
Packet scheduler	Round Robin scheduler
AMC delay	0 or 1 frames
FCS delay	0 or 2 frames
Spreading factor	15 or 32
Maximum number of codes for HS-DSCH	10 or 20
Power allocated for HS-DSCH	Macro – 40%; pico - 70 %

Appropriate MCS is selected based on the measurements made by the mobile station. When MCS is changed a certain delay due to signalling is assumed, and is a simulation parameter.

The selected loading does not reflect on the maximum load that can be served by HSDPA. Further the simulated bitrates and transfer delays do not correspond to the maximum values HSDPA could offer, but they are example values achieved by selected loading and parameters. In all cases Round-robin scheduling is used. Due to that simulated bitrates remain low.

The simulated macro-cell system is two-dimensional and consists of 18 hexagonal cells of radius of 933 meters with 3 sector directional antennas. In pico-cell environment an office building is assumed in which four base stations are located in corridors. The propagation, mobility and packet traffic models are based on UMTS30.03 [UMTS30.03]. The mean mobile speed is assumed to be 3 km/h. The assumed channel model is a single-tap Rayleigh fading channel. Most of the HSDPA parameters are according to [Nok00c] and listed in TABLE 5.8-2.

5.9 Performance Gain of Multi-Code Transmission

Here simulations for multi-code transmission are shown. Simulations are made in an indoor environment, with 3 km/h mobile station speed and a single tap channel model. Traffic model that is according to [UMTS30.03] models bursty incoming traffic from the internet. The incoming data rate is 2 Mbps. The following assumptions of HSDPA parameters are made: FCS is not used, Chase combining is used, the maximum spreading factor is 16 and the maximum number of codes per user is 10. The ideal measurements and signalling is assumed.

First a reference case is simulated in which all HS-DSCH power is allocated for a single code channel. With a single code channel the maximum data rate is 1.08 Mbps. Then the maximum number of multi-codes is increased and relative capacity improvement over the reference case simulated. With 10 code channels the maximum data rate becomes 10.8 Mbps. The simulation results are shown in FIGURE 5.9-1. As seen, multi-code transmission clearly offers better throughput. The case with 10 codes offers almost 4.5-fold capacity if compared to a single code. In the reference case, only one code channel per user is allocated, thus the data rate is adapted to the prevailing conditions through HARQ and AMC. When the maximum number of code channels is varied, better fine-tuning of the data rate can be obtained. This improves system adaptation and therefore throughput.

Naturally, maximum data rates also increase as more code channels are added. If we assume e.g. fixed 10 codes per user maximum data rate would become 10.8 Mbps. However, then the spreading factor would be reduced by factor 10. In this case only those users near to the serving base station would benefit from higher number of spreading codes.

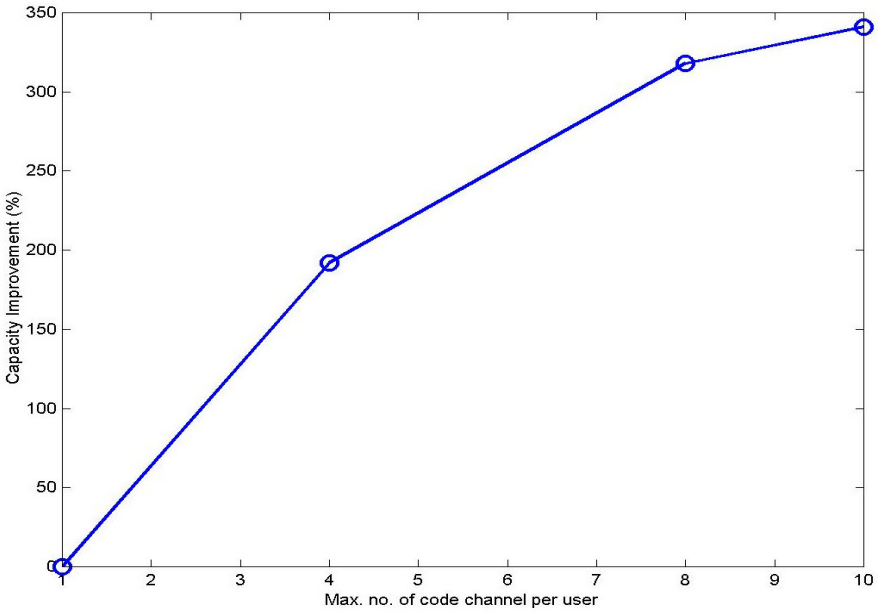

FIGURE 5.9-1. Gain of multi-code transmission over single code.

5.10 Performance of Adaptive Modulation and Coding

Next simulations are executed to find out the gains from AMC. The simulation parameters are as in the previous case, except measurement and signalling impairments are taken into account. 1.0 dB measurement error for AMC and FCS measurements is assumed. Signalling and processing delays are 1 frame and 2 frames for AMC and FCS, respectively. The simulated cases and used modulation and coding sets are given in TABLE 5.10-1.

TABLE 5.10-1. Simulation cases and used modulation and coding sets in them. Active AMC sets marked with dark colour.

Case	QPSK R = ¼	QPSK R = ¾	QPSK R = ½	QPSK R = ¾	16QAM R = ½	8PSK R = ¾	64QAM R= ¾
#1							
#2							
#3							
#4							
#5							
#6							
#7							

Simulation results for AMC can be seen in FIGURE 5.10-1. The relative capacity compared to case 1 is shown for the different sets of modulation and coding schemes. Simulations show a 2.5-fold capacity increase due to AMC. However, simulations do not show any capacity gain from 64QAM. Due to the fact that the high loading interference is already so high, that 64QAM cannot support

data transmission any more. This is an important result since it is a fact that 64QAM is rather complex to implement, see [TR25.848].

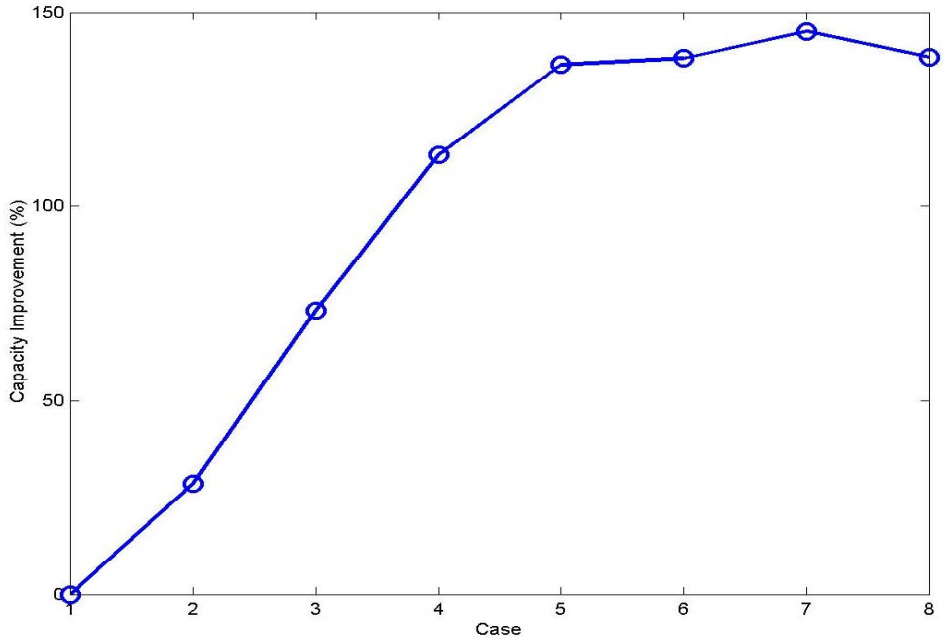

FIGURE 5.10-1. Relative capacity over QPSK R = ¼. Simulated cases are presented in TABLE 5.10-1.

FIGURE 5.10-2 shows the HS-DSCH throughput as a function of the maximum number of code channels per user ($N_{\max}$) with and without 64QAM. The result shows that the HS-DSCH performance improvement due to the presence of the 64QAM decreases with an increasing number of the HS-DSCH code channels per user. The reason for such an observation is that as $N_{\max}$ becomes greater, more choices are available for improving the HS-DSCH user bitrate. Thus, the use of higher order modulation would become less critical. From the system performance point of view, one major disadvantage of using 64QAM is that higher E_b/I_0 requirement is needed for a given frame error rate. If more multi-codes are used, the gain from the higher order modulations would not be significant. If the bitrate difference between the *N* th and *N*+1 th MCS is small due to the effect of multi-codes, the use of the *N* th MCS with a slightly lower retransmission might yield a slightly better system throughput than that of the *N*+1 th MCS. Thus, given a channel condition, if the use of multi-codes can provide a similar bitrate between the lower order modulation and the higher one, the system can "save" some retransmissions by using the lower order modulation.

These simulations assume Round-Robin scheduler. If C/I-based scheduler was used instead more gain from 64QAM could be seen since users with better quality are served first. Those users are also more likely to be able to use higher order modulation.

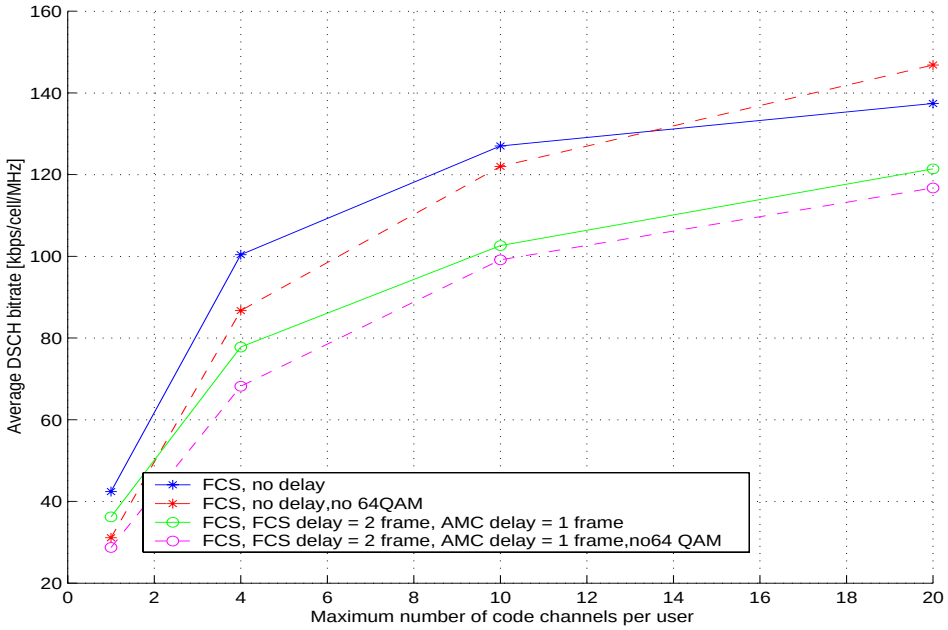

FIGURE 5.10-2. DSCH throughput as a function of N_{max} with and without 64QAM.

Next data rates obtained by different users are simulated. Data rates are shown as a function of distance to the serving base station. The simulated scenario is the hexagonal macro scenario with 3 km/h mobile speed and a single tap Rayleigh channel. In this case 70 % of the total base station power is allocated for HS-DSCH. AMC delay is assumed to be 1 frame and measurements ideal. According to these simulations users near the base station can achieve up to 6.5 Mbps instantaneous data rate, while users in the cell border can have 2 Mbps data rates, see FIGURE 5.10-3. These values also include re-transmission, thus they are values seen by the user. A lower data rate in the cell border is due to stronger MCS that leads to a lower data rate, but also due to more re-transmissions. The conventional ARQ provides almost equal data rates with HARQ with soft combining. Only in the cell border lower data rate can be seen for the conventional ARQ.

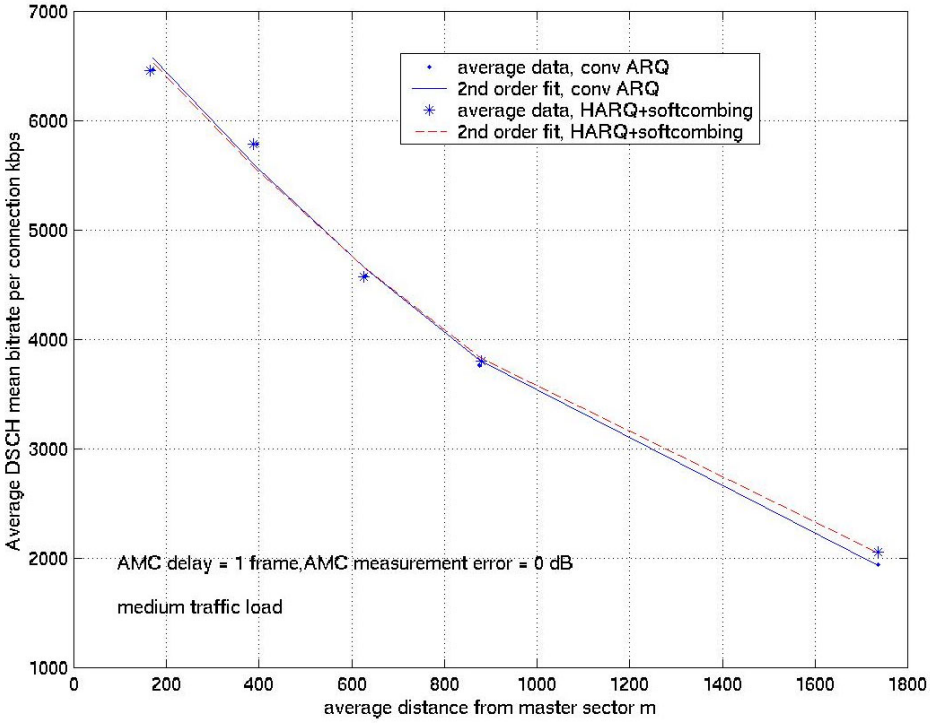

FIGURE 5.10-3. Average data rate as a function of distance.

5.11 Performance of Fast Hybrid-ARQ

Here the performance of FHARQ type-I and FHARQ type-I with soft combining (Chase combining) has been compared. Simulations are made in the hexagonal macro-cell environment with 3km/h mobile speed and a single tap Rayleigh fading channel. In this case AMC is without 64QAM. The simulation results are shown in FIGURE 5.11-1 as a function of AMC measurements error. Measurement error is modelled as a log-normally distributed error with a standard deviation as a parameter. When assuming ideal AMC measurements, the gain from soft combining is 10–14 %. For realistic measurement errors gain is 10–27 %

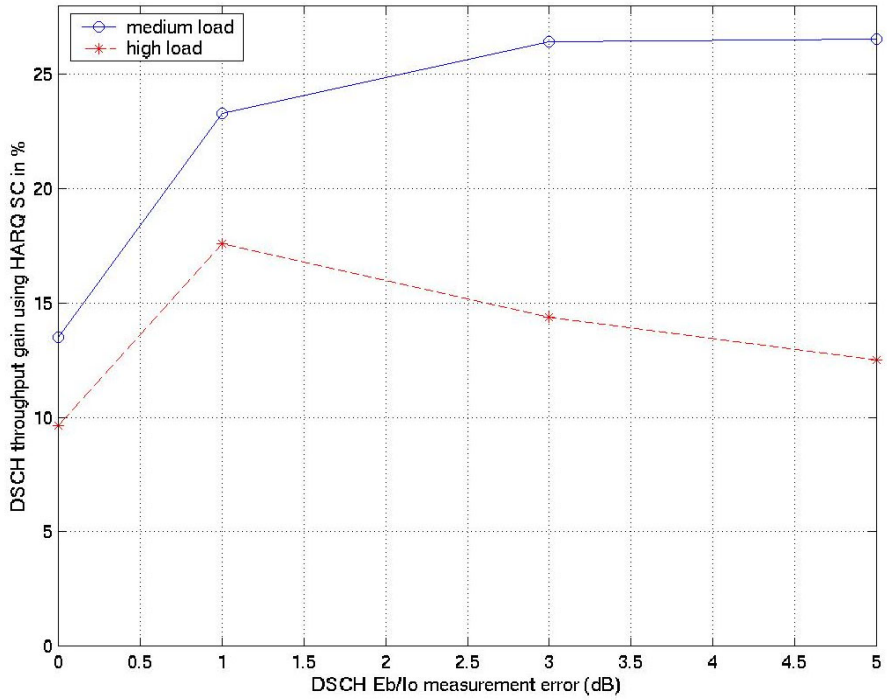

FIGURE 5.11-1. Gain from Chase combing over type-I HARQ as a function of AMC measurement error.

5.12 Performance of Fast Cell Selection

The fast cell selection performance has been simulated in the indoor environment with ideal signalling and measurements. The simulation results are shown in FIGURE 5.12-1. The capacity improvement over a single code is given as a function of a maximum number of multi-codes. As seen, the gain from FCS is in order of a few percentages at most. Since FCS introduces an overhead due to signalling, it is questionable whether FCS is reasonable in a HSDPA system.

In [Pou01] it was noticed that the gain from FCS is even smaller if realistic measurement and signalling impairments are assumed. The gain from FCS is significantly reduced when the delays are present. Almost no gain is achieved with a large $N_{\max}$, while only a small gain is visible with a small $N_{\max}$. The explanation is that even though the sector with the best channel condition is chosen via FCS, the AMC delay postpones the transmission with the allocated bitrate so that the transmitted bitrate no longer corresponds to the optimal channel condition. With the AMC delay, the HS-DSCH E_b/I_0 used to select the MCS would no longer reflect the most current HS-DSCH E_b/I_0. Thus, the observed HS-DSCH E_b/I_0 could either be higher or lower than the most current HS-DSCH E_b/I_0. If the former is higher than the latter, higher bitrate is allocated, resulting a higher FER. On the other hand, if the observed DSCH

E_b/I_0 is lower than the most current HS-DSCH E_b/I_0, a lower bitrate would be used than the optimum for the current situation. However, the selected low bitrate would lead to gain due to lower FER.

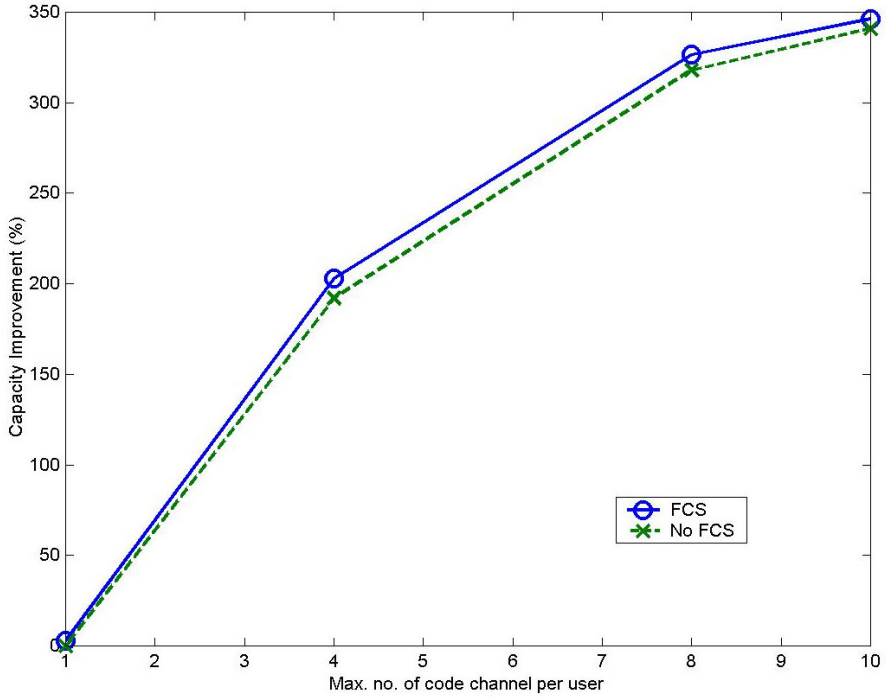

FIGURE 5.12-1. Capacity improvement over single code as a function of maximum number of multi-codes. Simulation results given for cases with and without FCS.

5.13 HSDPA Performance

Next HSDPA performance is simulated in the indoor and macro-cell environments. With these simulations FCS is not used. Signalling and measurements are assumed ideal. The simulation results for the indoor case are shown in FIGURE 5.13-1. Throughput is given as a function of a call arrival rate. When the call arrival rate is low the system load is also low and throughput is modest. When call arrival rate increases up to 100 calls/second, system reaches its maximum throughput. Then all the resources are effectively used. The simulated HSDPA throughput with 100 calls/second arrival rate becomes 5.25 Mbps/sector (1.05 Mbps/sector/MHz). When the call arrival rate is further increased, the throughput does not improve, as the resources are already fully in use.

In FIGURE 5.13-2 the corresponding simulation in the macro-cell environment is shown. In this simulation FCS and 64QAM are not used. A fixed number of users is assumed instead of the arrival process. It is further assumed that every user has all the time something to transmit in its buffer. Throughput is then given as a function of a users per cell. When the load is increased throughput first increases as the utilization of the system increases. Finally the

system will becomes fully loaded and some users are put into queue. Queuing disturbs ones connection thus throughput starts to decrease. Queuing causes delay to re-transmissions and since it is assumed that MCS is not changed in the middle of re-transmissions, some re-transmitted packets are sent by using a wrong MCS in the prevailing channel condition. Simulations show 4 Mbps/sector (800 kbps/sector/MHz) throughput in this case.

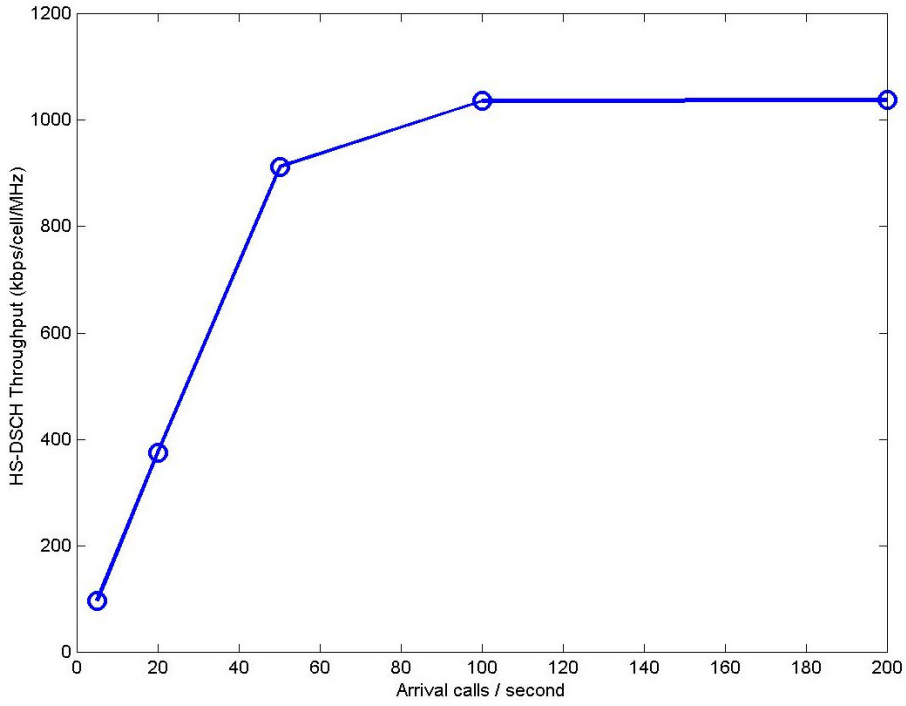

FIGURE 5.13-1. Simulated HSDPA performance in indoor environment. Throughput given as a function of call arrival rate. The used scheduler is Round-Robin.

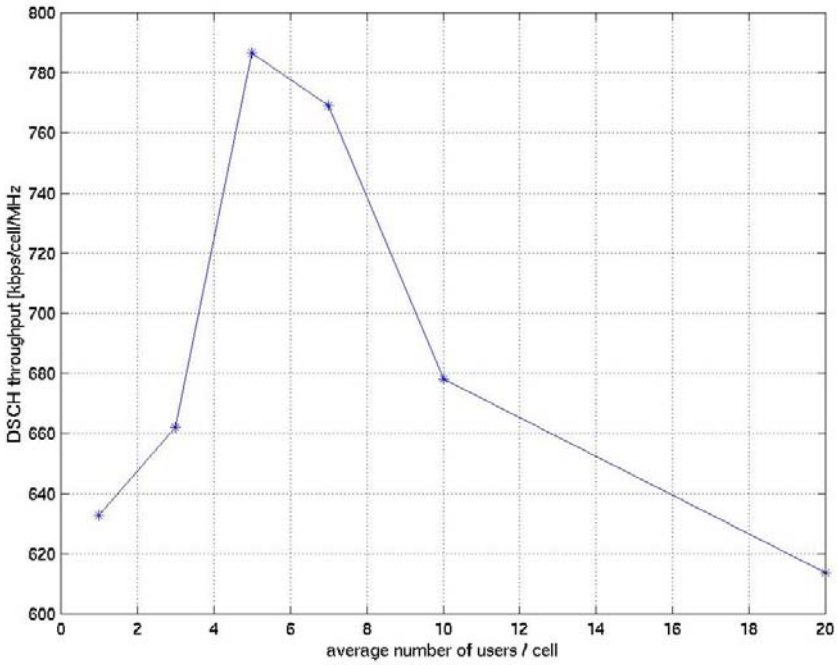

FIGURE 5.13-2. Simulated HSDPA performance in macro cell environment. Throughput given as a function of users per cell. The used scheduler is Round-Robin.

These simulations are made with Round-Robin scheduler. The Round-Robin scheduler allocates resources to users in a FIFO manner, i.e. those requests are first served that first arrive to the system. Round-Robin scheduler thus treats users in a fair manner since each user has an equal chance to get resources. This also means that users having bad channel quality are given as much resources as users having good channel quality. Due to that this scheduler gives very pessimistic cell throughputs. With for example, C/I-based scheduler much higher capacity figures could be achieved, since resources are allocated primarily to those users having good channel quality. However C/I-based scheduler is less fair - those users having poor quality or in a cell border are not served or having a much lower data rate than in case of round-robin.

5.14 HSDPA Performance Compared to Release 1999 DSCH

In this chapter performance of release 1999 DSCH and HS-DSCH are simulated and compared. When simulating DSCH HARQ type-I is used while for HS-DSCH Chase combining is used. For HS-DSCH FCS and 64QAM are not used. Simulations are executed in the macro cell-environment and realistic measurement and signalling delays are assumed. The simulation results are given in FIGURE 5.14-1. Capacity gain from HS-DSCH over DSCH is given as a function of the number of subscribers. For low loads HSDPA does not provide high gain. When system loading increases the gain improves, and capacity improvement as high as 130 % can be seen. The highest loads assumed very

high number of users. The same loading to the system would be generated if a lower number of users were using higher data rates.

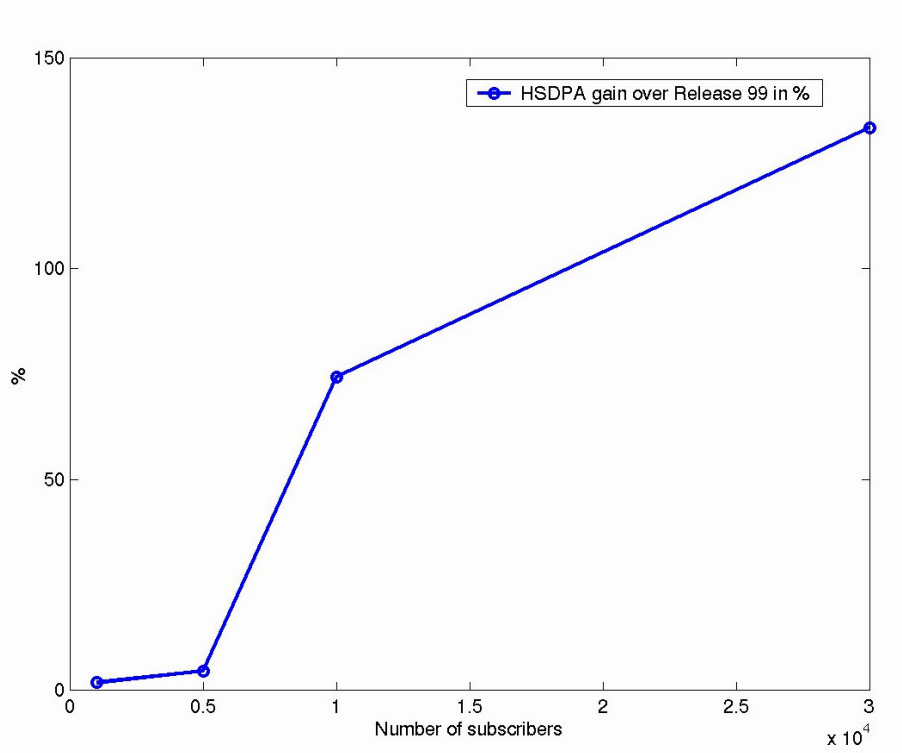

FIGURE 5.14-1. Gain of HS-DSCH over DSCH as a function of subscriber amount.

5.15 HSDPA Robustness

The next effect of AMC and FCS delays are studied, see FIGURE 5.15-1. Delays are due to processing in the mobile station and in the base station and delays due to signalling. According to these simulations FCS delay does not cause a big loss - only a 1 % loss is seen. AMC delay causes a larger loss. In this case capacity loss due to AMC delay is about 11 %. Since a realistic measurement and signalling impairments cause less than 15 % performance loss it can be concluded that HSDPA is thus rather robust against impairments.

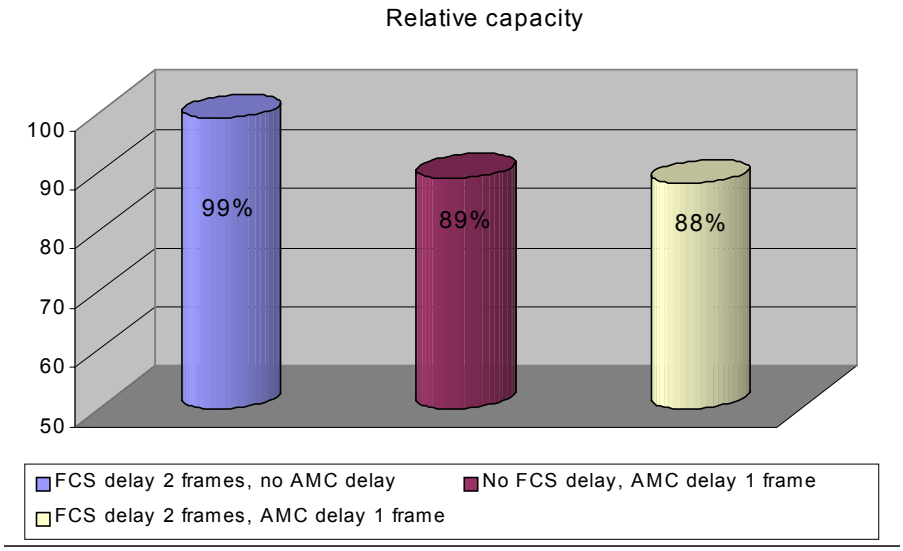

FIGURE 5.15-1. HSDPA Performance loss due to delays is FCS and AMC signalling and processing.

5.16 Discussions

In this chapter HSDPA performance was studied. HSDPA provides very high capacity - simulations show 5.25 Mbps/sector throughputs in the indoor environment and 4.0 Mbps/sector in the outdoor environment with a pessimistic Round-Robin scheduler. HS-DSCH capacity is 2.3-fold if compared to release 1999 DSCH. Simulations show that the gain from 64QAM or FCS is negligible. These are important results, especially since the implementation of 64QAM and FCS is rather complex. Instead AMC provides very high gain of 150 %. Multi-code transmission offers 4.5-fold capacity if compared to single code transmission. An analysis made for impairments shows that HSDPA is robust against signalling delays. According to this analysis HSDPA offers a very high throughput to the network and a solid basis for the system optimisation.

Here HSDPA performance in a single-tap Rayleigh channel has been analysed. Performance in a multi-tap channel might be worse as shown here. Simulations in multi-path faded channel are for study as well as simulations with C/I-based scheduler.

6 CONCLUSIONS

In this study WCDMA radio network and WCDMA radio resource management algorithm performance was analysed by using static and dynamic radio network level simulators. The used simulation tool and their modelling have been presented. The used tools are powerful tools for the radio resource management algorithm development, support for the network planning and optimisation of radio network parameters. However, this tool has the biggest importance in generating understanding of a very complex WCDMA radio network performance. This is in particular true as no live WCDMA networks yet exist. During the coming months the first live networks will be launched. This will not remove the need from these tools – WCDMA standards in 3GPP will continuously evolve and new features will be added. These tools are needed also in the future to generate understanding of how new algorithms and features behave and what kind of impacts they have on the network performance.

Simulations show that system parameters selected by 3GPP ensure good capacity. Here the performance of power control, random access, handover, compressed mode and HSDPA were simulated. Simulations show good capacity with the system parameters selected by 3GPP. Based on the simulations, mobile station power amplifier ACLR and receiver filter selectivity requirements were specified. Those values are selected so that the capacity impact even in very pessimistic scenarios would be minimal. Possible remaining problems can be then handled by radio resource management and especially by using inter-frequency handover.

Here two novel mechanisms – diversity random access and site selection diversity – were proposed. Both proposed mechanisms are now part of both cdma2000 and WCDMA system.

Based on the simulations presented here, the mobile station minimum power requirement and handover measurement quantities were selected in 3GPP. Handover measurements should be wideband SIR based, handover filtering should be sliding window and reporting event-based. Accordingly with the given analysis it is recommended to execute the downlink outer loop power control in the mobile station.

In the future network performance can be improved with advanced multi-user detection receivers. Simulations show high capacity gain for the uplink multi-user detection receiver. In the downlink, orthogonal codes readily take care of intra-cell interference, thus a smaller gain from interference cancellation receiver is expected.

In 3GPP release 5 High Speed Downlink Packet Access is introduced. HSDPA system can offer very high data rates and capacity to the network. Simulations, however, show that 64QAM that is a complex modulation method does not provide capacity gain. It is thus questionable to require a mobile station to support 64QAM. Another observation was that FCS does not provide capacity gain. As FCS would require the signalling between base stations in the active set, it is unnecessary to increase complexity to the system by requiring FCS.

Further work includes simulations for other radio resource management algorithms such as packet scheduling, admission control and load control. HSDPA system should be simulated with C/I-based schedulers as Round-Robin scheduler may give pessimistic capacity estimates for the system.

REFERENCES

[3GPP] http://www.3gpp.org

[3GPP2] http://www.3gpp2.org

[Abr70] Abramson N., "The ALOHA systems – another alternative for computer communications", Fall Joint Computer Conference, 1970

[Ada97] Adachi F., Sawahashi M., Okawa, K., "Tree structured generation of orthogonal codes with different lengths for forward link of DS-CDMA radio", IEE Electronics Letters, vol.33, No.1, pp. 27–28, 2nd of January, 1997

[Akh99] Akhtar S., Zeghlache D., "Capacity Evaluation of the UTRA WCDMA Interface", in proceedings of VTC99 fall conference, pp. 914–918, 19–22 September, Amsterdam, Netherlands

[Akh00] Akhtar S., Zeghlache D., "CIR Based Soft Handover for UTRA FDD Uplink", in proceedings of PIMRC00 conference, pp. 650–654, 18–21 September, 2000, London, UK

[Akh01] Akhtar S., Malik S.A., Zeghlache D., "A Comparative Study of Power Control Strategies for Soft Handover in UTRA FDD WCDMA System", in proceedings of VTC01 spring conference, pp. 2680–2684, 6–9 May, 2001, Rhodes, Greece

[And92] Andermo P.G., "System Flexibility and its Requirements on Third Generation Mobile Systems", in proceedings of PIMRC92 conference, pp. 1–3, 19–21 October, 1992, Boston, MA, USA

[And94] Anderson T., "Tuning the Macro Diversity Performance in a DS-CDMA System", in proceedings of VTC94 conference, pp. 41–45, 8–10 June, 1994, Stockholm, Sweden

[And95]] Andermo P.-G.(editor), "UMTS Code Division Testbed (CODIT)", CODIT Final Review Report, September 1995

[Ari91] Ariyavisitakul S., Chang L.F., "Simulation of CDMA System Performance with Feedback Power Control", IEE Electronics Letters, pp. 2127–2128, 7 November, Vol.27, No.23

[Ari92] Ariyavisitakul S., "SIR Based Power Control in a CDMA System", in proceedings of GLOBECOM´92 conference, pp. 862–873, 6–9 December, 1992, Orlando, Florida, USA

[Ari93] Ariyavisitakul S., Chang L.F., "Signal and Interference Statistics of a CDMA System with Feedback Power Control", IEEE Transactions on Communications, pp. 1626–1634, Vol. 41, No. 11, November, 1993

[Ari94] Ariyavisitakul S., "Signal and Interference Statistics of a CDMA System with Feedback Power Control – Part II", IEEE Transactions on Communications, pp. 597–605, Vol. 42, No. 2/3/4, February/March/April, 1994

[ARIB] http://www.arib.or.jp/index_English.html

[Att02] Attar R., Esteves E., "A Reverse Link Outer-Loop Power Control Algorithm for cdma2000 1xEV Systems", in proceedings of ICC02 conference, pp. 573–578, 28 April – 2 May, 2002, New York, NY, USA

[Aus93] Austin M.D., Stuber G.L., "Velocity Adaptive Handoff Algorithms for Micro cellular Systems", in proceedings of ICUPC93 conference, pp 793–797, 12–15 October, 1993, Ottawa, Ont., Canada

[Aus94] Austin M.D., Stuber G.L., "Velocity Adaptive Handoff Algorithms for Micro Cellular Systems", IEEE Transactions on Vehicular Technology, Vol. 43, No., 3, August 1994.

[Bai94] Baier A., Fiebig U.-C., Granzow W., Koch W., Teder P., Thielecke J., "Design Study for a CDMA-based Third-Generation Mobile System", IEEE Journal in Selected Areas of Communications, vol. 12, no. 4, pp.733- 743, May 1994

[Bak00] Baker M.J.P., Moulsley T.J., "Power Control in UMTS Release'99", in proceeding of 3G Mobile Communication Technologies –00 conference, pp. 36–30, 27–29 March, 2000, London, UK

[Ben98] Benn H., O'Neill R., Owen R., Johnson C., "UMTS Air Interface Simulation", IEE Colloquium on UMTS – the R Challenges, 6/1 – 6/8, 23 November, 1998, London, UK

[Ben00] Bender P., Black P., Grob M., Padovani, R., Sindhushayana N., Viterbi A., "CDMA/HDR: A Bandwidth-Efficient High-Speed Wireless Data Service for Nomadic Users", IEEE Communications Magazine, pp. 70–77, Volume 38, Issue 7, July, 2000

[Ber95] Berg J.E., "A recursive Method For Street Microcell Path Loss Calculations", in proceedings of PIMRC95 conference, Vol. 1, pp 140-143, 27–29 September, Toronto, Ottawa, Canada

[Ber00] Bernhard U., Pampel H., Mueckenheim J., Gunreben P., "Evaluation of W-CDMA Network Performance and Impact of Soft Handover Using Dynamic Network Simulation", in proceedings of 3G Mobile Communication Technologies conference, pp. 347–351, 27–29 March, 2000, London, UK

[Bi02] Bi Q., Vitebsky S., "Performance Analysis of 3G-1X EVDO High Data Rate System", in proceedings of WCNC02 conference, pp. 389–395, 17–21 March, 2002, Orlando, FL, USA

[Bin00] Binucci N., Hiltunen K., Caselli M., "Soft handover Gain in WCDMA", in proceedings of VTC00fall conference, pp. 1467–1472, 24–28 September, Boston, MA, USA

[Bur94] Burr A.G., "Bounds and Estimates of the Uplink Capacity of Cellular Systems", in proceedings of VTC94 conference, pp. 180–1484, 8–10 June, 1994, Stockholm, Sweden

[Cao02] Cao, S., "Standardization Activities of 3G and Beyond", in proceedings of B3G - International Forum on Mobile

Telecommunications, pp. 59–61, 20–22 November, 2002, Beijing, China

[Car00] Cardona N., Navarro A., "W-CDMA Capacity Analysis Using GIS Based Planning Tools and Matlab Simulation", in proceedings of 3G Mobile Communication Technologies conference, pp. 230–234, 27–29 March, 2000, London, UK

[Cas00] Castaneda-Camacho J., Lara-Rodriguez D., "Performance of New Microcell/Macrocell Cellular Architecture with CDMA Access", in proceedings of VTC00 spring conference, pp. 483–486, 15–18 May, 2000, Tokyo, Japan

[CCSS] http://www.synopsys.com/products/cocentric_studio/cocentric_studio.html

[Cha91] Chang L.F., Ariyavisitakul S., "Performance of a CDMA Radio Communications System with Feed-Back Power Control and Multipath Dispersion", in proceedings of GLOBECOM91 conference, pp. 1017–1021, 2–5 December, 1991, Phoenix, AZ, USA

[Cha85] Chase D., "Code combining - a maximum-likelihood decoding approach for combining an arbitrary number of noisy packets," IEEE Transactions in Communications, vol. COM-33, pp. 385-393, May 1985.

[Chh99] Chheda A., "A Performance Comparison of the CDMA IS-95B and IS-95A Soft Handoff Algorithms", in proceedings of VTC99, pp. 1407–1412, 16–20 May, 1999, Houston, TX, USA

[Chi91] Chia S.T.S., "The Control of Handover Initiation in Microcells", in proceedings of VTC91 conference, pp. 531–536, 19–22 May, 1991, St. Louis, MO, USA

[Cho95] Chopra M., Rohani K., Reed D., "Analysis of CDMA Range Extension due to Soft Handoff", in proceedings of VTC95 conference, pp. 917- 921, 25–28 July, 1995, Chicago, IL, USA

[Cho01] Choudhary P., Ghosh A., Jalloul L., "Simulated Performance of W-CDMA Random Access Channel", in proceedings of VTC01 conference, pp. 270–2704, 6–9 May, Rhodes, Greece

[Chu00] Chulajata T., Kwon H.M., "Combinations of Power Controls for cdma2000 Wireless Communications System", in proceedings of VTC00 fall conference, pp. 638–645, 24–28 September, 2000, Boston, MA, USA

[Coo02] Cooper W., Zeidler J.R., McLaughlin S., "Performance Analysis of Slotted Random Access Channels for W-CDMA Systems in Nakagami Fading Channels", IEEE Transactions on Vehicular Technology, Vol. 51, No.3, pp. 411- 422, May 2002

[COST231] Damosso E., Correia L.M., (editors), "Digital Mobile Radio Towards Future Generation Systems", COST231 Final Report,

[C.S0003-A] 3GPP2, "Medium Access Control (MAC) Standard for cdma2000 Spread Spectrum System", 3GPP2, Release A, June 9, 2000.

[C.S0004-A] 3GPP2, “Signaling Link Access Control (LAC) Specification for cdma2000 Spread Spectrum System”, 3GPP2, Release A, June 9, 2000.

[C.S0024] 3GPP2, “cdma2000 High Rate Packet Data Air Interface Specification”, 3GPP2, Version 4.0, October 25, 2002

[CWTS] http://www.cwts.org/cwts/index_eng.html

[Dar98] Daraiseh A.-G., Landolsi M., “Optimized CDMA Forward Link Power Allocation During Soft Handoff”, in proceedings of VTC98 conference, pp. 1548–1552, 18–21 May, 1998, Ottawa, Ont., Canada

[Das01] Das A., Khan F., Sampath A., Su H.-J., “Performance of Hybrid ARQ for High Speed Downlink Packet Access in UMTS”, in proceedings of VTC01 fall conference, pp. 2133–2137, 7–11 October, 2001, Atlantic City, NJ, USA

[Deh00] Dehghan S., Lister D., Owen R., Jones P., “W-CDMA Capacity and Planning Issues”, Electronics & Communication n Engineering Journal, pp. 101–118, June, 2000

[Dia92] Diaz P., Agusti R., “Analysis of a Fast CDMA Power Control Scheme in an Indoor Environment”, in proceedings of VTC92 conference, pp. 67–70, 10–13 May, 1992, Denver, CO, USA

[Due95] Duel-Hallen A., Holtzman J., Zvonar Z., “Multiuser Detection for CDMA Systems”, IEEE Personal Communications, pp. 46–58, April, 1995

[Dzi99] Dziong Z., Krishnan M., Kumar S., Nanda S., “Statistical “Snap-Shot” for Multi-Cell CDMA System Capacity Analysis”, in proceedings of WCNC99 conference, pp. 1234–1237, 21–24 September, 1999, New Orleans, LA, USA

[Eng99] Engström B., Ericson M., “WCDMA System Level Performance with Fast Fading and Non-Ideal Power Control”, in proceedings of VTC99fall conference, pp. 1129–1133, 19–22 September, Amsterdam, Netherlands

[Eri98a] Eriksson T,. Ojanperä T., ”Implementation Aspects”, Chapter 10, pp. 279–322 in book “Wideband CDMA for Third Generation Mobile Communications” edited by T.Ojanperä and R. Prasad. Artech House, 1998.

[Eri98b] Ericsson, "Adjacent Channel Interference in UTRA System", rev.1, Tdoc SMG2 UMTS-L1 100/98.

[Eri99a] Ericsson, “Evaluation of up- and downlink adjacent channel performance”, TSG RAN Working Group 4(Radio) meeting #2, TSGR4#2(99)048, 15–19 February, 1999, Turin, Italy

[Eri01a] Ericsson, "Compressed mode performance", TSG RAN working Group 4 (Radio) meeting #2, tdoc TSGR 4#15 R4-010013, 23–26 January, 1999, Boston, MA, USA,

[Esm97] Esmailzadeh R., Gustafsson, M., “A new Slotted ALOHA Based random Access Method for CDMA Systems”, in proceedings of

ICUPC97 conference, pp. 43–47, 12–16 October, 1997, San Diego, CA, USA

[Est02] Esteves E., "On the Reverse Link Capacity of cdma2000 High Data Rate Packet Data Systems", in proceedings of ICC02 conference, pp. 1823–1828, 28 April – 2 May, 2002, New York, NY, USA

[Ete01] Etemad K., "Enhanced Random Access and Reservation Scheme in CDMA2000", IEEE Personal Communications, pp. 30–36, April 2001

[ETSI] http://www.etsi.org

[Faw95] Fawer U., Aazhang, B., "A Multiuser Receiver for Code Division Multiple Access Communications over Multipath Channels", IEEE Transaction on Communications, Vol. COM-43, pp. 1556–1565, 1995

[Fla02] Flanagan J., Novosad T., "WCDMA Network Cost Function Minimization for Soft Handover Optimization with Variable User Load", in proceedings of VTC02 fall conference, pp. 2224–2228, 24–28 September, 2002, Vancouver, BC, Canada

[Fra99] Frank G., Weber R., "Random Access Scheme for ETSI/UTRA WCDMA", in proceedings of VTC99 conference, pp. 16–20, 16–20 May, 1999, Houston, Texas, USA

[Fre01] Frenger P., Parkvall S., Dahlman, E., "Performance Comparison of HARQ with Chase Combining and Incremental Redundancy for HSDPA", in proceedings of VTC01 fall conference, pp. 1829–1833, 7–11 October, 2001, Atlantic City, NJ, USA

[Fre02] Frederiksen F., Kolding T.E., "Performance and Modeling of WCDMA/HSDPA Transmission/H-ARQ Schemes", in proceedings of VTC02 fall conference, pp. 472–476, 24–28 September, 2002, Vancouver, BC, Canada

[Fur00] Furukawa H., Hamabe K., Ushirokawa A., "SSDT – Site Selection Diversity Transmit Power Control for CDMA Forward Link", IEEE Journal on Selected Areas in Communications, Vol.18, No.8, August 2000.

[Gej92a] Gejji R.R., "Forward-Link Power Control in CDMA Cellular Systems", in proceedings of VTC92 conference, pp. 981–984, 10–13 May, 1992, Denver, CO, USA

[Gej92b] Gejji R.R., "Forward-Link Power Control in CDMA Cellular Systems", IEEE Transactions on Vehicular Technology, pp. 532–536, Vol. 41, No. 4, November, 1992

[Gho99] Ghosh A., Cudak M., Felix K., "Shared Channels for Packet Data Transmission in W-CDMA", in proceedings of VTC99 fall conference, pp. 943–947, 19–22 September, 1999, Amsterdam, Netherlands.

[Gho00] Ghosh A, Jalloul L., Cudak M., Classon B., "Performance of Coded Higher Order Modulation and Hybrid ARQ for Next Generation Cellular CDMA Systems", in proceedings of VTC00

fall conference, pp. 500–505, 24–28 September, 2000, Boston, MA, USA

[Gho01] Ghosh A., Jalloul L., Love B., Cudack M., Classon B., "Air Interface for 1XTREME/1XEV-DV", in proceedings of VTC01 spring conference, pp. 2474–2478, 6–9 May, 2001, Rhodes, Greece

[Gil89] Gilhousen K., Padovani R., Wheatley C.E. III, "Soft Handoff in a CDMA Cellular Telephone System", US Pat. No. US5101501 A1, filed 11.07.1989

[Gil91] Gilhousen K.S., Jacobs, I.M., Padovani, R., Viterbi A.J., Weaver L.A., Wheatley C.E., "On the Capacity of a Cellular CDMA System", IEEE Transactions on Vehicular Technology, vol. 40, No. 2, pp.303–312, 1991

[Gio00] Giovanardi A., Mazzini G., Tralli V., Zorzi M., "Some Results on Power Control in Wideband CDMA Cellular Network", in proceedings of WCNC00 conference, pp. 365–369, 23–28 September, 1999, Chicago, IL, USA

[Gor96] Gorricho J.-L., Paradells J., "Evaluation of the Soft Handover Benefits on CDMA Systems", in proceedings of ICUPC96 conference, pp 305–309, 29 September – 2 October, 1996, Cambridge, MA, USA

[Gra95] Granlund S., Häkkinen H., Hämäläinen S., " Method for improving the reliability of a handover and call establishment, and a cellular radio system", PCT patent no WO96/37083, priority date 17 May, 1995

[Gra01] Grandell J., Salonaho O., "Closed-Loop Power Control Algorithms in Soft Handover for WCDMA Systems", in proceedings of ICC01 conference, pp. 791–795, 11–14 June, 2001, Helsinki, Finland

[Gri91] Grimlund O., Gudmundson B., "Handoff Strategies in Micro cellular Systems", in proceedings of VTC91 conference, pp. 505–510, 19–22 May, 1991, St. Louis, MO, USA

[Gud91a] Gudmundson M., "Correlation Model for Shadow Fading in Mobile Radio Systems," Electronics Letters, vol. 27, pp. 2145-2146, November 7, 1991, No 23

[Gud91b] Gudmundson M., "Analysis of Handover Algorithms", in proceedings of VTC91 conference, pp. 537–541, 19–22 May, 1991, St. Louis, MO, USA

[Gun01] Gunaratne S., Nourizadeh S., Jeans T., Tafazolli R., "Performance of SIR-Based Power Control for UMTS", in proceedings of 3G Mobile Communications Technologies –01 conference, pp. 16–20, 26–28 March, 2001, London, UK

[Gus97] Gustafsson M., Jamal K., Dahlman E., "Compressed Mode Techniques for Inter-Frequency Measurements in a Wide-band DS-CDMA System", in proceedings of PIMR97 conference, pp.231–235, 1–4.September, 1997, Helsinki, Finland

[Hei02] Heiska K., Posti H., Muszynski P., Aikio P., Numminen J., Hämäläinen M., ”Capacity Reduction of WCDMA Downlink in the Presence of Interference From Adjacent Channel Narrow-Band System”, IEEE Transactions on Vehicula Technology, pp. 37–51, Vol. 51, No. 1, January, 2002

[Hen01] Henttonen T., Hämäläinen S., “Network Effects of WCDMA Random Access and Acquisition Procedures", in proceedings of CIC2001 conference, 30 October – 2 November, 2001, Seoul, Korea

[Hig00] Higuchi K., Andoh H., Okawa K., Sawahashi M., Adachi F., “Experimental Evaluation of Combined Effect of Coherent Rake Combining and SIR-Based Fast Transmit Power Control for Reverse Link of DS-CDMA Mobile Radio”, IEEE Journal on Selected Areas in Communications, pp. 1526–1535, Vol. 18, No. 8, August, 2000

[Hil00a] Hiltunen K., de Bernardi R., “WCDMA Downlink Capacity Estimation”, in proceedings of VTC00 spring conference, pp. 992–996, 15–18 May, 2000, Tokyo, Japan

[Hil00b] Hiltunen K., Binucci N., Bergström J., “Comparison Between Periodic and Event-Triggered Intra-Frequency Handover Measurement Reporting in WCDMA”, in proceedings of WCNC2000 conference, pp.471–475, 23–28 September, 2000, Chicago, IL, USA

[Hil02] Hiltunen K., Binucci N., “WCDMA Downlink Coverage: Interference Margin for Users Located at the Cell Coverage Border“, in proceedings of VTC02 spring conference, pp. 270–272, 6- 9 May, 2002, Birmingham, AL, USA

[Hol92] Holzman J.M., “Adaptive Measurement Intervals for Handovers”, in proceedings of ICC92 conference, pp. 1032–1036, 14–18 June, 1992, Chicago, IL, USA

[Hol95] Holtzman J.M., “Adaptive Averaging Methodology for Handoffs in Cellular Systems”, IEEE Transactions on Vehicular Technology, Vol.44, No.1, pp. 59–66, February, 1995

[Hol97] Holma H, Hämäläinen S., Toskala A., ”Interference Analysis of CDMA Uplink with Hard and Soft Handovers, in the proceedings of CIC97 conference, pp. 37–41, 1997, Seoul, Korea.

[Hol98] Holma H., Toskala A., Hämäläinen S., Ojanperä T., "Performance Analysis" Chapter 7, pp. 195–247 in book “Wideband CDMA for Third Generation Mobile Communications” edited by T.Ojanperä and R. Prasad. Artech House, 1998

[Hol00] Holma H.A. Toskala (editors), "WCDMA for UMTS", John Wiley & Sons, Ltd, 2000, ISBN 0 471 72051 8

[Hol01] Holma H., Soldani D., Sipilä K., “Simulated and Measured WCDMA Uplink Performance”, in proceedings of VTC01 conference, pp.1148–1152, 7–11 October, Atlantic City, NJ, USA

[Hop01] Hoppe, R., Buddendick, H., Wölfle, G., Landstorfer, F., M., "Dynamic Simulator for Studying WCDMA Radio Network Performance", in proceedings of VTC01 spring conference, pp. 2771–2775, 6–9 May, 2001, Rhodes, Greece

[Hor02] Horng J.H., Vannucci G., Zhang J., "Capacity Enhancement for HSDPA in W-CDMA System", in proceedings VTC02 fall conference, 24–28 September, 2002, Vancouver, BC, Canada

[Hoz99] de Hoz A., Cordier C., "W-CDMA Downlink Performance Analysis", in proceedings of VTC99 fall conference, pp. 968–972, 19–22 September, 1999, Amsterdam, Netherlands

[Hua96] Huang W., Bhargava V.K., "Performance Evaluation of a DS/CDMA Cellular System with Voice and Data Services" in proceedings of PIMRC96 conference, pp. 588–592, 15–18 October, 1996, Taipei, Taiwan

[Häk96] Häkkinen H., Granlund S., Hämäläinen S., "A Connection Establishment method, a subscriber terminal unit and a radio system", Australian patent no. 719096. Application no AU199716041 B2, 1997.02.04. Priority data: number 960541, date 06.02.1996, filed with Finland.

[Häm96] Hämäläinen S., Toskala A., Holma H., "Capacity Evaluation of a Cellular CDMA Uplink with Multiuser Detection", in proceedings of ISSSTA96 conference, pp.339–343, 22–25 September, 1996, Mainz, Germany

[Häm97a] Hämäläinen S., Holma H., Toskala A., Laukkanen M., "Analysis of CDMA Downlink Capacity Enhancements", in proceedings of PIMRC97 conference, pp.241- 245, 1–4 September, 1997, Helsinki, Finland

[Häm97b] Hämäläinen S., Lilja H., Lokio J., Leinonen M., "Performance of a CDMA Based Hierarchical Cell Structure Network", in proceedings of PIMRC97 conference, pp.863–866, 1–4 September, 1997, Helsinki, Finland

[Häm97c] Hämäläinen S., Slanina P., Hartman M., Lappeteläinen A., Holma H., Salonaho O., "A Novel Interface Between Link and System Level Simulations", in proceedings of ACTS97 conference, p.599- 604, 7–10 October, 1997, Aalborg, Denmark

[Häm98] Hämäläinen S., Lilja H., Ojanperä T., " Hierarchical Cell Structures", Chapter 8, pp. 249–259 in book "Wideband CDMA for Third Generation Mobile Communications" edited by T.Ojanperä and R. Prasad. Artech House, 1998.

[Häm99a] Hämäläinen S., Lilja H., Hämäläinen A., "WCDMA Adjacent Channel Interference Requirements", in proceedings of VTC99fall conference, pp. 2591–2595, 19–22 May, 1999, Amsterdam, Netherlands

[Häm99b] Hämäläinen S., Holma H., Sipilä K., "Advanced WCDMA Radio Network Simulator", in proceedings of PIMRC99 conference, pp.951-955, 19–22 September, 1999, Osaka, Japan

[Häm00] Hämäläinen S., Numminen J., " Timing Method and Arrangement for Perfoming Prepatory Measurements for Inter-frequency Handover", EP Pat.No. EP00969618 EP, filed 24.10.2000

[Häm01] Hämäläinen S., "High Speed Packet Access in WCDMA", in proceedings of CIC2001 conference, 30 October – 2 November, Seoul, Korea, Invited paper to technical session

[Häm02] Hämäläinen S., Henttonen T., "Comparison of Filtering and Reporting Schemes for WCDMA Handover", in proceedings of ICT02 conference, pp. 178–182, 23–26 June, 2002, Beijing, China

[Häm03] Hämäläinen S., Henttonen T., Numminen J., Vikstedt J., "Network Effects of WCDMA Compressed Mode", submitted to VTC 2003 spring, Cheju, Korea

[Ism00] Ismail M.S., Rahman T.A., "Forward-link Performance of CDMA Cellular System", IEEE Transactions on Vehicular Technology, Vol. 49, No., 5, pp. 1692–1696, September, 2000

[ITU] http://www.out.org

[Jak74] Jakes W., Microwave Mobile Communications, pp. 57-77. Wiley & Sons, 1974.

[Jal93a] Jalali A., Mermelstein P., "Power Control and Diversity for the Downlink of CDMA Systems", in proceedings of ICUPC93 conference, pp. 980–984, 12–15 October, Ottawa, Ont., Canada

[Jal93b] Jalali A., Mermelstein P., "Effects of Multipath and Antenna Diversity on the Uplink Capacity of a CDMA Wireless System", in proceedings of GLOBECOM93 conference, pp. 1660–1664, 29 November – 2 December, 1993, Houston, TX, USA

[Jal94] Jalali A., Mermelstein P., "On the Bandwidth Efficiency of CDMA Systems", in proceedings of ICC94 conference, pp. 515–519, 1–5 May, 1994, New Orleans, LA, USA

[Jal97] Jalali L., Rohani K., "CDMA Forward Link Capacity and Coverage in Multipath Fading Channel", in proceedings of VTC97 conference, pp.1440–1444, 4–7 May, 1997, Phoenix, AZ, USA

[Jal98a] Jalali A., Gutierrez, A., "Performance Comparison of Alternative Wideband CDMA Systems", in proceedings of ICC98 conference, pp. 38–42, 7–11 June, 1998, Atlanta, GA, USA

[Jal98b] Jalali A., Gutierrez A., "Performance Comparison of Direct Spread and Multicarrier CDMA Systems", in proceedings of VTC98 conference, pp. 2042–2046, 18–21 May, 1998, Ottawa, Ont, Canada

[Jal00] Jalali A., Padovani R., Pankaj R., "Data Throughput of CDMA-HDR High Efficiency – High Data Rate Personal Communication Wireless System", in proceedings of VTC00 spring conference, pp. 1854–1858, 15–18 May, 2000, Tokyo, Japan

[Jan93] Jansen M.G., Prasad R., "Throughput Analysis of a Slotted CDMA System with Imperfect Power Control", in proceedings of

IEE Colloquium on Spread Spectrum Techniques for Radio Communication Systems 93, pp.8/1–8/4, 1993, London, UK

[Jan94] Jansen M.G., Prasad, R., "Throughput and Delay Analysis of a Cellular Slotted DS CDMA System with Imperfect Power Control and Sectorization", in proceedings of ISSSTA94 conference, pp. 420–424, 4–6 July, 1994, Oulu, Finland

[Jan95a] Jansen M.G., Prasad R., "Performance Analysis of a DS CDMA System Using Measured Delay Profiles in and Indoor Environment", in proceedings of PIMRC95 conference, pp. 169–172, 27–29 September, 1995, Toronto, Ont., Canada

[Jan95b] Jansen M.G., Prasad R., "Capacity, Throughput, and Delay Analysis of a Cellular DS CDMA System With Imperfect Power Control and Imperfect Sectorization", IEEE Transactions on Vehicular Technology, pp. 67–75, Vol. 44, No. 1, February, 1995

[Jes01] Jeske D.R., Sampath A., "Signal-to-Interference Ratio Estimation Based on Decision Feedback", in proceedings of VTC01 spring conference, pp. 2484–2488, 6–9 May, 2001, Rhodes, Greece

[Jim94] Jimenez J., (ed.), "Final Propagation Model", CODIT deliverable, R2020/TDE/PS/P/040/b1, June 1994

[Joh02] Johnson C., Khalab J., Hoglund A., "Inter and Intra Operator Coexistence of WCDMA HCS Layers", in proceedings of VTC02 spring conference, pp. 115–119, 6–9 May, 2002, Birmingham, AL, USA

[Jon00] Jones P.R. Owen, "Sensitivity of UMTS FDD System Capacity and Coverage to Model Parameters", in proceedings First International Conference on 3G Mobile Communications Technologies 00 conference, pp. 224–229, 27–29 March, 2000, London, UK

[Jug99] Jugl E., Boche H., "Limits of sectorization gain caused by mobility and soft handoff", Electronics Letters, pp. 119–120, Vol.35, No.2, 21 January, 1999

[Jun01] Jung Y.-S.., Jeon H.-C., Shin S.-M., Oh J.-H., Kwon B., Ihm J.-T., "Coverage and Capacity Analysis in cdma2000 Network for Voice and Packet Data Services", in proceedings of VTC01 fall conference, pp. 2028–2032, 7–11 October, 2002, Atlantic City, NJ, USA

[Keu95] Keurulainen J., Häkkinen H., Hämäläinen S., "Handover Method, and a Cellular System", US Pat. No. 6,198,928 B1, 6.3.2001. PCT filed 31.8.1995.

[Kha98] Khan F., Roobol C., Larsson J., "Performance of a Common Channel Packet Access in WCDMA", in proceedings of PIMRC98 conference, pp. 198–202, 8–11 September, Boston, MA, USA

[Kim01a] Kim J., Kim D.-H., Song P.-J., Kim S., "Design of Optimum Parameters for Handover Initiation in WCDMA", in proceedings of VTC01 fall conference, pp. 2768–2772, 7–11 October, 2001, Atlantic City, NJ, USA

[Kim01b] Kim J.-H., Kim J.,-I., Bang S.-C., ”Performance Analysis of Uplink Power Control in W-CDMA System for High Data Rate Transmission”, in proceedings of VTC01 fall conference, pp. 1937–1940, 7–11 October, 2001, Atlantic City, NJ, USA

[Kol02] Kolding T.E., Frederiksen F., Mogensen P., “Performance Aspects of WCDMA Systems with High Speed Packet Access (HSDPA)”, in proceedings of VTC02 fall conference, pp. 477–481, 24–28 September, 2002, Vancouver, BC, Canada

[Kor01] Korpela S., Hämäläinen S., ”Comparison of Narrow Band and Wide Band SIR Based Handover Criteria in WCDMA”, in proceedings of CIC2001 conference, 30 October – 2 November, 2001, Seoul, Korea

[Kum94] Kumar P.S., Holtzman J.M., “Analysis of Handoff Algorithms Using both Bit Error Rate (BER) and Relative Signal Strength”, in proceedings of ICUPC94 conference, pp. 1–5, 27 September – 1 Ocotober, 1994, San Diego, CA, USA

[Kwa01] Kwan R., Rinne M., “Performance analysis of the Downlink shared channel”, in proceedings of ICT01 conference, 2001, Bucharest, Romania

[Kwo99] Kwon D., Shin M., Kim M., Yoon Y., Park H.-K., “Performance Evaluation Between CDMA Systems by Mobile System Interference Simulator”, in proceedings of TENCON99 conference, pp. 1201–1204, 15–17 September, 1999, Cheju, Korea

[Lab96] Labedz G., Love R., Stewart K, Menich B.,”Predicting Real-World Performance for Key Parameters in a CDMA Cellular System”, in proceedings of VTC96 conference, pp. 1472–1476, 28 April – 1 May, 1996, Atlanta, GA, USA

[Lai99a] Laiho-Steffens J., Wacker A., Sipilä K., Heiska K., “The Impact of the Subscriber Profile on WCDMA Radio Network Performance”, in proceedings of VTC99 fall conference, pp. 2490–2494, 19–22 September, Amsterdam, Netherlands

[Lai99b] Laiho-Steffens J., Jäsberg M., Sipilä K., Wacker A., Kangas A., “Comparison of Three Diversity Handover Algorithms by Using Measured Propagation Data”, In proceedings of VTC99 spring conference, pp.1370–1374, 6–20 May, 1999, Houston, TX, USA

[Lai00a] Laiho-Seffens J., Wacker A., Sipilä K., “Verification of 3G Radio Network Dimensioning Rules with Static Network Simulator”, in Proceedings of VTC2000 spring conference, pp.478–482, 15–18 May, Tokyo, Japan

[Lai00b] Laiho-Seffens J., Wacker A., Aikio P., “The Impact of the Radio Network Planning and Site Configuration on the WCDMA Network Capacity and Quality of Service”, in Proceedings of VTC2000 spring conference, pp.1006–1010, 15–18 May, Tokyo, Japan

[Lai01] Laiho J., Wacker A., Novosad T., Hämäläinen A., “Verification of WCDMA Radio Network Planning Prediction Methods with

Fully Dynamic Network Simulator", in proceedings of VTC01 fall conference, pp. 526–530, 7–11 October, 2001, Atlantic City, NJ, USA

[Lat98] Latva-aho, M., "Advanced receivers for wideband systems", Acta Univ. Ouluensis, Finland, Doctoral Thesis, 1998

[Lau95] Lau F.C.M., Tam W.M., "Effects of Increased Capacity in CDMA Cellular Systems", in proceedings of ISSSE95 conference, pp. 579–582,25–27 October, 1995, San Francisco, CA, USA

[Lee91] Lee W.C.Y., "Overview of Cellular CDMA", IEEE Transaction on Vehicular Technology, pp. 291–302, Vol. 40, No. 2, May, 1991

[Lee98] Lee C.-C., "Effect of Soft and Softer Handoffs on CDMA System Capacity", IEEE Transactions on Vehicular Technology, pp. 830–841, Vol.47, No. 3, August 1998.

[Lee00] Lee W.C.Y., Lee D., "CDMA Capacity on Pathloss and Power Control", in proceedings of VTC00 fall conference, pp. 624–629, 24–28 September, 2000, Boston, MA, USA

[Lee01a] Lee W.C.Y., Lee D., "CDMA System Capacity Analysis", in proceedings of PACRIM01 conference, pp. 22–26, 26–28 August, 2001, Victoria, BC, Canada

[Lee01b] Lee W.C.Y., Lee D., "CDMA Capacity Analysis", in proceedings of PIMRC01 conference, pp. D-139 – D-143, 30 September – 3 October, 2001, san Diego, CA, USA

[Lil96] Lilja H., "Characterizing the effect of Nonlinear Amplifier and Pulse Shaping on the Adjacent Channel Interference with Different Data Modulations", Licenciate thesis, Oulu University, Finland, 1996

[Lil99a] Lilja H., Mattila H., "WCDMA Power Amplifier Requirements and Efficiency optimization Criteria", in proceedings of 1999 IEEE MTT-S International Microwave Symposium, pp. 1843–1846, 13-19 June, 1999, Anaheim, CA, USA

[Lil99b] Lilja H., Hämäläinen S., Pehkonen K., "Timing of Handover", US Pat.No. US6456847 B1, filed 12.09.1999

[Lim99] Lim S.S., Cao Q., Demetrescu C., Reader D.J., Lin J., "3rd Generation RACH Transmission – A Candidate", in proceedings of VTC99 spring conference, pp. 140–144, 16- 20 May, 1999, Houston, Texas, USA

[Lin94] Lin J.-C., Lee T.-H., Su Y.-T., "Power Control Algorithm for Cellular Radio Systems", IEE Electronics Letters, pp. 195–197, Vol. 30, No. 3, 3rd February, 1994

[Lin97] Ling F., Love B., Wang, M.M., "Behavior and Performance of Power Controlled IS-95 Reverse-Link Under Soft Handoff", in proceedings of VTC97 conference, pp. 924–928, 4–7 May, 1997, Phoenix, AZ, USA

[Lin00a] Lin C.-L., "Investigations of 3rd Generation Mobile Communication RACH Transmission", in proceedings of VTC00

fall conference, pp. 662–667, 24–28 September, 2000, Boston, MA, USA

[Lin00b] Ling F., Love R., Wang M.M., Brown T., Fleming P., Xu H., "Behavior and Performance of Power Controlled IS-95 Reverse-Link Under Soft Handoff", IEEE Transactions on Vehicular Technology, pp. 1697–1704, Vol.49, No. 5., September 2000

[Lov01] Lover R, Hgosh A., Nikides R., Jalloul L, Cudak M, Calsson M., "High Speed Downlink Packet Access Performance", in proceedings of VTC01 spring conference, pp. 2234–2238, 6–9 May, 2001, Rhodes, Greece

[Lov02] Love R., Classon B, Hhosh A., Cudak M., "Incremental Redundancy for Evolutions of 3G CDMA Systems", in proceedings of VTC02 spring conference, pp. 454–458, 6–9 May, 2002, Birmingham, AL, USA

[Luo00] Luo J.J., Dillinger M., Schulz E., "Research on Timer Settings for the Soft Handover Algorithm with Different System Loads in WCDMA", in proceedings of ICCT00 conference, pp. 741–747, 21–25 August, 2000, Beijing, PR China

[Luu01] Luukkanen, P., Rong Z., Ma L., "Performance of 1XTREME System for Mixed Voice and Data", in proceedings of ICC01 conference, pp. 1411–1415, 11- 14 June, 2001, Helsinki, Finland

[Mac00] Machauer R., Wiesler A., Joindral F., "Comparison of UTRA-FDD and cdma2000 with Intra- and Intercell Interference", in proceedings of ISSSTA00, pp. 652–656, 6–8 September, 2000, New Jersey, USA

[Mal95] Malkamäki E., Blanc P., Urie A., "Two Step Look-up Table Approach - the Link Between Transport and Control Simulations in ATDMA", in proceedings of RACE Mobile Telecommunications Summit 1995, pp. 432–436, November 1995

[Mal01] Malkamäki E., Mathew D., Hämäläinen S., "Performance of Hybrid ARQ Techniques for WCDMA High Data Rates", in proceedings of VTC2001 spring conference, pp. 2720–2724, 6–9 May, 2001, Rhodes, Greece

[Man95] Mandayam N.B., Holtzman J., Barberis S., "Erlang Capacity for an Integrated Voice/Data DS-CDMA Wireless System with Variable Bit Rate Sources", in proceedings of PIMRC95 conference, pp. 1078–1082, 27–29 September, Toronto, Ont., Canada

[Mat01] Mate A., Caldera C., Rinne M., "Performance of the Packet Traffic on the Downlink Shared Channel in a WCDMA Cell", in proceedings of ICT01 conference, June, 2001, Bucharest, Romania

[Mih99] Mihailescu C., Lagrange X., Godlewski P., "Soft Handover Analysis in Downlink UMTS WCDMA System", in proceedings of MoMuC99 conference, pp. 279–285, 15–17 November, 1999, san Diego, CA; USA

[Mil92] Milstein L.B., Rappaport T.S., Barghouti R., "Performance Evaluation for Cellular CDMA", IEEE Journal on Selected Areas in Communications, pp. 680–689, Vol.10, No. 4, May, 1992

[Moh99] Mohanty N., Voltz P., "Reverse Link Performance of Coherent DS-CDMA Cellular Systems with Power Control in Dynamic Fading Channel Conditions", in proceedings of VTC99 conference, pp. 39–44, 16–20 May, 1999, Houston, TX, USA

[Mor97] Morikawa H., Kajiya T., Aoyama T., Campbell A.T., "Distributed Power Control for Various QoS in a CDMA Wireless System", in proceedings of PIMRC97 conference, pp. 903–907, 1–4 September, Helsinki, Finland

[Mor01] Morimoto A., Higuchi K., Sawahashi M., "Site Independent Diversity Transmit Power Control for Inter-Cell Diversity in W-CDMA Forward Link", in proceedings of VTC01 fall conference, pp. 645–649, 7–11 October, 2001, Atlantic City, NJ, USA

[Mot88] Motley A.J., Keenan J.M.P., "Personal Communication Radio Coverage in Buildings at 900 MHz and 1700 MHz", Electronics letters, pp. 763–764, 9th June 1988, Vol 24, No.12

[Mot98] Motorola, "A Balanced Approach to Evaluating UTRA Adjacent Channel Interference Protection Requirements", Tdoc SMG2 UMTS-L1 46598.

[Mou01] Mousley T.J., "Throughput of High Speed Downlink Packet Access for UMTS", in proceedings of 3G Mobile Communication Technologies 01 conference, pp. 363–367, 26–28 March, 2001, London, UK

[Mur91] Murase A., Symington I.C., Green E., "Handover criterion for macro and microcellular systems", in proceedings of VTC91 conference, pp 524–530, 19–22 May, 1991, St. Louis, MO, USA

[Nag00] Nagate A., Murata M., Miyahara H., Sugano M., "An Integrated Approach for Performance Modeling and Evaluation of Soft Handoff in CDMA Mobile Cellular Systems", in proceedings of VTC00 fall conference, pp. 2605–2610, 24–28 September, 2000, Boston, MA, USA

[Neu00] Neubauer T., Baumgartner T., Bonek E., "Required Network Size for System Simulation in UMTS FDD Uplink", in proceedings of ISSSTA00 conference, pp. 481–485, 6–8 September, 2000, Parsippany, NJ, USA

[Nik98] Nikula E., Toskala A., Dahlman E., Girard L., Klein A., "FRAMES Multiple Access for UMTS and IMT-2000", IEEE Personal Communications, pp. 16–24, April, 1998

[Nok98a] Nokia, "Summary of the UTRA FDD ACP Simulations", Tdoc SMG2 UMTS-L1 310/98.

[Nok98b] Nokia, Ericsson "The Relationship Between Downlink ACS and Uplink ACP in UTRA System", Tdoc SMG2 UMTS-L1 69498.

[Nok99a] Nokia, "FDD UE minimum transmission power simulation results", TSG-RAN Working Group 4 (Radio) meeting #6, tdoc TSGR4#6(99)395, 26–29 July, 1999, South Queensferry, Scotland

[Nok99b] Nokia, " Outer loop power control", TSG-RAN Working Group 4 (Radio) meeting #8, Sophia Antipolis, France, 26–29 October, 1999

[Nok00a] Nokia, "UE minimum TX power", tdoc 016, TSG-RAN Working Group 4 (Radio) meeting #10, San Jose, California, US, 17-21 January 2000

[Nok00b] Nokia, "Mixed pico indoor and micro outdoor propagation and mobility model", tdoc 0630, TSG-RAN Working Group 4 (Radio) meeting #13, Turin, Italy, 4–8 September 2000

[Nok00c] Nokia, Ericsson, Motorola. Common HSDPA system simulation assumptions. TSG-R1 document, TSGR1#15(00)2094, 22–25th, August, 2000, Berlin, Germany, 12 pp

[Nok00d] Nokia, "UE Minimum Power", TSG RAN Working Group 4 (Radio) meeting #10, 29 February – 3 March, 2000, San Diego, California, USA

[Nok00e] Nokia, "Simulation Results in static propagation condition for RACH Performance Requirement Principle (Release '00)", tdoc0559, TSG RAN Working Group 4 (Radio) meeting #13, 4–8 September 2000, Turin, Italy

[Nok02] Press release, "Nokia launches new service solutions for operators at the 3GSM congress in Cannes", Nokia press release, February 20, 2002.

[Oja96a] Ojanperä T., Rikkinen K., Häkkinen H., Pehkonen K., Hottinen A., Lilleberg J., "Design of a 3rd Generation Multirate CDMA System with Multiuser Detection, MUD-CDMA" in proceedings of ISSSTA96 conference, pp. 334- 338, 22–25 September, 1996, Mainz, Germany

[Oja98] Ojanperä T., Prasad R., "Wideband CDMA for Third Generation Mobile Communications", Artech House Publishers, 1998

[Olo97] Olofsson H., Almgren M., Johansson C., Höök M., Kronestedt F., "Improved Interface Between Link Level and System Level Simulations Applied in GSM", in proceedings of UPCR97 conference, pp. 79–84, 12–16 October, 1997, San Diego, CA, USA

[OPNET] http://www.opnet.com/products/modeler/opnet_modeler.pdf

[Owe00] Owen R., Burley S., Jones P., Messer V., "Considerations for UMTS Capacity and Range Estimation", IEE Colloquium on Capacity and Range Enhancement Techniques for the Third Generation Mobile Communications and Beyond, pp. 5/1–5/6, 11 February, London, UK

[Pad94] Padovani R., "Reverse Link Performance of IS-95 Based Cellular Systems", IEEE Personal Communications, pp. 28–34, Third Quarter, 1994

[Par01] Parkval S., Dahlman E., Frenger P., Beming P., Persson M., "The High Speed Packet Data Evolution of WCDMA", in proceedings of PIMRC01 conference, pp. G-27 – G-31, 30 September – 3 October, 2001, san Diego, CA, USA

[Pic92] Pickholtz R.L., Schilling D.L., Milstein L.B., "Theory Spread-Spectrum Communications – A Tutorial", IEEE Transaction on Communications, vol. COM-30, pp. 855–884, May 1992

[Pie99] Pietilä A., "Simulations of Voice and Data Traffic in WCDMA Network", in proceedings of VTC99 conference, pp. 2070–2074, 16–20 May, 1999, Houston, TX, USA

[Pin00] Pinto H.B., "Uplink capacity of the WCDMA FDD Mode in UMTS Networks for Mixed Services", in proceedings of VTC00 fall conference, pp. 2167–2624, 24–28 September, 2000, Boston, MA, USA

[Pou01] Poutiainen E., Kwan R., Hämäläinen S., Chong, P., "Performance Study of the High Speed Downlink Packet Access (HSDPA) in a WCDMA Network", in proceedings of CIC2001 conference, 30 October – 2 November, 2001, Seoul, Korea

[Pro95] Proakis J.G., "Digital Communications", McGraww-Hill, 1995, ISBN 0-07-051726-6

[Qiu00] Qiu L., Zhu J., "Performance of Optimum Transmitter Power Control", in proceedings of VTC00 fall conference, pp. 601–607, 24–28 September, 2000, Boston, MA, USA

[Qua01] Qualcomm, Inc., "1xEV: 1x Evolution IS-856 TIAEIA Standard, Airlink Overview", November 7, 2001, revision 7.2

[Rao99] Rao Y.S., Kripalani A., "cdma2000 Mobile Radio Access for IMT 2000", in proceedings of ICPWC99 conference, pp. 6–15, 17–19 February, 1999, Jaipur, India

[Reg95] Rege K.M., Nanda S., Weaver C.F., Peng W.-C., "Analysis of Fade Margins for Soft and Hard Handoffs", in proceedings of PIMRC95, pp. 829–835, 27–29 September, 1995, Toronto, Ont., Canada

[Ren02] Rentel C.H., Krzymien, W.A., Darian B., Vanghi V., Elliot R., "Comparative Forward Link Traffic Channel Performance Evaluation of HDR and 1XTREME Systems", in proceedings of VTC02 spring conference, pp. 160–164, 6–9 May, 2002, Birmingham, AL, USA

[Rin99] Rinne M., Hämäläinen S., Lilja H., "Effects of Adjacent Channel Interference on WCDMA Capacity", in proceedings of ICT'99 conference, pp. 127–132, 1999, Cheju, Korea

[Rob75] Roberts L.G., "ALOHA Packet System with and without Slots and Capture", Computer Communications Review,vol.5, No 2, pp. 28–42, April 1975.

[Sam94] Sampath A., Holtzman J.M., "Adaptive Handoffs Through the Estimation of Fading Parameters", in proceedings of ICC94

conference, pp. 1131–1135, 1–5 May, 1994, New Orleans, LA, USA

[Sam95] Sampath A, Kumar P.S., Holzman J.M., "Power Control and Resource Management for a Multimedia CDMA Wireless System", in proceedings of PIMRC95 conference, pp. 21–25, 27–29 September, Toronto, Ont., Canada

[Sam97a] Sampath A., Kumar P.S., Holzman J.M., "On Setting Reverse Link Target SIR in a CDMA System", In proceedings of VTC97 conference, pp. 929–933, May 4–7, 1997, Phoenix, Arizona

[Sam97b] Sampath A, Mandayam N.B., Holtzman J.M., "Erlang Capacity of a Power Controlled Integrated Voice and Data CDMA System", in proceedings of VTC97 conference, pp. 1557–1561, 4–7 May, 1997, Phoenix, AZ, USA

[Sam01] Sampath. A., Jeske D.R., "Analysis of Signal-to-Interference Ratio Estimation Methods for Wireless Communication Systems", in proceedings of ICC01 conference, pp. 2499–2503, 11–14 June, 2001, Helsinki, Finland

[Sar00] Sarkar S., Chen T., Leung G., Blessent L., Tiedemann E., "cdma2000 Reverse Link; Design and System Performance", in proceedings of VTC00 fall conference, pp. 2713–2719, 24–28 September, 2000, Boston, MA, USA

[Sar01] Sarkar S., "Reverse Link Capacity for cdma2000", in proceedings of VTC01 spring conference, pp. 2397–2401, 6–9 May, 2001, Rhodes, Greece

[Sch98] Schneider W., Cordier C., Fratti M., "On the Maximum Uplink Capacity per km^2 of CDMA Systems", in proceedings of ISSSTA98 conference, pp. 798–801, 2–4 September, 1998, Sun City, South Africa

[Sch99] Schulist M., Weber R., "Link level performance results for a WCDMA random access scheme with preamble power ramping and fast acquisition indication", in proceedings of VTC99 fall conference, pp. 2581–2585, 19–22 September, 1999, Amsterdam, Netherlands

[Sch01] Schulist M., "Acknowledgement of 3GPP WCDMA Random and Packet Access Applying Space-Time Transmit-Diversity", in proceedings of VTC01 spring conference, pp. 2519–2523, 6–9 May, 2001, Rhodes, Greece

[Sch02] Schwab M., Seidenberg P., "Analysis of Mobile-originated Interference in Coexisting UMTS Networks", in proceedings of VTC02 spring conference, pp. 1636–1639, 6–9 May, 2002, Birmingham, AL, USA

[Sei94] Seita P., "Soft Handoff in a DS-CDMA Microcellular Network", in proceedings of VTC94 conference, pp. 530–534, 8–10 June, Stockholm, Sweden

[Sha92] Shapira J., Padovani, R., "Spatial Topology and Dynamics in CDMA Cellular Networks", in proceedings of VTC92 conference, pp. 213–216, 10–13 May, 1992, Denver, CO, USA

[Sha94] Shapira J., "Micro Cell Engineering in CDMA Cellular Networks", IEEE Transactions on Vehicular Technology, pp. 817-825, Vol. 43., No. 4., November, 1994

[Shi01] Shin S., Ko G., Kim K., "Performance Comparison of Two Common Control Channels for 3G Systems", in proceedings of ICATM01 conference, pp. 231–234, 22–25 April, 2001, Seoul, South Korea

[Sim93] Simpson F., Holtzman J., "Direct Sequence CDMA Power Control, Interleaving and Coding", IEEE Journal on Selected Areas in Communications, pp. 1085–1095, Vol.11, No. 7, September, 1993

[Sip99a] Sipilä K., Jäsberg M. Laiho-Steffens J., Wacker A., "Soft Handover Gains in Fast Power Controlled WCDMA Uplink", in proceedings of VTC99 conference, pp. 1594–1598, 16- 20 May, 1999, Houston, TX, USA

[Sip99b] Sipilä K., Laiho-Steffens J., Wacker A., Jäsberg M., "Modeling the Impact of the Fast Power Control on the WCDMA Uplink", In proceedings VTC'99 conference, pp. 1266–1270, 16- 20 May, 1999, Houston, TX, USA

[Sip00] Sipilä K., Honkasalo Z.-C., Laiho-Seffens J., Wacker A. "Estimation of Capacity and Required Transmission Power of WCDMA Downlink Based on a Downlink Pole Equation", in Proceedings of VTC2000 conference, pp.1002–1005, 15–18 May, 2000, Tokyo, Japan

[Smi02] Smida B., Sampath V., Marinier P., "Capacity Degradation due to Coexistence Between Second Generation and 3G/WCDMA Systems", in proceedings of VTC02 spring conference, pp. 95–99, 6–9 May, 2002, Birmingham, AL, USA

[Sol92] Soliman S., Wheatley C., Padovani R., "CDMA Reverse Link Open Loop Power Control", in proceedings of GLOBECOM92 conference, pp. 69–72, 6–9 December, 1992, Orlando, FL, USA

[Sol96] Soleimanipour M., Freeman G.H., "A Realistic Approach to the Capacity of Cellular CDMA Systems", in proceedings of VTC96 conference, pp. 1125–1128, 28 April – 1 May, 1996, Atlanta, GA, SA

[Son98] Song L., Holzman, J.M., "CDMA Dynamic Downlink Power Control", in proceedings of VTC98 conference, pp. 1101–1105, 18–21 May, 1998, Ottawa, Ont., Canada

[SPW] http://www.cadence.com/products/spw.html

[Sta01] Staehle D., Leibnitz K., Heck K., Schröder B., Weller B., Tran-Gia P., "Analytical Characterization of the Soft Handover Gain in UMTS", in proceedings of VTC01 fall conference, pp. 291–295, 6–9 May, 2001, Rhodes, Greece

[Sto98] Stocks M. (editor), "Third Generation Partnership Project Agreement", 3gpp agreement, 4.12.1998

[Str93] Strasser G., (ed.), "Propagation Model issue 1", R2084/ESG/CC3/ DS/P/012/b1, April 1993

[T1] http://www.t1.org

[Tak01] Takano N., Hamabe K., "Enhancement of Site Diversity Transmit Power Control in CDMA Systems", in proceedings of VTC01 fall conference, pp. 635–639, 7–11 October, 2001, Atlantic City, NJ, USA

[Tam97a] Tam W.M., Lau F.C.M., "Analysis of Imperfect Power Control in CDMA Cellular Systems", in proceedings of PIMRC97 conference, pp. 892–897, 1–4 September, 1997, Helsinki, Finland

[Tam97b] Tam W.M., Lau F.C.M., "Capacity Analysis of a CDMA Cellular System with Power Control Schemes", in proceedings of ICUPC97 conference, pp. 608–612, 12–16 October, 1997, San Diego, CA, USA

[Tel99] Telia, "RSCP/ISCP for HO and cell selection purposes", 3GPP TSG-RAN Working group 2 (Radio layer 2 and radio layer 3) meeting #9, tdoc TSGR2#9(99)h64, 29 November – 3 December, 1999, Sophia Antipolis, France

[Tel00a] Telia, " Impact of compressed mode on the capacity of a WCDMA system", 3GPP TSG-RAN Working group 4 (Radio) meeting #4, tdoc TSGR 4#14(00)0960, 10–12 May, 1999, Kista, Sweden

[Tel02] http://www.telecoms.com, Global Mobile, Issue 16, 11 September, 2002

[TIA] http://tiaonline.org

[Tig01] Tigerstedt K., Heiska K., "Static WCDMA System Simulator for Indoor Environments", in proceedings of VTC2001 spring conference, pp. 2800–2803, 6–9 May, 2001, Rhodes, Greece

[Tos98] Toskala A., Holma H., Hämäläinen S., "Link and System Level Performance of Multiuser Detection CDMA Uplink", Wireless Personal Communications, vol.8, pp 301–302, 1998.

[Tra01] Tralli V., Zorzi M., "Quality of Service and Power Consumption in WCDMA Cellular Systems with SIR-based Closed Loop Power Control", in proceedings of PIMRC01, pp. D-22 – D-26, 30 September – 3 October, 2001, San Diego, CA, USA

[Tri01] Tripathi N.D., "Simulation Based Analysis of the Radio Interface Performance of an IS-2000 System for Various Data Services", in proceedings of VTC01 fall conference, pp. 2665–2669, 7–11 October, 2001, Atlantic City, NJ, USA

[TS25.101] 3GPP TS25.101, "UE Radio transmission and reception (FDD)", Release 1999, v3.6.0, March, 2001

[TS25.104] 3GPP TS25.104, "UTRA (BS) FDD; Radio Transmission and Reception", Release 1999, v.3.6.0, March, 2001

[TS25.133] 3GPP TS25.133, “Requirements for Support of Radio Resource Management”, release 1999, v.3.5.0, March, 2001

[TS25.211] 3GPP TS25.211, “Physical channels and mapping of transport channels onto physical channels (FDD)”, Release 1999, v.3.6.0, March, 2001

[TS25.212] 3GPP TS25.212, “Multiplexing and channel coding(FDD)”, release 1999, v.3.5.0, March, 2001

[TS25.213] 3GPP TS25.212, “Multiplexing and channel coding (FDD)”, release 1999, v.3.5.0, March, 2001.

[TS25.214] 3GPP TS25.214, “Physical Layer procedures (FDD)”, Release 1999, v3.6.0, March, 2001

[TS25.215] 3GPP TS25.215, “Physical layer - Measurements (FDD)”, release 1999, v.3.6.0, March, 2001.

[TS25.306] 3GPP TS25.303, “UE Radio Access Capabilities”, release 1999, v.3.1.0, March, 2001

[TS25.322] 3GPP TS25.322, “RLC protocol specification”, release 1999, v.3.6.0, March, 2001.

[TS25.331] 3GPP TS25-331. v. 3.50, “RRC Protocol Specification”, Release 1999, v.3.6.0, March, 2001.

[TR25.848] 3GPP TR25.848, “Physical Layer Aspects of UTRA High Speed Downlink Access”, Release 4., v.4.0.0, March 2001.

[TR25.922] 3GPP TR25.922, “Radio Resource Management Strategies”, release 1999, v3.5.0, March, 2001

[TR25.942] 3GPP TR25.942, “RF System Scenarios”, release 1999, v3.0.0, March 2001

[TTA] http://www.tta.or.kr/HDnewenglish/main/index.htm

[TTC] http://www.ttc.or.jp/e/index.html

[Ucr01] Uc-Rios C.E., Lara-Rodriguez D., “Forward Link Capacity Losses for Soft and Softer Handoff in Cellular Systems”, in proceedings of PIMRC01 conference, pp. D-48 – D-53, 30 September – 3 October, San Diego, CA, USA

[UMTS30.01] UMTS30.01, “UMTS Baseline Document; Position of UMTS agreed by SMG”, ETSI SMG, v3.3.0, 1998-06

[UMTS30.03] TR 101 112 (UMTS 30.03): "Universal Mobile Telecommunications System (UMTS); Selection procedures for the choice of radio transmission technologies of the UMTS".

[UMTS30.06] UMTS30.06, “Universal Mobile Telecommunications System (UMTS); UMTS Terrestrial Radio Access (UTRA); Concept Evaluation”, TR 101 146, v3.0.0, 1997-12.

[Var90] Varanasi M.K., Aazhang, B., “Multistage Detection in Asynchronous Code-Division Multiple-Access Communications”, IEEE Transactions on Communications, Vol. COM-38, pp.509–519, 1990

[Var91] Varanasi M.K., Aazhang, B., “Near-Optimum Detection in Synchronous Code-Division Multiple-Access Communications”,

IEEE Transactions on Communications, Vol. COM-39, pp.725–736, 1991

[Vem96] Vembu S., Viterbi, A.J., "Two Different Philosophies in CDMA – A Comparison", in proceedings of VTC96 conference, pp. 869–873, 28 April – 1 May, 1996, Atlanta, GA, USA

[Vij93a] Vijayan R., Holtzman J.M., "A Model for Analysing Handoff Algorithms", IEEE Transactions on Vehicular Technology, pp 351- 356, Vol. 42, No.3, August 1993

[Vij93b] Vijayan R., Holtzman J.M., "Sensitivity of handoff algorithms to variations in the propagation environment", in proceedings of ICUPC93 conference, pp. 158–162, 12–15 October, 1993, Ottawa, Ont., canada

[Vit93a] Viterbi A.J., Viterbi A.M., Zehavi E., "Performance of Power-Controlled Wideband Terrestrial Digital Communication", IEEE Transactions on Communications, Vol. 41, No. 4, April, 1993

[Vit93b] Viterbi A.M., Viterbi A.J., "Erlang Capacity of a Power Controlled CDMA Systems", IEEE Journal on Selected Areas in Communications, Vol.11., No.6, August 1993.

[Vit94a] Viterbi A.J., Viterbi A.M., Zhavi E., "Other-cell interference in Cellular Power-Controlled CDMA", IEEE Transactions on Communications, Vol. 42, No. 2/3/4, February/March/April, pp. 1501–1504, 1994.

[Vit94b] Viterbi A.J., Viterbi A.M., Gilhousen K.S., "Soft Handover Extends CDMA Cell Coverage and Increases Reverse Link Capacity", IEEE Journal in Selected Areas of Communications, Vol 12, No. 8, pp. 1281- 1288, October, 1994

[Vuk01] Vukovic I.N., Brown T., "Performance Analysis of the Random Access Channel (RACH) in WCDMA", in proceedings of VTC01 spring conference, pp. 532–536, 6–9 May, 2001, Rhodes, Greece

[Wac99a] Wacker A., Laiho-Steffens J., Sipilä K., Jäsberg M., "Static Simulator for Studying WCDMA Radio Network Planning Issues", in proceedings of VTC99 conference, pp. 2436–2440, 16–20 May, 1999, Houston, Texas, USA

[Wac99b] Wacker A., Laiho-Steffens J., Sipilä K., Heiska K., "The Impact of the Base Station Sectorization on WCDMA Radio Network Performance", in proceedings of VTC99fall conference, pp. 2611–2615, 19–22 September, Amsterdam, Netherlands

[Wac01] Wacker A., Laiho J., "Mutual Impact of Two Operators' WCDMA Radio Network on Coverage, Capacity and QoS in a Macro Cellular Environment", in proceedings of VTC01 fall conference, pp. 2077–2081, 7–11 October, 2001, Atlantic City, NJ, USA

[Wal94] Wallace M., Walton R., "CDMA Radio Network Planning", in proceedings of ICUPC94 conference, pp. 62–67, 27 September – 1 October, 1994, san Diego, CA, USA

[Wan93] Wang M.M., Tonguz O.K., "Forward Link Power Control for Cellular CDMA Networks", IEEE Electronics Letters, pp. 1195–1197, Vol. 29, No. 13, 24th June, 1993

[Wan00] Wang Y.-P., Ottoson T., "Cell Search in W-CDMA", IEEE Journal on Selected Areas of Communications, pp.1470–1482, Vol.18, No. 8, 2000

[Wan01] Wang Y.-P., Bottomley G.E., "CDMA Downlink System Capacity Enhancement Through Generalized RAKE Reception", in proceedings of VTC01 fall conference, pp. 1177–1181, 7–11 October, 2001, Atlantic City, NJ, USA

[Wen01] Wen J.-H., Sheu J.-S., Chen J.-L., "Performance of Optimum Transmitter Power Control in Multimedia CDMA Cellular Mobile Systems", in proceedings of VTC01 spring conference, pp. 2883–2887, 6- 9 May, 2001, Rhodes, Greece

[Wib01] Wibisono G., Darsilo R., "The Effect of Imperfect Power Control and Sectorization on the Capacity of CDMA System with Variable Spreading Gain", in proceedings of PACRIM01 conference, pp. 31–34, 26–28 August, 2001, Victoria, BC, Canada

[Wic97] Wichman R., Hottinen, A "Multiuser Detection for Downlink CDMA Communications in Multipath Fading Channels" in proceedings of VTC97 conference, pp. 572-576, 4–7 May, 1997, Phoenix, USA

[Wig96] Wigard J., "A Simple Mapping from C/I to FER for a GSM Type of Air-Interface", in proceedings of PIMRC96 conference, pp. 78–82, 15–18 October, 1996, Taipei, Taiwan

[Won97] Wong D., Lim, T.J., "Soft Handoffs in CDMA Mobile Systems", IEEE Personal Communications Magazine, pp. 6–17, December 1997

[Wor99] Worley B., Takawira F., "Power Reduction and Threshold Adjustment for Soft Handoff in CDMA Cellular Systems", in proceedings of Africon99 conference, pp. 263–268, 28 September – 1 October, 1999, Cape Town, South Africa

[Wu97] Wu J.-S., Sze M.-T., Chung J.-K., "Uplink and Downlink Capacity Analysis for Two-Tier CDMA Cellular Systems", in proceedings of INFOCOM97 conference, pp. 626–633, 7–11 April, 1997, Kobe, Japan

[Wu99] Wu Q., "Performance of Optimum Transmitter Power Control in CDMA Cellular Mobile Systems", IEEE Transaction on Vehicular Technology, pp. 571–575, Vol. 48, No. 2, March, 1999

[Wu02] Wu H., "The Environment Characteristics of Telecom Services in China", in proceedings of 2002 Euro-China Co-operation Forum on the Information Society, 16–20 April, 2002, Beijing China

[Xia97] Xia H.H., "Reference Models for Evaluation of Third-Generation Radio Transmission Technologies", in proceedings of ACTS97 conference, pp.235–240, 7–10 October, 1997, Aalborg, Denmark

[Yan97] Yang J., Lee W.C.Y., “Design Aspects and System Evaluations of IS-95 based CDMA Systems”, in proceedings of ICUPC97 conference, pp. 381–385, 12–16 October, 1996, San Diego, CA, USA

[Yan00a] Yang X., Ghareri-Niri S., Tafazolli R., ”Evaluation of Soft Handover Algorithms for UMTS”, in proceedings of PIMRC00 conference, pp. 772–776, 18–21 September, 2000, London, UK

[Yan00b] Yang X., Ghaheri-Niri S., Tafazolli R., ”Enhanced Soft Handover Algorithms for UMTS System”, in proceedings of VTC00 fall conference, pp. 1539–1543, 24–28 September, 2000, Boston, MA, USA

[Yin02a] Ying W., Fei G., Ping Z., Hai W., “Performance of RSCP-Triggered and Ec/No-Triggered Inter-Frequency Handover Criteria for UTRA”, in proceedings of VTC02 spring conference, pp. 704–708, 6–9 May, 2002, Birmingham, AL, USA

[Yin02b] Ying W., Dan S., Ping Z., Hai W., “Comparison between the Periodic and Event-Triggered Compressed Mode”, in the proceedings of VTC02 spring conference, pp. 1331–1335, 6–9 May, 2002, Birmingham, AL, USA

[Yun94] Yun L.C., Messerschmitt D.G., ”Power Control for Variable QOS on a CDMA Channel”, in proceedings of MILCOM94 conference, pp. 178–182, 2–5 October, 1994, Fort Monmouth, NJ, USA

[Yun95] Yun L.C., Messerschmitt D.G., ” Variable quality of service in CDMA systems by statistical power control”, in proceedings of GLOBECOM95 conference, pp. 713–719, 18–22 June, 1995, Seattle, WA, USA

[Zan92] Zander J., “Performance of Optimum Transmitter Power Control in Cellular Radio Systems”, IEEE Transactions on Vehicular Technology, pp. 57–62, Vol.41, No.1, February, 1992

[Zan94] Zander J., Frodigh M., “Comment on “Performance of Optimum Transmitter Power Control in Cellular Radio Systems””, IEEE Transactions on Vehicular Technology, pp. 636, Vol.43, No.3, August, 1994

[Zha94] Zhang N., Holtzman J.M., “Analysis of Handoff Algorithms Using both Absolute and Relative Measurements”, in proceedings of VTC94 conference, pp. 82–86, 8–10 June, 1994, Stockholm, Sweden

[Zha96] Zhang N., Holtzman J.M., “Analysis of Handoff Algorithms Using both Absolute and Relative Measurements”, IEEE Transactions on Vehicular Technology, pp. 174–179, Vol. 45, No. 1, February 1996

[Zha98] Zhang N., Holtzman J.M., “Analysis of CDMA Soft-Handoff Algorithm”, IEEE Transactions on Vehicular Technology, pp. 710–714, Vol.47, No.2, May, 1998

[Zha01a] Zhang Q., Yue O.-C., "UMTS Air Interface Voice/Data Capacity – Part 1: Reverse Link Analysis", in proceedings of VTC01 spring conference, pp. 2725–2729, 6–9 May, 2001, Rhodes, Greece

[Zha01b] Zhang Q., "UMTS Air Interface Voice/Data Capacity – Part 2: Forward Link Analysis", in proceedings of VTC01 spring conference, pp. 2730–2734, 6–9 May, 2001, Rhodes, Greece

[Zor94] Zorzi M., "Simplified Forward-Link Power Control Law in Cellular CDMA", IEEE Transaction on Vehicular Technology, pp. 1088–1093, Vol. 43, No. 4, November, 1994

APPENDIX A: CHANNEL MODELS USED WITH SIMULATIONS

TABLE A.1 CODIT Macro-Cell Channel.

Tap	Relative Delay (ns)	Relative Power (dB)	Doppler Spectra
1	100	-3.2	CLASSIC
2	200	-5.0	CLASSIC
3	500	-4.5	CLASSIC
4	600	-3.6	CLASSIC
5	850	-3.9	CLASSIC
6	900	0.0	CLASSIC
7	1050	-3.0	CLASSIC
8	1350	-1.2	CLASSIC
9	1450	-5.0	CLASSIC
10	1500	-3.5	CLASSIC

TABLE A.2 CODIT Micro-Cell Channel.

Tap	Relative Delay (ns)	Relative Power (dB)	Doppler Spectra
1	0	-2.3	RICE (Ricean factor -7.3 dB, Doppler shift 0.6066)
2	0	0.0	RICE (Ricean factor -3.5 dB, Doppler shift 0.6066)
3	0	-13.6	CLASSIC
4	50	-3.6	RICE (Ricean factor -3.5 dB, Doppler shift 0.6066)
5	50	-8.1	CLASSIC
6	100	-10.0	CLASSIC
7	1700	-12.6	RICE (Ricean factor -2.2 dB, Doppler shift 0.6066)

TABLE A.3 ATDMA Macro-Cell Channel.

Tap	Relative Delay (ns)	Relative Power (dB)	Doppler Spectra
1	0	0.0	CLASSIC
2	380	-10.0	CLASSIC
3	930	-22.7	CLASSIC
4	1940	-24.7	CLASSIC
5	2290	-20.7	CLASSIC
6	2910	-22.1	CLASSIC

TABLE A.4 ATDMA Micro-Cell Channel.

Tap	Relative Delay (ns)	Relative Power (dB)	Doppler Spectra
1	0	-4.9	CLASSIC
2	230	0.0	CLASSIC
3	630	-11.3	CLASSIC
4	1110	-13.9	CLASSIC
5	1440	-16.1	CLASSIC
6	1840	-23.5	CLASSIC

TABLE A.5 ETSI Macro-Cell Channel.

Tap	Channel A		Channel B		Doppler
	Rel. Delay (nsec)	Avg. Power (dB)	Rel. Delay (nsec)	Avg. Power (dB)	Spectrum
1	0	0.0	0	-2.5	CLASSIC
2	310	-1.0	300	0	CLASSIC
3	710	-9.0	8900	-12.8	CLASSIC
4	1090	-10.0	12900	-10.0	CLASSIC
5	1730	-15.0	17100	-25.2	CLASSIC
6	2510	-20.0	20000	-16.0	CLASSIC

TABLE A.6 ETSI Micro-Cell Channel.

Tap	Channel A		Channel B		Doppler
	Rel. Delay (nsec)	Avg. Power (dB)	Rel. Delay (nsec)	Avg. Power (dB)	Spectrum
1	0	0	0	0	CLASSIC
2	110	-9.7	200	-0.9	CLASSIC
3	190	-19.2	800	-4.9	CLASSIC
4	410	-22.8	1200	-8.0	CLASSIC
5	-	-	2300	-7.8	CLASSIC
6	-	-	3700	-23.9	CLASSIC

YHTEENVETO (FINNISH SUMMARY)

Väitöskirja käsittelee WCDMA- järjestelmän suorituskykyyn ja sen simulointiin liittyviä kysymyksiä. Tutkimuksen tuloksena on kehitetty työkaluja, joita käyttäen on mahdollista tutkia WCDMA- järjestelmän radioverkon kapasiteettia, eri parametrien ja algoritmien vaikutusta kapasiteettiin sekä simulointeihin perustuva suorituskykyanalyysi joukolle WCDMA- järjestelmän parametreja ja algoritmeja. Lisäksi on kehitetty kaksi uutta menetelmää, joilla pyritään parantamaan WCDMA- ja cdma2000- järjestelmien suorituskykyä.

Kehitettyä radioverkkosimulointityökalua voidaan hyväksikäyttää tutkittaessa WCDMA- järjestelmän parametreja ja algoritmeja standardointitarkoituksia varten, radioresurssienhallinta-algoritmien kehitystyön apuvälineenä, kehitettäessä verkkosuunnittelutyökaluja sekä WCDMA- radioverkkojärjestelmän optimointityökaluna. Työssä on käsitelty kahdenlaisia radioverkkosimulointityökaluja – staattisia sekä dynaamisia simulaattoreja. Staattinen radioverkkosimulaattori on yksinkertainen tietokoneohjelma, jolla voidaan lyhyessä ajassa generoida suhteellisen luotettavia simulointituloksia. Staattiset radioverkkosimulaattorit ovat riittäviä esimerkiksi radioverkkosuunnittelun tarpeisiin. Dynaaminen radioverkkosimulaattori on suhteellisen monimutkainen työkalu, joka mallintaa ajan kulumisen, käyttäjien liikkumisen sekä liikenteen generoimisen, monikäyttömenetelmän sekä oikeankaltaiset radioresurssienhallinta-algoritmit.

Työssä tutkittiin WCDMA- järjestelmän kapasiteettia käyttäen hyväksi kehitettyä staattista radioverkkosimulaattoria. WCDMA- tukiaseman vastaanotin voidaan toteuttaa käyttäen ns. monen käyttäjän ilmaisimia. Tässä työssä tutkittiin monen käyttäjän ilmaisimen mahdollistamaa järjestelmän kapasiteettihyötyä. Tukiaseman lähetys liikkuvalle asemalle voidaan toteuttaa käyttäen ortogonaalisia hajautuskoodeja tai liikkuvassa asemassa voidaan käyttää häiriönpoistoa. Tässä työssä tutkittiin mahdollista kapasiteettihyötyä ortogonaalisista hajautuskoodeista sekä häiriönpoistosta. Lisäksi tutkittiin ns. pehmeän kanavanvaihdon mahdollista kapasiteettihyötyä siirtosuunnassa tukiasemalta liikkuvalle asemalle.

Liikkuvan aseman tehovahvistimen epälineaarisuudesta sekä vastaanotinsuodattimen selektiivisyydestä johtuen viereisillä kanavilla kommunikoivat liikkuvat asemat tai tukiasemat saattavat aiheuttaa häiriötä vastaanotossa. Tässä työssä on tutkittu vaatimuksia tehovahvistimen lineaarisuudelle ja vastaanotinsuodattimen selektiivisyydelle perustuen staattisiin simulointeihin. Simulointien perusteella on arvioitu viereisen kanavan häiriön aiheuttamaa järjestelmän kapasiteettihäviöitä.

Tässä työssä on tutkittu tehonsäädön sekä sen parametrien, puhelunmuodostukseen liittyvien algoritmien, erilaisten tukiasemanvaihtoalgoritmien sekä niiden parametrien ja epäjatkuvan toimintatilan (compressed mode) vaikutusta järjestelmän kapasiteettiin käyttäen dynaamista radioverkkosimulaattoria. Suuret datanopeudet mahdollistavan HSDPA -menetelmän suorituskykyä on tutkittu dynaamisella simulaattorilla.

CDMA- järjestelmien suorituskyvyn parantamiseksi tässä työssä esitellään kaksi uutta menetelmää – diversiteetti puhelunmuodostus (diversity random access) sekä tukiasemadiversiteetti (Site Selection Diversity Transmit, SSDT, Fast Cell Selection, FCS). Molemmat menetelmät ovat käytössä sekä WCDMA että cdma2000 –järjestelmissä.

Useita WCDMA- järjestelmän parametreja on muutettu tai sovittu 3GPP-standardointiprojektissa perustuen tässä työssä esitettyyn tutkimukseen. Tällaisia parametreja ovat mm. liikkuvan aseman tehovahvistimen lineaarisuusvaatimus, vastaanotinsuodattimen selektiivisyysvaatimus sekä liikkuvan aseman minimitehovaatimus.

JYVÄSKYLÄ STUDIES IN COMPUTING

1 ROPPONEN, JANNE, Software risk management - foundations, principles and empirical findings. 273 p. Yhteenveto 1 p. 1999.
2 KUZMIN, DMITRI, Numerical simulation of reactive bubbly flows. 110 p. Yhteenveto 1 p. 1999.
3 KARSTEN, HELENA, Weaving tapestry: collaborative information technology and organisational change. 266 p. Yhteenveto 3 p. 2000.
4 KOSKINEN, JUSSI, Automated transient hypertext support for software maintenance. 98 p. (250 p.) Yhteenveto 1 p. 2000.
5 RISTANIEMI, TAPANI, Synchronization and blind signal processing in CDMA systems. - Synkronointi ja sokea signaalinkäsittely CDMA järjestelmässä. 112 p. Yhteenveto 1 p. 2000.
6 LAITINEN, MIKA, Mathematical modelling of conductive-radiative heat transfer. 20 p. (108 p.) Yhteenveto 1 p. 2000.
7 KOSKINEN, MINNA, Process metamodelling. Conceptual foundations and application. 213 p. Yhteenveto 1 p. 2000.
8 SMOLIANSKI, ANTON, Numerical modeling of two-fluid interfacial flows. 109 p. Yhteenveto 1 p. 2001.
9 NAHAR, NAZMUN, Information technology supported technology transfer process. A multi-site case study of high-tech enterprises. 377 p. Yhteenveto 3 p. 2001.
10 FOMIN, VLADISLAV V., The process of standard making. The case of cellular mobile telephony. - Standardin kehittämisen prosessi. Tapaustutkimus solukkoverkkoon perustuvasta matkapuhelintekniikasta. 107 p. (208 p.) Yhteenveto 1 p. 2001.
11 PÄIVÄRINTA, TERO, A genre-based approach to developing electronic document management in the organization. 190 p. Yhteenveto 1 p. 2001.
12 HÄKKINEN, ERKKI, Design, implementation and evaluation of neural data analysis environment. 229 p. Yhteenveto 1 p. 2001.
13 HIRVONEN, KULLERVO, Towards Better Employment Using Adaptive Control of Labour Costs of an Enterprise. 118 p. Yhteenveto 4 p. 2001.
14 MAJAVA, KIRSI, Optimization-based techniques for image restoration. 27 p. (142 p.) Yhteenveto 1 p. 2001.
15 SAARINEN, KARI, Near infra-red measurement based control system for thermo-mechanical refiners. 84 p. (186 p.) Yhteenveto 1 p. 2001.
16 FORSELL, MARKO, Improving Component Reuse in Software Development. 169 p. Yhteenveto 1 p. 2002.
17 VIRTANEN, PAULI, Neuro-fuzzy expert systems in financial and control engineering. 245 p. Yhteenveto 1 p. 2002.
18 KOVALAINEN, MIKKO, Computer mediated organizational memory for process control. Moving CSCW research from an idea to a product. 57 p. (146 p.) Yhteenveto 4 p. 2002.
19 HÄMÄLÄINEN, TIMO, Broadband network quality of service and pricing. 140 p. Yhteenveto 1 p. 2002.
20 MARTIKAINEN, JANNE, Efficient solvers for discretized elliptic vector-valued problems. 25 p. (109 p.) Yhteenveto 1 p. 2002.
21 MURSU, ANJA, Information systems development in developing countries. Risk management and sustainability analysis in Nigerian software companies. 296 p. Yhteenveto 3 p. 2002.
22 SELEZNYOV, ALEXANDR, An anomaly intrusion detection system based on intelligent user recognition. 186 p. Yhteenveto 3 p. 2002.
23 LENSU, ANSSI, Computationally intelligent methods for qualitative data analysis. 57 p. (180 p.) Yhteenveto 1 p. 2002.
24 RYABOV, VLADIMIR, Handling imperfect temporal relations. 75 p. (145 p.) Yhteenveto 2 p. 2002.
25 TSYMBAL, ALEXEY, Dynamic integration of data mining methods in knowledge discovery systems. 69 p. (170 p.) Yhteenveto 2 p. 2002.
26 AKIMOV, VLADIMIR, Domain Decomposition Methods for the Problems with Boundary Layers. 30 p. (84 p.). Yhteenveto 1 p. 2002.
27 SEYUKOVA-RIVKIND, LUDMILA, Mathematical and Numerical Analysis of Boundary Value Problems for Fluid Flow. 30 p. (126 p.) Yhteenveto 1 p. 2002.
28 HÄMÄLÄINEN, SEPPO, WCDMA Radio Network Performance. 235 p. Yhteenveto 2 p. 2003.